Control Algorithms for Optimisation of Engine Combustion Process with Continuously Changing Fuel Composition

By

KinYip Chan

Supervised by

Prof. Andrzej Ordys

Dr. Olga Duran

Dr. Konstantin Volkov

Dr. Jiamei Deng

Thesis submitted in partial fulfilment of the requirements of Kingston University for the Degree of Doctor of Philosophy

Faculty of Science, Engineering and Computing
Kingston University, London

April 2014

Abstract

Current research efforts in the areas of automotive control aim at developing new control algorithms so engine can work efficiently with different fuel compositions. Progressing in this direction, this thesis pioneers and researches novel control strategies to reduce the engine emissions gasses, Carbon Dioxide (CO_2), Oxygen (O_2), Carbon Monoxide (CO) and Nitric Oxide (NOx), while keeping optimum performance with unknown fuel mixtures.

A two-zone engine combustion model is developed and thoroughly validated against the computational data from commercial engine simulation packages. The engine model is suited for the development and testing of control systems. The simulation uses the following fuel mixtures: isooctane (C_8-H_{18}), methanol (C_1-H_4-O_1) and ethanol (C_2-H_6-O_1). The results obtained provide better understanding of the control parameters, including fuel-to-air ratio, ignition timing, exhaust-valve timing and intake-valve timing. Moreover, the model facilitates control design.

The novel engine controller is studied on the fuel composition as the additional parameter where such parameter has not been widely considered in engine control research. Efficient methodologies to estimate the original fuel composition by using the exhaust gas composition obtained from the engine are proposed and investigated. Two novel approaches based on feed-forward neural network and Adaptive Neuro-Fuzzy Interface System (ANFIS), respectively, are proposed. The portion of mixture for Isooctane-Methanol and Isooctane-Ethanol are effectively calculated. Moreover, results suggest that the feed-forward neural network outperforms the ANFIS approach and that the performance of the fuel estimator is stable in the continuous time process.

Further in this research, a Multi-Input-Multi-Output (MIMO) engine control system is developed. The methodology used is a system identification employing a state-space model. In order to reduce the complexity of the state-space model, the developed AI fuel estimator is used to facilitate on the model reduction by feeding gains to controllers for the individual components. In addition, it uses the linear quadric regulator (LQR) method to find the closed-loop gain in the development of the closed-loop control system.

The above techniques have been evaluated and results show that the controller is able to identify the minimum levels of the emission gases in terms of CO_2, O_2, CO and NOx in a continuously changing engine speed.

Acknowledgments

I would like to thank all involved in this project to make its completion of possible. I would earnestly express my special thanks to all of my supervisors: Prof. Andrzej Ordys, who gave the best support and guidance to me so that I can focus my work directly on the project. Dr. Olga Duran, who advised me on artificial intelligence strategies used in the project. Dr. Konstantin Volkov, who provided me the knowledge of thermodynamics in the development of engine simulation platform. Dr. Jiamei Deng, who shared her valuable engine control experience to improve the controller. Also thanks to all correspondent technical staff in Kingston University SEC department who spent their time on all technical supports needed in this thesis.

Finally, I would like to thank my parents, Anson and Angela and my brother Kin Wang who give me their dedicated support outside the project which had been very encouraging.

Contents

List of Figure

List of Table

Abbreviations

3D	3 Dimensional
ADC	Analogue to Digital Converter
ALU	Arithmetic Logic Unit
ANFIS	Adaptive Neuro-Fuzzy Interface System
ANN	Artificial Neural Network
BDC	Bottom Dead Centre
BMEP	Break Mean Effective Pressure
C	Carbon atom
CFD	Computation Fluid Dynamic
CI	Charge Ignition
CO	Carbon Monoxide
CO2	Carbon Dioxide
ECU	Engine Control Unit
EGR	Exhaust Gas Recirculation
EVC	Exhaust Valve Closed
FAR	Fuel-to-air Ratio
H	Hydrogen atom
H2O	Water Vapour
HCCI	Homogenous Charge Compression Ignition
ICE	Internal Combustion Engine
IVO	Intake Valve Opened
LESoft	Lotus Engine Simulation Software
LQG	Linear Quadratic Gaussian
LQR	Linear Quadratic Regulator
LTR	Loop Transfer Recovery
MAP	Manifold Absolute Pressure
MESC	MATLAB Engine Simulation Code
MIMO	Multi-Input-Multi-Output
MISO	Multi-Input-Single-Output
N	Nitrogen atom
NO	Nitrogen Monoxide
NOx	Nitrogen Oxide
O	Oxygen atom
O2	Oxygen
O3	Ozone
PCA	Principle Component Analysis
PCCI	Premixed Charge Compression Ignition
pem	Predictive Error Measurement
PM	Particulate Matter
ppm	Parts Per Million
RW	Ricardo Wave
SI	Spark Ignition
SISO	Single-Input-Single-Output
SSr	Sum of Squared Residual

SSt	Total Sum of Square
VCR	Variable Compression Ratio
TDC	Top Dead Centre
VVT	Variable Valve Timing
ZrO2	Zirconium Oxide

Chapter 1 Introduction

1.1 Introduction

This thesis proposes novel control strategies for optimal Spark-Ignition (SI) engine control when engine uses different unknown fuel compositions. The target is to find the optimal engine operating parameters aiming to keep the similar performance with different mixture where engines produce the cleanest emissions. The controller should be capable, on the one hand, of estimating the original fuel composition using the residual gas composition after combustion. On the other hand, after fuel estimation is achieved, the controller should adjust to the optimal set of engine operating parameters. This thesis contributes towards the research on control strategies able to optimise the engine operating parameters while utilising different types of fuels. The end product will provide vehicle users with more choices on purchasing the fuel with different compositions without compromising the engine performance.

The overall methodology builds a two-zone combustion model which describes mathematically the behaviour of the engine, then it utilises different Artificial Intelligence (AI) approaches for fuel identification and employs closed-loop state-space-based control strategies to provide optimal parameters.

1.2 Contents of the thesis

This thesis is organised as follow:-

Chapter 1 provides the introductory discussion of the thesis, includes the aims and objectives of the project, literature review, motivation, methodology and contributions.

Chapter 2 presents an overview of internal combustion engines (ICE). The chapter begins with the background, and then discusses the availability of electronic engine controls including the Engine Control Unit (ECU), sensors and actuators. The chapter also discusses commercial engine simulation software packages available for engine simulation studies.

Chapter 3 discusses a model for engine simulation that uses combustion theory with different sub-models. This thesis uses an in-house engine simulation model MATLAB Engine Simulation Code (MESC) and the development of this model is discussed throughout the chapter. The code estimates engine combustion process and energy conversion based on zero-dimensional thermodynamic theory.

Chapter 4 compares the engine simulation model developed in Chapter 3 with two reference software packages for the validation of MESC. Two commonly used commercial engine simulation software packages, Ricardo Wave (RW) and Lotus Engine Simulation (LESoft), are used as tools to compare the engine operation, in terms of temperature and pressure during combustion stroke. The comparisons include three steady-state tests for three engine operating parameters, which are fuel-to-air ratio, ignition timing and compression ratio. The results showed that the MESC developed provide the similar cylinder temperature and pressure envelopes.

Chapter 5 presents the development of non-linear system identification of original fuel composition, which can be used as an additional parameter in engine control. This required the artificial intelligence methodologies to model the inverse engine composition process between emission content and fuel composition. Neural network models are trained which are capable of estimating the type of fuel composition. Three compositions, Isooctane, Methanol and Ethanol are used. The virtual engine model is built up, and its control parameters, which can capture the behaviours of fuels, are identified. The neural network is aiming at finding the inverse model in order to estimate the fuel composition based on the exhaust gas composition. Two algorithms, feed-forward neural network and Adaptive Neuro-Fuzzy Interface System (ANFIS), are tested and results are compared.

Chapter 6 studies a closed-loop Multi-Input-Multi-Output (MIMO) control algorithm capable of minimising exhaust gas emission without affecting the engine performance. The control parameters use in the controller include fuel-to-air ratio, ignition time, and valve events. Three closed-loop controllers, PI controller, Nonlinear Auto-Regressive (NAR) neural network and state-space with LQR, are tested. The controller is combined with the fuel estimator developed in Chapter 5, and the performances of all controllers are investigated.

Chapter 7 is the final chapter which summarises the thesis with conclusions, and recommendations for future work.

1.3 Motivations

The growing number of vehicles running in urban areas has raised the problem of the consumption of fossil oil which is a scarce natural resource. Different fuel producers may use diverse fuel additives in fuels which may be unknown to the general public. Car fuels are usually classified into 'Gasoline' and 'Diesel'. Quality measurement is introduced to ensure smooth combustion process. The quality measurement in 'Gasoline' is counted by Octane number, and 'Diesel' is counted by Cetane number. The composition of fuels varies since fuel producers blend fuels with some other chemicals. Methanol and ethanol are commonly used alcohols to enhance the reduction of Carbon Monoxide (CO) emission [25][75][77].

The other concern is the growing number of vehicles around the world leading to the increase of the production of emissions which contaminate our world partly contributing to global warming. Authorities are concerned about the vehicle pollutions especially in urban areas. Thus they introduced legislations to lower the level of engine emission to alleviate public concern about worsening air quality [15][55]. The act gives guidelines to car manufacturers and car users to protect from engine pollution [53]. In order to optimise engine performance to meet the tightening emission limits, the approach of advanced electronic engine control is one of the alternatives to satisfy the laws.

The main challenge ahead is the control of engine emission without affecting the engine performance. The pattern of engine emission is determined by both of the fuel composition and the engine combustion process. In chemical terms, the combustion process is a chemical exchange process which involves chemical atoms found in fuel and air. Engines work in high temperature and high pressure where the energy conversion process takes place in a cylinder of small volume. The high temperature process produces a residual gas which contains portions of toxic gases, including Carbon Monoxide (CO), Nitric Oxide (NOx) and Particulate Matter (PM). They adversely affect the environment and human health. The products of such process form emissions that may be altered from different engine operating parameters and different fuel compositions.

One possibility of improvement on combustion process is to adjust the geometries of the engine cylinders. However, the geometry of the engine is fixed, and it is very hard to adjust or modify adaptively in present technologies. The improvement of the engine geometries relies on laboratory tests and research results design the geometries with the end product during manufacture. Another identified area to improve engine combustion is to adjust the fluid flow process. This can be achieved by optimising the engine operating parameters such as fuel-to-air ratio, ignition timing, valve timing, etc. The engine operating parameters concerned are in-cylinder pressure and temperature and hence the starting time of the ignition of fuel.

The other challenge in engine control is the improvement of fuel consumption. Although this is not limited by law, less fuel consumption is a pecuniary concern to vehicle drivers. Fuel consumption can be reduced by better engine design as to the approach of complete combustion. Complete combustion may mean less unwanted end products. Combustion involves Oxygen (O_2) and the end products are Carbon Dioxide (CO_2) and H_2O [15]. Modern engines are equipped with Engine Control Units (ECU) and various sensors and actuators where engines are capable of adjusting the engine operating parameters to achieve certain performance. It is noted that these requirements can lead to contradictory constraints to be satisfied by the control algorithms [56].

While mechanical engineers are making efforts to develop actuators capable of working in high pressure engine processes, control engineers are developing control algorithms in parallel to achieve better engine operation. Recent works on engine control are based on the data obtained from real engine-bed test. However, engine tests may require mechanical modifications to install the correspondent components to the engines for special needs. For example current variable valve timing (VVT) system and variable compression ratio (VCR) require a large mechanical system to operate. A more flexible way to investigate control algorithms substitutes the engine bed with computer based virtual engines which allow better observation of behaviours and relationships of engine parameter changes without any laboratory works.

This thesis proposes novel engine Multi-Input-Multi-Output (MIMO) control algorithms to be used with engines fill with blended fuel of unknown composition. Results are simulated in a computer based engine simulation code, and can be validated using the data of real engine log. The objective is to prove the possibility of using more choice of fuel to run the engine. Vehicle users could use fuels with different compositions without concerns on engine performance, while the optimised engine control should achieve the desired level of emissions and performance.

1.4 Aims and objectives

The aim of this thesis is to control an engine with the optimal engine operating parameters with an unknown fuel composition.

The objectives of this thesis are:-

a) To estimate the original fuel composition by using the exhaust gas composition obtained from the real engine.

b) To run the engine with the unknown mixture of fuel so that the lowest possible emissions in all constraints are achieved while the engine is kept in the optimal performance by developing novel control strategies.

The overview of this thesis is first to identify the parameters for the engine control. Two commercial engine simulation software packages, Ricardo Wave and Lotus Engine Simulation, are used as tools for parameter identification. Such engine simulations are off-laboratory way to observe the behaviour of emission in the variation of different engine operating parameters. Those engine simulation packages have been validated by comparing the simulated results with real engines. Once parameters are identified, an engine simulation platform based on MATLAB/Simulink has been developed, and hence underlined the minimum set of parameters needed.

The advantages of using engine simulation compared to real engine bed test are:-

1) Simulation has more flexibility in the engine operating parameter research. In real engine development, such research may require heavy demand of mechanical systems or even engine modifications which usually are not cost-effective on commercial engines. For example, if a research is on exhaust or intake valve timing control, a mechanical Variable Valve Timing (VVT) system is required to be fitted onto the normal engine. This requires the modification of the intake manifold. Another example is a cylinder pressure sensor that requires drilling holes for its installation into the cylinder.

2) Actuators for engine control may not be practically ready. Mechanical engineers are working on the possibility of camless engines. For example, to modify the valve lift profile, engine cam needs to be replaced. Camless valve can provide a pulse event which gives better control of pressure and temperature inside the engine cylinders. Camless valves are currently under development but they are not practically ready due to high pressure engine process. Simulation can go further while the valve events are generated virtually on the computer.

Once the engine simulation code is developed, the engine can be used for fuel estimation and control algorithm development. The fuel estimation can be achieved by using artificial intelligence methods, including feed-forward neural network and Adaptive Neuro-Fuzzy Interface System ANFIS. The fuel estimator provides further control to the optimal engine operating parameters.

1.5 Literature review

Engine components determine the engine operation timings. The timings of the engine operations are controlled mechanically by engine cams, whose lack of flexibility does not allow making adjustments. This thesis starts with reviewing the available engine components in order to outline the following:-

a) Understanding of the engine behaviours by varying the engine operating parameters.
b) The limitations of implementation of electronic engine systems in practice.
c) Possible solutions by replacing the mechanical system with electronic actuators.

The outlined system includes the Variable Valve Timing (VVT), the Variable Compression Ratio (VCR), the variable intake manifold length and exhaust gas recirculation systems. The literature review covers the outlined engine systems which can be found in Spark-Ignition (SI) engines and Compression-Ignition (CI) engines, and even the possible Homogenous Charge Compression Ignition (HCCI) engines and Premixed Charge Compression Ignition (PCCI) engines, with discussion on the relationship against engine performance and emissions from 1.5.2 to 1.5.15.

The second half on the literature review discusses the control algorithms implemented onto the engine and experimental works that had been done in practice. Most studies focus on the ideas of HCCI or PCCI, which involves the control of the valve timings, injection and ignition control, and exhaust gas recirculation. The emissions can be estimated and controlled through the algorithms including artificial system identifications by using ANN and fuzzy-logic controller. These are analysed in 1.5.16 and 1.5.17. In order to apply the controller to the virtual engine, engine simulation models and platforms are needed. Those are discussed in 1.5.19.

1.5.1 Engine control algorithm

Desired engine control aims to develop engines which can cover the advantages of two engine combustion processes; Spark Ignition (SI) and Compression Ignition (CI) combustion processes (see Appendix A). By comparing the advantages and disadvantages of both combustion processes, it is noted that if engines generate lower combustion temperature, the emission products in SI engines are at lower level of $CO2$ and NOx. Lower combustion temperature also makes engines more durable and cheaper to manufacture. On the other hand, CI engines are more efficient to generate high power due to higher compression ratio resulting in higher combustion temperature. CI engines are also found to have better fuel economy [16]. One limitation of SI engines is that they are unable to perform compression ignition as the material used in SI engines cannot achieve such high compression ratio. An overview written by Brijesh discussed the emission behaviours in these two combustion techniques [16]. Brijesh underlined that the challenges to achieve the new combustion techniques are the handle of the trade-off between different parameters.

The possibility of the next generation of internal combustion engines (ICE) needs new ideas of engine combustion process which utilises charge ignition using gasoline as fuel, with the aid of electronic engine control. Such combustion process is called Homogenous Charge Compression Ignition (HCCI) and Premixed Charge Compression Ignition (PCCI) (also see Appendix A). Yao et al. presented the recent trends of HCCI combustion process. They found that engine simulation tool is a good method to investigate HCCI [111]. HCCI process applied to various fuel types, and air and fuel mixing process are important to control the combustion process. PCCI studies shared similar ideas, but used the premixed charge where the air and fuel mixture are well mixed to enhance the homogenous charge to perform compression ignition [51][67].

1.5.2 Variable Valve Timing (VVT)

The period of valves opening determines the amount of air/fuel mixture entering through intake valve into the engine cylinder or exiting through exhaust valve from the engine cylinder. This determines the mixture flow rate which affects the pressure and temperature once combustion starts. The effective compression ratio is also varying from different valve timings. Studies from Walter and Ye have shown that engines perform differently at different rotational speeds and at different loads [104][114].

In engines using camshaft valve opening control, the duration of valves opening is fixed due to mechanical action of camshaft and valve lobe. Current variable valve timing systems, using in commercial engines, have limitation on the design of valve profiles. The limitation lies on dimension of lobe which is fixed in shape and the shape cannot be adjusted during the running of engine.

Two methodologies currently use in variable valve timing (VVT) control. Firstly, the 'Cam Phasing' approach uses additional gear components to shift the valve opening angle to optimal range. Secondly, the 'Cam Changing' approach is fitted more than one lobe and additional mechanical components allow the lobe shift to different valve profile according to the speed range. More detail of the systematic description in commercial VVT system will be discussed later in 2.7.5. Camshaft valve control limits the valve profile curve leads to a one-off open and close action in exhaust and intake stroke. Electronic camless valves are under research aiming at more valve timing profiles such that valves can be opened in compression stroke allowing optimal control in cylinder pressure and temperature happening in the engine operation.

1.5.3 Reaction of engine combustion using different valve timing

For reduction of engine emission using different valve timing, Walter et al. discussed about the emission of CO, NOx and particulate matter (PM) against different valve timing [104], and Kapus et al. discussed the fitting of valve timing system to improve the emission of CO_2 [66]. The principle of valve timing control acts as possible Exhaust Gas Recirculation (EGR) where part of the exhaust gas returns into the cylinder from the exhaust valve end. VVT also boost the possibility of homogenous charge mixture. Yap and Verhelst discussed the gasoline HCCI engine which used the VVT method to minimize the emission of NOx. The exhaust gas has higher pressure and temperature compared to atmospheric air, thus a certain portion of it returns to the engine cylinder to boost the initial pressure and temperature of engine cycle [92][103][112]. Walter also found that VVT reduced fuel consumption by the EGR approach which re-burned the fuel.

1.5.4 Valve overlapping

Valve overlapping happens when both intake and exhaust valves open for the same period [47]. A sketch of the valve overlapping timing against piston position of the complete engine event is shown in Figure 1 [71]. Typically, valve overlapping is performed at the period when the intake valve opens at the timing before the piston reaches the TDC in exhaust stroke (at position 1 in Figure 1); and exhaust valve closes after the piston moves beyond the TDC in the intake stroke (at position 5 in Figure 1). The advantage for valve overlapping is a continuous variable valve timing (VVT) that provides adaptive adjustment to improve engine torque delivery across different revolution range [102]. When the engine speed is high, more air is needed for higher energy combustion; therefore duration of intake valve opening needs to be longer. A portion of exhaust gas will suck back to the combustion chamber while the exhaust valve is opening, and hence increase the mixture pressure and temperature.

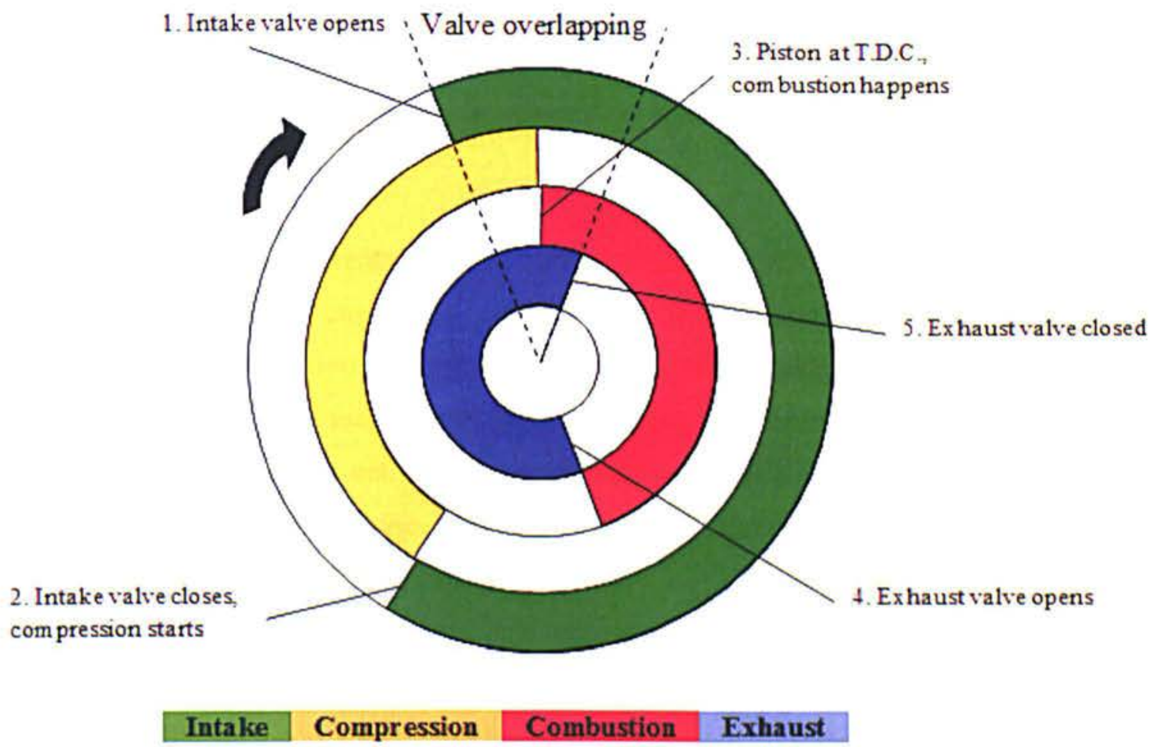

Figure 1 Valve overlapping in term of piston position [71].

1.5.5 Negative Valve Overlapping (NVO)

The other approach in VVT is Negative valve overlapping (NVO). Urushihara studied the possibility of NVO [102]. Negative valve overlapping uses the valve timing when both exhaust and intake valves close for a period of time during exhaust/intake stroke. Exhaust valve closes before piston reaches the TDC (at position 1 in Figure 1and intake valve opens after piston moves beyond the TDC (at position 5 in Figure 1). The concept is similar to the role of the exhaust valve in exhaust gas recirculation systems. When the intake valve opens, the hot residual gas heats up the fresh mixture and the high temperature mixture is enhanced for compression ignition. The results, presented in [102], showed that the injection timing is an important parameter in conjunction with NVO. The new fuel injection strategy is injecting a portion of fuel during the negative valve closing interval and injects the rest in the intake stroke that was also examined in [102].

1.5.6 Late intake valve closing on diesel engine

Another VVT approach is late intake valve closing (LIVC) which is found in diesel engine research. There are some researches investigating the performance on LIVC on diesel engines [81][86]. The idea behind LIVC is that the mixture combusts at a lower combustion temperature, and hence emissions of Nitrogen Oxide (NOx) are reduced. However, the trade-off of the approach is that the concentration of Hydrocarbons (HC) and Carbon Monoxide (CO) increases. Detailed description of exhaust gas behaviour is given in 2.5.5.1 and 5.3.

1.5.7 Valve Event Control

Valve profiles and valve events are important in the achievement of HCCI and PCCI control. Jang studied in the HCCI engines by using different valve lift and engine camshaft profiles and the effect in combustion efficiency [62]. He found that by using three different cam dimensions in the valve timing control, the engine produced the EGR effect by reducing exhaust valve profile and event. The higher exhaust valve lift is benefited in the high load condition but demerits the engine at low load. The EGR effect occurs due to the Negative Valve Overlapping (NVO) valve events where a portion of the exhaust gas is tapped and compressed before the fresh mixture enters the engine cylinder, providing boost in pressure and temperature while the engine is induced [62]. The study concluded that the fuel conversion efficiency was higher with higher exhaust valve lift rather than that with lower. The late exhaust and intake maximum opening point made the fuel conversion efficiency improve.

In the study of valve timing, Yap et al. give the overview of valve phasing control [112]. The engine sets the optimum valve timing aiming at the lowest NOx. The valve timing is then adjusted according to the performance. They discussed the effects on combustion temperature and compression ratio with valve timing variations. Results also show the reduction in NOx with optimising the exhaust valve event.

1.5.8 Variable Compression Ratio (VCR)

The compression ratio for a given internal combustion engine is almost always constant since the geometrical shapes of the engine components in the cylinders are unmodifiable. The typically values of compression ratio are ranging from 8 to 12 for spark-ignition engines, and from 12 to 24 for compression-ignition engines [55]. When compression ratio is high, the fuel and air particles are closely packed together and a higher explosive velocity during combustion is obtained, i.e. better performance and less fuel consumption. However, compression ratio is limited in two respects: 1) the material strength is limited due to maximum stress at certain pressure; 2) engine knock occurs in SI engines in combination of the compression ratio exceeding the range and fuels with incorrect value of 'Octane number' used. A study from Turner and Barclay tested variable compression ratio systems where they changed geometries of combustion chambers [13][101].

To design engines for different driving compression ratio profiles, engineers develop engines which are capable of varying the position of piston or shape of combustion chamber [8][13][69][80][101]. To achieve the optimal engine compression ratio, the geometries of engine cylinders can be adjusted by varying the geometries configuration of mechanical component by either vary the position of TDC [13] or vary the length of connecting rod to modify piston position [8][80]. The other possible VCR approach is a 'tilting' methodology where the engine cylinder is hinged to the crank case and can be tilted by a hydraulic adjuster. Different tilt angles result in different clearance volumes which give different compression ratios [34]. Although VCR technologies are practically possible, they involve heavy mechanical systems and engine modifications which are not desirable.

1.5.9 Reaction of engine combustion using different compression ratio

Debnath et.al discussed the effect of VCR using a single cylinder engine [27]. They found the implementation of VCR affects engines with reduced entropy, increased cooling water and exhaust gas flow availability, resulting in increased energy release after combustion. Shivakumar et.al estimated that different compression ratio achieved lower NOx level by using neural network estimation [98]. Drangel found that VCR approach improved on fuel economy by 30% [34]. Ye also studied the improvement on fuel economy with VCR combined with VVT on a four-cylinder engine [114]. By consideration of practical use, Ye found that the VCR method performed significantly better at light engine loading, but limited or zero improvement at heavy loading. It can be summarised that VCR technologies are far from mature. VCR systems are suitable for light loading engines, with reduction on NOx emission, better fuel economy, but they are hard to install in internal combustion engines due to the heavy mechanical components that are required to modify cylinder geometries.

1.5.10 Variable Length of intake manifold

Airflow is one of the main factors in controlling the performance of engine combustion. The pipe geometries determine the air flow, and affect the pressure and temperature of air/fuel mixture inside engine cylinders. The amount of air and the flow velocity entering the cylinders depends on its shape (circular or rectangular).

1.5.11 Reaction of engine combustion using different length of intake manifold

Ceviz et al. [18][19] tested on the variation of the length of intake manifold against the engine performance. They found the improvement on fuel consumption at high load and low speed by extending the length while low speed condition. Soares et al. studied on the variable intake manifold length engine in different intake air temperature relationship [95]. They found there was 3% difference in acceleration time at a set speed (40km/h) in a 1000m. Another study by Yan investigated the component design of intake manifolds and the reconstruction of manifold temperature without manifold modification [109]. Yan found that EGR optimised the manifold pressure and temperature. However variable length of intake manifold systems can be very hard to implement onto engines as they also involve heavy mechanical systems, which make the technology not practical for commercial use.

1.5.12 Exhaust gas recirculation

Exhaust gas recirculation (EGR) is the idea of emissions control and act as turbocharge in engines by feeding back some portion of the exhaust gas back to the cylinder. Due to current emission standard is getting tightened; engines are designed to use relatively leaner mixture for combustion [58]. The disadvantage in leaner mixture is the increase in the emissions of Carbon Monoxide (CO). EGR is one of the solutions to tackle the lean mixture problem. An additional path is installed which allows the exhaust manifold to connect to the intake manifold. Fresh air is then mixed with exhaust gas to produce rises in the initial temperature of mixture in compression stroke. The amount of exhaust gas that returns to the intake manifold is determined by ECU regarding to the level of emissions and exhaust temperature.

1.5.13 Reaction of engine combustion in exhaust gas recirculation

Studies show that the EGR heated up the intake air by feeding hot exhaust gas into intake manifold, which acts as a pre-heater to boost the initial temperature of air in the compression stroke. Ibrahim et al. studied the use of EGR in SI engines [58]. Their investigation found a significant reduction on NOx emissions by 50% where stoichiometric air/fuel mixture was used in their engine bed test. Ghazikhani and Ishida studied EGR effects in CI engines [46][59]. Ghazikhani found that EGR can reduce the engine combustion temperature while Ishida et al. found improvements in NOx-PM trade-off. NOx and PM have an inverse relationship against each other but they can both be reduced with lower combustion temperature. By summarising all studies it may be concluded that EGR affects the lower combustion temperature, leading to the reduction of toxic emissions of NOx, and PM.

1.5.14 Fuel composition mixture control

For PCCI combustion process, the main control parameter is the quality of mixture between air and fuel particles. Two studies from Hanson and Kokjohn respectively investigated the possibility of running a PCCI heavy duty engine with different blend of gasoline and diesel composition [51][67]. The studies use the engine operating parameters including injection timing, injection mass and intake valve closing timing. Results show that the methodology is able to achieve 50% thermal efficiency of the engine combustion.

1.5.15 Ignition and injection control

In the HCCI and PCCI studies, the engine bed experiments use fuel of gasoline or gasoline blended with other composition such as ethanol and methanol. With electronic engine control, engines can be fitted with a spark-plug. The ECU can make the decision on whether the engine should run in SI mode which requires a spark on, or run HCCI/PCCI mode without spark on. Gao researched camless VVT and EGR methodologies with and without spark assistance [44]. The method used a modified engine with self-developed ECU. Results show that the method is able to run HCCI processes by controlling the cylinder pressure profile and that it is able to switch modes according to the engine load. Misztal studied the particulate matter and found that the injection timing and the homogeneity of the mixture is decisive to PM level and that it lowers the variation by split injection [78].

1.5.16 Engine control systems

Bosch GmbH developed a SI engine control system called 'Motronic' fitted with emission sensors and a single ECU to control electronic fuel injection and electronic ignition [15]. Motronic used both open-loop and closed-loop control algorithms. The objectives were to reduce engine emissions, reduce fuel consumption and improve engine performance, driving comfort and driving safety. Engine control strategies, included idle speed control, emission control by using EGR and second-air system, camshaft control for operating timing, and component protection such as anti-engine knocking control, provided the advantages on electronic control compared to mechanical engine system.

The other single system called 'Jetronic' is a single system for fuel injection control [15]. Fuel injection is essential to engine control to comply with the emission regulations [55]. Bendix produced the first commercial fuel injection control system [55]. Various sensors are fitted in the air path to monitor the condition of the air path, such as throttle; and control the fuel path, such as the electronic fuel injector [15]. Fuel injection system can be operated as single point injection or multi point injection depends on the system chosen.

1.5.17 System identification algorithm

Engine emissions are considered to have non-linear relationships against engine operating parameters, therefore it is impossible to obtain the transfer function for the controller. The emission compositions can by estimated by using system identification method [35].

- Artificial neural network

One outlined method for system identification is the artificial neural network [52][72][87][113][118]. Such estimation can be optimised by using additional gain in the closed-loop controller. Atkinson developed the neural network based engine control in order to reduce NOx and PM emissions [11]. Arsie studied on the recurrent neural network which is able to estimate NOx in transient SI engine cycle [9]. He estimated NOx with an error of less than 2% in given transient engine cycle. Deng developed the regressive artificial neural network able to model the estimation of emission in Particulate Matter (PM) using CI engines [30]. They also studied the methodologies by using Principle Component Analysis (PCA) and observed the power spectral density to minimize the number of data needed to train the neural network models while accuracy had no significant drops [31].

- State-space model

The other system identification method is the state-space approach [65]. The dynamics of the system may be represented by a set of n^{th} order differential equations in the vector valued state. State-space can be controlled by using state-feedback controller by designing the feedback gain. One problem in the development of state-space in multi variable systems is order number in the differential equations that can be high, hence producing a complex controller. Zolotas et al. presented the MISO robust controller in a non-linear oscillatory system. They were able to reduce the number of order by using Linear Quadric Gaussian (LQG) control [119], in addition the Loop Transfer Recovery (LTR) was used improve the effect of unknown disturbances. Jaimoukha proposed model reduction in linear parameter-varying systems [60], by using the synthesis Riccati inequalities to define appropriate Gramians. It can be useful in engine control providing that the system is linearized using state-space.

1.5.18 Emission control algorithms

In combination of the emission estimation, various studies used PID [36][42] and fuzzy logic as the closed-loop control. Zhang studied on the artificial neural network emission estimation combined with closed-loop fuzzy-PID control [115]. The results of Zhang showed the reduction in emissions included the composition of NOx. Ghaffari used the fuzzy-PID control algorithm to tune the fuel-to-air ratio [45]. The results showed that the controller was able to match the actual response of the specifications.

1.5.19 Engine simulations

The engine simulations can be generated by 'simple' approach using zero/one dimensional estimations or by 'detailed' approach using three dimensional (3D) estimations. For 'simple' approaches, the engine performance can be calculated by using zero or one dimensional sub-models based on thermo-dynamic theories. Two common commercial engine simulation software packages, Ricardo Wave [91] and Lotus Engine Simulation [71], and two studies from Ferguson [39] and Ohyana [83] generated engine simulations using this approach. The 'detailed' approach uses the detail description of Computation Fluid-Dynamic (CFD). CFD simulations contain 3D meshes which describe the behaviours of particles movement in consideration of all directions, and has been widely used in fire frame spread in safety studies [28][29] and the turbulence studies [33]. The 'detailed' engine simulations are aimed for studies in designing the geometries of engine components rather than engine performance control simulations. Three commercial software packages, AVL fire [12], Ricardo Wave3D [91] and GT-Power [110] use 'detailed' approaches for engine simulations.

1.5.20 Sub-models of engine simulations

The sub-model used in the commercial engine simulation packages covered the heat transfer, heat release with the combustion model, piston motions and gas exchanges. Woschni developed the heat transfer model [107] which is commonly used nowadays. The heat release model, also can be called combustion model, estimated the mass fraction burned and can be represented by the Wiebe model [39]. However the emission estimation may not be included in every software packages. Ricardo Wave [91] package included the emission sub-models which covered the level of Carbon Monoxide (CO), Nitric Oxide (NO_2) and Particulate Matter (PM).

1.6 Methodology of the thesis

The engine control can be divided into three parts, the engine simulation model, fuel estimation system and engine control system.

1.6.1 Engine simulation model

This thesis develops the virtual SI engine simulation using the 'simple' approach based on the first law of thermo-dynamic. Various sub-models are used to generate the estimations in heat release, heat transfer and gas exchange process. The engine simulation is able to calculate the engine performance of four-stroke medium size engine, and return the emission compositions of CO_2, O_2, CO and NOx, and exhaust gas temperature. The developed model is validated by comparing the calculations with the reference models. Three models are used as reference tools, including two commercial engine simulation packages, Ricardo Wave and Lotus Engine Simulation, and a book from Ferguson [39] who developed an in-house engine simulation. The comparisons are made based on the parameters affecting the combustion performance, including the peak pressure timing and peak temperature timing during combustion stroke.

1.6.2 Fuel estimation system

The engine may tolerate different compositions of blended fuel. Different compositions in engines are valid by matching the standard of 'Octane number'. The 'Octane number' is the value to ensure fuel injected into engines is able to avoid the resulting incorrect portion of mixture. Engines cannot operate or combustion happens at the wrong moment, hence affecting emission and performance control. The typical value of 'Octane number' should be in the range of 0.93 to 1.

The original fuel composition can be estimated by using Artificial Neural Network (ANN) using the concept of modelling the inverse behaviour of combustion process. To collect the dataset to train the neural network, sampling engine tests are needed. Therefore the tests are run on the given engine cycles which should be able to cover most of the behaviours that can be found in different condition of the engine, including different fuel-to-air ratio, different ignition timing, different valve events, and different speeds. During the engine cycle testes, past information of exhaust products, including the level of Carbon Dioxide (CO_2), Oxygen (O_2), Carbon Monoxide (CO), Nitric Oxide (NOx) and exhaust temperature, are recorded for the dataset. Two ANN algorithms, feed-forward ANN and Adaptive Neuro-Fuzzy Interface System (ANFIS), are used for fuel estimation and results are compared.

1.6.3 Engine control system

The engine operation parameters can be updated by the Engine Control Unit (ECU) where the computer optimises the fuel-to-air ratio; ignition timing and valves event are investigated by the emission composition. The controller is built as Multi-Input-Multi-Output (MIMO) system. The number of inputs needed for the controller is investigated. The behaviour of engine combustion is considered as a non-linear behaviour [64]. System identification method, such as state-space and neural network is used and parameters can be optimised by a closed-loop control.

1.7 Contributions

The contributions of this thesis are outlined as follows:-

- Artificial Intelligence (AI)

Fuel estimation current SI engine combustion studies are focused on the design geometries of the engine [74], which ignore the fact that the minor effects of fuel composition in 'Gasoline' can be different for each fuel producer. The thesis studies an AI fuel estimation method, which is able to provide additional control according to the exhaust gas behaviours. The fuel estimator captures the inverse engine process and estimates the original fuel composition and hence feeds gains to controllers for individual components according to the composition of blended fuel.

- Control algorithms

Engine control is the trend of future engine development. This requires innovative ideas covering possible engine variables in different conditions, such as different fuel compositions, different speed and torque. This thesis investigates on novel engine control algorithms aiming to minimise engine emissions while maintaining the performance for engines with different unknown compositions. The controller uses exhaust gases including CO_2, O_2, CO and NOx to return the single engine control variable in the development of Multi-Input-Multi-Output (MIMO) systems. The controller is simulated on the virtual engine which has also been developed in this thesis. Results and performances are being compared. Recommendation of the most suitable controller is discussed.

- Development of engine simulation model

The advantage of using engine simulation was discussed in 1.4, which concluded that electronic engine control requires the modification of engine with high costs involved. This thesis develops the virtual engine in such a way that it facilitates its use for control research purposes.

1.8 Conclusions

The introduction chapter discussed the detail of the ideas and the setup of this thesis. The literature review analyses current engine control systems and methodologies of modelling such systems in practice. This included the availability of engine sensors and actuators which are able to monitor and control engine combustion process respectively. The literature reviews also covered different control techniques, such as variable valve timing (VVT), variable compression ratio (VCR), variable length of intake manifold and exhaust gas recirculation (EGR) system. The possibilities of developing those techniques are discussed. This can be concluded that both VCR and variable length of intake manifold systems required large mechanical components in order to control and will not be considered in this thesis. This chapter is also discussed the methodologies of this thesis which are outlined as follows:-

1) An engine simulation method is needed to develop. The engine simulation returns the level of emission and exhaust temperature with different engine operating parameters
2) A fuel estimator is going to develop, enable an additional parameter in engine control. It can also able to find probability distribution of given fuels, namely Isooctane, Methanol and Ethanol, while the mixture of fuel is unknown.
3) The novel Multi-Input-Multi-Output (MIMO) controller aims to optimise engine combustion performance.

Chapter 2 Working processes in ICEs and their control

This chapter gives an overview of engine control systems. An understanding of the form of emissions and their behaviours is required in order to identify the control parameters which control the emissions while achieving maximum performance. Emissions can be divided into toxic and non-toxic categories. The cause and behaviours of the emissions depend on the combustion performance. To improve the existing internal combustion engine, the mechanical components of the engine are to be replaced by computer controllable components. This chapter also studies the background of the sensors and actuators which draw the possibility of achieving camless engines where the engine is completely controlled by electronic elements.

2.1 Introduction

The internal combustion engine (ICE) performs energy transfer from combustion power into kinetic energy. The main components of the internal combustion engine consist of the combustion chamber (which can be referred as to engine cylinder due to its shape), a piston and a crank. The concept of ICE can be described as follows: - By considering the ICE as a volumetric pump, air and fuel particles mix together and pack inside a limited volume of the combustion chamber. The movement of the piston then reduces the cylinder volume and compresses the air/fuel mixture to higher pressure and temperature. As air contains oxygen which acts as a reactor, the mixture reacts once it reaches the ignition temperature either using a spark or possibly self-ignition through compression. The mixture reacts and the resultant expansion of the mixture propagates throughout the space in the chamber and hence applies force to push the piston in the downward direction. As the volume increases, the pressure and temperature drop. The piston connects to a crank, and converts the motion mechanically to angular motion to complete the energy transfer. A detail description of different engine combustion processes is discussed in Appendix A.

2.2 Internal combustion engine history in brief

Before the use of the internal combustion engine in vehicles, engines existed in various applications on heavy works. The power generated in engines is massive which humans and animals cannot achieve. In the 1860s, the internal combustion engine was practically invented and built for commercial use [54]. The first internal combustion engine available in the market was developed by J.J. Etienne Lenoir. He used the idea of a cylinder, a piston and a crank, and the burned coal-gas-air mixture was injected into a cylinder and mixture was ignited by a spark. This drew the first shape of an internal combustion engine. Although this was a good start, the efficiency was low at best about 5%.

A later idea from Nicolaus A. Otto in 1876 developed a more successful engine. Otto introduced the idea where one engine cycle worked on four-strokes, hence generated power in every 720° of crank angle. Air and fuel mixed before entering into the cylinder and produced a homogeneous charge mixture. The mixture entered into the cylinder and was compressed. The mixture ignited by a spark, hence called Spark-Ignition (SI) process. The combustion transfers the power large enough for four strokes piston movements. This was a further improvement of the prototype shape of engine commonly used in vehicle in the past one hundred years.

In 1892, Rudolf Diesel developed a new type of internal combustion engine. The new feature of Diesel's idea was that the ignition was not started by a spark. Air entered into the cylinder and was compressed to higher pressure and temperature. Diesel was injecting a liquid fuel, with a lower boiling point, to ignite the combustion. This new type of engine resulted in doubling the efficiency and a higher expansion ratio, without the effect of engine knocking. The combustion process was called the Compression-Ignition (CI) process. Diesel invented an alternative idea which was also commonly used in vehicle in the past one hundred years. The fuel that he used was named as Diesel for his contribution [54].

2.3 Overview of engine control

To control an engine, a micro-processor is fitted onto the car. The micro-processor is called the Engine Control Unit (ECU). It is an electronic device which takes information from engine sensors and provides algorithms to control the actuators which give the optimal parameters to perform efficient combustion. It also aims to provide cleaner exhaust gas, better fuel economy and better engine performance [55].

2.3.1 Types of controller

The type of controller can be divided into two types, open-loop control and closed-loop control:-

2.3.1.1 Open-loop system

In an open-loop system, a control criterion is sent to the main system and computes the output. The block diagram of an open-loop system is shown in Figure 2. The open-loop system usually stores past experimental data in the program and controls the system through a look-up table or a network. It is not capable of optimizing performance when the condition, which is not included in the dataset, has changed.

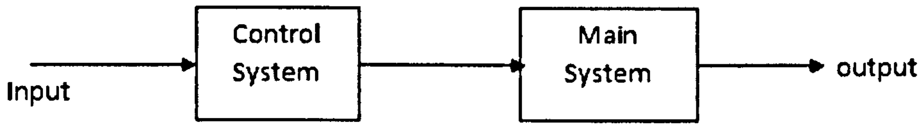

Figure 2 Block diagram of an open-loop control system

Engine control algorithms considered as open-loop system include the use of look-up tables and system identification methodologies. The engine data is collected from engine tests in the laboratories where the data recorded is able to cover a wide range of engine behaviours, such as different speeds and loads, by using engine cycles. This dataset can be used as a set of reference parameters in the look-up tables, or can be trained for system identification. System identification can be achieved by artificial feed-forward neural networks, which use neurons to update weights between parameters or state-space, whose weights are updated by state changes.

2.3.1.2 Closed-loop system

A closed-loop system uses the output of the plant (i.e. SI engine in this thesis) to compensate the new set of parameters and the control settings by feedback signals. Figure 3 shows the block-diagram of a closed-loop system. There is an output comparator which corrects the setting when the criteria meet the threshold.

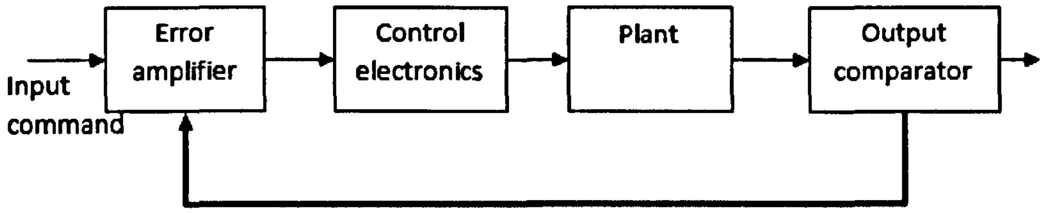

Figure 3 Block diagram of a closed-loop control system [55]

The closed-loop control algorithms which are used in engine control include PID, fuzzy logic and regressive neural network controllers. PID algorithm is the most commonly used closed-loop control algorithm. The disadvantage of using PID in engine control is that the PID approach cannot return the fast enough response in the situation of the rapid changes in engine behaviours, while the speed, engine load and other factors such as resistance force and frictions etc. vary arbitrarily in function of time. Faster controller is needed and fuzzy logic and ANN based nonlinear auto regressive (NAR) are used in engine control provides faster control in closed-loop algorithm where the results of real-time engine information are used as feedback.

2.4 Engine Control Unit (ECU)

Engine control units (ECU) compute units which give digital control to adjust the mechanical part of the engine when needed. The ECU consists of an arithmetic logic unit (ALU) which communicates with long and short term storage of data embedded in the system. Engineers can program and store in programmable EPROM, which is able to make changes of the program with flash memory for data manipulation. The computer calculates the adjustment in real-time to optimize the combustion parameters. The operating parameters include fuel-to-air ratio, ignition timing (SI engine only), or injection timing, intake and exhaust valve timing and event and other parameters which the internal combustion engine needs to keep running [15]. The aim of engine control is to increase the efficiency and control the emission to minimum. Various sensors are installed onto the engine to monitor the combustion process. The microprocessor collects information of engine combustion product. The signals are converted into digital format through analogue to digital converter (ADC). The converted digital signals are sent to the program. Overviews of commonly used sensors and actuators are shown in Figure 4.

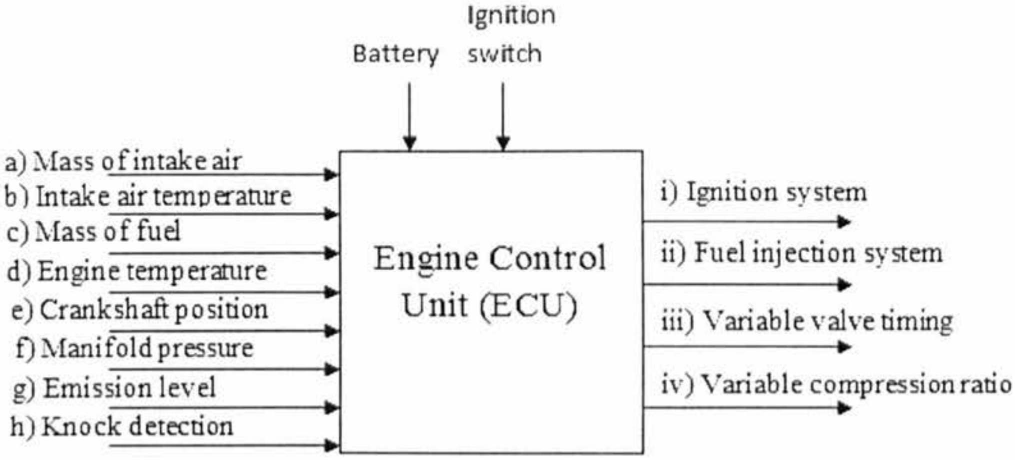

Figure 4 Electronic Control Unit and few available sensors and actuators examples

Some sensors that connect to the ECU, as shown in Figure 5, use open-loop control strategies including air-flow sensor, air temperature sensor and throttle position sensor. In open-loop configuration, the ECU adjusts the engine parameters according to the sensor outputs with the help of past dataset information. Some other sensors, such as lambda sensors, engine temperature sensors or knock sensors, shown in Figure 5, use the closed-loop control configuration. The engine parameters, such as the ignition timing and fuel-to-air ratio, are then continuously optimised according to the feedback of the respective sensors.

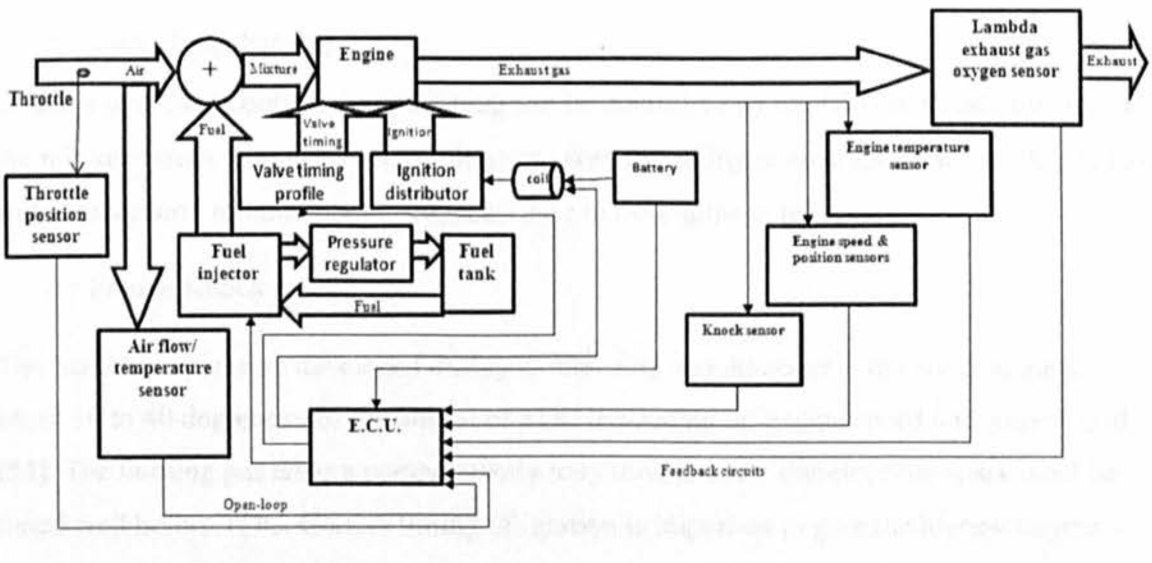

Figure 5 Block diagram of an engine control system.

In order to develop the suitable controls strategies, engine simulation has been a valuable tool to predict and optimise key parameters in the engine control system. Engine simulation allows flexible and low cost development of control algorithms without the need for an engine bed, or modification of engines by installing the needed components. Once the algorithm has been developed and tested, it may be installed into the ECU.

2.5 Operating parameters against engine performance

The performance of ICEs depends on several geometric and thermodynamic parameters. The volume of the combustion chamber is calculated from the dimension of the cylinder. The cylinder is assumed to have a fixed bore size and a stroke length. When the piston is moving, the volume is calculated according to crank-slider model which depends on the connecting rod length as a function of crank angle. The piston movement is also a factor that estimates heat transfer, blow-by losses and energy losses due to friction. The combustion performance is treated using thermodynamic calculations with heat release sub-models.

2.5.1 Intake manifold length and volume

The geometry of intake manifold affects the flow of air/fuel mixture. The intake manifold length can be varied in some engines using adjustable mechanical parts [18][19]. The dimension of the length affects the mixture turbulence inside the combustion chamber, and hence affects pressure and the burning velocity duration.

2.5.2 Start of combustion

In terms of engine control, the spark plug can be controlled by the ECU to decide the timing the mixture needs to ignite by spark. It gives more flexibility to an engine with spark ignition and compression ignition combined, according to the engine condition.

- Engine Knock

The maximum pressure developed during combustion should occur at the crank angle at about 10 to 40 degrees prior the arrival of TDC depending on engine speed and engine load [54]. The burning gas takes a comparatively long time to burn; therefore the spark must be timed well before TDC. Correct timing of ignition is important to give the highest engine power without knocking. If the timing of spark happens too early, a rapid burning leaded to engine knocks; conversely a late spark causes slow burning and produces low engine power and poor fuel economy. The optimal moment of ignition is a function of several variables, such as the engine speed and the engine load.

- Auto-Ignition

Another factor that should be avoided in the engine design is auto-ignition. This happens when the mixture reaches auto-ignition temperature and ignites in the random part of combustion chamber. While spark plug ignites, auto-ignition causes more than one frame envelope generate in the combustion chamber. Resulting in the needed energy does not locate in the desired position to push the piston, hence produces poor engine performance or even damages the engine. Different fuel compositions have their auto-ignition temperatures, for example, gasoline's is 540 °C and for diesel fuel is 260 °C.

2.5.3 Valve timing and valve lift

Valves in the cylinder determine the amount of gas entering (intake valve) or exiting (exhaust valve) the combustion chamber. Valve events have effect on the fluid flow inside the cylinder; hence affect cylinder pressure and temperature distribution. The reason of changes in fluid flow is due to the pressure and temperature differences between the working engine and atmosphere. The optimal valve timing also optimises the reduction on effective compression ratio [2][5][64][68][96] and improves the benefit of Exhaust Gas Recirculation (EGR) [104][111][112].

Valve events are controlled mechanically by the engine cam and the lobe which pushes the valve to open. Due to the geometry of the valve components, the valves have fixed valve lift event and timing. However the valves events can possibly be optimised at high cost, by fitting a heavy mechanical control component to add a few more profiles.

2.5.4 Exhaust gas recirculation

Engine emission can be reduced by the methodology of Exhaust Gas Recirculation (EGR). EGR is based on the idea of feeding back a portion of the exhaust gas back to the cylinder for re-burning. The block diagram of EGR is shown in Figure 6. EGR provides a boost effect on the starting temperature and pressure at the intake stroke. The fresh mixture at its atmosphere pressure and temperature mixes with exhaust gas at its exhaust gas pressure and temperature, in which the averaged pressure and temperature of the mixture is boosted. EGR also provides a 're-burn' process for any un-burned fuel and Oxygen left in the previous cycle.

EGR system connects to the exhaust manifold to the position in conjunction with the throttle. Fresh air is mixed with exhaust gas through the throttle and consequently the temperature of the gas rises. The amount of EGR is controlled by ECU. Temperature of air is heated up by exhaust gas, which acts as a pre-heater before entering the combustion chamber at low speed.

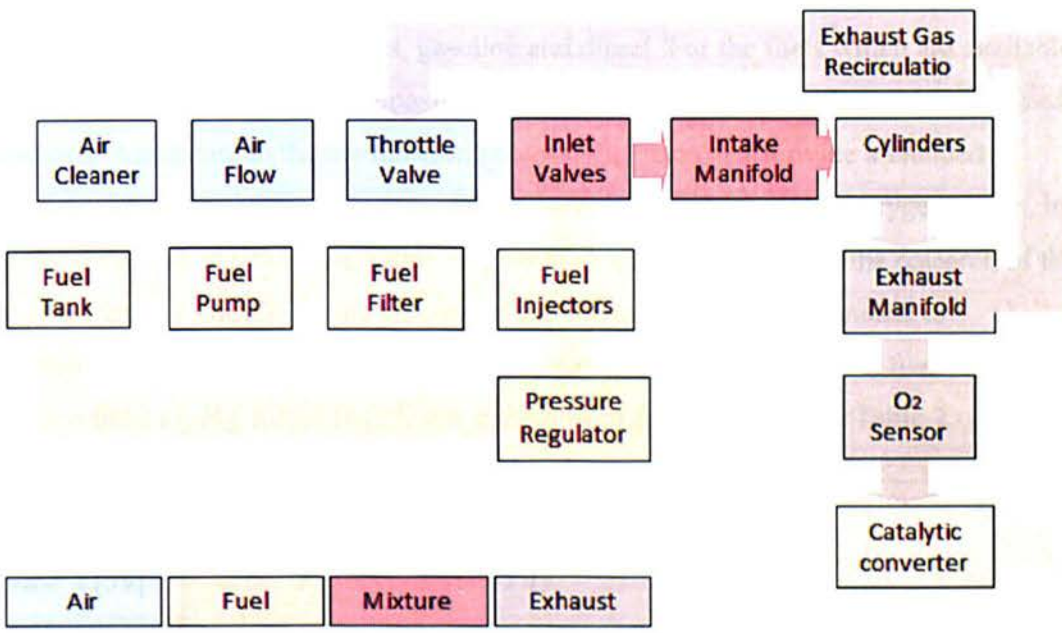

Figure 6 Air and fuel flow in ICE.

2.5.5 Composition of air and fuel

- Air

An engine acts as a gas exchanger. Engines take air at the atmosphere condition. Dry air consists of roughly 79% of nitrogen and 21% of oxygen. More detailed compositions of dry air with the common species are shown in Table 1.

Gas	ppm by volume	Molecular weight	Mole fraction	Molar ratio
Oxygen	209500	31.998	0.2095	1
Nitrogen	780900	28.012	0.7905	3.773
Argon	9300	38.948	NIL	NIL

Carbon dioxide	300	40.009	NIL	NIL
Air	1000000	28.962	1.000	4.773

Table 1 Principle constituents of dry air [54]

- Fuel

Fuels can be divided in two categories, gasoline and diesel. For the fuels which are available for commercial vehicle uses, the composition of fuel form in a compound contains atoms of hydrocarbons. According to the combustion process, fuel suppliers provide a blended composition with alcohol type substances which includes small amount of oxygen atoms, in helping the reduction of CO in emissions. Within such composite mixture the research of the fuel suppliers ensure smooth engine process within the range. Gasoline consists of hydrocarbon with 4 to 12 carbon atoms per molecular in the mix [17]. Diesel fuel consists of hydrocarbon from $C_{10}H_{20}$ to C_{20} H_{28}. A few examples of fuels are listed in Table 2.

Fuel	C	H	O	N
Gasoline_f [39]	7	17	0	C7-H17
Gasoline_h1 [54]	8.26	15.5	0	C8.26-H15.5
Gasoline_h2 [54]	7.76	13.1	0	$C_{7.76}$-$H_{13.1}$
Diesel_f [54]	14.4	24.9	0	$C_{14.4}$-$H_{24.9}$
Diesel_h [54]	10.8	18.7	0	$C_{10.8}$-$H_{18.7}$

Table 2 Examples of fuel composition used in different combustion processes

2.5.5.1 <u>Complete and incomplete combustion</u>

Ideal complete combustion happens without any secondary reactions. The product of the complete combustion of hydrocarbons would contain only Water Vapour (H_2O) and Carbon Dioxide (CO_2) without the unwanted by-products. In reality, it is not possible to achieve the complete combustion in continuous engine process since there will be minority of other species presents in the mixture. The combustion condition cannot be kept constant all the time. Therefore in real situations, exhaust gas would form combustion by-products.

Bosch [15] explained other unwanted species available during combustion while the combustion is not ideal. Fuels consist of the compound of hydrocarbons. After the combustion, any unburned hydrocarbons (HC) left in the exhaust gas are considered as unwanted species. The partially burned hydrocarbons react with oxide that produces unwanted species of combustion such as Carbon Monoxide (CO), Aldehydes (CH.CHO), Ketones (CH.CO), Carboxylic Acids (CH.COOH), etc.

The other important factor of incomplete combustion is the combustion temperature. High temperature combustion generates emissions contain Carbon Monoxide (CO), Nitrogen (N), Carbon (C), Nitrogen Oxide (NO/NOx), etc. Diesel engines works in higher temperature combustion compared to gasoline engines, therefore NOx emission control is focused more in diesel engine studies although smaller amount of NOx can be found in gasoline engine.

Combustion by products can be divided into a) non-toxic emissions which have not many negative effects to environment and b) toxic emissions, which are to be controlled as lowest as possible. Detailed discussion is presented in the next sections.

2.5.5.2 Non-toxic emissions

- Oxygen (O_2)

Oxygen (O_2) is a natural component which is presents in the atmosphere as intake air (Table 1). Any unburned oxygen will be emitted as oxygen compounds. Oxygen level in the exhaust gas can be treated as a measure of the mixture quantity in fuel-to-air ratio. The level of oxygen can be obtained from a lambda sensor (refers to 2.6.5) and the measurement of Oxygen is typically in terms of mass fraction (% by volume).

- Carbon Dioxide (CO_2)

Carbon Dioxide (CO_2) can be found through human activity or reaction between an oxide and Carbon (C). Although CO_2 is naturally presented in the atmosphere (Table 1), it is treated as waste gas. It is considered as one of the causes in the greenhouse effect. Authorities concern of the growth of the number of automobiles and target the level of CO_2 emissions are needed to control in vehicles. The measurement of CO_2 is typically in terms of mass fraction (% by volume). Statistic in 1995 found the atmosphere has increased by approximate 20% since 1920 [15].

- Water Vapour (H_2O)

Water vapour (H_2O) can be found in the engine emission after the reaction of hydrogen and oxygen. It is a natural resource on the Earth with no harm to human nor the environment. No measurement is necessary in engine emissions.

- Nitrogen (N_2)

Nitrogen (N_2) is a natural component which presents in the atmosphere. It is a natural gas and not consider as toxic. Any unused nitrogen during engine combustion will be emitted as nitrogen compound. No measurement is necessary in engine emissions.

2.5.5.3 Toxic-emissions

- Carbon Monoxide (CO)

Carbon Monoxide (CO) can be found in the partially burned engine combustion. If the distribution of the fuel-to-air ratio is unequal [53], Carbon Monoxide is formed with the reaction of carbon and oxygen. It is a colourless, odourless and tasteless gas. Carbon Monoxide is harmful to human and can cause death even with small concentration in a short moment [15]. The measurement of CO is typically in terms of mass fraction (% of volume).

- Nitrogen Oxide (NOx)

The term NOx refers to together with Nitrogen Monoxide (NO) and Nitrogen Dioxide (NO_2). Both NO and NO_2 are the product of the reaction after Nitrogen (N) and Oxygen (O) in high temperature combustion process. Engines aim to design as highest compression ratio as possible, leading to the higher frame speed and work in higher temperature [55], and hence level of NOx becomes more significant. NOx is harmful to human health and has negative effects on environment, i.e. acid rain to forest [15][74]. The measurement of NOx is typically in terms of Parts per Million (ppm).

- Hydrocarbon (HC)

Hydrocarbon is the compound of the fuel or the by-product of Hydrogen and Carbon, therefore this can be divided into two form of HC emission:-

One form of the HC is any unused HC is emitted as exhaust gas. There are two reasons of HC atom left unused. Firstly it happens when the frame speed is slow, resulted in not all the HC atoms are burnt during the short duration of combustion [54]. Secondly the incorrect amount of fuel-to-air ratio use in fuel air/fuel mixture, resulted in HC atoms are not fully burnt while all air is reacted with HC.

The other form of HC is happen as the by-product of combustion reaction between Hydrogen and Carbon. In this case, HC presents in various forms [15], alkanes, alkenes, alkines, cyclic aromatic, namelybenzene, toluene, and polycyclic hydrocarbons. Most of hydrocarbons have no harm on human, but some hydrocarbons are considered as cancer causing [53].

- Particulates Matter (PM)

Particulates in the form of particulates matter occurs during an incomplete combustion [6]. They can be found in diesel engine. Particulates matter consists of tiny particles of unburned Carbon (can be referred as soot), or a small portion of PM is form of burned HC, works in high temperature combustion and being cooling and forms in the expansion stroke. PM considers as toxic emission and cause health hazard to human [53]. The measurement of PM is typically in terms of Parts per Million (ppm).

- Ozone (O_3)

Ozone is the production of Oxygen. It has the compound of three Oxygen (O) atoms. However, ozone is a toxic emission, which is harmful to human [15].

2.5.6 Combustion chamber design

One of the study areas in engine emission reduction is the combustion chamber design. It is the main factor of the frame propagation speed in cylinder and has effect on the combustion quality. If mixture burns too fast, exhaust gas found higher level of NOx. But when the mixture burns too slow, this produces higher level of HC [55]. The geometries of the engine are fixed. The combustion chamber design is based on laboratory works so it is almost impossible to use electronic control to modify the shape in real-time.

2.5.7 After treatment system

The emissions reduction of modern passenger vehicles relies on the after-treatment system. Vehicles fit with catalytic converter in the exhaust pipe decompose engine emissions, i.e. re-burn the exhaust gas to perform the second reaction to reduce CO, NOx and HC [55]. It is the post-combustion process for the exhaust gas based the decomposition method of the chemical reaction, but no engine parameters optimization is involved.

2.5.8 Fuel-to-air ratio control

The exhaust gas composition is highly influenced by the distribution of fuel-to-air ratio. Heisler and Ferguson discussed the behaviour of the emission with different fuel-to-air ratio [39][53]. The minimum Hydrocarbon (HC) is found at the ratio slightly richer than stoichiometric but maximum level found at the ratio went to more extreme to leaner or richer. However, the level of Nitric Oxide (NOx) found in exhaust gas trend to have opposite relationship against HC. The highest level of NOx happens when the HC level is about the lowest, and level of NOx decreases with the ratio went to extreme to leaner or richer. The lowest Carbon Monoxide (CO) level happens when the mixture is rich, and increases when the mixture becomes richer.

2.5.9 Combustion temperature control

The combustion temperature is possibly controlled by the engine ignition timing and valve timing. Ignition timing holds the key of the peak temperature happens at the optimal piston position, and the valve timing holds the key of the peak pressure during compression stroke. Combustion at higher temperature produces higher level of NOx, and hence exhaust compositions vary with those two engine operating parameters.

2.6 Engine sensors

Engines performance is different under different speed and engine loads. Old-type engines are operated by mechanical components which are controlled by crankshaft. There is no flexibility of making adjustment to mechanical components. The engine operating parameter design, such as ignition timing and valve timing, are calibrated on crankshaft experimentally. The main advantage to computer engine control is that engine parts will have tears and wears after operates at high speed at long period which affect performance. To overcome those problems, vehicles fit with various sensors to monitor the engine condition in real-time. The microcomputer adjusts engine performing parameters through control algorithms and controls the appropriate actuators. Some actuators can be detached from cam tear and wear free to operate engines.

2.6.1 Intake air mass and temperature sensor

The amount of air entering the cylinder has big influence on the performance combustion and emission. The flow rate affects the fuel-to-air ratio and the pressure in the cylinders. The engine speed is determined by the manifold pressure [49]. Therefore, the amount of air drawn into the engine is a measurement of the engine loading condition. An intake air mass sensor is positioned at the entrance of the air pipe and measure the air flow and temperature. There are two types of intake air mass sensors, flap-type air-flow meter and hot-wired air-flow meter:-

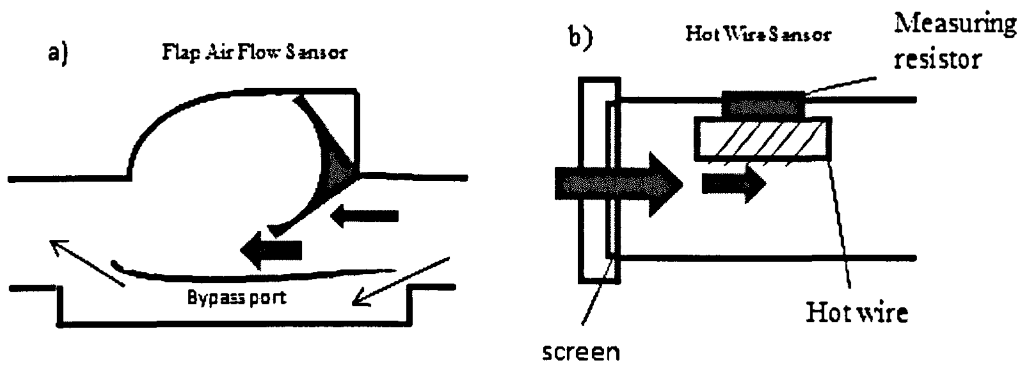

Figure 7a) Left picture, diagram of Flap-type air-flow meter, b) right picture, Hot-wired air-flow meter [55][56]

- Flap-type air-flow meter

The systematic diagram of a flap type air flow sensor showed in Figure 7a. The sensor records the flow rate by measuring the angle of deflection of a flap. Air passes the entrance and flow into the sensor. As the air speed or density increased, the force acting on the flap also increases. The air current produce a force pushes the flap and this opposing force counteract the return spring. The angular position of the flap is determined by the potentiometer measures in voltage, the calibration of which is such that the relationship between the air throughput and the voltage output is inversely proportional.

- Hot-wired air-flow meter

The hot wire air mass meters, shown in Figure 7b, rely on the cooling effect of air as it passes over a heated wire. Due to the difference of atmospheric air temperature and heated wire temperature the sensor temperature fell as air flow increased. The cooling effect on the wire changes its resistance. The measurement of this changes and determines the amount of air flowing into the engine. It can also record the air temperature and act as an intake air temperature sensor.

2.6.2 Manifold absolute pressure (MAP) sensor

Intake manifold locates between throttle and cylinder. It is the path of air in the engine. The cylinder pressure is proportional to the manifold pressure since the manifold pressure can be considered as initial pressure of mixture before entering into cylinder. Reflecting on the mixture turbine inside manifold, in the situation when throttle is wide open, the intake manifold is usually at ambient atmospheric pressure. In other situations, when throttle is partially closed, cylinder does not have enough air, therefore manifold become vacuum and cylinder pressure drops. The dimensions and geometries of intake manifold are factor of engine performance. Length and curve has to be as match as possible for different cylinders to match combustion.

Measurement of the amount of air entering the engine can be determined by utilising a manifold absolute pressure sensor. The engine load determines the air pressure within the manifold. The manifold absolute pressure sensor can either be located within the ECU or mounted remotely on the engine (usually on the inlet manifold). In the cases of MAP sensors are located within the ECU; they are connected to the inlet manifold via a small bore hose. The manifold absolute pressure sensor converts the relative air pressure within the inlet manifold into an electrical signal. The ECU interprets the signal and deduces the quantity of air entering the engine.

2.6.3 Crankshaft position sensor

Crankshaft is the disc which transfers the piston energy into engine torque. It connects to the piston through a connector, and connects to the wheel through gears and axle. Therefore it holds information of the piston position and engine speed. Crankshaft collects the position in degree and sent to the ECU with an input signal. ECU uses the information in combinations with ignition system and fuel injection to determine the timing of ignition and the amount of fuel needed. It is typically use Hall Effect sensor to measure the position of the valves and signal is sent to ECU for reference.

It should be noted that the ECU cannot determine the exact position of the engine within its four stroke cycle from the crankshaft position sensor alone. The camshaft position sensor must also be referenced to provide sufficient data for ignition control and sequential injection.

2.6.4 Camshaft position sensor

Camshaft of a vehicle is used in conjunction with crankshaft. The main function of camshaft is to covert the rotational force of crankshaft into a linear motion to active the intake valve, exhaust valve and mechanical ignition system. The open timing of the valve is proportional to the piston position. The duration of the open valve is determined by the size of the cam lobe, which has a fixed geometry and only able to optimise the timing with a large mechanical system (refers to 2.7.5). Camshaft sensors are similar to crankshaft sensors where typically use Hall Effect sensor to determine their position.

2.6.5 Oxygen (Lambda) sensor

Oxygen sensors, usually refer to Lambda sensors, are the sensors which records the value of oxygen level in exhaust gas. In the prefect case, oxygen is expected to burn completely with fuel. However during the fast engine process, there will be certain level of oxygen left unburned and exhausted. Oxygen is an oxide which is the resource of burning. During the engine combustion, a minimum amount of oxygen is needed to maintain a long enough duration of combustion for the desired power, especially while accelerating. However if the mixture is leaner than needed, there will be an amount of oxygen left unburned and exhaust as waste. It can be adjusted by the fuel-to-air ratio and hence oxygen sensor determines the fuel-to-air ratio whether it is lean or rich in real time. The production of oxygen sensor normally uses zirconium oxide (ZrO_2) for its active material. It consists of a thimble-shaped portion of ZrO_2 covers with two thin and porous platinum electrodes [55].

The operation of the oxygen sensors are similar to galvanic battery cell, in the case of the sensor the ZrO_2 acts as the electrolyte. At high temperature, this electrolyte becomes conductive so if the two plates are in contact with different amounts of oxygen, then a small voltage will be generated across the two plates. This action is produced because of oxygen atoms carry two free electrons so this means that the atom carries a negative charge. The ZrO_2 attracts oxygen ions with the result that negative charges build up on the surface of the ZrO_2 adjacent to the platinum electrode. The sensors do not actually measure oxygen concentration, but measure the amount of oxygen needs to completely oxidise any remaining combustibles in the exhaust gas. Therefore they measure the change of voltage. Rich mixture causes an oxygen demand. This demand causes a voltage to build up, due to transportation of oxygen ions through the sensor layer. Lean mixture causes low voltage, since there is an oxygen excess. Because the sensors function in high temperature, it cannot function at engine start, or cold start, and requires some period of time to warm up.

2.6.6 Emission (NOx) sensors

NO and NO2 is a toxic emission and usually grouped as Nitric Oxide (NOx) (refers to 2.5.5.3). Many countries and European Union are determined to limit emission of NOx. NOx sensors are currently available in research engines because they cannot take measurements in real-time [106]. Engineers and authorities are pushing hard to introduce NOx sensors which can take real-time measurement. But for commercial engines, NOx sensors are under development at the time of this thesis. Therefore current tasks on lower NOx emission are depended on laboratory works.

The principle of NOx sensors is based on the concept of oxygen sensors which NOx sensors find the decompose rate of NOx to oxygen to determine the level of NOx. The material uses in making NOx sensors includes gold or titanium electrode, which are able to find the decay of the dioxide and taking residual of oxygen level to estimate the NOx. There is other approach by Akbar et al. [3] and Figueroa et al. [40] use the ceramic material and the exhaust temperature to determine the level of NOx in exhaust gas.

2.6.7 Cylinder pressure and temperature sensor

Cylinder pressure and temperature hold valuable information of combustion process. The peak pressure and temperature during compression stroke are crucial to the combustion performance. By considering the engine life, commercial engines do not fit with in-cylinder sensors. Engines are calibrated during production based on laboratory work, therefore in-cylinder pressure and temperature sensor available in research and development engines. Such research engine requires drilling holes to fit the sensors.

2.6.8 Knock sensor

The cause of engine knock has discussed in 2.5.2. The principle of knock sensors is detecting vibrations from combustion knock in the frequency range 1-10 kHz. The piezo-electric knock sensor, a microphone, bolts to the engine block responds to unique frequencies causes by engine knock. The Engine Control Unit uses a filter to filter away background noise and detects actual engine knock.

2.7 Engine actuators

Engine actuators can be divided into the control of air path/fuel path and ignition. In SI engine, the main factors of combustion performances are fuel-to-air ratio and the ignition timing. To control fuel-to-air ratio, control algorithm can be simplified by control either path. SI engines have throttle for the air path which determines the amount of air. The further control can be done by adjusting valve timing in which ERG produces a boost effect of mixture pressure, has been discussed in 2.5.4. SI engines also have the fuel injector in which the mass of fuel injects to the cylinder can be controlled by ECU. The consideration in ignition timing can be controlled by spark plugs.

2.7.1 Air/fuel mixture control

Fuel-to-air ratio is the ratio of mass of fuel and mass of air in the fuel mixture. In the ideal situation, the stoichiometric fuel-to-air ratio is found when the fuel mixes with all free oxygen; the combustion burns all the gas and converts the combustion energy into highest kinetic energy and least pollution chemically. The stoichiometric ratio can be defined as the ideal ratio which all air are burned with all fuel available, results in only Carbon Dioxide and Water Vapour. Hillier [56] defined the ratio as shown in Equation 1.

$$\frac{25}{2}O_2 + C_8H_{18} \rightarrow 8CO_2 + 9H_2O$$

Equation 1

The ratio of mass of fuel against the mass of air to achieve stoichiometric is approximately 14.7:1 (by mass) or fuel-to-air ratio, ϕ, of 1. The highest explosive velocity and highest power is obtained from a ratio which is slightly higher than ϕ of 1. When the rich mixture is used, the explosive velocity decreases considerably. When ϕ is larger than 1, the mixture is considered as rich mixture, and when ϕ is smaller than 1, the mixture is considered as a lean mixture. Table 3 outlined the effect when the mixture is leaner or richer.

Fault	Effect	Symptom
Rich mixture	Incomplete combustion	Black smoke from exhaust High exhaust pollution

	Slow burning	Low power output High fuel consumption
	Sparking plugs soon soot-up	Misfiring Poor starting
Lean mixture	Slow burning	Low power output High fuel consumption Overheating
	Detonation	Pinking (excessive knocking) Low power and if condition persists will give blue smoke from exhaust showing piston failure

Table 3 Effects of incorrect mixture strengths [8]

The fuel-to-air ratio can be adjusted by electronic control. ECU gets the information of mass of air from air flow sensor. The response signal gives adjustment to fuel injector, allow a fine and precise adjustment to the amount of fuel needs for combustion.

2.7.2 Engine throttle

Throttle is the valve which controls the amount of air enter engine, locates at the entrance of intake manifold. The main function of a throttle regulates the fuel-to-air ratio and hence optimises the manifold pressure by controlling the air flow rate where it has effect on the power output of the engine and composition of exhaust gas. The air flow sensor locates after the throttle valve to measure the amount of air enters i.e. the amount of air enter into cylinder represents the engine load, and also a throttle position sensor sends signals to E.C.U to determine the amount of fuel needed. In the study of Verhelst et.al, and experiment is carries out while the engine speed is fixed of 1500rpm, the throttle affects the break torque and NOx emission [102]. The results showed that the NOx emission is exponential increase against throttle position. The best break torque is at throttle 80% open. However, compression ignition (CI) engines do not fit with a throttle since there is no need to control air volume.

In one practice, a throttle position system is run using National Instrument CompactRio as shown in Figure 8. The throttle has 6 pins, two sets connects to 12V power; two sets receive PWM from ECU control the opening position of the throttle and one pin output the position in voltage. There is a return spring pull the throttle to close position. The opening of throttle determine by the PWM signal from ECU The PWM gives the DC motor enough power against the spring and throttle open therefore the pulse width determine the position. The detail discussion can be referred to Appendix B.

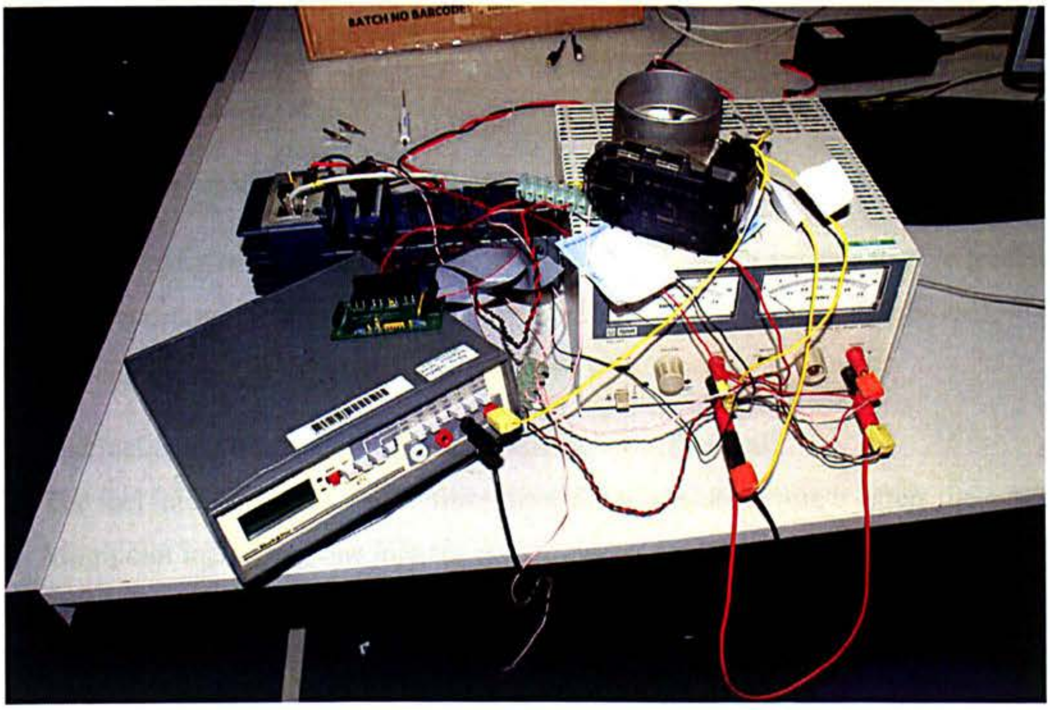

Figure 8 Throttle connected to computer to program

2.7.3 Fuel injection system

Fuel injection systems control amount of fuel needs to perform combustion. An example of an electronic fuel injection system is shown in Figure 9. The mixing process of fuel and air happens in this stage to blend mixture before entering the engine cylinder. Fuel injection system injects fuel in a fine spray form to generate a better mix process with air. In old-type engines, air and fuel is blended in a carburettors, but carburettors perform poorly in terms of emission. Current engines replaced carburettors with electronic fuel injection system, which gives the flexibility of adjusting settings in different engine loads and speed. In this section, both systems are discussed.

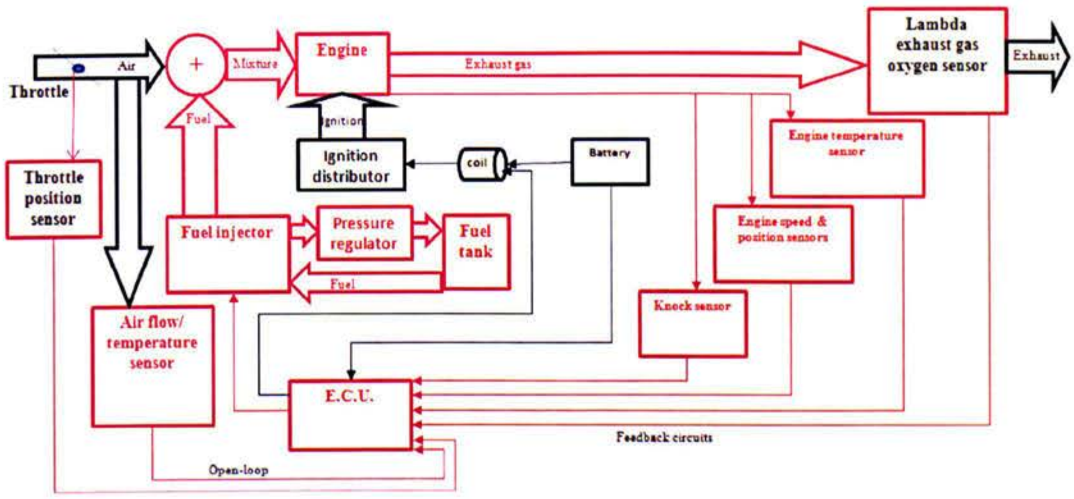

Figure 9 Fuel control system in red

- Closed-loop electronic injection system

Electronic fuel injection systems consist of various sensors which are able to give feedbacks of real-time conditions and optimizing actuator settings when necessary. The procedure of electronic fuel injection system can be summarised as follows:-

1) The fuel pump sends fuel to the injectors from the fuel tank.
2) The fuel injector injects fuel to form the air/fuel mixture before it enters the cylinders.
3) Multipoint injection – one injector per cylinder just before the cylinders
4) Throttle body injection – one injector only that discharges fuel into air stream
5) Pressure regulator controls the fuel pressure and sends the surplus fuel un-use by fuel injector bank to tank.
6) ECU controls the fuel injectors by controlling the pressure and the opening time of the head, according to the amount of air flow throw air flow sensor.
7) While the engine is working, ECU takes information of crankshaft position and speed, engine temperature and oxygen of exhaust gas and calculates the amount of fuel needs for next cycle.

- Electronic fuel injector

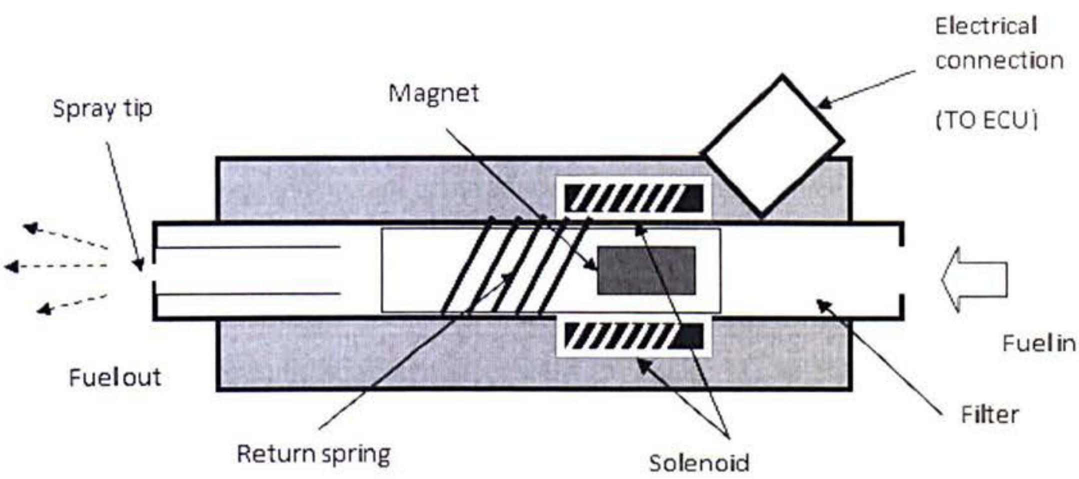

Figure 10 System diagram of a fuel injector operation [55]

Air and fuel mixture is formed by spraying finely-atomized fuel into the throat of the inlet port. Injector valves are solenoid operated. Fuels are delivered by opening the valve using a solenoid winding of resistance about 16Ω, overcomes a return spring which is fitted to hold a nozzle against its seat when it is closed. Needle valve is lifted by approximately 0.1mm. The front end of the needle valve is provided with a specially ground pintle for atomising the fuel. The pull in and release times of the valve lie in the range of 1 to 1.5 ms. A particular spray angle in connection with a specific distance of the injector relative to the engine inlet valve must be maintained to ensure good fuel distribution with low condensation loss. A system diagram of a fuel injector is shown in Figure 10 [15].

2.7.4 Ignition system

In SI engines, combustion starts when the engine control fire a spark to the compressed air and fuel mixture [48]. The spark plugs are needed to assist the engine combustion because the temperature of the compressed mixture is not high enough to perform compression ignition. Spark plug sends a high voltage spark to ignite air/fuel mixture in the most appropriate moment. The engine combustion performs in function of time; means the combustion spend a period for the reacted air and fuel particles propagate throughout the space inside the cylinder, therefore, the mixture should be ignited before the TDC (represents by minus degrees in the controller prior to TDC) in considerations of frame propagation. To provide the highest efficiency, the timing of the highest combustion energy occurs when the piston is typically at around 12° beyond the TDC, which such timing can be transferring the highest energy to the crankshaft mechanically.

2.7.4.1 Electronic ignition system

Since the mechanical ignition system cannot improve on engine performance and reduce emission, electronic ignition system is introduced to replace mechanical ignition system in providing more precise timings of spark during different engine speed and engine loads. The system replaced the distributor by a pulse generator.

The system of the electronic ignition system shows in Figure 11. To eliminate the cam event, electronic systems use engine control unit (ECU) to take information of the position of the crankshaft. The engine load is also measure by investigating the intake air flow rate and air temperature. ECU also takes information of the engine speed, piston temperature and camshaft position to calculate the best time for sending the spark for combustion. The ECU also checks from the knock sensor if a knock would happen and starts ignition through spark plug.

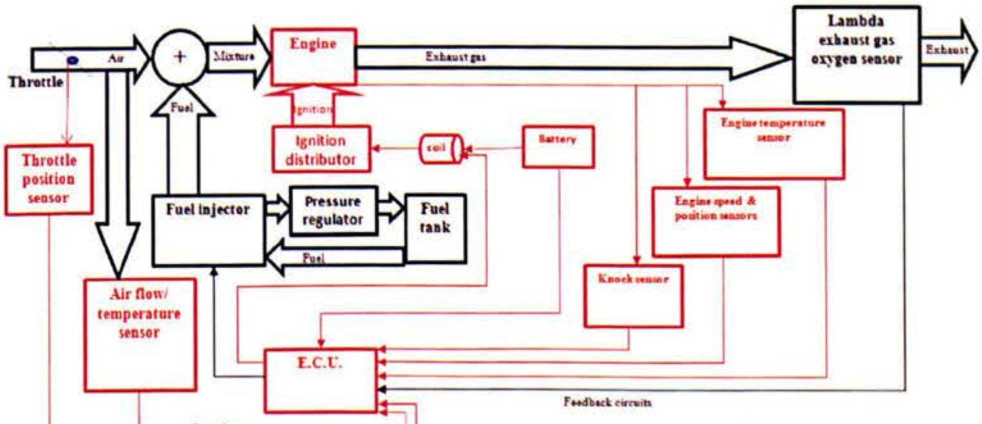

Figure 11 Block diagram of electronic ignition system in red

2.7.5 Valve timing

An example of cam valve presents in Figure 12. The shape of the cam lobe is similar to a 'waterdrop'. When the cam turns to the longer end of the lobe, the valve is being pushed to the opening position. Mechanical valve events are controlled by a cam. The valve profiles can be represented by the amount of valve lifts and the duration of the opening period, where they are determined by the geometries of the cam lobe. To optimise the valve event, study on variable cam timing can be found in the earlier stage [63]. Later study focus on variable valve timing. It can be given additional profiles in different speed and load by fitting mechanical system. There are two types of cam VVT available in current vehicle engines, cam phasing and cam changing. Those two methods can be combined to provide more profiles to match the best performance for different revolution and power range.

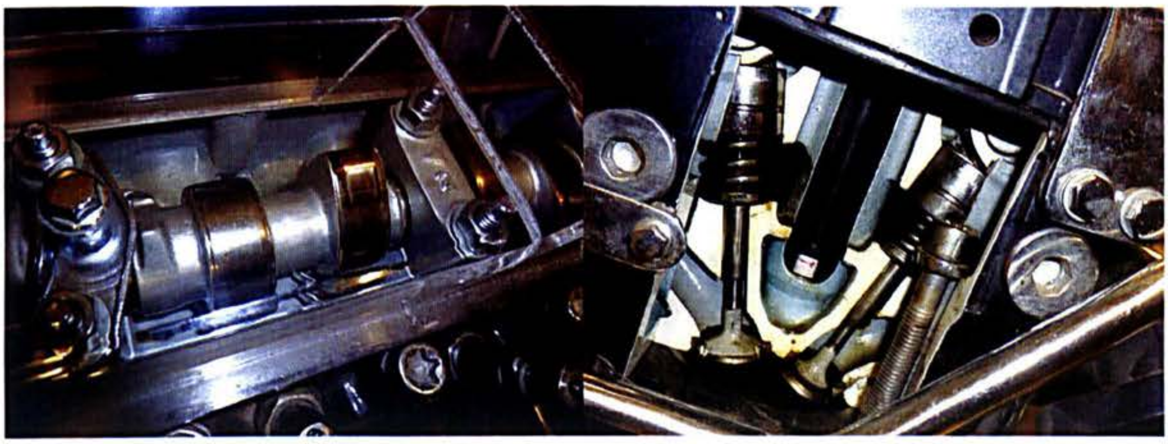

Figure 12 a) The left picture shows the shape of cam lobes and b) the right picture the left valve is closed and right valve is being pushed down

- Cam phasing VVT

Cam phasing VVT varies the valve timing by shifting the phase angle of the camshaft actuates by mechanical parts controlling by ECU. The phase angle can be changing in advance to let intake valve opening earlier and can also control the duration of valve opening. The phase angle can be controlled continuously or in fixed angles.

- Cam changing

Cam changing VVT uses two different cam lobes profile. The system changes profile depends on engine load and speed. One of the lobes is longer, which allows longer opening time at high speed. There is a pin, which controlling by ECU, locks the rocker arms with the longer lobes, allows more aggressive cam profile and longer valve opening at high speed. When the engine speed decrease the pin detach and the short lobe controls the opening of valve.

2.7.6 Camless VVT system

Compare to cam controlled VVT, camless VVT uses valve control which is isolated from the camshaft. Both ideas prove VVT theory improves fuel consumption, engine performance and emissions [103][114]. However, valve lifting is still depends on mechanical part which limited the cam VVT systems to certain valve settings or profiles. Cam-phasing VVT shifts opening and closing timing but it has no ability to change the amount of valve lift. Cam-changing VVT controls the lifting duration and the amount of lift of the valve, but only limited to certain profiles at certain speeds or/and loads. Recent engine technologies use the combinations of cam phasing and cam changing to provide the significant flexibility to optimize the engine parameters. However the cost is expensive, heavy and rather complex to design. To overcome those limitations the valves need to be isolated from the camshaft. The position and the timing and duration of opening of the valve are determined by ECU. The ECU sends signal to the actuator and active the valve. Traditional electric and hydraulic servo systems require low bandwidth, therefore new ideas for actuators is needed. There are few approaches to achieve of camless valves and actuators are under research.

- Electromagnetic valves

One approach is using a spring system to stable the valve in the middle position [32][85][116][117]. Two springs are supported the position of the valve while two solenoid magnets are employed to control the force of movement of the valve to open or close position. There are discovered challenges against electromagnetic valves. The problems occur in the nonlinear force to current relationship of solenoids at small air gap, and valve lash. This is because the high compression pressure inside the cylinder against the valve and valves must open with sufficient force. The other problem is the noise and wear associated with high contact velocity while opening and closing if the valve [57]. To overcome those problems will be costly.

- Electro-Hydraulic valves

Electro-Hydraulic valve is another solution for camless valve. The system consists of hydraulic pump and servo valves which the flow of the fluid is controlled by ECU [1][7][44][50][99]. The viscosity of the fluid is strong enough to hold the valve in the position needed. The main disadvantage for hydraulic valve is the valve lift function is affected by viscosity changes in some temperature range.

- Piezoelectric valve

Piezoelectric valves use the 'piezoelectric effect' to control the position of the valve. The piezoelectric effect, as it named 'piezo', means piezoelectric materials (such as quartz and ceramics) expands or contracts according to the voltages supplies to the material. One study from Jalili used ceramic as the piezoelectric material to control the position of the valve. The valve end is connected to the ceramic. The position of the valve changes due to the expansions and contractions of the ceramic which the amount of voltage supply is controlled by ECU. The reaction of piezo-ceramic is amplified by summing into a larger displacement, using a ratchet-type mechanism [61].

2.8 Engine simulation software

Various commercial packages have been developed to solve engineering problems relates to design and optimisation of internal combustion engines (ICE). There are four primary engine simulation commercial packages uses in the automotive industry today: Ricardo Wave (RW), Lotus Engine Simulation (LESoft), AVL fire, and GT-Power. These packages are similar in purpose and functionality. They require detailed input parameters to simulate the engine operation in an integrated manner rather than using different sub-systems.

2.8.1 Lotus Engine Simulation

LESoft is an in-house code developed by Lotus Engineering. The package processes engine simulation in two modules, the data module and the solver module [71]. The data module allows user to input the engine dimension data. The solver module is a built in combustion and heat transfer zero-dimensional equations and fuel/gas composition solver according to user input data in data module. The code is able to predict gas flow, combustion and overall performance of ICEs.

2.8.2 Ricardo Wave

RW is an engine simulation package designed to analyse the dynamics of pressure waves, mass flows, energy losses in ducts, plenums and manifolds of various systems and machines [91]. RW provides simulation of time-dependent fluid dynamics and thermodynamics using two-zone model.

However, software costs generally prohibit use in small organizations, primarily making them industry-specific software packages. Moreover, commercial software packages are based on Computation Fluid Dynamics (CFD) since they are designed to improve mechanical aspects of the engine. While mechanical models are used to calculate the moving parts of the engine in order to obtain the engine torque and acceleration, control models are used to allow calculations in feedback control schemes to optimise engine performance, such as variable valve timing, ignition timing, fuel-to-air ratio, and other variable engine geometries systems. Open source packages have been developed by small research groups to solve specific issues.

2.8.3 MATLAB

The in-house package, MATLAB Engine Simulation Code (MESC), has been developed for the solution of optimisation problems relating to the development and operation of ICEs. The code solves a full engine cycle with compression, combustion, expansion, exhaust and intake strokes in a single cylinder model. The user is able to specify the cylinder geometry and input data such as air and fuel composition, valve and ignition timing, engine speed, parameters for heat transfer and heat release sub-models. The solver is based on a two-zone model and uses the first law of thermodynamics and real-gas law to calculate pressure, temperature, heat flux and other functions. On top compared to commercial software packages, the code gives more flexibility on engine control using various fuel compositions.

2.9 Conclusions

This thesis focuses on control algorithms in SI engines. The background chapter gave an overview of the internal combustion engine and the related engine combustion performance. The chapter investigates the relationships between the engine operating parameters and engine emissions and shortlisted the possible parameters which can be obtained from various sensors and can be controlled by the existing actuators in practice. It can be concluded that the parameters needed to realistically control the engine emissions and performance have been identified, and include the following:

1) The engine operating parameters which are important to engine combustion are fuel-to-air ratio, ignition timing, exhaust valve closed timing and intake valve opening timing.
2) The emission compositions targets to be kept to the minimum and also used to monitor the fuel compositions are Carbon Dioxide (CO_2), Oxygen (O_2), Carbon Monoxide (CO) and Nitric Oxide (NOx).
3) The exhaust gas temperature can be used to understand the combustion performance.

These parameters are used for building the engine simulation model and the engine controller.

2.10 Summary of Chapter 2

This chapter gave discussions of the background knowledge of engine parameters and an overview of control systems. The brief engine history is introduced in 2.2, which concluded in 2.3 and 2.4 that electronic controlled engine is needed to improve engine performance. Exhaust gas product is formed of natural and toxic substances after the high temperature combustion process. Behaviour of different exhaust compositions against different engine operating parameters is discussed in 2.5. The cause of toxic emission draw the idea on the control parameters needed to reduce toxic emission to a minimum. 2.6 and 2.7 summarised the availability of various engine sensors and actuators, and also the possibilities of future engine control components, such as camless engine system. The contribution of this background gave a valuable discussion in 2.8 in order to find the possibilities of engine control and parameters needed to build the engine simulation platform and the control model.

Chapter 3 Development of mathematical model and its implementation

The development of a computer based engine simulation of a four strokes SI engine has been discussed in this chapter. The in-house engine simulation software package is developed based of the 1st law of thermodynamic. The sub-models that are used in the simulation, involves in heat transfer, heat release, gas exchanges and any other engine dynamic factors, such as blow-by and frictions has been explained. The estimation of cylinder temperature is divided into two zones, burned zone and unburned zone; and the estimation of pressure is treated as a single zone. All of the mathematical representations used in sub-models are compared with the commercial software, namely Ricardo Wave and Lotus Engine Simulation. The advantage of using MESC in this application is it allows the engine run in transient condition where the controller updates engine operating parameters in continuous time. Also MESC is able to estimate the level of CO_2 and O_2, whereas RW and LESoft cannot obtain such components (refer to 1.5.20). The result of the development of this engine simulation provides the platform which researches on the engine controller.

3.1 Introduction

This chapter describes the virtual engine model development of a 4-stroke spark-ignited (SI) engine which is the most commonly used in vehicles. To match the thermodynamic process of real engines, a category of sub-models is needed to provide the detailed description of all relevant processes such as burned gas composition, mass burning rate, heat transfer, blow-by and others [39][83]. Engine sub-models are divided into various categories, including the cylinder geometry and piston motion, combustion models, heat transfer models, and some others factor such as friction and blow-by. The descriptions of sub-models are based on data presents in user's guides [71][91] and literature [39][54].

3.2 Simulation of 4-stroke engine cycle

The engine simulation divides the engine cycles into processes which follow the changes in thermodynamic and chemical state of the working fluid. The virtual engine used in this thesis is a 4-stroke engine. The division of simulations includes different engine process of intake process, compression process, combustion process, expansion process, and exhaust process. Calculations in each process are generated as functions of time. The starting point of these cycle simulations is using the first law of thermodynamics in an open system. The structure of this type of engine simulation is indicated in Figure 13. During each cylinder process, sub-models are used to describe geometric features of the cylinder and valves/ports, the thermodynamic properties of unburned and burned gases, the mass and energy transfers across the system boundary, and the combustion process needed only in the combustion stroke.

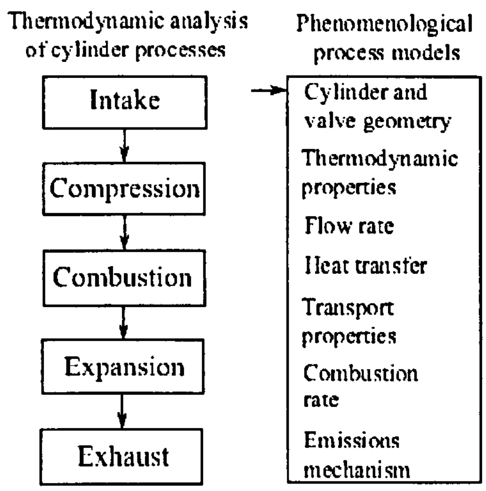

Figure 13 Structure of thermodynamic based simulation of ICE operating cycle.

3.2.1 Compression stroke

During the compression stroke, the working fluid has no reaction (referred as 'frozen' in Ricardo Wave as the contents of the charge assumed to be 'frozen' as all reaction cease [91]). The thermodynamic properties, in terms of the rate of change in pressure ($\frac{\delta p}{\delta \theta}$) (full description is in Equation 18) and temperature$\frac{\delta \vartheta}{\delta \theta}$ (Equation 19 and Equation 20), are determined using sub-models to calculate the thermodynamic behaviours. Sub-models including geometries of cylinder, heat-transfer, and gas exchanges are required in compression stroke. The mixture compositions are calculated based on thermo equilibrium state .The heat transfer is calculated using one of the Nusselt–Reynolds number correlations for turbulent convective heat transfer [54]. The transport properties, viscosity, and thermal conductivity use in these correlations are obtained from semi-empirical relations.

3.2.2 Combustion stroke

During the combustion stroke, the combustion process starts. The equations of generating thermodynamic properties including geometries of cylinder; heat-transfer and gas exchanges are the same as equations found in the compression stroke. In addition, heat release sub-model representing the behaviour of the combustion is included to virtualise the engine. This sub-model can estimate the combustion process in one or two zones, burned zone and unburned zone, although two zones calculations are considered in this thesis.

Many approaches can be used to predict the burning or chemical energy release rate. They are successfully meet the specifications of different simulation objectives [39][54][71][91]. The simplest approach uses a one-zone model where a single thermodynamic system represents the entire combustion chamber contents. The energy release rate is defined by empirically based functions specified as part of the simulation input. Quasi-geometric models of turbulent premixed flames are used with a two-zone analysis of the combustion chamber contents (an unburned and a burned gas region) in more sophisticated simulations of ICEs [54].

3.2.3 Expansion stroke

The simulation of the expansion stroke is similar to the compression stroke. The expansion process is either treated as a continuation of the combustion process or, once combustion is over. The information of burned gas is used as the initial condition of the expansion stroke. Sub-models include geometries of cylinder, heat-transfer, gas exchanges are needed in expansion stroke.

3.2.4 Exhaust and intake stroke

The exhaust process uses conservation equations for a one-zone open-system model of the cylinder contents, means no 3D meshes are involved. Mass flows across open valves are usually calculated using one-dimensional compressible flow equations for flow through a restriction or filling and emptying models [39][54]. The more accurate unsteady gas dynamic intake and exhaust flow models are sometimes used to calculate the mass flow into the engine cylinder in complete engine cycle simulations when the variation in engine flow rate with speed is an important (the disadvantage is much increased computing time).

3.3 Cylinder geometry

Geometric sub-model is used to define the topology of the combustion chamber as well as to specify geometric surfaces and volume zones use for heat transfer and combustion sub-models. The cylinder volume depends on the engine geometry (bore, stroke, connecting rod length and compression ratio), and is a function of crank angle and the rate of change of cylinder volume.

The model uses to specify the cylinder geometry is piston, head and cylindrical liner [54]. Both of the piston and head surface area are assumed to be equivalent to the area derives from the bore diameter with multipliers of this area allows in the Woschni heat transfer model. The sketch of the engine geometry including the cylinder and the crank is shown in Figure 14. Typical values of these parameters are $b/s = 0.8$ to 1.2 for small and medium size SI engines, decreasing to about 0.5 for large slow-speed CI engines, $l/a = 3$ to 4 for small and medium size engines, and 5 to 9 for large slow-speed engines.

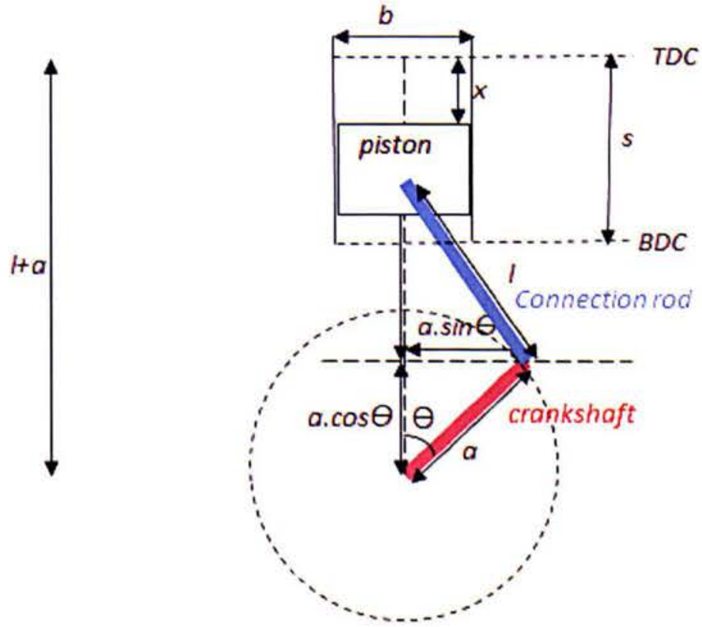

Figure 14 Geometric solutions for slider volume

where,

l is the length of connection rod

a is the crank radius

b is the bore diameter

s is the length of stroke

x is the distance between the surface of the piston head and the TDC

3.4 Piston motion

Piston motion sub-model is used to determine the instantaneous position of the piston in the cylinder and the volume of the combustion chamber as a function of crank angle. The piston position is fed to other sub-models.

The crank–slider model, shown in Figure 14, used to characterize the arrangement of mechanical parts is designed to convert translational motion into rotational motion. The piston motion is defined by including geometric inputs for the cylindrical combustion chamber, crankshaft and connecting rod. The position of piston is derived from basic trigonometry equations [39]. The cylinder volume can be calculated by Equation 2.

$$\frac{V}{V_d} = \frac{1}{r_{cr}-1} + \frac{1}{2}\left[1 + R - \cos\theta - \sqrt{(R^2 - \sin^2\theta)}\right]$$

Equation 2

where,

v is the cylinder volume

v_d is the displacement volume

r_{cr} is the compression ratio

R is $2l/s$

Upon differentiation, the volume change in function of crank position in degree defines in Equation 3.

$$\frac{dV}{d\theta} = \frac{v_d}{2}\sin\theta\left[1 + \cos\theta(R^2 - \sin^2\theta)^{-\frac{1}{2}}\right]$$

Equation 3

The movement of the piston in the cylinder can be considered as a volumetric pump, the formulation of such model can be defined by calculating the mass flow rate:-

$$\dot{m}(t) = \rho_{in}(t).\dot{V}(t) = \rho_{in}(t).\lambda_l(p_m,\omega_e).\frac{V_d}{N}.\frac{\omega_e(t)}{2\pi}$$

Equation 4

where,

ρ_{in} is the density of gas at engine intake

λ_l is the volumetric efficient

V_d is the displaced volume

N is the number of revolutions ($N = 2$ for four stroke engine)

Ω_e is the engine speed

The term volumetric efficiency, λ_l, determines the amount the combustion power generates to push the piston and the power of engine can move. However it is hard to predict since many factors affect it. To approximate the volumetric efficiency, assume the ideal engine cycle is applied:-

$$\lambda_l = \frac{V_c+V_d}{V_d} - \left(\frac{p_{out}}{p_m}\right)^{\frac{1}{K}} \cdot \frac{V_c}{V_d}$$

Equation 5

where,

p_{out} is the pressure of exhaust side

p_m is the manifold pressure

V_c is the compression volume

K is the constant for most of working fluid $K = 1.4$

3.5 Air and fuel properties

The air properties use in this thesis have been discussed in Chapter 2.5.5. The simulation which uses the same composition found in atmosphere air consists of 21% oxygen and 79% of nitrogen (for each mole of O_2 there are 3.76 moles of N_2). Selected physical properties of oxygen and nitrogen are given in the textbooks and tables [54]. Extension of the analysis to different air mixtures encountered in practice is straightforward. The most frequent differences are the presence of water vapour, carbon dioxide and argon in the atmospheric air. The amount of water vapour in the atmospheric air normally depends on temperature and degree of saturation. The gas species considered in software packages include:-

CO_2, CO, N_2, H_2O, O2, H_2, C_8H_{18}, $C_{12}H_{26}$, CH_4, H, N, NO, O, OH

In RW and MESC calculations, the fuel is a user-defined composition of C, H, O and N atoms (the most common hydrocarbon fuels have no O or N unless mixed with ethers or alcohols). In LESoft calculations, the fuel types are limited to those compose of C, H and O atoms [71].

Combustion products are a mixture of some gases. The gas properties are based on the appropriate governing relations, e.g. perfect gas equations for air-only thermo-chemistry or ideal/real gas equations for the thermo-chemistry of hydrocarbon/air mixture for general C/H/O/N fuel types. The thermodynamic properties of the individual gases are calculated as functions of temperature with these properties being averaged as molar functions to give the overall properties of the mixture [39]. The real-gas enthalpy and internal energy are calculated from their ideal-gas counterparts shown in Equation 6, along with the specific heats at constant pressure and volume.

$$H = U + pV$$

Equation 6

where,

H is the enthalpy (Joules)

U is the Internal Energy (Joules)

p is pressure (Pa)

V is volume (m^3)

The gas property sub-model is based on polynomial curve fits to thermodynamic data for each species [54] shown in Equation 7. In a real gas model, the compressibility factor is calculated using empirical correlation [91]. For a gas mixture, the critical temperature and pressure, and acentric factor are calculated according to the mixing rule.

$$\frac{h}{RT} = a_1 + \frac{a_2}{2}T + \frac{a_3}{3}T^2 + \frac{a_4}{4}T^3 + \frac{a_5}{5}T^4 + \frac{a_6}{T}$$

Equation 7

where,

h is the specific enthalpy

R is the gas constant

T is the temperature

a_1 to a_6 are constants of integration determined by matching the specific enthalpy at some reference temperature

Dissociation effect on effective heat release is developed through the use of maldistribution factor [71]. The maldistribution factor is incorporated to allow for a reduction in effective caloric value of the fuel due to poor charge mixing and dissociation. A factor of 0 implies almost perfect mixing and a high effective caloric value for the fuel. A typical gasoline engine would have a maldistribution factor of between 1.0 and 3.0. Values less than 1.0 imply better combustion and may be appropriate for gas fuelled engines.

The coefficients of chemical reactions are determined from the equilibrium calculations [39]. Fuel evaporation and condensation are not taken into account in the calculations (these sub-models are available in RW).

3.6 Heat release model

The amount of heat releases during combustion transfer to energy pushes down the piston in an appropriate time. The burning rate is defined as the rate at which the fuel mass in the cylinder is consumed in the combustion process to become products of combustion. Regardless of the final state of the air/fuel mixture (emissions products, free radicals), the initial fresh air and fuel no longer exist in their natural states when combustion has completed.

The heat release rate is calculated using empirical heat release function derived from the Wiebe equation. The Wiebe model is widely used to describe the rate of fuel mass burned in thermodynamic calculations, and this model is available in all packages. The Wiebe function is described in Equation 8 [39].

$$x_b = 1 - a\exp\left[\left(\frac{\theta - \theta_s}{\theta_d}\right)^n\right]$$

Equation 8

where,

x_b is the mass fraction burned from 0% to 100%

a is a burn rate cover 10–90% of mixture burned

θ is the crank position in degree

θ_s is the angle of start of burn

θ_d is burn duration is degree

n is the exponential factor

The combustion duration is defined as the number of crank degrees between 10% and 90% of mass fraction burnt. The combustion phasing is defined as the number of crank degrees after TDC firing at which 50% of the fuel has been burnt.

Wiebe model allows the independent input of function shape parameters, combustion duration and combustion phasing which are functions of the type of fuel being used [54]. It is known to represent quite well the experimentally observed trends of premixed combustion. By adjusting the individual Wiebe function component shapes and their relative proportions through the fuel mass fractions, a complicated overall burn rate curve is defined. Varying the 50% burn point simply shifts the entire curve forward or backward. Varying the 10–90% duration extends the total combustion duration, making the profile extend longer or compress shorter. Varying the Wiebe exponent shifts the curve to burn mass earlier or later.

The two-part Wiebe function takes into account the mass fraction burned in the premixed combustion period and the mass fraction burned during the diffusion combustion period [71][91].

As an alternative to Wiebe combustion models, the user may choose to enter a complete profile of combustion [91]. This way allows the user to enter a cylinder pressure profile obtained from testing, internally derived from a heat release profile using the applied heat transfer model and thermodynamic properties, and output a fuel mass burn profile for combustion calculations.

A more advanced sub-model, turbulent flame combustion model, calculates the rate of fuel burned using the turbulent flame speed and of instantaneous flame area [39]. It responds to changes in cylinder flows and in combustion chamber geometry. The model also provides spatial resolution as to the instantaneous flame location needed for heat transfer calculations.

A combustion model follows a constant combustion fuel-to-air ratio under the assumption that the air/fuel mixture is fully premixed. In certain engine designs (e.g. Spark Injection Direct Ignition engines), the fuel and air are not fully mixed at the start of combustion. The spark-ignition stratified sub-model is used in [91] to impose a combustion equivalence ratio that is different from the overall equivalence ratio of the cylinder, for the purpose of simulating a stratified charge mixture. This model allows combustion stoichiometry to vary during combustion, and is used to improve accuracy of results for systems that add or remove air or fuel during combustion, since the system will respond more accurately to changes in cylinder contents. The spark-ignition stratified sub-model creates an adaptive mixture which begins at a user-entered equivalence ratio and adjusts as burn progresses to consume the available air.

3.7 Conduction

Conduction sub-model is used to calculate cylinder surface temperature. Accurate surface temperature improves boundary conditions for the in-cylinder heat transfer sub-model, and is used to assist in engine component design. One conduction sub-model is available in MESC (it is referred to as 'simple'), two conduction sub-models are available in LESoft [71] (they are referred to as 'simple' and 'conduction'), and three sub-models are implemented in RW [91] (they are referred to as 'simple', 'conduction' and 'swing').

The 'simple' engine conduction sub-model uses a pre-defined thermal network which represents the cylinder liner, cylinder head, piston, and intake and exhaust valves. This model enables the prediction of the surface temperature of the combustion chamber and heat rejection of the engine to the coolant. This model is offered by all packages.

Other conduction sub-models, offered by LESoft and RW, use a more detailed pre-defined thermal network than 'simple' model.

In the 'conduction' sub-model used in LESoft and RW, the cylinder wall temperature is specified or calculated via a simple one-dimensional heat transfer calculations for cylinder head, piston and linear walls. The cylinder walls are assumed to have a wall thickness that is directly proportional to the bore. The heat transfer coefficients of coolant and cylinder head are constant values, and conductivity of material is specified by choosing material used. The cylinder head temperature is calculated as the area average of the wall temperature and the valve temperature. Valve head temperatures are calculated for both inlet and exhaust valves as a function of fuel type and fuel-to-air ratio. The piston temperature is assumed that it is equal to the area averaged cylinder head temperature. In the RW, this sub-model has more spatial resolution and also allows substituting portions of the pre-defined mesh with existing finite element models built using other commercial software [91].

The 'swing' sub-model from the RW accounts for cyclic temperature transients on combustion chamber surfaces and other engine surfaces exposed to gases, which are produced by the peaked nature of the gas-wall heat fluxes [91]. This is especially relevant for in-cylinder surfaces with low conductivity where temperature fluctuation is quite high (100–200 K).

The calculations presented are based on 'simple' conduction model, and cylinder wall temperature is fixed in all calculations.

3.8 <u>Heat transfer model</u>

Two non-dimensional parameters, the Nusselt number and the Reynolds number, are used to estimate the heat transfer correlated with fluid conditions. Those two parameters vary in time, therefore heat transfer to and from the cylinder gases are calculated at every crank angle increment. These calculations require knowledge of wall area, wall temperatures, and surface heat transfer coefficient. The cylinder surface areas are calculated using surface area to bore area ratio which are a function of combustion system. The linear area is calculated at each increment by the piston displacement from TDC. Gas velocity depends on piston mean speed, amount of swirl, the amount of combustion and the gas turbulence [39].

Various heat transfer sub-models are offered by each package for the calculation of the convective heat transfer coefficient in the engine cylinder [71][91]. The heat transfer models proposed by Annand, Woschni and Eichleberg are available in LESoft and MESC. Heat transfer models offered by the RW include Woschni, Annand and model referred to as 'flow' model [91].

Woschni, Annand and Eichleberg models are derived from a basic Nusselt number correlation for flow in pipes [39][54]. The equation to calculate Nusselt number is shown in Equation 9. Each model employs coefficients that have been developed to best reproduce the heat transfer results obtained by experiment. The Woschni heat transfer sub-model is the most commonly used heat transfer model since Woschni accounts for the increase in the gas velocity inside the engine cylinder during combustion. It views the charge as having a uniform heat flow coefficient and velocity on all surfaces of the cylinder, and calculates the amount of heat transferred to and from the charge based on these assumptions [107]. The Annand and Eichleberg heat transfer models are typically used as a mean of comparison for the results from the Woschni model. Annand and Eichleberg are rarely used in practical applications [54]. Different from the Woschni model, the Annand model assumes a constant gas velocity equal to the mean piston speed. The heat transfer coefficient can be calculated using the Equation 11.

Since the Woschni heat transfer correlation is the most commonly used, the engine simulation use Woschni as the primary heat release model:-

$$Nu = 0.0035{R_e}^{0.8}$$

Equation 9

where,

Nu is the Nusselt's number

Re is the Reynold's number

The Annand heat transfer sub-model is typically used as a mean of comparison for the results from Woschni heat transfer sub-model. It is rarely used in practical applications. Different from the Woschni model, where the increase in the gas velocity in the cylinder during combustion is accounted for, the Annand model assumes a constant gas velocity is equal to the mean piston speed. The Annand correlation is

$$\boldsymbol{Nu = a{R_e}^{0.7}}$$

Equation 10

The constant, a, is 0.49 for four-stroke engines and 0.26 for two-stroke engines.

The heat transfer coefficient is [107]:-

$$h = 128 h_c b^{-0.2} p^{0.8} T^{-0.53} \left(C_1 u_{pm} + C_2 T_r \frac{V}{V_r} \frac{p - p_m}{p_r} \right)^{0.8}$$

Equation 11

where,

b is the bore (m)

V is the cylinder volume (m^3)

p is the cylinder pressure (kPa)

T is the cylinder temperature (K)

u_{pm} is the mean piston velocity (m/s)

p_m is the motored cylinder pressure (kPa).

Subscript r corresponds to the reference pressure p_r (kPa), reference temperature T_r (K) and reference volume V_r (m^3). User specific multiplier constant h_c is 1. The constant C_1 is 2.28 for combustion and is changed to 6.18 for scavenging. The constant C_2 defines the combustion term. Its value is 3.24×10^{-3} in closed cycle, and 0 before combustion and scavenging therefore the term $\left[C2.\frac{T_r V}{V_r P_r}.(p-p_m)\right]$ can be ignored during compression, and exhaust and intake stroke [91].

The detailed finite heat release model presented in Equation 12 includes the cylinder wall heat transfer, dQ_w/dt, if the instantaneous average cylinder heat transfer coefficient h and engine speed N are known.

$$\frac{dQ_w}{dt} = h(\theta)A_w(\theta)\frac{T(\theta)-T_w}{N}$$

Equation 12

where,

T_w is the area-weighted mean of the temperatures of the exposed cylinder wall, the head and the piston crown.

h is the heat transfer coefficient calculated from Woschni model

A_w is the exposed cylinder area, which is the sum of the cylinder bore area, A_{wall}, the cylinder head area, A_{head}, and the piston crown area, A_{piston}, assuming a flat cylinder head shown in Equation 13.

$$A_w(\theta) = A_{wall} + A_{head} + A_{piston} = \pi by + \frac{\pi}{2}b^2$$

Equation 13

where,

y is the exposed cylinder wall height

b is the bore size

$A_{piston} = \pi b^2/4$

The ratio of the cylinder head surface area to the piston surface area, A_{head}/A_{piston}, is a measurable quantity, and it is about 1.2.

The 'flow' model, implemented in RW, predicts convective heat transfer from gases to combustion chamber walls, and its spatial and cyclic temporal variations are driven by the instantaneous mean and turbulent gas motions [91]. Prediction of heat transfer coefficient is linked to the fluid dynamics of combustion gases, which is determined by periodic piston motion, valve flows, injection process, combustion, motion of piston and chamber geometry. The multi-zone flow model solves differential equations for swirl and turbulence and an algebraic equation for squish in a number of combustion chamber flow zones. The heat transfer coefficient for each surface is obtained from the Colburn analogy of heat and momentum transfer and is directly linked to the effective velocities. One of the main benefits of this approach is that it captures the dependence of the heat transfer coefficient on the magnitude of instantaneous in-cylinder flow velocities. Another benefit is the improved ability of the model to represent the spatial non-uniformity of the heat transfer coefficients.

Thermal radiation from gases to surrounding combustion chamber surfaces is a significant component of heat transfer for diesel engines, due to soot formation during diesel combustion [39]. Instantaneous and mean levels of heat radiation are functions of the volume and distribution of burning gas, amount of soot present in the burning gas, combustion chamber geometry, and surface emissivity and temperature. The sub-models employed in the radiation model calculate the soot loading in the burned zone, volume of the radiating burned zone and radiation temperature.

3.9 Friction

The Chen–Flynn friction model is used to calculate the work done by friction in the engine and accompanying systems [71][91]. Friction model takes into account engine speed, mean piston speed, maximum cylinder pressure and compression ratio. The Chen–Flynn correlation has a constant term (for accessory friction), a term which varies with peak cylinder pressure, a term linearly dependent on mean piston velocity (for hydrodynamic friction) and a term quadratic with mean piston velocity (for windage losses).

3.10 Blow-by

Blow-by occurs when a portion of gas escapes through the gap between piston and cylinder wall into the crankcase [39]. The consequence is the pressure inside the cylinder decreased by a portion. This is also taking into account when sub-model calculates the enthalpy. The blow-by model calculates how much gas is removed from the cylinder during the cycle and blown by the cylinder's rings, optionally into the crankcase.

In MESC calculations, the fraction of blow-by is specified with initial value of 0.8. In RW calculations, blow-by sub-model assumes the net gas flow past the first ring is zero and enables the thermodynamic model for the first crevice [91]. The input parameters for the model are cold piston liner clearance and distance of the top ring from piston top. During compression, the air/fuel mixture is packed into the crevice volume (absorption process) allowing unburned hydrocarbons to escape the combustion process occurring in the main chamber. The absorbed unburned hydrocarbons return to the cylinder during expansion as a source of hydrocarbons emissions.

3.11 Emissions

Emissions sub-models are used to calculate the in-cylinder formation and destruction of common engine emissions species [39][54]. Emissions sub-models for the engine include CO, HC, and NOx. The CO emissions sub-model predicts CO production during combustion and exhaust in an engine cylinder element. The HC emissions sub-model predicts HC production during combustion and exhaust in an engine cylinder element as well as in the flow network. The NOx emissions sub-model predicts NOx production during combustion and exhaust in an engine cylinder element.

The emissions sub-models are available in RW packages. The calculation is only valid in two temperature zones model, therefore it is not available in LESoft. Thus the require constant is based on the arrhenius relationship rate constant multiplier. RW has the recommended value but such constant has no other supporting articles. The initial setting in RW does not switch on this option. Therefore emission sub-models are not used in the simulations presented.

3.12 Valve motion

Valve motion is specified by means of a few simple parameters such as diameter, maximum lift, and duration of opening and closing ramps [39][49][54]. The lift valve sub-model defines a lift profile using polynomial lift curves. The mass can be estimated using Equation 14, where flow function shown in Equation 15 determines the constant related to direction of flow.

$$m(t) = c_d A(t) \frac{p_{in}(t)}{\sqrt{R\vartheta_{in}(t)}} \Psi\left(\frac{p_{in}(t)}{p_{out}(t)}\right)$$

Equation 14

where,

m is the mass of the flow

c_d is the discharge coefficient

A is the cross section area of the valve

p_{in} is the intake pressure

p_{out} is the output pressure

R is the gas constant

ϑ_{in} is the intake temperature

ψ is the flow function which is defines in Equation 15.

$$\Psi\left(\frac{p_{in}(t)}{p_{out}(t)}\right)=\begin{cases}\sqrt{K\left[\frac{2}{K+1}\right]^{\frac{K+1}{K-1}}} & for\ p_{out}<p_{in}\\ \left[\frac{p_{out}}{p_{in}}\right]^{1/K}\sqrt{\frac{2K}{K-1}\left[1-\frac{p_{out}}{p_{in}}\right]^{\frac{K-1}{K}}} & for\ p_{out}\geq p_{in}\end{cases}.$$

Equation 15

the critical pressure where the flow reaches sonic conditions in the narrowest part [49] in determines by:-

$$p_{cr}=\left[\frac{2}{K+1}\right]^{\frac{K}{K-1}}\cdot p_{in}$$

Equation 16

In this thesis, assume $K\sim 1.4$, Equation 15 can be simplified as:-

$$\Psi\left(\frac{p_{in}(t)}{p_{out}(t)}\right)=\begin{cases}\frac{1}{\sqrt{2}} & for\quad p_{out}<\frac{1}{2}p_{in}\\ \sqrt{\frac{2p_{out}}{p_{in}}\left[1-\frac{p_{out}}{p_{in}}\right]} & for\quad p_{out}\geq\frac{1}{2}p_{in}\end{cases}$$

Equation 17

The valve lift duration is specified by the number of crank degrees between valve opening and valve closing. The valve-flow model assumes a steady, adiabatic and reversible flow of an ideal fluid through a duct. The valve flow in an engine is not an ideal flow, and the discharge coefficient is introduced to account for real gas effects. The mass flow through the valves depends on the effective open area, pressure ratio, upstream pressure, specific heat, upstream temperature and ratio of specific heats.

3.13 Scavenging

The gas exchange process in the four-stroke engine is driven primarily by the piston motion, and a fully mixed scavenging model is most commonly used [39]. With the perfect mixing model any charge gas entering the cylinder is instantaneously and homogeneously mixed with the gas currently in the cylinder.

3.14 Overview of engine model

Various sub-models found in engine simulation have been discussed in 3.3 to 3.13. Such sub-models calculate the mass flow of the correspondent areas, including heat release, heat transfer, gas exchange and type of injection. The results generate different engine condition if different sub-models are used. The final engine is developed as standard engine geometries and set of sub-models are used as default unless further study is conducted. The parameters used in this thesis are shown in Table 4.

Engine simulation model	Definition in simulation
Combustion process	Spark ignition
Number of stroke	4
Heat release model	Wiebe
Heat transfer model	Woschni
Injection type	Port injection
Number of valve	1 exhaust valve, 1 intake valve
Gas exchange	Thermal equilibrium

Table 4 Default model used in the thesis

The engine simulation is treated the engine air system as a receiver. The inputs and the outputs are the mass and energy flow. By considering the engine at constant time, t, the volume, V, gas constant, R, and the specific heat at constant pressure, c_p, and volume, c_v, are constant. The block diagram of the air system is shown in Figure 15 [49].

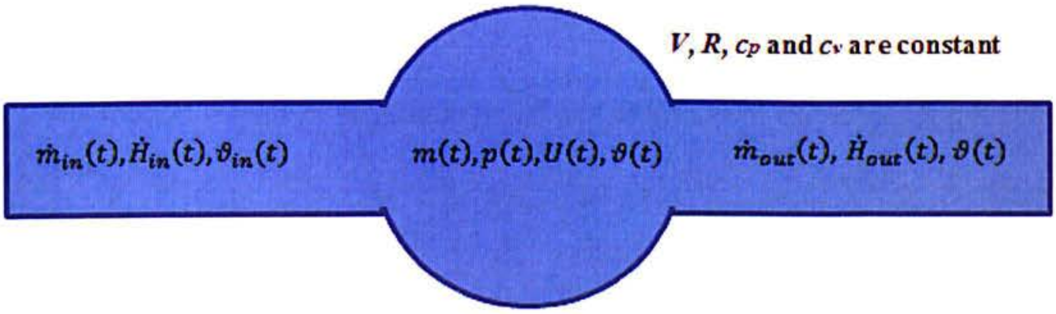

Figure 15 Input, states and output of the engine as an air system

where,

m is the mass flow, the subscripts indicate the related direction of the flow

H is the heat

p is the cylinder pressure

ϑ is the temperature

U is the energy

V is the volume

R is the ideal gas constant

c_p is the specific heat at constant pressure

c_v is the specific heat at constant volume

The engine condition of four stroke can be solved by the differential equation of pressure, p, and temperature, ϑ, based on ideal gas law and portion in the different in mass flow rate in and out of the cylinder. The unburned and burnt mixture zones are considered as separate open systems. The differential equation of the cylinder pressure with respective of crankangle ($d\theta$) is presented in Equation 18.

$$\frac{dp}{d\theta} = \frac{\frac{1}{m}\frac{dV}{dt} + \frac{VC_b}{m\omega} - x\frac{v_b}{\vartheta_b}\frac{d\ln v_b}{d\ln \vartheta_b}\frac{d\vartheta_b}{d\theta} - (1-x)\frac{v_u}{\vartheta_u}\frac{d\ln v_u}{\partial \ln \vartheta_u}\frac{d\vartheta_u}{d\theta} - +(v_b - v_u)\frac{dx}{d\theta}}{\left[x\frac{v_b}{p}\frac{d\ln v_b}{d\ln p} + (1-x)\frac{v_u}{p}\frac{d\ln v_u}{d\ln p}\right]}$$

Equation 18

where,

v is specific volume of the gas, subscript u of unburn zone and subscript b for burned zone

x is the mass fraction burned

ϑ is the cylinder temperature, subscript u of unburn zone and subscript b for burned zone

p is the cylinder pressure, subscript u of unburn zone and subscript b for burned zone

V is the volume

m is the mass of the piston

C_b is is the blow-by coefficient, $C_b = \frac{\dot{m}_l}{m}$, and $\dot{m}_l$ is the leakage due to blow-by

For two zones temperature, the rates of change in temperature in function of crankangle are presented in Equation 19 for burned zones and Equation 20 for unburned zone.

$$\frac{d\vartheta_b}{d\theta} = -\frac{h}{m\omega c_{pb} x}\sum A_{bi}(\vartheta_b - \vartheta_{\omega i}) + \frac{v_b}{c_{pb}}\frac{d\ln v_b}{d\ln \vartheta_b}\frac{dp}{d\theta} + \frac{h_u - h_b}{x c_{pb}}\left[\frac{dx}{dt} - \left(x - x^2\frac{C_b}{\omega}\right)\right]$$

Equation 19

$$\frac{d\vartheta_u}{d\theta} = -\frac{h}{m\omega c_{pu}(1-x)}\sum A_{ui}(\vartheta_u - \vartheta_{\omega i}) + \frac{v_u}{c_{pu}}\frac{d\ln v_u}{d\ln \vartheta_u}\frac{dp}{d\theta}$$

Equation 20

where,

ω is the engine speed

h ,heat transfer coefficient, subscript u of unburn zone and subscript b for burned zone

Calculations in different strokes have different mass flow, since the sub-models may not be valid in certain stroke. For example, the combustion model is used in combustion stroke but not in other stokes, and mass flow calculation in valve events only valid in intake stroke. The detail of the strokes modelling is discussed in 3.2. Here is the list of the mass flow calculations used in different strokes:-

- Compression stroke

The mass flow includes the calculation the cylinder volume in Equation 3 and the heat is generated in the heat transfer in Equation 11. The specific heat changes during the gas exchange. The calculation of change in temperature is only for unburned zone because engine process is beyond combustion.

- Combustion stroke

The pressure is calculated in a single zone. The mass flow of the burned zone and unburned zone is the sum of two zones. However the temperature calculates in two zones, the calculations of change in temperature have two results where the mass flow of burned zone and unburned zone is not combined. In combustion stroke the heat is added from the combustion model in Equation 8.

- Expansion stroke

The calculation of is similar to compression stroke, since it acts as a volumetric pump. The different is the change in temperature in expansion zone only considers the burned zone. The temperature at the starting point of expansion zone uses the value calculated as the last point in the temperature of burned zone in combustion stroke.

- Exhaust and intake stroke

The start temperature used is the finishing point of temperature in burned zone. The mass flow changes as valve opens. The mass is calculated from the change in volume and flow events shown in Equation 17.

3.15 Network model

Flow elements are used to construct the flow network, which is the primary part of any model. The collection of flow elements available are organized into groups, representing element types. These elements are similar in various packages [71][91].

Ambient element is used as flow sources and sinks in a model and attach to the rest of the flow network via a single duct. This is most-commonly used element to represent an infinite reservoir at standard atmospheric conditions.

Cylinder elements is typically used to model the cylinder of an engine, however additional elements includes to model piston compressors and crankcases. Cylinder element is zero-dimensional and simply represents a volume changing with time. Cylinder connects to multiple flow elements via valves and usually require numerous sub-models in order to correctly represent the desired system.

Duct element represents a portion of a flow network which is long (in respect to cross sectional area) creating one-dimensional flow. It is automatically discretized into a series of computational cells based on a discretization length. A duct must be connected at each end to one ambient or cylinder element.

A fuel-to-air injector element injects the amount of fuel into a cylinder which enough to meet a specified fuel-to-air ratio, based on the total air flow through throttle. The actual fuel-to-air ratio is more or less than the demand ratio based on some of the air or fuel exiting through the valves.

3.16 Full engine simulation

The output of the engine is the power generates by the combustion and the resultant thermal expansion develops a force which pushes the piston to downward position and hence converts the mechanical movement into forward direction. The full engine simulation is required to achieve the increase and decrease of the speed, and the torque. Two additional models, intake manifold model and torque estimation model, are required to compute the full engine simulation.

3.16.1 Engine torque

The definition of torque is the angular moment which generates the mechanical power of the engine. However the relationship between torque and speed is that speed is represents by the level variable, which is not arbitrarily assignable, but torque can be arbitrarily. While engine is generated torque in the forward direction, there is torque push in the resist direction. This resistance force includes the weight of vehicle, air resistance and friction etc. Therefore, the engine torque has direct relationship with vehicle speed but also arbitrarily affects by the engine load.

The definition of torque can be explained by the pressure that has to act on piston during expansion. This pressure is called brake effective pressure (BMEP). BMEP is the mean pressure therefore it gives the averaged pressure of one cycle. Since engine torque depends on the engine displacement volume, the mathematics representation of brake mean effective pressure presents in Equation 21.

$$p_{me} = \frac{T_e.4\pi}{V_d}$$

Equation 21

where,

P_{me} is the break mean effective pressure

T_e is the engine torque

V_d is the cylinder displacement volume

In this thesis, the engine torque calculation is simplified by using the BMEP. The brake torque is presented in Equation 22, it defines as the difference between engine torque and load torque. The assumption is the load torque known where this value can be calculated with vehicle free body model but such calculations are not consider in this thesis.

$$Torque = T_e(t) - T_l(t)$$

Equation 22

where,

T_e is the engine torque

T_l is the load torque

3.16.2 Intake manifold

The speed of the engine increases by opening the throttle. The effect of the intake manifold pressure changes the initial pressure of the cylinder when the intake valve opens. An intake manifold model is needed to generate the change in speed. To calculate the rate of change in pressure, the intake manifold model can be modelled by Equation 23 [49]:-

$$\frac{d}{dt}p(t) = \frac{RT_m}{V_m}\left(A(t)\frac{p_a}{\sqrt{R.T_m}}.\frac{1}{\sqrt{2}} - \frac{p(t)}{R.T_m}.\frac{V_d.\omega_{e0}}{4\pi}\right)$$

Equation 23

where,

R is gas constant

T_m is manifold temperature

V_m is manifold volume

p_a is atmosphere pressure/ throttle pressure

V_d is cylinder volume

ω_{e0} is engine speed

The throttle is considered as a valve with the mass flow can be estimated using Equation 17.

3.17 Conclusions

The virtual engine is developed in this chapter. The implementation of the sub models use for detailed descriptions of engine process, including heat release (Wiebe), heat transfer (Woschni), gas exchange (thermal equilibriums), valve motions, and other factors such as friction and blowby have been discussed. The engine is further developed as a full engine simulation by implement the intake manifold allowing the estimation of engine speed according to the throttle opening event.

The engine simulation development can be concluded and the outlined contribution summarised as follows:-

1) The virtual engine simulation development is done as a 4-stroke medium size SI engine.
2) The engine simulation is generated based on the 1st law of thermo-dynamics, including various zero-dimensional sub-models contain detailed engine process descriptions.
3) The variable of the engine simulation includes the engine operating parameters outlined in 2.9, which are fuel-to-air ratio, ignition timing, exhaust valve closed timing and intake valve opening timing.
4) The outputs of the engine simulation return the exhaust composition including CO_2, O_2, CO and NOx, and the exhaust gas temperature.
5) The speed can be updated by throttle event.

3.18 Summary of Chapter 3

This chapter can be summarised by the development of a complete engine simulation in all considerations. The engine simulation is developed in four strokes combustion process, where the differences of simulation development approach is discussed in 3.2. The combustion in the engine processes in a tiny cylinder shape space and the geometry of the engine and mathematics approached in piston motion is explained in 3.3 and 3.4 respectively. Sub-models are required for the detailed combustion estimation, such as heat release (in 3.6), heat transfer (in 3.7 & 3.8) and the other matters including friction (in 3.9), blowby (in 3.10), emissions (in 3.11), valve motion (in 3.12) and exhaust factor (in 3.13) are explained. The network model which packs up the intake has been addressed in 3.15. The model is finished by the consideration of application in real engine, where engine speed and torque are the measurement for the engine output. Such model has been discussed in 3.16. The conclusion of this chapter is the engine model is developed for engine control simulation where most of possible factors in real application are included.

Chapter 4 Validation of engine simulation model

This chapter discusses the validation of the engine simulation developed in Chapter 3. The capabilities between different platforms are compared. The scenario is to build a single cylinder engine with same volume and geometries. All sub-models are applied with the same parameters. The comparison has been made through sets of steady state input parameters with varying fuel-to-air ratio, ignition timing and compression ratio. The comparison shows that the developed model agreed the performance of reference model, namely Ricardo Wave and Lotus Engine Simulation.

4.1 Introduction

The newly developed engine simulation is built and the detail of such development has been discussed in Chapter 3. The advantage to develop the engine simulation platform is that this thesis can focus on the required parameters for engine control [83]. To validate the model, the performance of the in-house engine simulation code is compared with three reference engine simulation platforms, namely Ricardo Wave, Lotus Engine Simulation and a book written by Ferguson [39].

The comparison of combustion performance can be determined by investigating the moment peak pressure and temperature in function of crank angle in the combustion stroke. Those two parameters drew the frame of combustion envelope. Therefore the engine performance and the form of emission can be incorrect if such timing of peak temperature and pressure between the model and reference are very different.

4.2 Capabilities

Cylinder and plenum are zero-dimensional elements in that they have properties of mass, pressure, temperature and volume but not length. The conditions within these elements are calculated at each crank angle by solving the mass equation and the energy equation derived from the first law of thermodynamics.

The mass equation accounts for changes in in-cylinder mass due to flow through valves, and due to fuel injection. A separate accounting is made for fluxes of air, fuel and products of combustion. The energy equation equates the change of internal energy of in-cylinder gases to the sum of enthalpy fluxes in and out of the chamber, heat transfer, and piston work.

There are two options: one-zone and two-zones. In the one-zone model implemented in LESoft [71], the whole cylinder is treated as one region. Whereas in the two-zone model implemented in RW and MESC, the cylinder is divided into two regions: an unburned zone and a burned zone which share a common pressure [91]. This thesis chose the two-zone model in which it can capture more detail of the engine processes taking place during the combustion period. It is noted that all combustion models may be used in either one or two-zone model, but emissions models generally require the two-zone model [39].

Table 5 shows the capabilities of different engine simulating software. The sub-models use in simulations is only presented in the table, with + means yes and – means no.

Sub-model/Controlled parameter	LESoft	RW	MESC
Geometry	+	+	+
Compression ratio	+	+	+
Air/fuel properties	C/H/O	C/H/O/N	C/H/O/N
Fuel composition	+	+	+
Air/fuel ratio	+	+	+
Injection timing	–	–	–
Heat release	Wiebe/Others	Wiebe/Others	Wiebe
Ignition timing	+	+	+
Conduction	Simple	Simple	Simple
Heat transfer	Woschni Annand Eichelberg	Woschni	Woschni
Friction	+	+	+
Blow-by	Simple	Simple	Percentage

Emission	+	+	+
Valve motion	Simple	Simple	Simple
Valve lift	+	+	+
Valve timing	+	+	+
Scavenging	Simple	Simple	Simple

Table 5 The capability of different engine simulation software packages.

4.3 Development of engine models

The solver reads a model from a main input file which contains all data required for a simulation (the model network, initial conditions for the flow field and all control data for the run). The solver produces an output file when run. The output file contains information, important in understanding the input, run-time processing and output of a model (time step output, engine summary, fuel burn progress summary, engine geometry, operating conditions, engine cylinder heat transfer, and performance). A general flow diagram for the development of a model is shown in Figure 16.

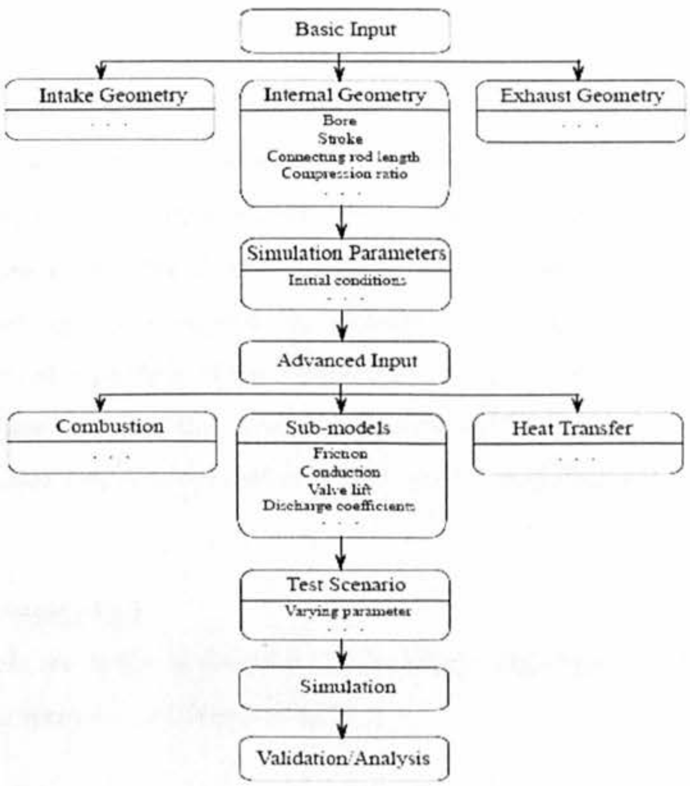

Figure 16 Development of engine model.

The basic engine data include engine geometry (bore, stroke, connector rod length, and compression ratio), engine inertia (mass and inertia of various components), cylinder and valve event phasing. Initial conditions such as exhaust temperatures, intake temperatures, and wall temperatures need to be input as reasonable values. The motion of the piston is calculated based on the data specified for bore, stroke, and connecting rod length. The clearance volume is calculated based on the compression ratio.

Once the basic inputs are defined, the advanced inputs need to be defined. These inputs are port flow coefficients, valve lift per crankshaft rotation, combustion and heat transfer modeling (types of models to be used for representing the combustion and heat transfer processes and the surface areas and temperatures of various components within the cylinder, phasing of cylinder firing with respect to TDC). Some intuition is used to determine the parameters due to the large difference in engine operating speed and difference in engine type.

To define the operation of the cylinder head, the valve lift per incremental camshaft rotation is defined. The results of valve lift versus incremental camshaft rotation are related to crankshaft rotation based on published valve opening points with reference to crankshaft position. Flow versus valve lift is defined. The input is in the form of flow coefficients or discharge coefficients taken from the empirical data [54].

Once these basic and advanced inputs have been satisfied, the simulation format is specified. Convergence detection allows the package to move on to the next case once a user-specified tolerance for convergence (tolerance is about 1%) towards a solution is attained on the active case. Simulation duration sets the number of cycles for the engine to run before settling on a solution. If auto-convergence is enabled, the package will move on to the next case once convergence is reached regardless of the number of cycles specified. If convergence is not reached by the number of specified cycles, the package will output a warning to let the user know that convergence was not reached within desired tolerances and will continue on to the next case.

4.4 Validation of engine model

Three engine models are designed with various packages, and engine operating parameters and sub-models are chosen to perform the tests.

4.5 Scenarios of tests

The tests with three packages, RW, LESoft and MESC, are performed for fixed engine geometry and different engine operating parameters. Test 1 is focused on comparison of the results computed with various packages and reference results presented in [39]. Ignition timing, fuel-to-air ratio and compression ratio are varied in the Test 2, Test 3 and Test 4 respectively. Profiles of pressure and temperature are plotted for various tests, and discrepancies of the results computed with various packages are discussed.

The engine model, used in the tests, represents a simple single-cylinder four-stroke engine. The engine geometry and engine operating parameters, which are fixed in the tests, are specified in Table 6. The engine cylinder has a bore of 0.1 m, stroke of 0.08 m and connecting rod length of 0.15 m. The engine speed is fixed at 2000 rpm. The intake temperature and pressure are 300 K and 1 bar. The exhaust temperature and pressure are 700 K and 1 bar. Initial temperature and pressure of the cylinder are 350 K and 1 bar. The fuel is gasoline (C_8H_{18}) with an equivalence ratio of 0.8. The Wiebe combustion model is used in all tests with parameters which fit many experimental data [39][54] (a = 5 and n = 3). The burning duration is fixed at 60 degrees although crank angle corresponding to the start of combustion may be varied in calculations. Heat transfer in the cylinder is described using Woschni correlation (C_1 = 2.28 while valves closed and C_1 = 6.18 for scavenging) [91]. The averaged cylinder wall temperature is fixed at 420 K. Exhaust valve opens and closes at 170 and 390 degrees, and intake valve opens and closes at 330 and 550 degrees (valve overlapping).

Parameter	Value
Bore, m	0.10
Stroke, m	0.08
Connecting rod length, m	0.16
Engine speed, rpm	2000
Intake pressure, bar	1
Intake temperature, K	350

Exhaust pressure, bar	1
Exhaust temperature, K	700
Fuel	C_8H_{18}
Equivalence ratio	0.8
Combustion model	Wiebe model
Combustion duration (deg)	60
Heat transfer model	Woschni model
Wall temperature, K	420
Valve timing, deg	EVO 170, EVC 390, IVO 330, IVC 550

Table 6. Geometry of the engine and engine operating parameters used in the test.

The engine operating parameters, which are varied in the tests performed, are presented in Table 7. All engine operating parameters are fixed for the Test 1. The burning initiation time is varied in the Test 2, fuel-to-air ratio is varied in the Test 3, and compression ratio is varied in the Test 4.

Test	Varied parameter	Interval of values
Test 1	No	Fixed values
Test 2	Ignition timing, deg	From –60 to 10 with step 10
Test 3	Fuel-to-air ratio	From 0.8 to 1.2 with step 0.1
Test 4	Compression ratio	From 6 to 14 with step 2

Table 7 Varied engine operating parameters.

Detailed verification and validation of sub-models describing chemical composition of combustion products, heat transfer, friction and combustion processes, and gas dynamics of intake and exhaust systems have been performed. The results obtained have been compared with the reference data presented in [39][54], and these results are not presented in the paper. Main attention of the thesis presented is drawn on predicting cylinder pressure and temperature distributions with various packages, and the use of the engine simulation packages in development of control systems.

Three packages are used to model the cycle of single-cylinder four-stroke engine, and three engine models are designed with various packages. The engine model itself consists of the flow network designed using flow elements, sub-models applied to the flow elements, and a control network, built using control elements. The piping and manifolds of the intake and exhaust systems are also modelled using the flow elements. The flow network, and intake and exhaust networks are then linked together through engine elements and sub-models.

4.5.1 Ricardo Wave

The engine model, designed with RW, is shown in Figure 17. The engine model consists of cylinder ('cyl1' element), and intake and exhaust networks each of which is designed using ambient and duct elements. The intake network consists of 'Intake' ambient element containing a fresh air at the temperature of 350 K and pressure of 1 bar, and 'duct2' duct element connecting manifold and cylinder. The exhaust network consists of 'Exhaust' ambient element containing exhaust gases at the temperature of 700 K and pressure of 1 bar, and 'duct3' duct element connecting cylinder and manifold. The fuel injector ('injector1' element) is installed in the middle of the connecting duct ('duct 2' element). Fuel is mixed with fresh air, and pre-mixed air and fuel mixture enters the cylinder. The cross-sectional area of intake pipe is 35 mm² ('duct2' element), and cross-sectional area of exhaust pipe is 28 mm² ('duct3' element). The maximum valve lift is 9 mm, and the default lift profile is used. The friction and blow-by parameters are by default. Other engine operating parameters are specified in Table 6.

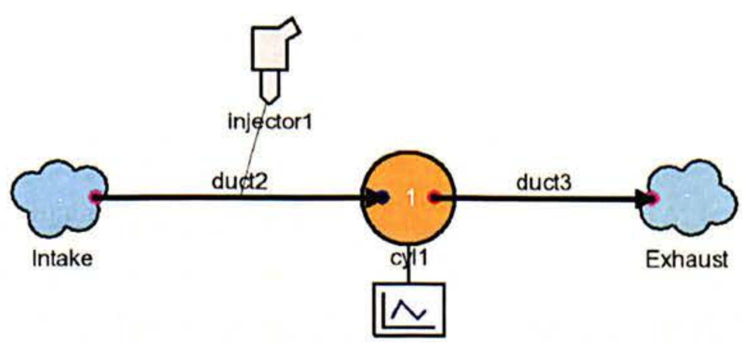

Figure 17 Engine model designed with RW.

4.5.2 Lotus Engine Simulation

The engine model, designed with LESoft, is shown in Figure 18. The engine model consists of the cylinder ('CYL1' element), and intake and exhaust networks each of which is designed using three elements representing connector, port and valve. The inlet connector ('INL1' element) contains fresh air at the temperature of 350 K and pressure of 1 bar. Fresh air goes through an intake port ('PORT1' element) with the diameter of 35 mm. The intake port is connected with the intake valve ('PVAL1' element). The exhaust gases leave the cylinder through the exhaust valve ('PVAL2' element) and exhaust port ('PORT2' element) with the diameter of 28 mm. The exhaust port is attached to the exit pipe ('EXT1' element), and the boundary conditions for exhaust gases are fixed at the temperature of 700 K and pressure of 1 bar. The maximum valve lift for both intake and exhaust valves are 9 mm, and the lift profile is 'fast lift' profile. The friction and blow-by parameters are by default. Other engine operating parameters are specified in Table 6.

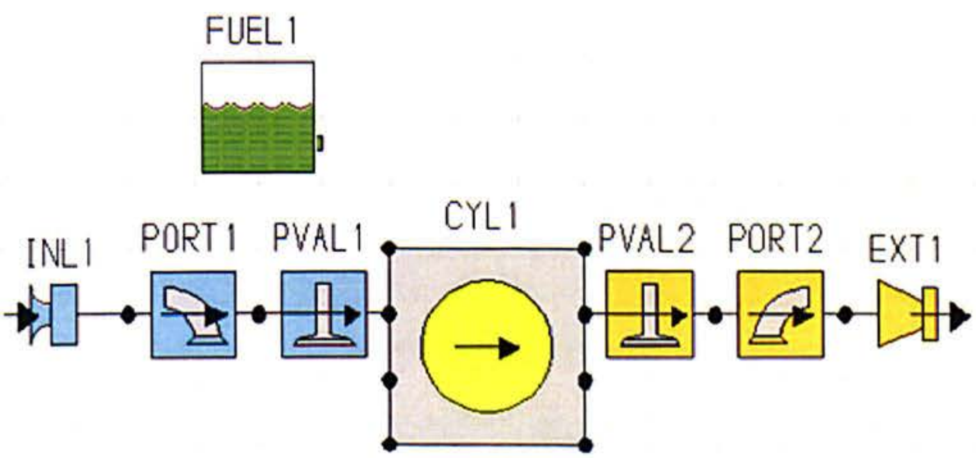

Figure 18 Engine model designed with LESoft.

4.5.3 MATLAB Engine Simulation Code (MESC)

The engine model, implemented with in-house package, MESC, is designed using flow and control elements specified in the text file (there is no graphics user interface, as this is in-house package). The friction and blow-by parameters are the same as in RW and LESoft engine models. Other engine operating parameters are specified in Table 6.

4.6 Comparison with reference results

The reference test is intended to match input parameters and settings for three packages as similar as possible. The engine models, designed with various packages, have been validated by comparing the results computed with reference results presented in [39]. The geometric parameters and operating parameters of engine are shown in Table 6, and three engine operating parameters, which are specific for this test, are presented in Table 8. The engine is a basic single-cylinder engine. The ignition timing is 35 degrees prior to TDC in the combustion stroke, compression ratio is 10, and fuel-to-air ratio of 1 (equivalent to fuel to air ratio is 14.7 by mass).

Parameter	Value
Ignition timing, deg	–35
Compression ratio	10
Fuel-to-air ratio	1

Table 8 Input parameters for reference test.

The accuracy of the curve coefficients that are used to describe the thermodynamic properties of the fuel, air and combustion products is established through internal consistency check and comparison to well established properties at the reference conditions ($T = 298.15$ K and $p = 1$ bar). Based on these results, it is concluded that the fundamental thermodynamic properties of the fuel, air and combustion product species are in agreement with published results in [39] to within the scatter of those results (typically less than 1%).

The pressure and temperature distributions in the engine cylinder, computed with various packages, are compared with the tabulated outputs from [39]. Comparisons between the results computed and those from [39] confirm that three packages produce reasonable data.

- Pressure distributions

The pressure profiles in the compression and combustion strokes are presented in Figure 19. The pressure distributions are started with crank angle of –180 degrees when the piston is at BDC. The pressure increases when the piston moves up to compress the air and fuel mixture. Ignition starts at –35 degrees before TDC when the combustion model starts to estimate the heat generated during combustion. The pressure rises due to the heat added to the compressed gas. The energy generated in the combustion process pushes piston down, volume increases and pressure drops. The results, predicted with RW and LESoft, are very close. The pressure profile, predicted with MESC, has a slightly delay in the maximum pressure point (this shift is about 2 degrees), and the maximum pressure level is about 6% lower compared to RW and LESoft results. Comparing the results obtained with the reference results of [39], calculations give delay in the maximum pressure point (this shift is about 10 degrees for RW and LESoft calculations, and it is about 8 degrees for MESC calculations), although the maximum pressure level, predicted with various packages, is close to reference data (discrepancy is about 3% for all packages).

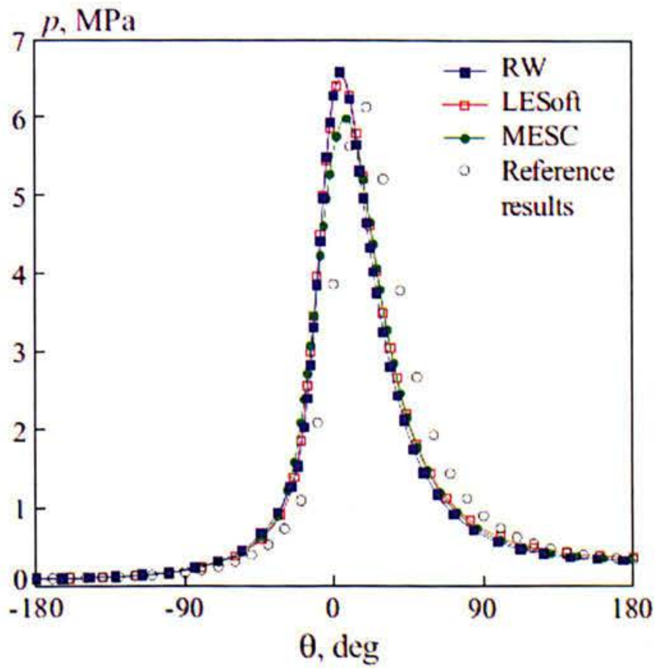

Figure 19 Comparison of pressure profiles with reference data of [39]

- Temperature distributions (two zones)

The results, presented in Figure 20, show the distributions of temperatures of burned and unburned mixture during compression and combustion strokes. Ignition starts at –35 degrees before TDC, when the combustion model starts to work in the burned zone. Calculations in the unburned zone continue without addition of heat due to combustion. Ignition duration is 60 degrees, and work of combustion model is finished at 25 degrees after the TDC. The temperature profiles corresponding to the burned and unburned mixtures are overlapped during the combustion interval (it is fixed at 60 degrees). The calculations after combustion depend on the temperature level reached in the burned zone. The reference results from [39] are plotted with the temperature step of 10 degrees. The reference results show a slightly lower level of temperature in the unburned zone and slightly higher level of temperature in the burned zone compared to the results computed with RW and MESC. Calculations with LESoft are based on one-zone model allowing prediction of averaged temperature in the engine cylinder. Discrepancy of the results computed with various packages may be explained by the different implementation of combustion models (there are some parameters and settings which are not controlled by the user) and small discrepancy in physical and chemical properties of fuel and combustion products.

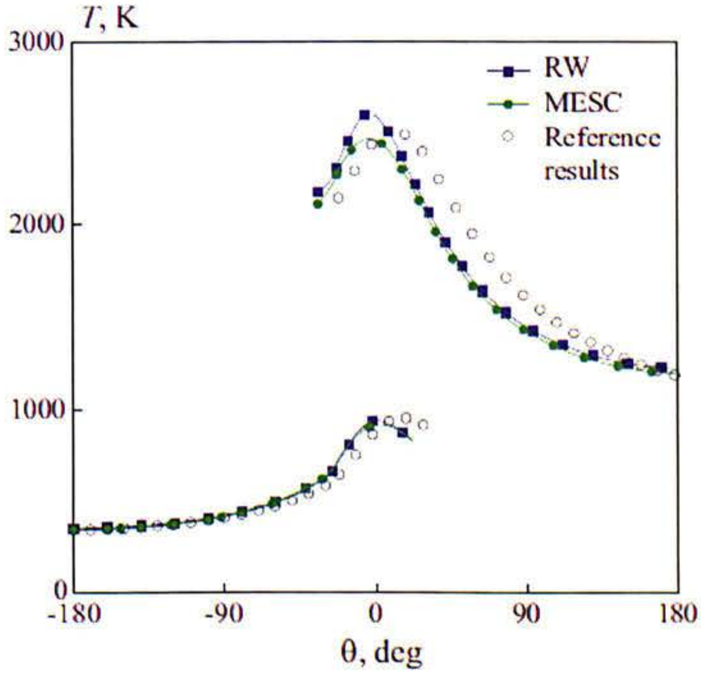

Figure 20 Comparison of unburned and burned temperature profiles with reference data of [39].

- Temperature distributions (averaged single zones)

The results, presented in Figure 21, show distributions of temperature averaged over burned and unburned zones (averaged temperature is not presented in [39] but may be calculated using results computed in burned and unburned zones). LESoft calculations are based on one-zone model, whereas results predicted with RW and MESC calculations are based on two-zone models. The temperature profiles out of combustion interval, which is fixed at 60 degrees, are very close for all packages. As for the profiles of temperature, presented in Figure 21, main discrepancy of the profiles of averaged temperature is related to the results corresponding to the combustion interval. LESoft and RW results are similar, although there is a slight delay in the peak of temperature occurring in RW calculations compared to LESoft calculations. MESC calculations have a visible delay in the occurrence of peak of averaged temperature and the maximum level of temperature which are about 3 degrees and 5% respectively.

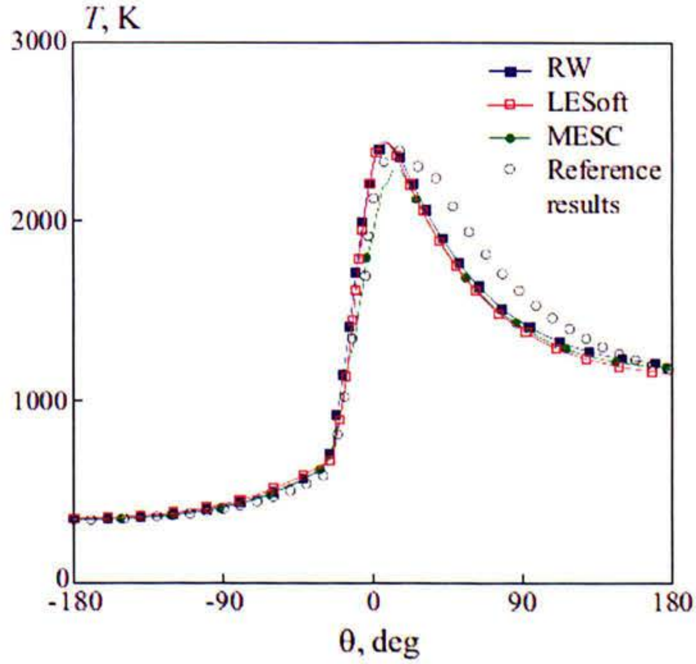

Figure 21 Comparison of averaged temperature profiles with reference data of [39].

The main factor affecting the pressure and temperature distributions in the engine cylinder is the calculation of heat generated during combustion (combustion sub-model). Although the heat release equation is matched in various packages considered, other factors may affect the results computed. In MESC and reference calculations from [39], the heat release escapes through the piston and cylinder wall gap using a blow-by fraction of 0.8, whereas RW and LESoft use default settings. Other factor affecting pressure and temperature profiles is heat transfer sub-model, which is not flexible to modify in RW. Inlet and exhaust pipe dimensions also affect the flows of air and combustion products in the cylinder, but these factors are not considered in the calculations presented.

The indicated mean effective pressure from the calculations with MESC package is 0.9528 MPa, whereas a value of 0.9510 MPa was obtained in [39] (a difference is about 0.2%). Discrepancies in the conservation of mass and energy are about 0.05% for all calculations.

4.7 Varying ignition timing

Ignition timing is one of the most important parameters in engine combustion control. In this test, different ignition timings are examined in terms of distributions of pressure and temperature in the combustion chamber. The geometric parameters and operating parameters of engine are shown in Table 6, and some other input parameters, which are specific for this test, are presented in Table 9.

Parameter	Value
Ignition timing, deg	–60, -50, -10, 0
Compression ratio	10
Fuel-to-air ratio (Fuel to air ratio)	1(14.7)
Valve timing, deg	EVO 170, EVC 330, IVO 390, IVC 550

Table 9 Input parameters for varying ignition timing test.

- Pressure distributions in different ignition timing

The pressure distributions, predicted with three packages, are presented in Figure 22. The results obtained are very similar in early ignition timing. For the late ignition timing, the discrepancy of the results computed is more significant in terms of occurrence of pressure peak. LESoft gives the earliest self-ignition which takes place just before crank angle of –10 degrees. The pressure peaks, predicted with RW and MESC calculations, are in a good agreement.

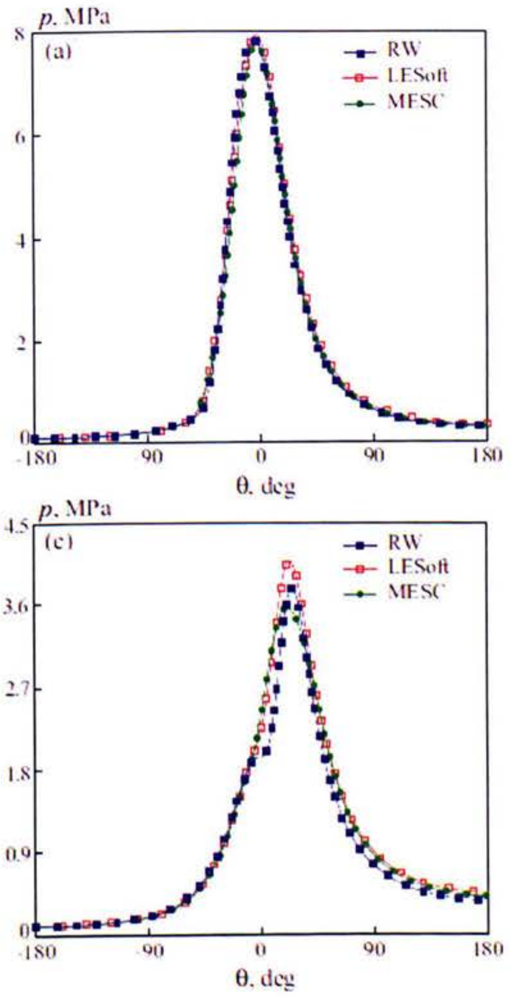

Figure 22 Profiles of pressure for different ignition timing of (a) is –60°, (b) is –50°, (c) is –10° and (d) is 0°.

There is a small difference in the maximum value of pressure, predicted with various packages. The location of pressure peak, predicted with three packages, is shown in Table 10. RW calculations give the earliest location of pressure peak, and LESoft calculations give the latest location of pressure peak in terms of crank angle.

Start of ignition, deg	RW	MESC	LESoft
–60	–2	–2	–4
–50	2	0	–6
–40	2	6	2
–30	8	10	8

–20	14	14	16
–10	22	20	24
0	32	30	34

Table 10 Location of pressure peak predicted with various packages.

- Temperature distributions in different ignition timing (averaged one zone)

The profiles of averaged temperature are shown in Figure 23. The profiles of temperature are very similar for three packages. There are, however, small differences in the maximum level of temperature and small differences in the corresponding crank angle. Those differences are caused by different assumptions on energy transfer in intake manifold, and intake and exhaust valves, and extra parameters like the cylinder materials.

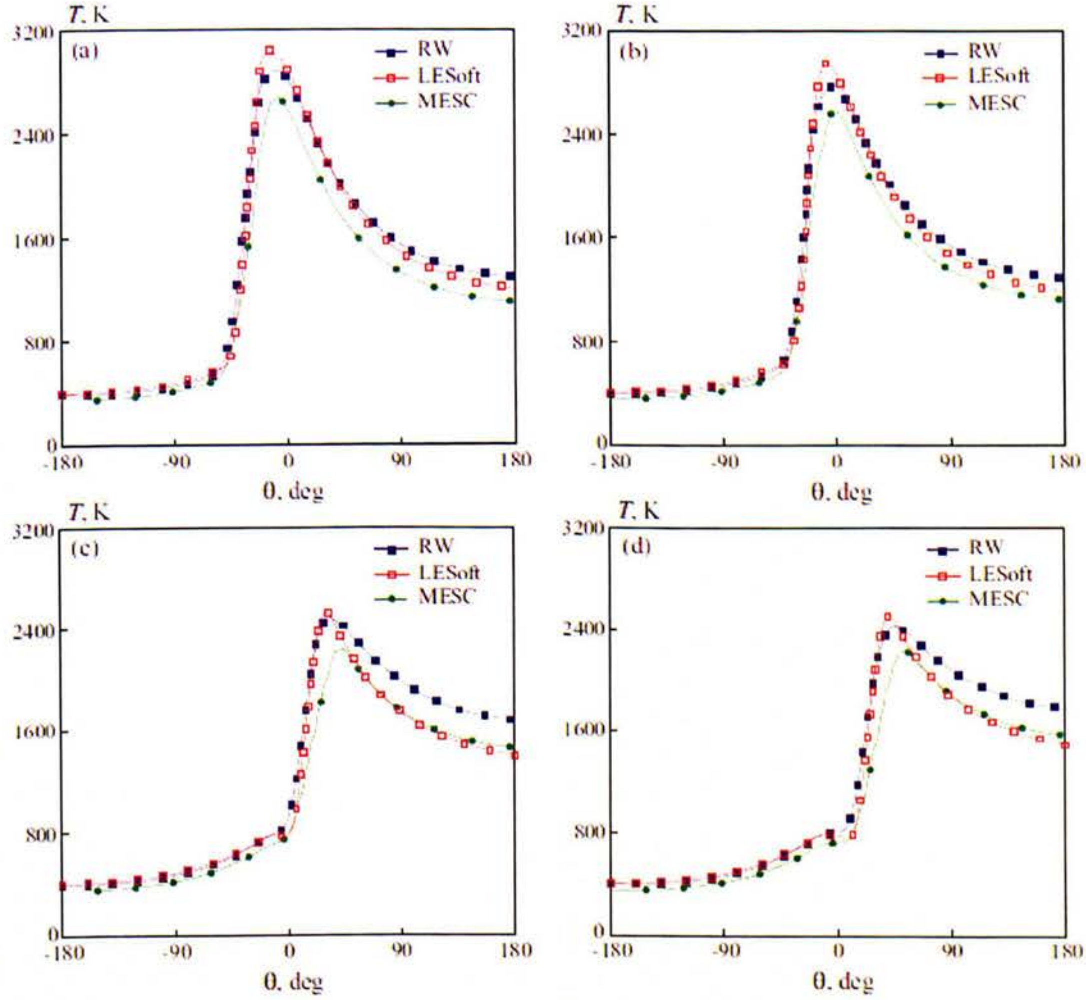

Figure 23 Profiles of temperature for different ignition timing of (a) is –60°, (b) is –50°, (c) is –10° and (d) is 0°.

The main discrepancy of the distributions of temperature, predicted with various packages, is related to the location of peak of temperature. These results are shown in Table 11. The temperature profiles, before crank angle corresponding to the ignition, are very similar. The location of peak of temperature, predicted with LESoft and MESC, takes place earlier than peak of temperature, predicted with RW. The sharp temperature decreasing taking place after the maximum of temperature during the expansion stroke is also similar between LESoft and MESC calculations. RW gives more slowly temperature decreasing during the expansion stroke. This behaviour may be explained by the combustion sub-model implemented in various packages. In the combustion model, implemented in RW, the timing is determined by the moment of 50% burned, rather than the start of ignition. The curve of mass fraction burned in LESoft and MESC packages may not be the same as in RW simulation. There is a more rapid increase in temperature when ignition started, until maximum of temperature reached. This result leads to a higher temperature when combustion finished even though the duration of burn is the same.

Start of ignition, deg	RW burned	RW averaged	MESC burned	LESoft
60	-8	-8	-16	-16
-50	-2	0	-12	-6
-40	-6	2	-8	2
-30	0	12	-4	10
-20	12	24	2	20
-10	22	34	10	30
0	28	46	20	40

Table 11 Location of temperature peak predicted with various packages.

If the start of heat release begins too late, it occurs in an expending volume, resulting in lower combustion pressure and lower network. If the start of heat release begins too early during the compression stroke, the negative compression work increases, since the piston is doing work against the expanding combustion gases. Delay of the initiation of combustion leads to the pressure peak occurring later during the expansion stroke. The pressure rise at $\theta_s = -10°$ is almost double that at $\theta_s = 10°$. As the start of heat release is changed from $\theta_s = -10°$ to $\theta_s = 10°$, the work input and the mean effective pressure decrease.

4.8 Varying fuel-to-air ratio

The other important parameters in engine combustion control in fuel-to-air ratio. Similar approach is done as in 4.7, but replaced the variable to fuel-to-air ratio. It is noted in some simulation platforms the input of the parameters of fuel-to-air ratio can be presented as fuel-to-air ratio (as shown in bold number inside bracket in Table 12). The geometric parameters and operating parameters of engine are shown in Table 6, and some other input parameters, which are specific for this test, are presented in Table 12.

Parameter	Value
Ignition timing, deg	-25
Compression ratio	10
Fuel-to-air ratio (Fuel to air ratio)	0.8 (18.38), 0.9 (16.33), 1.0 (14.7), 1.1 (13.36)
Valve timing, deg	EVO 170, EVC 330, IVO 390, IVC 550

Table 12 Input parameters for varying ignition timing test.

- Pressure distributions in different fuel-to-air ratio

The profiles of pressure computed with various packages in different fuel-to-air ratios are presented in Figure 24. All packages predict the maximum pressure level when the fuel-to-air ratio is stoichiometric. For leaner mixture, RW results are closer to those predicted with LESoft, whereas RW results for richer mixture are closer to the data computed with MESC. The comparison of the pressure profiles show that the shape of profiles is very similar for various packages, but the maximum pressure level is slightly different. The location of pressure peak takes place at the same crank angle for various packages.

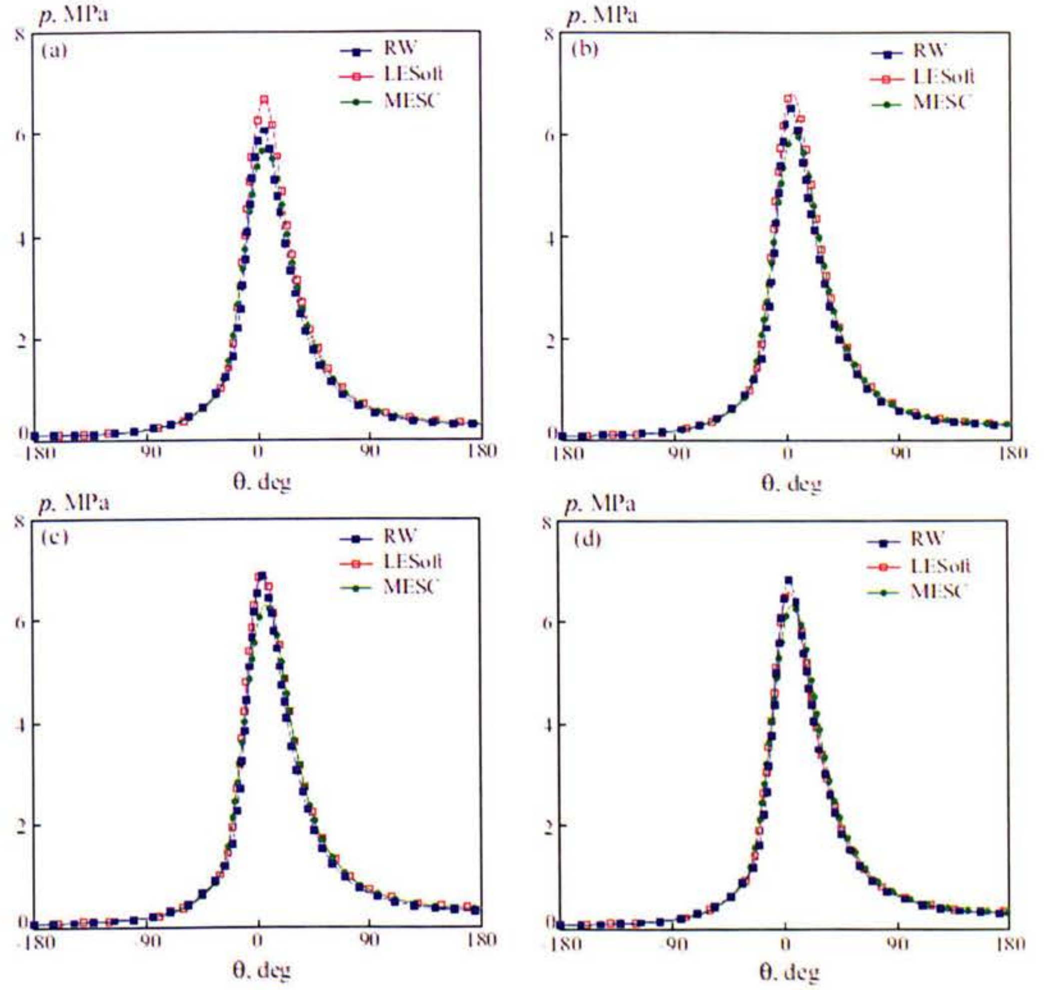

Figure 24 Profiles of pressure for fuel-to-air ratio of (a) is 0.8, (b) is 0.9, (c) is 1.0 and (d) is 1.1.

- Temperature distributions in different fuel-to-air ratio (averaged one zone)

The impact of fuel-to-air ratio on temperature profiles is similar to pressure as this is presented in Figure 24. The maximum temperature occurs when the fuel to ratio is stoichiometric. RW results are closer to LESoft results for learner mixture and closer to those predicted with MESC for richer mixture. In leaner mixture, RW predicts the location of temperature peak closer to the ignition point compared to MESC results. This may be because RW considers the position of the injection in a pipe, which affects the flow of mixture, and hence takes into account this effect in pressure and temperature distributions computed in the engine cylinder.

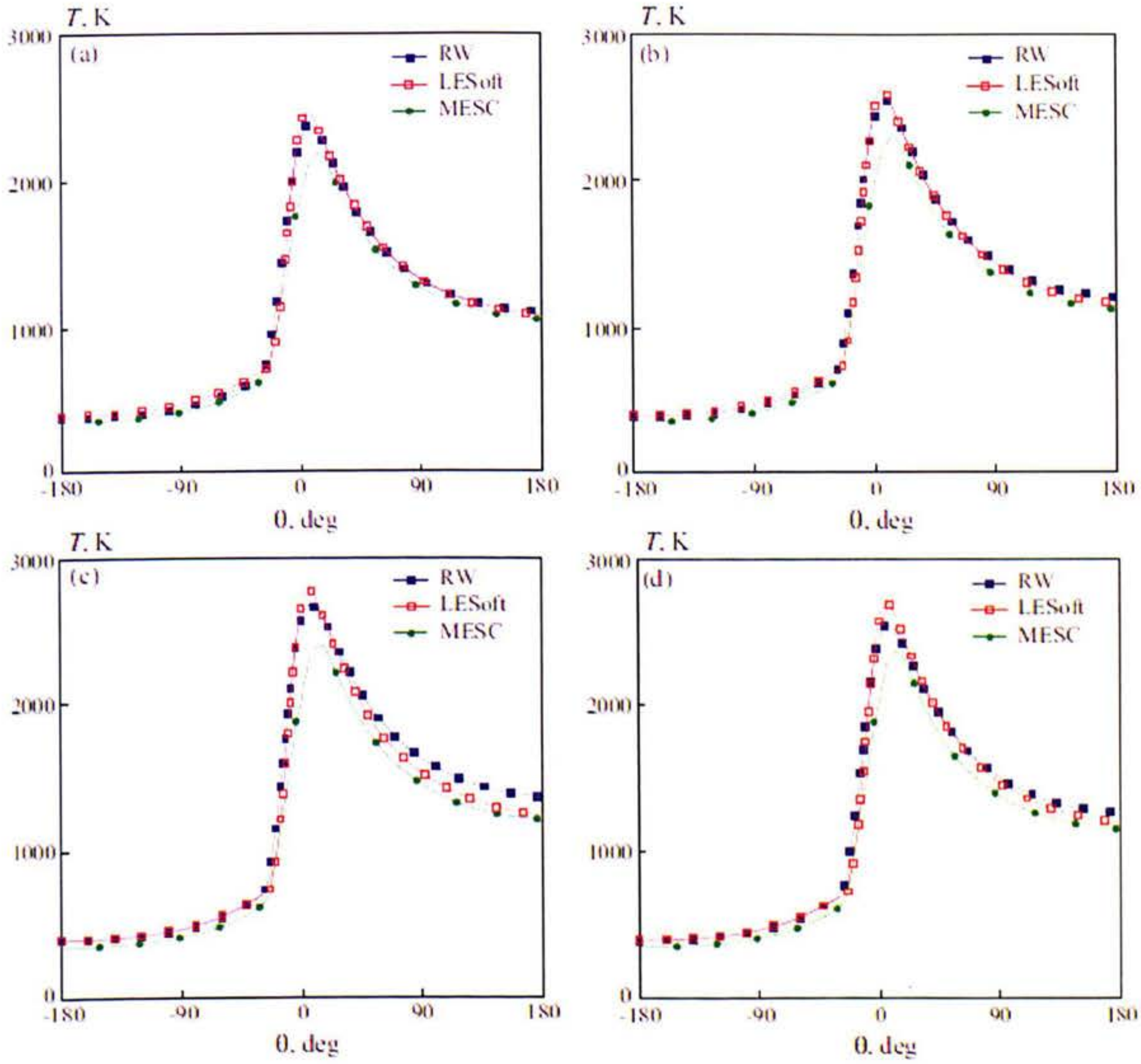

Figure 25 Profiles of temperature for fuel-to-air ratios of (a) is 0.8, (b) is 0.9, (c) is 1.0 and (d) is 1.1.

4.9 Varying compression ratio

Compression ratio is defined as the ratio of the maximum cylinder volume to the minimum volume. The compression ratio determines the peak pressure and the peak temperature in the cycle. The efficiency of the engine and formation of pollutants are strong functions of the compression ratio. The compression ratio is limited by the material strength and engine knock. Engine heads and blocks have a design a maximum stress, which should not be exceeded, limiting the compression ratio. Compression ratio is difficult to control due to fixed geometry of cylinder. In practice, compression ratio can be varied by changing the piston head surface shape. The geometric parameters and operating parameters of engine are shown in Table 6, and some other input parameters, which are specific for this test, are presented in Table 13.

Parameter	Value
Ignition timing, deg	-25
Compression ratio	6, 8, 10, 12
Fuel-to-air ratio	1.0
Valve timing, deg	EVO 170, EVC 330, IVO 390, IVC 550

Table 13 Input parameters for varying ignition timing test.

- Pressure distributions in different compression ratio

The results of pressure distributions computed with three packages are presented in Figure 26. The pressure increases as compression ratio increases, and the data obtained are in agreement with theory [39][54]. The position of maximum level of pressure slightly depends on the compression ratio.

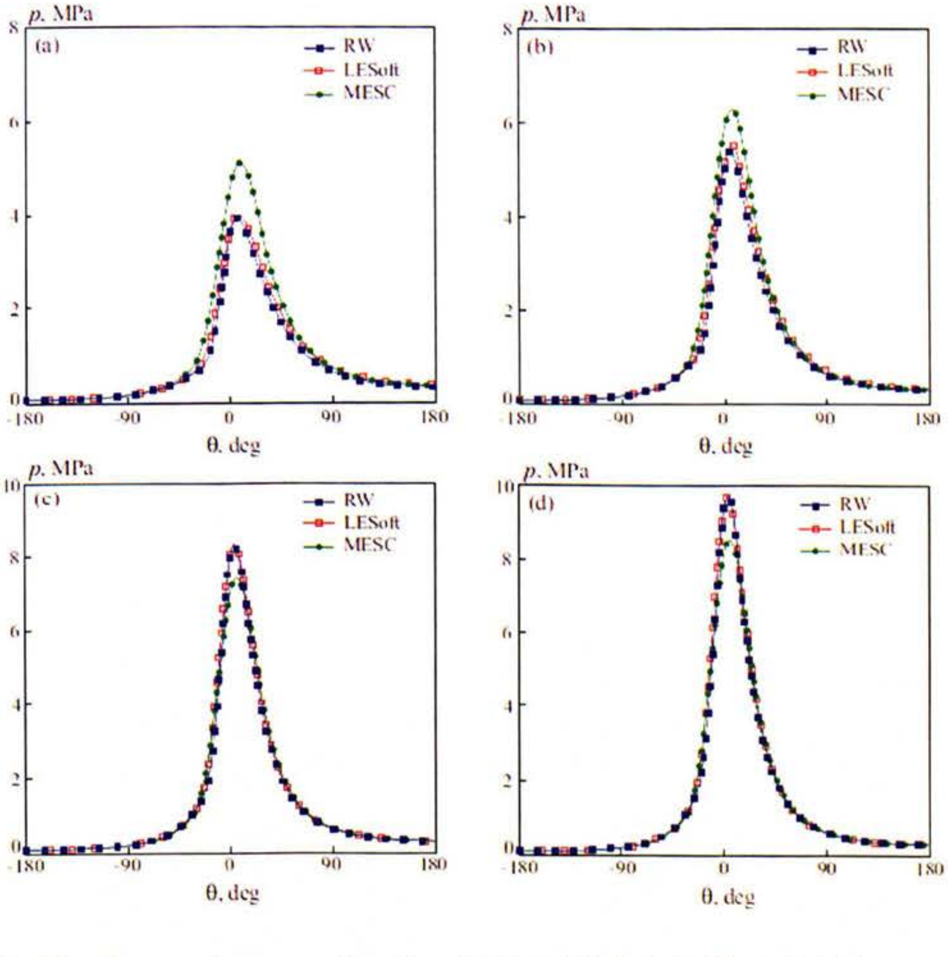

Figure 26 Profiles of pressure for compression ratios of (a) is 6, (b) is 8, (c) is 12 and (d) is 14

- Temperature distributions in different compression ratio (averaged one zone)

In LESoft and MESC calculations, the temperature slightly increases as the compression ratio increases as this is presented in Figure 27. In RW calculations, the highest temperature is observed at the compression ratio of 10. There is no significant change to observe in different compression ratio used in simulations.

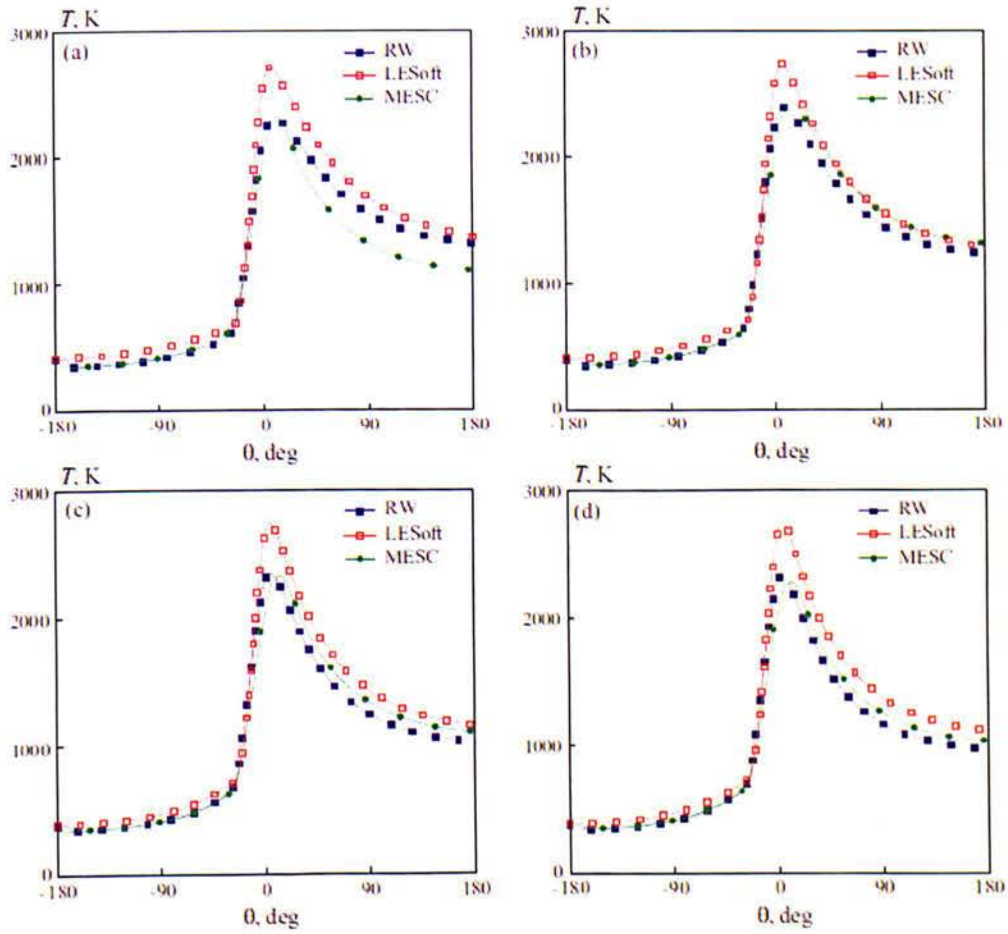

Figure 27 Profiles of temperature for compression ratios of (a) is 6, (b) is 8, (c) is 12 and (d) is 14.

4.10 Comparison of level of emissions

In practice, the level of emissions between different packages are worth to investigate for theirs' performance. However the comparison is not valid while the resultant emissions cannot be obtained from reference book [39]. Compare to the commercial package, the LESoft package has no emission data as output [71]. The only comparison can be made is the MESC and Ricardo Wave. Ricardo Wave has the emission sub-models which covered the level of CO, NO_2 and PM. The level of CO_2 can be estimated from the level of CO [91]. With such limitations, the comparison of emissions is not considered in this thesis.

4.11 Conclusions

The engine model used in this thesis has been developed in Chapter 3. This chapter gave the validation check for the in-house developed code for further use in this thesis. Two commercial engine simulation packages, Ricardo Wave (RW) and Lotus Engine Simulation (LESoft) have been used as reference as those two shortlisted packages had developed such codes based on many Laboratory works. In addition, the results presented in [39] have been also used as reference for comparisons of results. The conclusions of this chapter can be drawn as follow:-

1) The performance between different packages has been compared in terms of the distributions in engine combustion, including the investigation of timing of peak pressure and peak temperature.
2) Further comparisons include different variables, namely, fuel-to-air ratio, ignition timing and compression ratio.
3) The in-house model has similar performance compared to the two commercial engine simulations packages, and better than the results published by Ferguson [39].
4) The results including the engine simulation model and the validations discussed in Chapter 3 and Chapter 4 have been published [21].

4.12 Summary of Chapter 4

This chapter completed the validation of the developed engine simulation code using MATLAB. The capability between different simulation software packages has been discussed in 4.2. The developed software and candidates of comparison are explained in 4.3 & 4.4. The setting of the test is given in 4.5. The initial test was based on a set of fixed engine operating parameters and results are explained in 4.6. The next step is to test the variable engine operating parameters. They are set to a single variable input while other parameters are fixed. The test results, including variable ignition timing in 4.7, variable fuel-to-air ratio in 4.8 and variable compression ratio in 4.9, agreed that the MATLAB engine simulation estimation of combustion envelope is similar to the ones provided by the two commercial software. These two commercial software packages include more detail in the engine modelling with respect to the developed code; however, this does not affect the overall performance of the MATLAB code.

Chapter 5 Artificial Intelligence for Fuel Estimation

This Chapter develops an artificial intelligence fuel estimator which is able to identify the likelihood of given fuel compositions input into the engine. The outcome of fuel estimator is aimed to provide further engine parameters control while fuel composition is continuously changing after refuelled.

Three different fuel compositions, Isooctane, Methanol and Ethanol, are used as input composition. Dataset contains engine operating parameters and levels of emission, are collected using random engine operating parameter. The development of the fuel estimator generates the model which is able to find the relationship between emissions and input fuel by developing the neural network of inverse the engine process. The original fuel composition can be estimated through the composition of emissions, include the level of CO_2, O_2, CO and NOx.

Two methodologies, Adaptive Neuro-Fuzzy Interface System (ANFIS) and artificial feed-forward neural network, are used to achieve the AI fuel estimation. The original tests are targeted the estimation of fuel in number of atom of Hydrocarbons. The results show the comparison between two models of feed-forward neural network and ANFIS. Former one performed better than the latter. As a matter of facts that ANFIS requires a large set of fuzzy rules which are extremely difficult to handle a large set of engine data unless the method for data reduction is found. Further study develops the feed-forward fuel estimator which is able to estimate the number of the given fuels by likelihood, providing proportional control in engine operating parameters.

5.1 Introduction

The composition of the exhaust gas is determined by the original fuel composition and combustion performance; therefore by inversing the combustion process, the combustion performance can be computed through the engine exhaust gas. Although the actual composition of the fuel contains number of atoms of Hydrocarbon, this information remains unknown by the engine since the fuel mixture provides from fuel suppliers do not give any of this information. Fuels are categorised by name and standardised by Octane number. The importance of using fuel as parameter against combustion performance has been discussed in Chapter 2.5.5. Therefore, fuel composition information is believed to be an important parameter in engine control if it is obtainable.

In practical situation, the information of exhaust gas can be obtained from the sensors discussed in Chapter 2.6, which includes CO_2, CO, O_2 and NOx. In simulations, exhaust gas compositions can be estimated using engine model which is discussed in Chapter 3. In order to develop the artificial intelligence system to estimate fuel through idea of inverse engine process, dataset recording the exhaust gas data and various engine operating parameters are needed. The dataset should be able to cover most of engine behaviours in various situations. The dataset can be treated as reference training set to generate the system identification models. The investigation of two system identification methods, artificial neural network and ANFIS, will be discussed later in this chapter.

5.2 Artificial Neural Network (ANN)

Artificial Neural Network (ANN, refer as Neural Network) is a model which can be used as system identification, pattern recognition and model linearization. Engine emissions are arbitrarily affects by engine loads, engine speeds and engine operating parameters, and formed as nonlinear response which is unlikely to obtain the transfer function. Artificial neural network methodologies can generate the model capable of defining the relationship between the input and output and also predicting the desired variables through the statistical training process. The artificial neural network is inspired by biological nerves system. The model finds the correlation of non-linear behaviour and stores the weighting as interconnected neurons. Neurons are generated are based on the adjustment on the weight according to the difference between the network output and the targeted value.

5.2.1 Feed-forward Neural Network

A simple feed-forward neural network is the methodology of ANN considers as an open-loop control. Different from a look-up table, the network is able to update the weighting through the learning process. Dataset of past data is trained using the back-propagation method. The network is developed including neurons in hidden layer and in output layer. Figure 28 shows the block diagram of the hidden layer. Inside the hidden layer, the inputs are weighted and stored as neurons. These neurons are added and bias if needed. Finally the net input will be passed through the artificial transfer function, normally uses 'tansig'. In any ANN, the neural network can have more than one hidden layer. The output layer is similar to hidden layer. The inputs of the 'output layer' are the weighted net output from the 'hidden layer'.

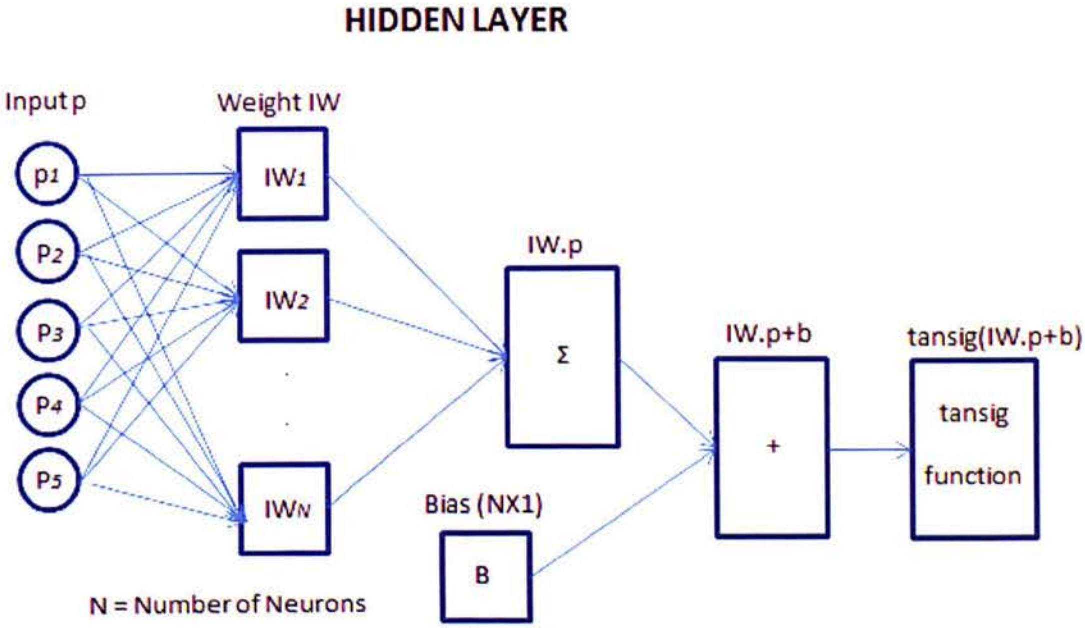

Figure 28 Block diagram of a hidden layer in an ANN

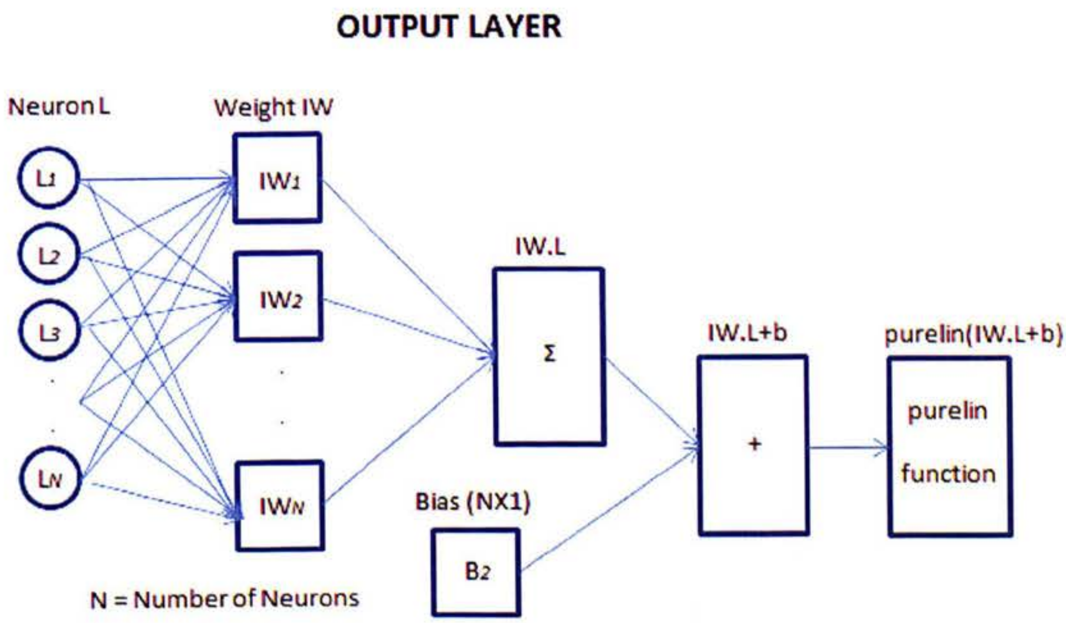

Figure 29 Block diagram of a output layer in an ANN

5.2.2 ANFIS model

Adaptive Neuro-Fuzzy Interface System (ANFIS) is an ANN method based on Takagi-Sugeno type fuzzy interface system. ANFIS only returns to a single output only although there is no limit on the number of inputs [24]. Such system contains both fuzzy logic and neural learning principle in a single framework. The structure of ANFIS for two inputs model is shown in Figure 30.

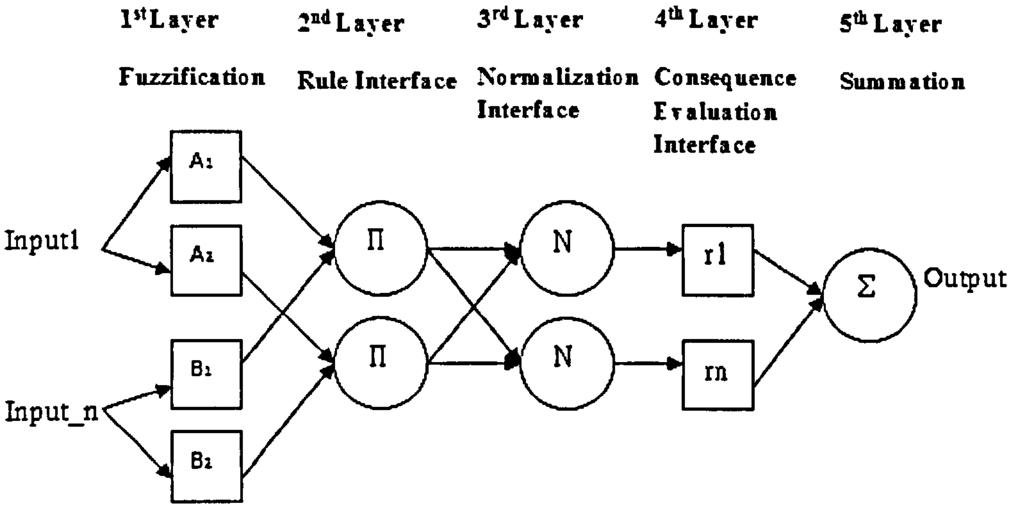

Figure 30 Block diagram of an ANFIS model

The procedure of ANFIS can be summarised as follow:-

1) Once the dataset is collected, the data is fuzzified and the If-Then rules are used to generate rules for neural training.
2) The fuzzy sub-set is used as the input of the neural network. The learning algorithm uses a hybrid method combines with least-square and back-propagation gradient descent.
3) The output is the summation of the weighted value of neurons evaluating from the neural network.

5.2.3 Neural network data collection

The preparation of the experimental dataset before training can enhance the performance of the neural network. In the development of fuel estimator, the data records the emission using three different fuels, which are Isooctane, Methane and Ethanol. The dataset also records the behaviours of engine using random engine operating parameters, including fuel-to-air ratio, ignition timing and valves event and the ranges of these parameters are shown in Table 14. The species of emission compositions record are CO_2, O_2, CO and NOx.

Parameters	Range
Fuel used	Isooctane (C_8H_{18}) Methanol ($C_1H_4O_1$) Ethanol ($C_2H_6O_1$)

Fuel-to-air ratio	0.8 to 1.2
Ignition	-10 to -50 deg
Exhaust valve open timing	330 to 390 deg
Intake valve open timing	330 to 390 deg

Table 14 Parameters and the ranges are used to record the experimental simulation dataset

The engine model is shown in Figure 31.

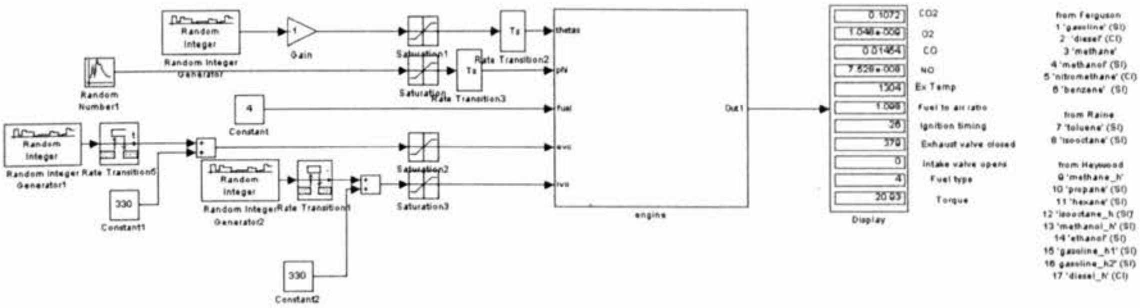

Figure 31 Engine data collection model

5.2.4 Division of dataset

The dataset are divided into two parts:-

Training set – The number of data are recorded for training in 1092 seconds. This training set is only used in training for development the engine control model.

Validation set- The number of data are recorded for validation in 630 seconds. This validation set is not used in training and treats as blind data. The dataset is used for testing data when needed.

5.2.5 Data normalisation

Data normalisation is important to the improvement of ANN performance. By considering the values of data collected in different range, for example, the valve timing has the range between 330° to 390° whereas the emission is CO_2 in range between 0.07 and 0.12. The difference which can be very large compared one parameter with another, produces a bigger bias to some parameters. The recommendation of developing better neural network performance is always a good practice to normalise the data. The dataset is also normalised by calculation of Equation 24.

$$Normalise = \frac{x_{max} - x(t)}{x_{max} - x_{min}}$$

Equation 24

The performance of the neural network can be represented by r-square. R-square is a statistic term where the calculation of the square of residuals finds the correlation between the response values and the predicted response values. The equation to calculate r-square is shown in Equation 27.

Sum of squared residual (SSr)

$$SSr = \sum (y(t) - u(t))^2$$

Equation 25

where,

y(t) is the predicted data

u(t) is the experimental data

Total sum of square (SSt)

$$SSt = \sum (y(t) - \bar{y}(t))^2$$

Equation 26

where,

$\bar{y}(t)$ is the mean value of the experimental data

$$RSquare = 1 - \frac{SSr}{SSt}$$

Equation 27

Figure 32 shows the r-square calculated from feed-forward neural network and ANFIS system. The r-square of feed-forward neural network is 0.8415, which is higher than that of

ANFIS system r-square which is 0.7116. The feed-forward neural network has the higher accuracy in the fuel estimation.

```
>> for i = 1:1500
SSr(i) = (fuel_val(i,1)-NN_val1(1+i,1))^2;
SSt(i) = (fuel_val(i,1)-fuel_mean(1,1))^2;
end
SSres = sum(SSr);
SStot = sum(SSt);
RSquare_NN = 1-(SSres/SStot)

for i = 1:1500
SSr(i) = (fuel_val(i,1)-ANFIS_val(1+i,1))^2;
SSt(i) = (fuel_val(i,1)-fuel_mean(1,1))^2;
end
SSres = sum(SSr);
SStot = sum(SSt);
RSquare_ANFIS = 1-(SSres/SStot)

RSquare_NN =

    0.8415


RSquare_ANFIS =

    0.7116

>>
```

Figure 32 MATLAB code for computation of R-sqaure of feed-forward NN and ANFIS

5.3 Behaviour of exhaust gas composition

The product of an internal combustion engine contains Carbon Monoxide (CO) and Nitric Oxide (NO). The amounts of these two compositions which are the major source of pollution to urban areas need to be limited to the level stipulated by law. Fuels consist of a number of carbon and hydrogen atoms. When fuel reacts with atmospheric air, air contains oxygen and large amount of nitrogen formed the products of Carbon, Hydrogen, Oxygen and Nitrogen.

CO, forms of reaction in Carbon and Oxygen, can be generated when the engine performs incomplete combustion. Insufficient amount of fuel and air injected into engine cylinder results in some oxygen left unburned and a portion of the carbon reacts with un-used oxygen during the combustion stroke producing CO. NOx forms due to the high temperature burning process. The high temperature burns gas behind the frame. It contains nitrogen and oxygen which form when they do not reach chemical equilibrium. Both toxic compositions, CO and NOx, cool down during the temperature drop in the expansion stroke and are emitted during the exhaust stroke.

5.3.1 Fuel-to-air ratio (FAR)

One of the most important engine operating parameters in emission control is fuel-to-air ratio (ϕ). The engine has been designed to run the engine with fully burned and the ratio is stoichiometric (see 2.7.1), at which ϕ can be calculated from Equation 28 and has a value of 1. The fuel-to-air ratio can be obtained from Equation 28. When the value of FAR is less than 1, the mass of air increases and the mixture is considered as leaner mixture (excess in air) [76]. When FAR is bigger than 1, it is considered as richer mixture (insufficient air) [76].

$$FAR(\phi) = \frac{mass_{fuel}}{mass_{air}} \cdot \frac{1}{14.7}$$

Equation 28

where,

$mass_{fuel}$ is the mass of fuel

$mass_{air}$ is the mass of air.

Engine normally operates close to stoichiometric combustion or slightly leaner to ensure reliable operation [54].

However, engine control can adjust fuel-to-air ratio slightly richer or leaner. In a cold engine temperature fuel vaporization is slow. Mixture is easier to be combusted with more fuel particles enter and flow in the cylinder, that means cold temperature is better operates at richer mixture [55]. When the engine is warmed up, the enrichment is no longer valid. More fuel particles produce higher level of CO so FAR ϕ needs to be adjusted.

Figure 33 shows the engine simulation of the behaviour of CO_2, O_2, CO and NOx at different fuel-to-air ratio. Assuming the engine temperature and all other engine parameters are fixed, CO_2 level is the highest at stoichiometric state. When the mixture is lean, higher level of NOx is produced and more O_2 is left unburned after combustion. When the mixture is rich, higher level of CO emitted. Same behaviours of exhaust composition also found in various articles [54][55].

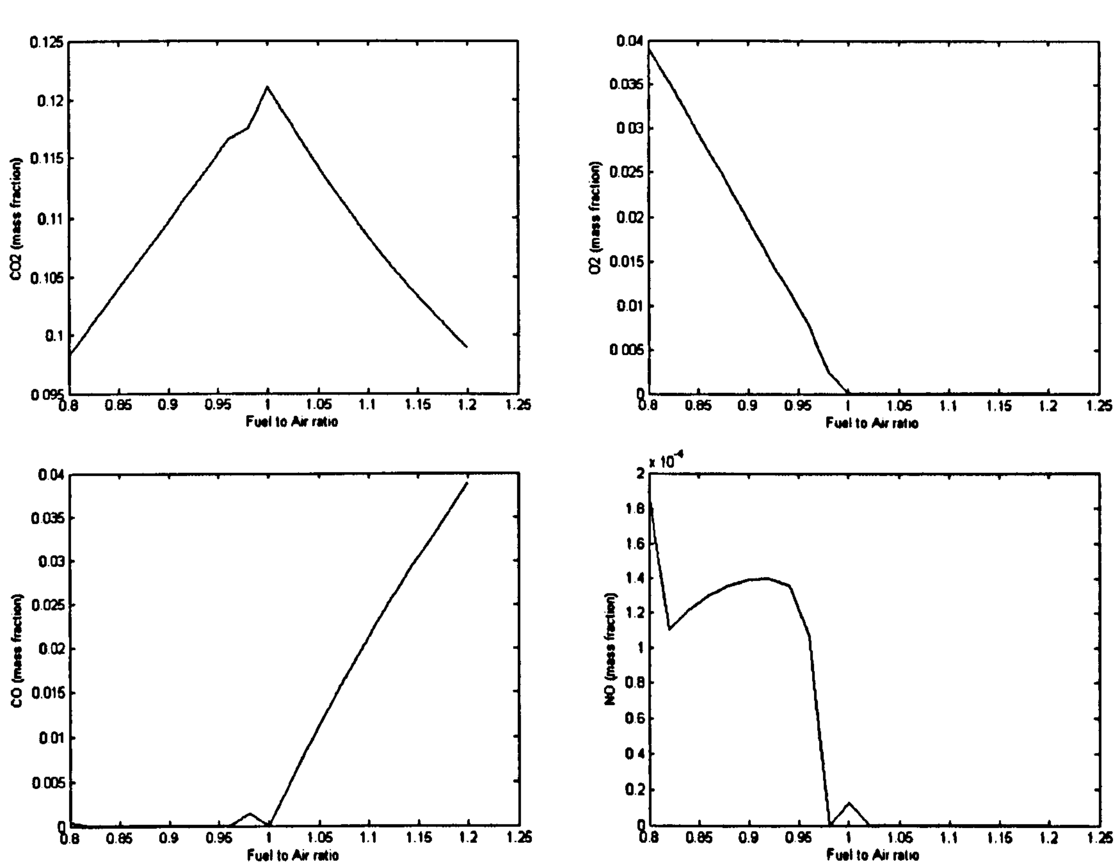

Figure 33 Behaviour of CO_2, O_2, CO and NOx at different fuel-to-air ratio

5.3.2 Ignition timing

The other important engine operating parameter which can be controlled is the emission spark timing, sometimes called ignition timing. The maximum pressure which is developed during combustion should occur at about 10° to 40° beyond TDC, depending on engine speed and engine load. Ignition timing is designed to achieve this. The timing of ignition determines the duration the frame propagates before cylinder volume expands, and hence it determines the combustion temperature. Discussed in 5.3, temperature is a factor of the formation of CO and NOx. By slightly adjusting the ignition timing improves emissions. However, ignition timing needs to be carefully determined to avoid engine knock.

Figure 34 shows the behaviour of CO_2, O_2, CO and NOx at different ignition timing. Other parameters, fuel-to-air ratio, valve events, engine speed and engine torque are fixed. The least level of O_2, CO and NOx is found at the correct ignition timing at about -26° to -28°. The trade-off is at the same ignition timing, the maximum of CO_2 level is found in that range at

0.1211. By comparing the minimum level of CO_2 found at other ignition timing, which is 0.1209, the increase is not significant (i.e. 0.0002) at the optimal ignition timing.

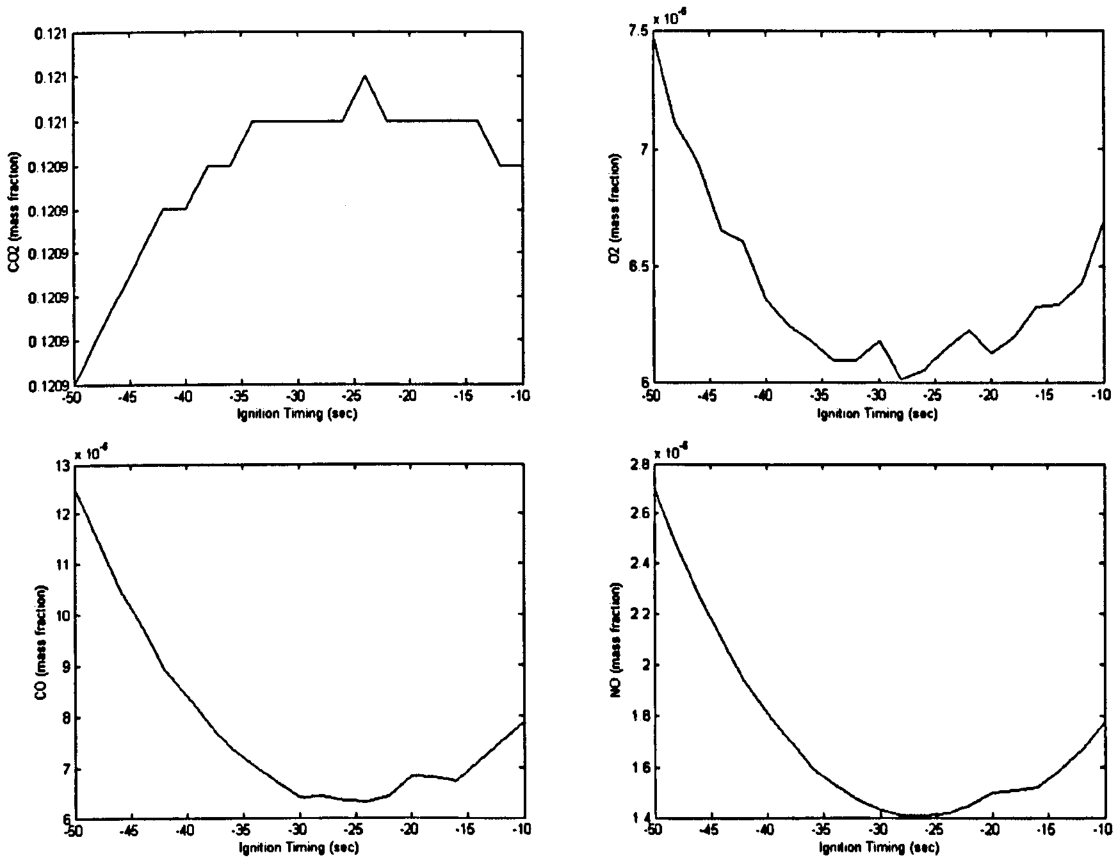

Figure 34 Behaviour of CO_2, O_2, CO and NOx at different ignition timings

5.3.3 Valve timing

The intake valve event determines the temperature and pressure during the compression stroke, whereas the exhaust valve timing determines the end temperature in the exhaust stroke and the amount of exhaust gas trapped in the cylinder (EGR process). Both valves event also determine the amount of air enter the cylinder and hence change the fuel-to-air ratio. However the ratio can be adjusted by the actuation of the throttle and the fuel injector. There are various studies in valve timing and have been discussed in 1.5.2. The studies on valve timing are mainly focus in different speed ranges although they also have effect on emission. In this thesis, the assumption is made on the envelope of the valve profiles are fixed. The controller only optimises the exhaust valve closed timing and intake valve opening timing in unit of crank degree.

5.3.4 Fuel composition

The combustion product is the reaction between air and fuel in a high temperature process. Fuel composition determines the form of emission after engine combustion process. Simulation results are used to compare the different fuel compositions with different fuel-to-air ratio and ignition timing.

The behaviour of emissions using different fuel-to-air ratios has been discussed in 5.3. Figure 35 and Figure 36 show the simulation results of CO and NOx using different fuel compositions and operates at different fuel-to-air ratios. Different colours represent different fuel compositions and the behaviours are shown in curve diagram with fuel compositions against different fuel-to-air ratios such that the level of emissions varies.

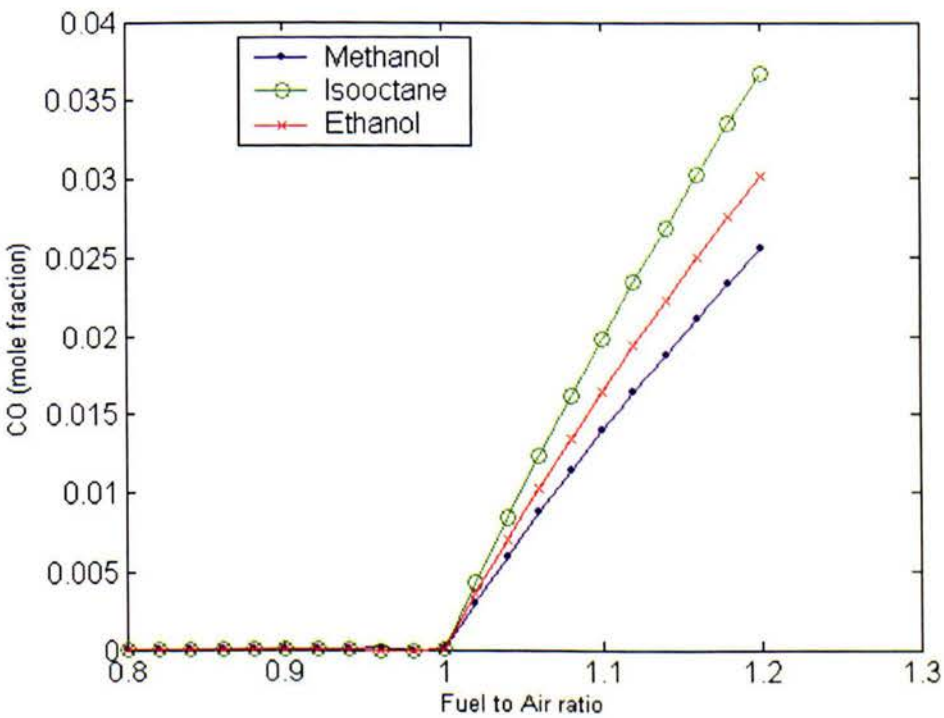

Figure 35 CO level found at different fuel-to-air ratios

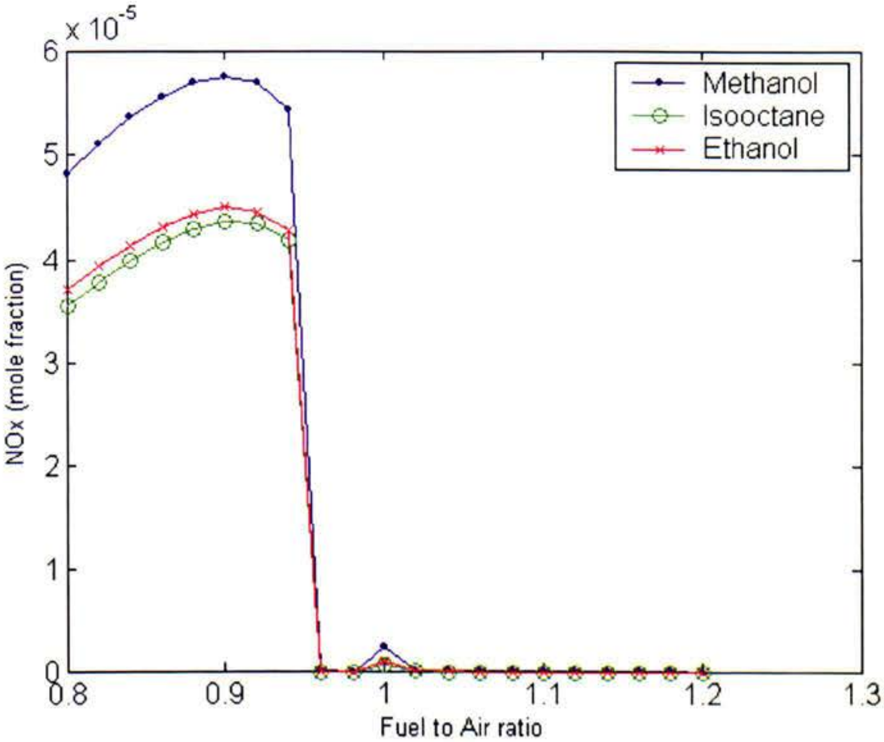

Figure 36 NO level found at different fuel-to-air ratios

Figure 37 and Figure 38 show the result of simulation which varies ignition timing when FAR ϕ is at stoichiometric ratio. The simulation is to observe the behaviour of CO and NO. At certain ignition timing, mixture almost burned completely before the beginning of expansion stroke. The red line denoted in both Figure 37 and Figure 38 represent results in Methanol which is found to have the highest CO and NOx level. In reality, Methanol can be the source of fuel mixture only in a certain portion of it added in the fuel.

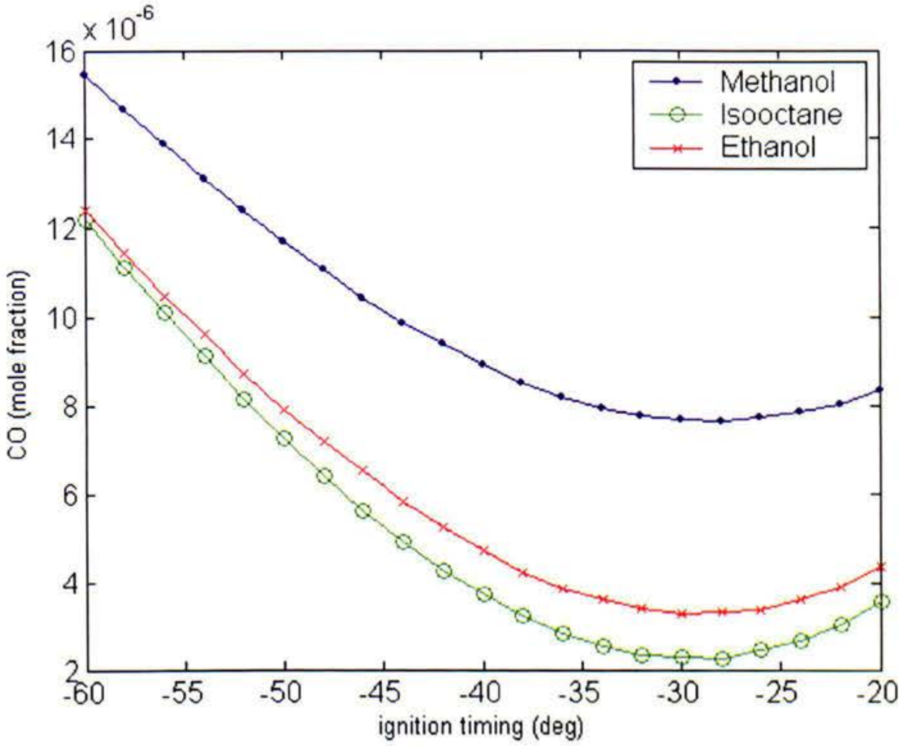

Figure 37 CO level found at different ignition timings. The red line represents Methanol

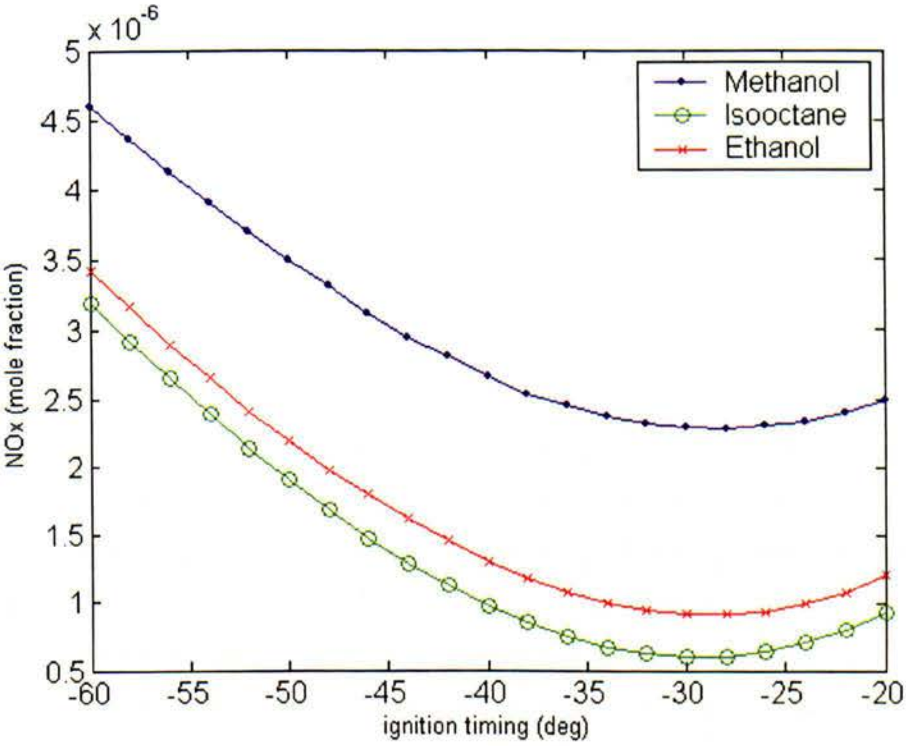

Figure 38 NO level found at different ignition timings. The red line represents Methanol

5.4 Fuel composition estimation

In this thesis, two methods are investigated, i.e. feed-forward neural network and Adaptive Neuro-Fuzzy Interface System (ANFIS). The dataset is collected from a random set of engine parameters such as fuel-to-air ratio, ignition timing, and valve timing events. The dataset is taken data from three different set speeds, 1000rpm, 2000rpm and 4000rpm, and 3 different fuel compositions. The idea for the network is to build a neural network which is capable of finding the portion of different fuel mixture and gives the switch to the engine controller modelled with different fuels.

5.4.1 Engine model

The simulation is aimed to estimate the number of atoms in Carbon and Hydrogen using four exhaust gas parameters, which are the levels of CO_2, O_2, CO and NOx. The block diagram of the fuel estimator is shown in Figure 39. The fuel estimator is trained with two methodologies, using a feed-forward neural network and ANFIS for comparison.

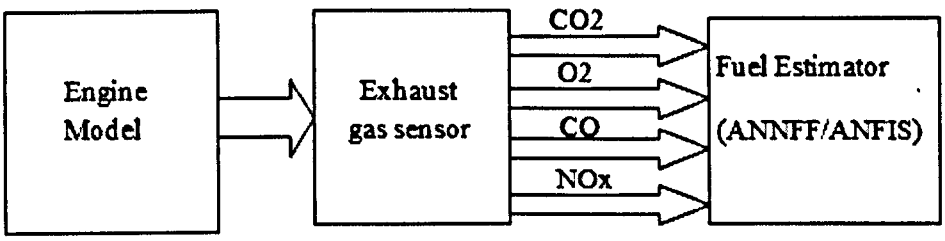

Figure 39 Block diagram of fuel estimation system

5.4.2 Fuel-to-air ratio

The simulation runs on a fixed value of ignition timing (-25°) and on different fuel-to-air ratios, Φ. The results of fuel composition estimation against different fuel compositions and Φ are shown in Figure 40. The results in feed-forward neural network, blue line denotes Carbon and red line for Hydrogen. The results provide reasonable estimations. Most of the results allow distinguishing between Isooctane (C_8H_{18}) as shown in Figure 40a, Ethanol ($C_2H_6O_1$) as shown in Figure 40b and Methanol ($C_1H_4O_1$) as shown in Figure 40c. The fuel-to-air ratio is a very sensitive parameter. When the fuel-to-air ratio is 1.2, the errors in the number of carbon and hydrogen atoms estimated are greater. The error compared to the difference in the Hydrocarbon atom found between Isooctane, and alcohol type substance

Methanol and Ethanol are treated as one category so no further study is conducted on the distinction between them. The other fuel estimation method using ANFIS shows Figure 40, red dotted line denotes Carbon and yellow dotted line denotes Hydrogen, found the similar results compared to feed-forward network. The errors in ANFIS as shown in Table 16, are larger than feed-forward neural network as shown in Table 15. ANFIS has worse performance therefore feed-forward neural network is recommended to be the fuel estimation.

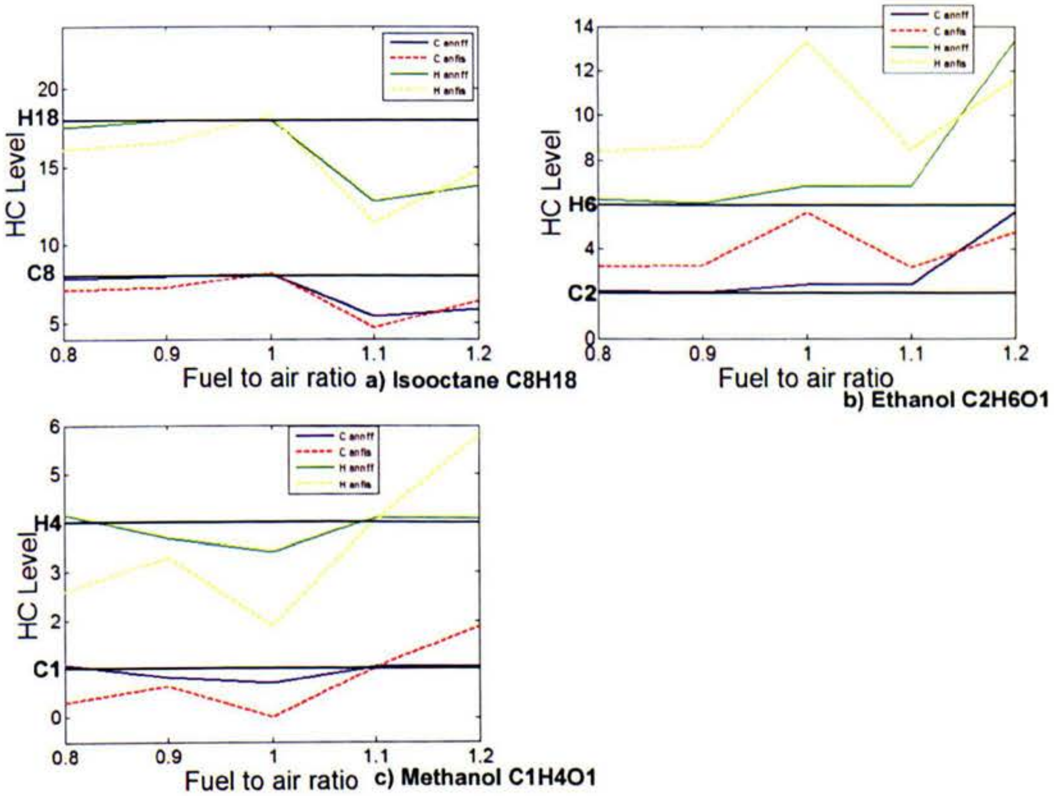

Figure 40 Fuel composition estimation, atoms in C and H against different fuel-to-air ratios with fixed ignition timing. a) Isooctane (top left), b) Ethanol (top right), and c) Methanol (bottom left)

Fuel-to-air ratio	Isooctane		Ethanol		Methanol	
	error of C atom	error of H atom	error of C atom	error of H atom	error of C atom	error of H atom
0.8	2.79%	2.5%	7.90%	5.27%	7.90%	3.98%
0.9	0.31%	0.28%	3.55%	2.35%	16.20%	8.10%
1.0	0.85%	0.11%	22.70%	15.12%	29.10%	14.53%

1.1	32.45%	28.83%	21.45%	14.30%	5.20%	2.60%
1.2	25.83%	22.94%	184.95%	123.33%	5.20%	2.58%

Table 15 Fuel composition estimation errors of feed-forward neural network at different fuel-to-air ratios with fixed ignition timing

Fuel-to-air ratio	Isooctane		Ethanol		Methanol	
	error of C atom	error of H atom	error of C atom	error of H atom	error of C atom	error of H atom
0.8	12.09%	10.72%	59.30%	39.55%	71.00%	35.25%
0.9	9.21%	8.17%	65.00%	43.32%	27.00%	18.25%
1.0	1.73%	1.56%	182.50%	121.67%	100.00%	53.25%
1.1	41.58%	36.94%	61.05%	40.72%	1.80%	1.00%
1.2	13.71%	17.89%	139.00%	92.50%	89.50%	44.75%

Table 16 Fuel composition estimation errors of ANFIS at different fuel-to-air ratio with fixed ignition timings

5.4.3 Ignition timing

The simulation runs with a fixed value of fuel-to-air ratio of 1 and in different ignition timings. The results of fuel composition estimation against different ignition timings are shown in Figure 41. The feed-forward neural network shows good results. The estimation of the three fuels, Isooctane (Figure 41a), Ethanol (Figure 41b), and Methanol (Figure 41c) in number of atoms in Carbon and Hydrogen have less than one atom different at different ignition timing. In Isooctane, the results are in the range between C_7H_{17} to C_9H_{19} from originally C_8H_{18}, and same for Methanol and Ethanol. Compared to ANFIS, the estimation in ethanol has a bigger error. The ignition timing is not a sensitive parameter. The variation is acceptable and the fuel estimation system is able to distinguish between all three fuels. In the comparison between two methods, feed-forward neural network is recommended which has smaller error compared to ANFIS, as shown in Table 17 and Table 18.

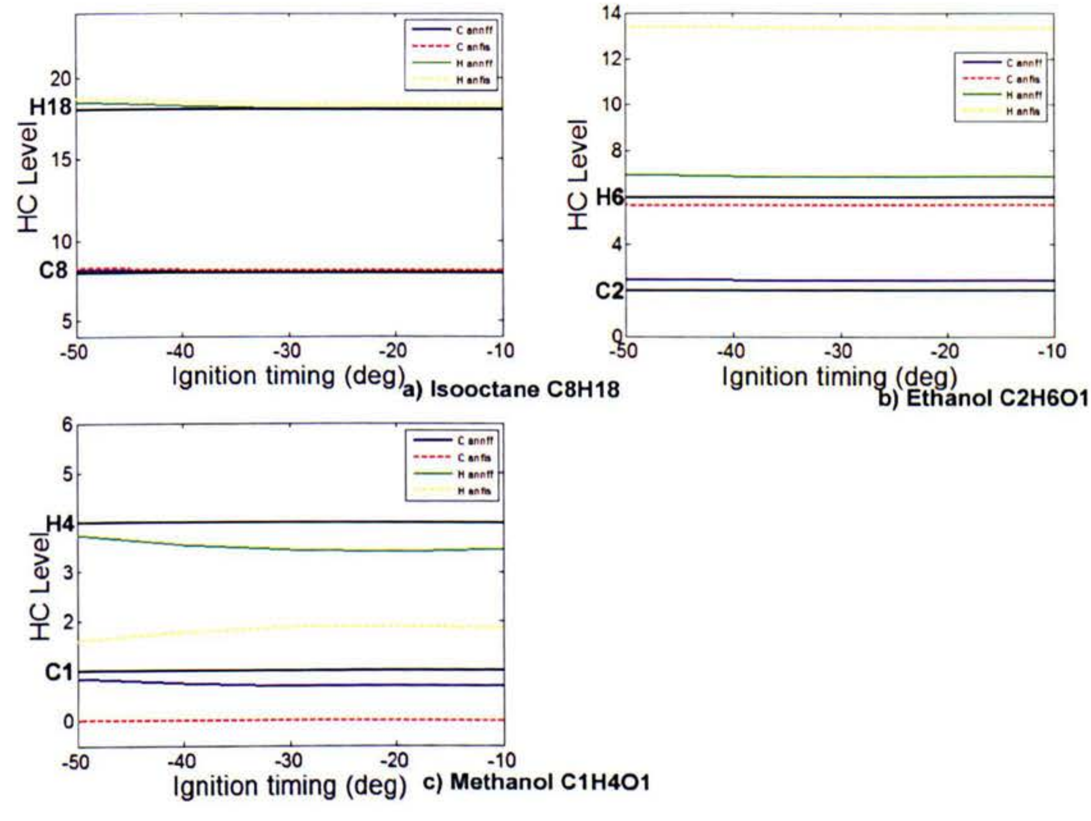

Figure 41 Fuel composition estimation, atoms in C and H against ignition timing, with fixed fuel-to-air ratio equals to 1, a) Isooctane (top left), b) Ethanol (top right), c) and c) Methanol (bottom left)

Ignition timing (deg)	Isooctane		Ethanol		Methanol	
	# of C atom	# of H atom	# of C atom	# of H atom	# of C atom	# of H atom
-10	0.52%	0.44%	22.95%	15.28%	27.02%	13.50%
-20	0.09%	0.06%	22.65%	15.12%	29.33%	14.68%
-30	0.29%	0.27%	22.80%	15.20%	27.91%	13.95%
-40	1.19%	1.06%	23.55%	15.70%	22.58%	28.18%
-50	2.99%	2.67%	25.90%	17.27%	13.11%	6.55%

Table 17 Fuel composition estimation errors of feed-forward neural network at ignition timing, with fixed fuel-to-air ratio equals to 1

Ignition timing (deg)	Isooctane		Ethanol		Methanol	
	# of C atom	# of H atom	# of C atom	# of H atom	# of C atom	# of H atom
-10	2.10%	1.89%	183.00%	122.00%	100.00%	54.13%
-20	1.70%	1.50%	182.50%	121.67%	100.00%	53.18%
-30	1.88%	1.67%	182.50%	121.83%	100.00%	53.73%
-40	2.68%	2.39%	183.50%	122.33%	100.00%	55.98%
-50	4.31%	3.83%	184.50%	123.00%	100.00%	60.20%

Table 18 Fuel composition estimation errors of ANFIS at different ignition timing, with fixed fuel-to-air ratio equals to 1

5.4.4 Fuel mixture

The exact chemical composition of gasoline is unknown and varies between different fuel producers. In section 5.4.2 and 5.4.3, fuel composition estimation is performed and results have been discussed. Here, the intention is to provide the same neural network to estimate the different mixed fuel composition. One assumption is made that the fuels were perfectly mixed. Two case studies, isooctane-methanol and isooctane-ethanol mixtures, have been used for the simulation, with 100% of Isooctane used as initial fuel and blended with Methanol and Ethanol with percentage of 5%, 10%, 15%, and 20% into isooctane.

- Case 1 Isooctane-Ethanol mixture

The time of the simulation is run for 5 cycles; the first set of tests used the blending of Isooctane ($C_8.H_{18}$) and Ethanol ($C_2.H_6.O_1$). The original composition estimation is shown in Table 21, and percentage error is shown in Table 22. The error is higher while the percentage of methanol increases. To improve the results, laboratory experiments may be conducted to find the specific heat capacity, enthalpy and entropy for the new mixed fuel compositions.

Fuel		Feed-forward NN		ANFIS		Calculated Composition
Isooctane	Ethanol	# of C atom	# of H atom	# of C atom	# of H atom	
100%	0%	8.009	18.02	8.138	18.28	$C_{8.0}H_{18.0}O_{0}$
95%	5%	7.940	17.88	8.105	18.21	$C_{7.7}H_{17.4}O_{0.05}$
90%	10%	7.865	17.73	8.069	18.14	$C_{7.4}H_{16.8}O_{0.1}$
85%	15%	7.784	17.57	8.031	18.06	$C_{7.1}H_{16.2}O_{0.15}$
80%	20%	7.694	17.39	7.989	17.98	$C_{6.8}H_{15.6}O_{0.2}$
75%	25%	7.596	17.19	7.943	17.89	$C_{6.5}H_{15.0}O_{0.25}$
70%	30%	7.488	16.98	7.893	17.79	$C_{6.2}H_{14.4}O_{0.3}$

Table 19 Number of C and H estimation with isooctane- ethanol mixture

Fuel		Feed-forward NN		ANFIS		Calculated Composition
Isooctane	Ethanol	Error C atom	Error H atom	Error C atom	Error H atom	
100%	0%	0.11%	0.11%	1.73%	1.56%	$C_{8.0}H_{18.0}O_{0}$
95%	5%	3.12%	2.76%	5.26%	4.66%	$C_{7.7}H_{17.4}O_{0.05}$
90%	10%	6.28%	5.57%	9.04%	7.98%	$C_{7.4}H_{16.8}O_{0.1}$
85%	15%	9.63%	8.46%	13.11%	11.48%	$C_{7.1}H_{16.2}O_{0.15}$
80%	20%	13.15%	11.47%	17.49%	15.26%	$C_{6.8}H_{15.6}O_{0.2}$
75%	25%	16.86%	14.60%	22.20%	19.27%	$C_{6.5}H_{15.0}O_{0.25}$
70%	30%	20.77%	17.92%	27.31%	23.54%	$C_{6.2}H_{14.4}O_{0.3}$

Table 20 Error of the mixture in C and H estimation with isooctane- ethanol mixture

- Case 2 Isooctane- Methanol mixture

Similar experiment is run but the second test replaced Ethanol with Methanol, which has different composition ($C_1.H_4.O_1$). The original composition estimation is shown in Table 19, and percentage error is shown in Table 20. The errors have same trend, therefore we can draw the same conclusion as in Case 1.

Fuel		Feed-forward NN		ANFIS		Calculated Composition
Isooctane	Methanol	# of C atom	# of H atom	# of C atom	# of H atom	
100%	0%	8.009	18.02	8.138	18.28	$C_{8.0}H_{18.0}O_0$
95%	5%	7.858	17.70	8.062	18.12	$C_{7.65}H_{17.3}O_{0.05}$
90%	10%	7.673	17.35	7.979	17.96	$C_{7.3}H_{16.6}O_{0.1}$
85%	15%	7.477	16.95	7.888	17.78	$C_{6.95}H_{15.9}O_{0.15}$
80%	20%	7.261	16.52	7.787	17.57	$C_{6.6}H_{15.2}O_{0.2}$
75%	25%	7.022	16.04	7.675	17.35	$C_{6.25}H_{14.5}O_{0.25}$
70%	30%	6.763	15.53	7.550	17.10	$C_{5.9}H_{13.8}O_{0.3}$

Table 21 Number of C and H estimation with isooctane- methanol mixture

Fuel		Feed-forward NN		ANFIS		Calculated Composition
Isooctane	Methanol	Error C atom	Error H atom	Error C atom	Error H atom	
100%	0%	0.11%	0.11%	1.73%	1.56%	$C_{8.0}H_{18.0}O_0$
95%	5%	2.72%	2.31%	5.39%	4.74%	$C_{7.65}H_{17.3}O_{0.05}$
90%	10%	5.11%	4.52%	9.30%	8.19%	$C_{7.3}H_{16.6}O_{0.1}$
85%	15%	7.58%	6.60%	13.50%	11.82%	$C_{6.95}H_{15.9}O_{0.15}$
80%	20%	10.02%	8.68%	17.98%	15.59%	$C_{6.6}H_{15.2}O_{0.2}$

75%	25%	12.35%	10.62%	22.80%	19.66%	$C_{6.25}H_{14.5}O_{0.25}$
70%	30%	14.63%	12.54%	27.97%	23.91%	$C_{5.9}H_{13.8}O_{0.3}$

Table 22 Error of the mixture in C and H estimation with isooctane- methanol mixture

5.4.5 Fuel composition estimation by likelihood

The performance of two artificial intelligence approaches, feed-forward neural network and ANFIS has been discussed in 5.4.4. The results proved that the feed-forward neural network, which performs better, has been chosen for further study of fuel estimation. However in engine control, the controller needs to understand the fuel probability of the mixed fuel rather than their actual chemical contents. Another approach, the pattern recognition feed-forward neural network, is used to identify the fuel for engine control. The block diagram of such neural network is shown in Figure 42. The transfer function of the output layer is replaced by the 'softmax' function in which the sum of the output is added up to one and it is able to find the probability distribution of the fuel. The pattern recognition neural network is able to classify the percentage of similarity of the given fuels. In this experiment, three fuel compositions listed in Table 14 are used for the classification.

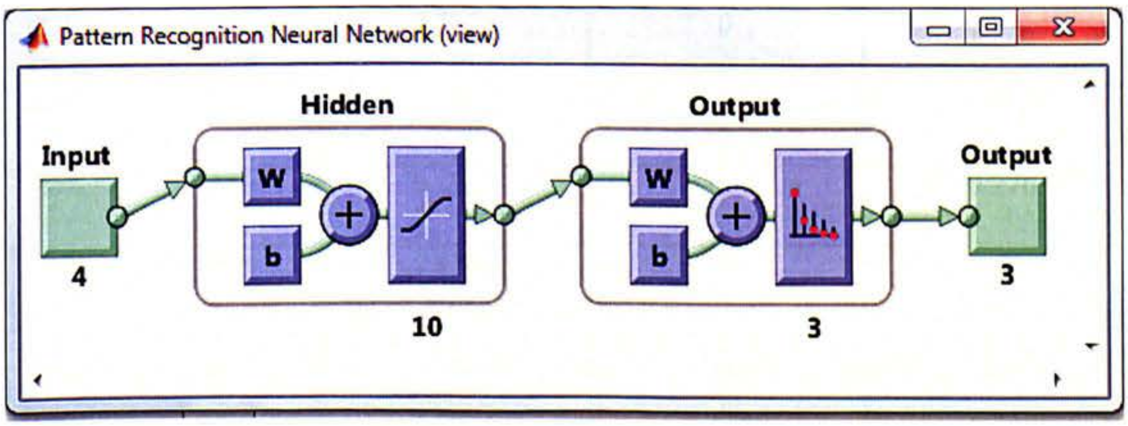

Figure 42 Block diagram of a feed-forward pattern recognition neural network

The dataset uses to train and validate the network is the same as the dataset used in 5.2.3. The performance is counted by the R-square which is equal to 0.7892. The engine operating parameters and fuel mixtures of pure Isooctane, Isooctane-Ethanol and Isooctane-Methanol used are the same as in 5.4.4.

- Case 1 Isooctane-Ethanol mixture

The first case study is the estimation of probability between Isooctane, Methanol and Ethanol with the mixture of Isooctane (C_8H_{18}) and Ethanol ($C_2H_6O_1$) mixture. The mixture contains Isooctane ranging between 70% to 100% and Ethanol ranging between 0% to 30%, and one case with 100% Ethanol for reference of pure Ethanol. The Results show in Table 23, the estimation pure Isooctane is not accuracy with the fuel composition with 100% Isooctane contains 20% of Ethanol. When the Isooctane contains a portion of Ethanol, the neural network estimated with the changing in the portion of mixture. The estimation of 100% Ethanol is 0.9876 which has a high accuracy. The neural network is able to provide further control to different portion of mixture of Isooctane-Ethanol.

Fuel		Probability (%)		
Isooctane	Ethanol	Isooctane	Methanol	Ethanol
100%	0%	0.8045	0	0.1955
95%	5%	0.7820	0	0.2180
90%	10%	0.7586	0	0.2414
85%	15%	0.7394	0	0.2606
80%	20%	0.7237	0	0.2763
75%	25%	0.6787	0	0.3212
70%	30%	0.6680	0	0.3320
0%	100%	0.0036	0.0088	0.9876

Table 23 The probability of isooctane, methanol and ethanol estimated with isooctane- methanol mixture

- Case 2 Isooctane-Methanol mixture

The second case is the estimation of probability between Isooctane, Methanol and Ethanol with the mixture of Isooctane (C_8H_{18}) and Methanol ($C_1H_4O_1$) mixture. The mixture contains Isooctane ranging between 70% to 100% and Methanol ranging between 0% to 30%, and one case with 100% Ethanol for reference. The Results show in Table 24, the result of 100% Isooctane estimation is the same as Case 1. When the portion of Methanol is mixed with

Isooctane, the estimation of the mixture is resulted as Isooctane-Ethanol mixture because both Methanol and Ethanol are considered as alcohol type substance. The mixed composition in hydrocarbon is closer to composition of Isooctane-Ethanol mixture. The estimation of 100% Methanol is 0.9970 of Methanol which the probability is high. The neural network is developed for further control to different portion of mixture of Isooctane-Methanol.

Fuel		Probability (%)		
Isooctane	Methanol	Isooctane	Methanol	Ethanol
100%	0%	0.8045	0	0.1955
95%	5%	0.7778	0	0.2222
90%	10%	0.7307	0	0.2693
85%	15%	0.6532	0	0.3468
80%	20%	0.5415	0	0.4584
75%	25%	0.4262	0	0.5738
70%	30%	0.3656	0.0001	0.6343
0%	100%	0.0001	0.9970	0.0029

Table 24 The probability of isooctane, methanol and ethanol estimated with isooctane- methanol mixture

5.4.6 Comparison of the two networks

The Results show in 5.4.2 & 5.4.3 agreed that feed-forward neural has higher accuracy. ANFIS system is also included in large set of fuzzy rule. The time needs to train or control is slow. The conclusion of the comparison can be made that feed-forward neural network is more suitable in fuel estimation compared to ANFIS which is more suitable in Single-Input-Single-Output (SISO) systems or systems with small number of input parameters.

5.5 Fuel composition estimation in continuous time

The results show in 5.4 have used a fixed set of parameters to test the network. It has been agreed that feed-forward neural network performs better than ANFIS. To perform further test on the performance of the fuel estimator perform in use of real application, the simulations run in continuous time. The fuel estimation is using the same feed-forward neural network developed in 5.4.6. The engine model is run at a fixed speed at 2000rpm and fixed torque. Two mixtures are under investigation, Isooctane-Ethanol and Isooctane-Methanol. Figure 43 shows the setting of the fuel estimation test is the continuous time. The engine is running for 5 seconds for each mixture. The fuel used the 100% Isooctane and blended with Methanol and Ethanol by 10%, 20%, 30% and 40%. It is noted that the engine operating used is different from 5.4.5. The fuel-to-air ratio used is slightly richer mixture between the values of 1.02 and 1.05. The tests also included the intake manifold model developed in 3.16.2 allows tiny variations in the air mass.

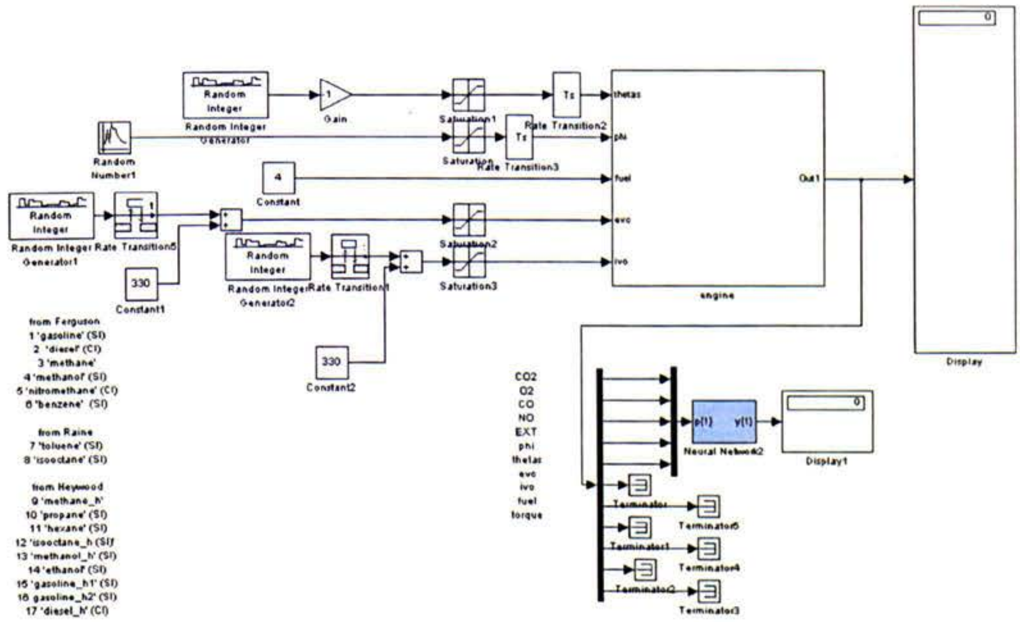

Figure 43 Engine simulation model with fuel estimator which is run in continuous time

5.5.1 Case 1 Isooctane-Ethanol mixture

The simulation is run for 5 seconds to see the performance of the fuel estimator developed in continuous time. The results present in the likelihood of three given fuel Isooctane (Figure 44), Methanol (Figure 45) and Ethanol (Figure 46). The estimations between the fuel with 100% and 80% of Isooctane generated the similar estimation, with the probability of likelihood is at around 83% of Isooctane and 17% of Ethanol. The performance of the fuel estimator is improved by increase the percentage of Ethanol to 30% (equivalent to 70% of Isooctane) and 40% (equivalent to 60% of Isooctane), the fuel estimator is able to pick up the variations. During the five seconds tests, the Results show few cases have slightly different estimations, but the errors are not significant. Therefore the trends and the conclusion is the same as 5.4.5.

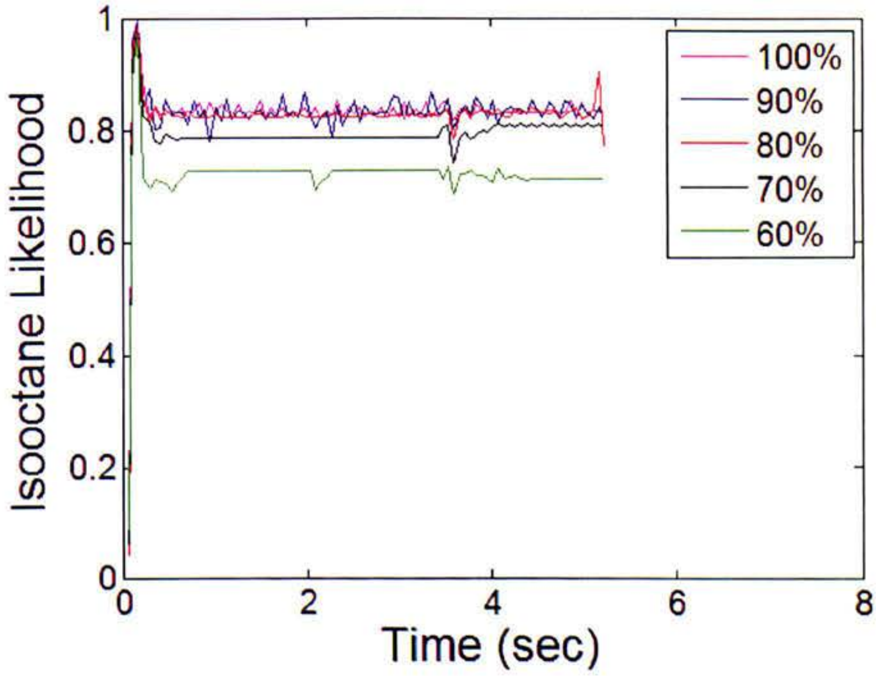

Figure 44 Results of Isooctane estimation by likelihood percentage in continuous time. Magenta line denotes 100% of Isooctane, blue line denotes 90% of Isooctane and 10% Ethanol, red line denotes 80% of Isooctane, black line denotes 70% of Isooctane, and green line denotes 60% Isooctane.

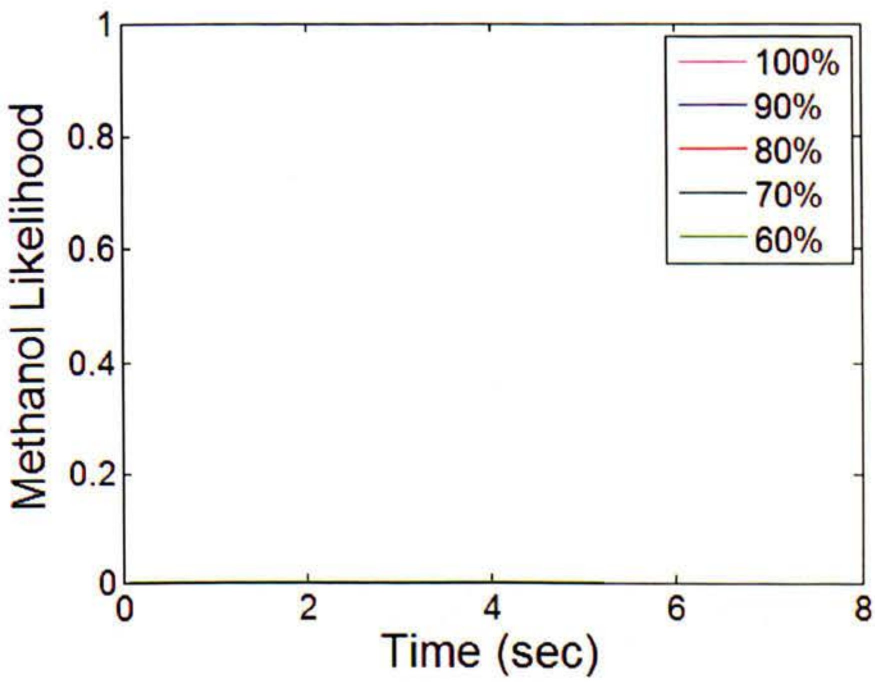

Figure 45 Results of Isooctane estimation by likelihood percentage in continuous time. Magenta line denotes 100% of Isooctane, blue line denotes 90% of Isooctane and 10% Ethanol, red line denotes 80% of Isooctane, black line denotes 70% of Isooctane, and green line denotes 60% Isooctane.

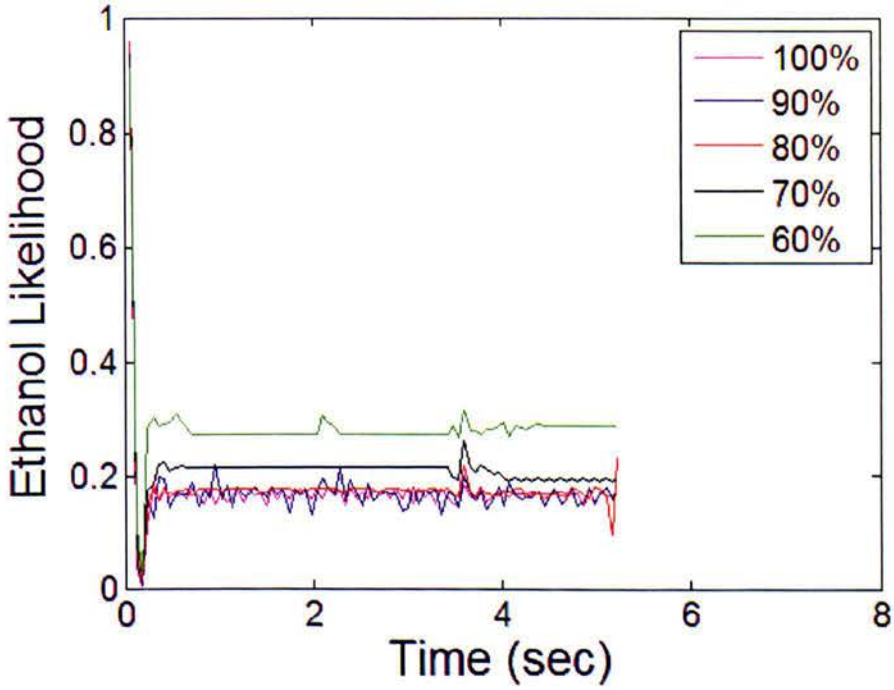

Figure 46 Results of Isooctane estimation by likelihood percentage in continuous time. Magenta line denotes 100% of Isooctane, blue line denotes 90% of Isooctane and 10% Ethanol, red line denotes 80% of Isooctane, black line denotes 70% of Isooctane, and green line denotes 60% Isooctane.

5.5.2 Case 2 Isooctane-Methanol mixture

A similar test has been done compared to 5.5.1 but replaced with the Isooctane-Methanol mixture. The performance of the fuel estimator is the same as case one. The Isooctane-Methanol is again estimated as Isooctane-Ethanol and concluded the same reason which has been explained in 5.4.5.

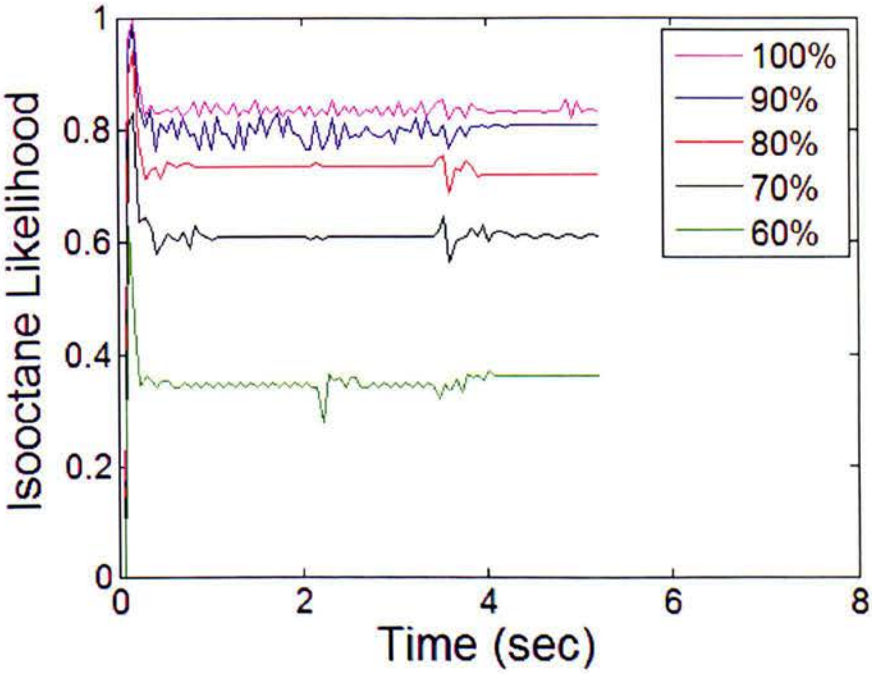

Figure 47 Results of Isooctane estimation by likelihood percentage in continuous time. Magenta line denotes 100% of Isooctane, blue line denotes 90% of Isooctane and 10% Methanol, red line denotes 80% of Isooctane, black line denotes 70% of Isooctane, and green line denotes 60% Isooctane.

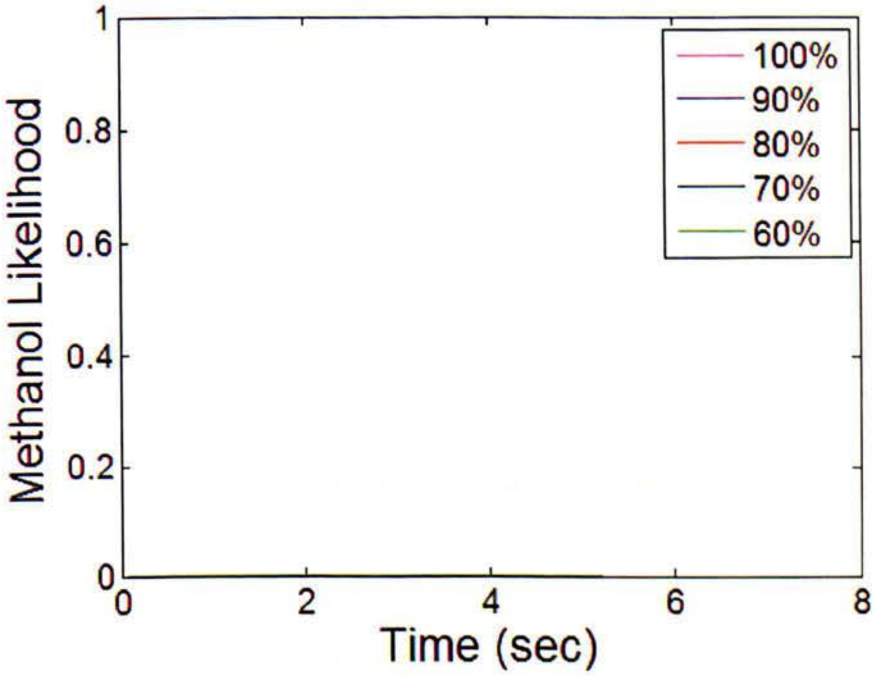

Figure 48 Results of Methanol estimation by likelihood percentage in continuous time. Magenta line denotes 100% of Isooctane, blue line denotes 90% of Isooctane and 10% Methanol, red line denotes 80% of Isooctane, black line denotes 70% of Isooctane, and green line denotes 60% Isooctane.

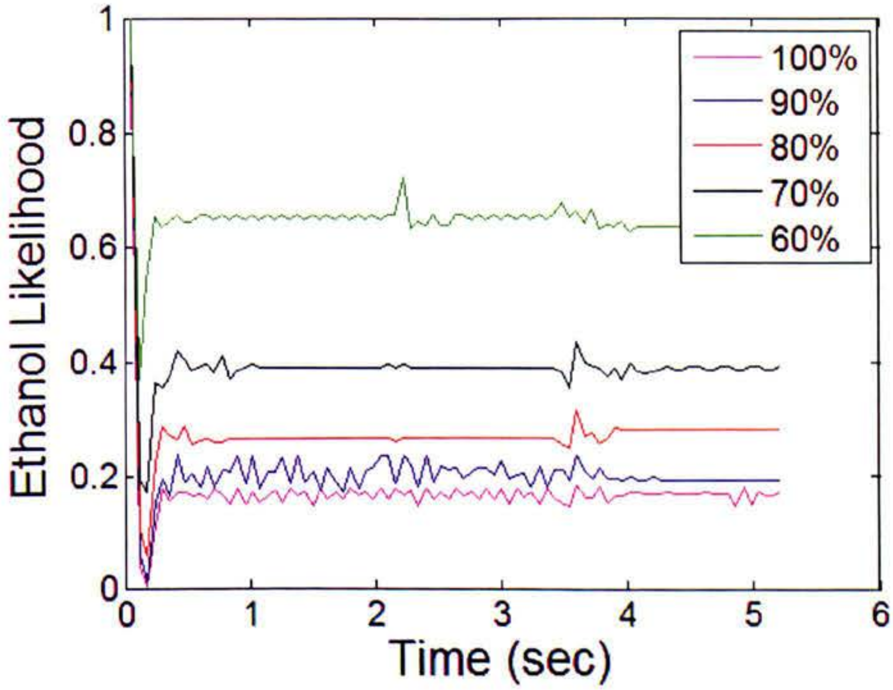

Figure 49 Results of Ethanol estimation by likelihood percentage in continuous time. Magenta line denotes 100% of Isooctane, blue line denotes 90% of Isooctane and 10% Methanol, red line denotes 80% of Isooctane, black line denotes 70% of Isooctane, and green line denotes 60% Isooctane.

5.6 Conclusions

This chapter develops the fuel estimator which is capable to provide further control on different fuel mixtures. Three fuels, Isooctane, Methanol and Ethanol have been used in the development of the fuel estimator. The input parameters of the system have been identified as the level of CO_2, O_2, CO and NOx in addition of the exhaust gas temperature. Two artificial intelligence methods, ANFIS and feed-forward neural network have been investigated and the conclusion can be drawn as follows:-

1) The performance of feed-forward neural network approach is better than ANFIS.
2) One negative factor of ANFIS is that it is more suitable for SISO systems. Large fuzzy-rules are difficult to handle in multi-variable system, as it happened in this thesis.
3) The fuel estimator can provide the proportional control by the likelihood of given fuels.
4) Results show that the fuel estimator can handle the changes of different percentage used in blending mixture of Isooctane-Methanol and Isooctane-Ethanol fuel.

5.7 Summary of Chapter 5

This chapter studies the development of AI fuel estimators. Two methodologies are investigated, ANFIS, which is a neuro-fuzzy system, and feed-forward neural network, which is a neural network system control through the learning process. The mathematical representations of the two methodologies have been discussed in 5.2. To identify the parameters needed in the network, the behaviour of emission composition between different fuels against engine operating parameters, i.e. fuel-to-air ratio and ignition timing, were analysed in 5.3. The observation of the emission behaviours determined the range of the control parameters used in the fuel estimation. The two methodologies for fuel estimation and the comparison are also discussed. The initial tests ran through the pure fuel composition and gradually mixtures of Isooctane with Methanol and Ethanol respectively. The portions of mixture varied in steps of 5%, 10%, 15%, 20%, 25% and 30%. The results shown in 5.4 confirm that the feed-forward neural network performed better in the fuel estimation application. Further simulations tested the fuel estimator in continuous time. Results shown in 5.5 draw the same conclusion as in 5.4 where the performance of the fuel estimator is not affected in the continuous time process.

Chapter 6 Engine Control

This chapter studies three closed-loop control algorithms in engine control, including PI control, Nonlinear Auto-Regressive (NAR) neural network and state-space model with LQR. The mathematical representation of those controllers will be discussed throughout the chapter. Each controller is tested based on the engine simulation platform developed in Chapter 3. The objective of the controller is to provide optimal control where the fuel composition and speed are changing. Results show that the state-space with LQR combined with the fuel estimator developed in Chapter 5 are able to achieve the minimum levels of emission in all constraints while the performance is reasonably maintained.

6.1 Introduction

Engine operating parameters, including fuel-to-air ratio, ignition timing, and the valve opening and closing event affect the combustion performance. These four engine operating parameters can be obtained from existing engine systems. It is noted that there are other factors related to the engine combustion process but they are not commonly used since those parameters cannot be easily obtained or controlled. Two of the outlined parameters discussed in 1.5.8 and 1.5.10, namely variable compression ratio and the variable manifold length, require large mechanical components to adjust the engine geometries and they are not practical to fit onto the engine. Thus, compression ratio information is hard to obtain in real-time engine process. Therefore the identified engine operating parameters to use in this thesis are outlined as the four parameters that can be obtained.

This chapter discusses the development of the engine control algorithm which can be used in real engines. The objective of the controller is to identify the optimal engine operating parameters with unknown composition of mixture and produce engine emission at the lowest level in all constraints, while the performance of the engine running in different speed ranges is not affected. The controller is tested using the engine simulation described in Chapter 3. The engine simulation is able to generate the exhaust gas composition and allows off-line research on control algorithm. The outlined emission composition is considered the obtainable parameters. Modern engines which are fitted with engine sensors, as discussed in 2.6 those are able to measure the levels of Carbon Dioxide (CO_2), Oxygen (O_2), Carbon Monoxide (CO) and Nitric Oxide (NOx) of exhaust gas.

6.2 Engine model and assumptions

The engine control simulation consists of three parts, namely, the engine model, the exhaust gas sensor block which records the discrete exhaust emission, and the engine parameter control system. The block diagram is shown in Figure 50. The emission control is considered as a multi-variable system. The controller takes the exhaust data from the engine simulation against CO_2, O_2, CO and NOx and additional parameters of exhaust gas temperature (Tex). The engine runs according to the control parameters, which are fuel-to-air ratio Φ, ignition timing Θ_{ig}, exhaust valve closed timing Θ_{evc} and intake valve opening timing Θ_{ivc}. The simulation is run on a single cylinder engine with the assumption that the controller developed is suitable on the same geometries with other cylinders.

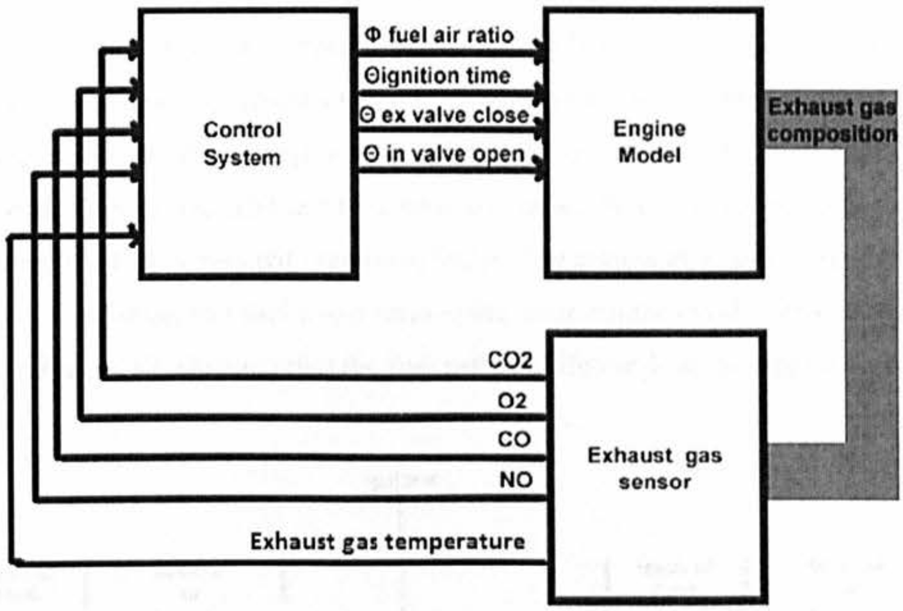

Figure 50 Engine emission control system

Engine control can be considered as a discrete engine event of a single cylinder working in a 4-strokes process. Most of the common vehicle engines usually contain more than one cylinder. However, an engine research usually tests under the single-cylinder engine. The reason for using the idea of a single-cylinder engine is that research treats the improvement of engine design on the cylinder combustion [10]. Single engine cylinder is connected to one exhaust path which removes the unwanted effects in the flow of emissions in several exhaust paths. The multi-cylinder researches are mainly focused on the design on manifold geometries or turbo-charge design. Therefore the engine simulation considers single-cylinder engines in this thesis. Once the controller is developed, it can be implemented and the optimal engine operating parameters can be found in a multi-cylinder engine.

6.3 Engine control event and data collection

Although the engine runs in continuous time, engine operating timing can be considered as a discrete event due to the engine process being divided into strokes [49]. The collection of exhaust gas information is valid while the exhaust gas valve is opened, and finishes when the valve is closed. The optimal ignition timing related to the past emission information can be updated during to the time gap between the timing of exhaust valve closed and the igniting timing in the coming stroke.

However the fuel injection timing and the amount of fuel injected into the cylinder are being updated in the next engine cycle because there is no time gap between the timing of exhaust valve closed and the intake valve opens where fuel is mixing at that moment. The controller has no time to calculate the correct values of parameters in the fuel path. Figure 51 presents the engine event in the SI engine process timeline. To compare the different of engine event of CI, the difference between SI and CI engine events are that CI engines ignite at the moment when the fuel is injected into the cylinder. The computer is able to update the optimal injection timing and fuel-to-air ratio in the same engine cycle. The CI engine event is presented in Figure 52, showing that the fuel path is different from SI engine event.

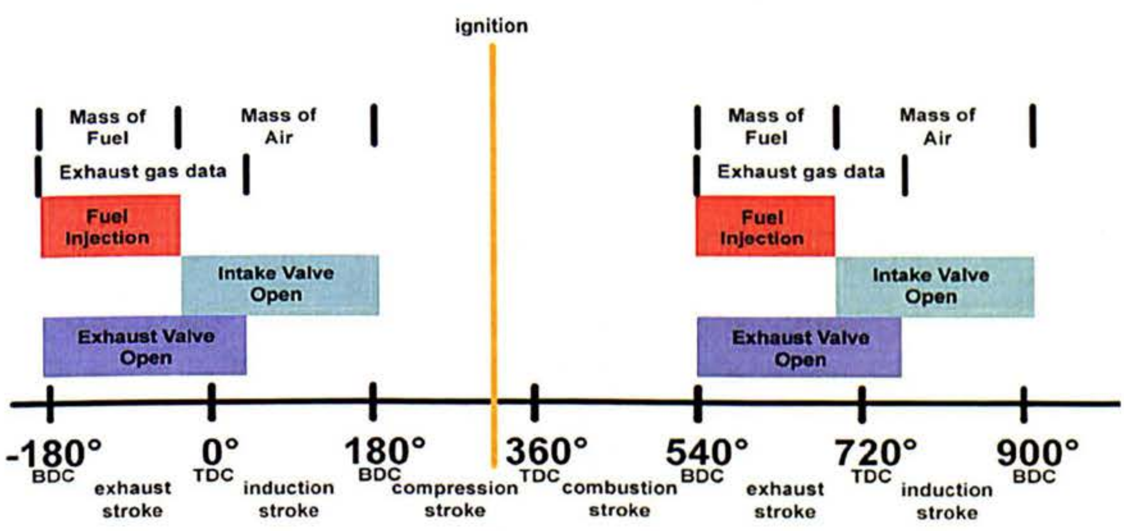

Figure 51 The control event of a SI engine.

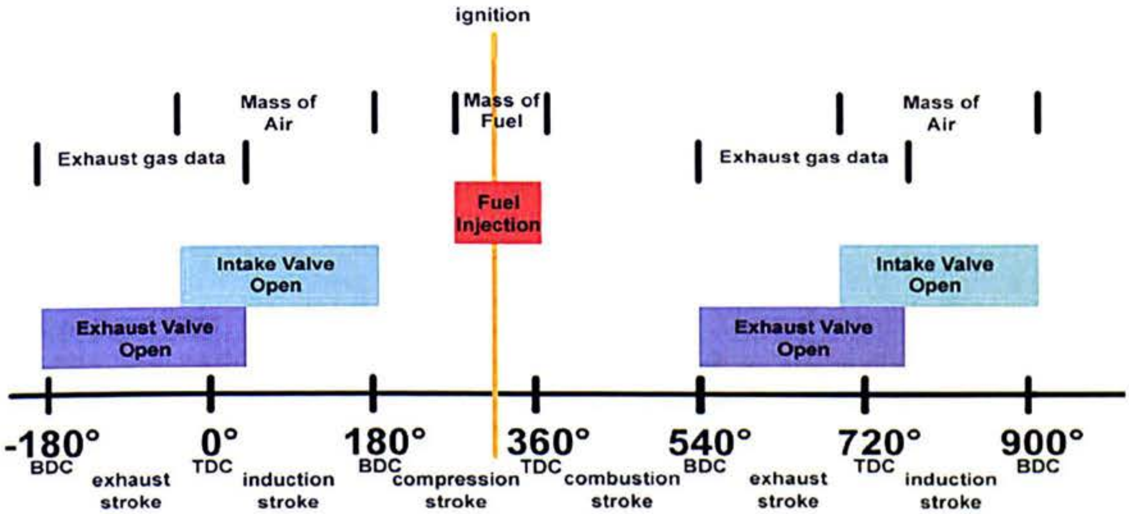

Figure 52 The control event of a CI engine.

6.3.1 Closed-loop engine control

In the closed-loop control, the input parameters can be optimised by computing the error between the output and the desired values. The controller provides a gain in order to update the optimal value to the new input variable.

Figure 53 shows the block diagram of a closed-loop control system design. Assume the engine has a transfer function *G(s)* which represents the relationship between the engine operating parameter and the condition of the exhaust gas. The error, *E*, is determined from the difference between output *Y(t-1)* and the current input *X(t)*. The updated input, *U*, can be compensated by finding the dynamics of the system which can be represented by the transfer function *D(s)*.

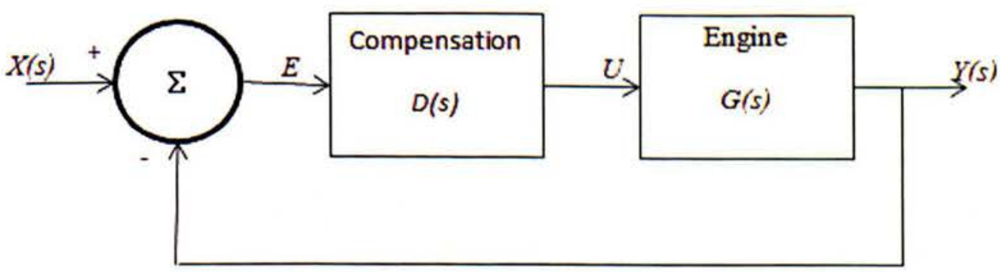

Figure 53 A Closed-loop Control System design definition

However, one concern in engine control is the behaviour between some of the engine operating parameters, namely, the emission and performance which are considered as non-linear behaviours [64]. This generates an obstacle as there is no existing formulation representing the non-linear behaviours due to the dynamic of the engine, G(s). If the transfer function of the system is not obtainable, the behaviour can be represented by other models including artificial neural networks or state-space representations.

6.4 PID Controller

PID control is the simplest approach in closed-loop control algorithm and has been widely used throughout different systems. The control system has three terms, proportional, integral, and derivative. Each term has its own gain, *kp*, *ki* and *kd* respectively, to provide the bias to each term. The proportional term updates the plant input accordingly to the error response. To increase the stability of the system, the integral term and derivative term are added for controlling the steady state and transient response from the past values and prediction response respectively. The expression of the PID controller is shown in Equation 29.

$$u(s) = kp.e(s) + ki.\frac{e(s)}{s} + kd.e(s).s$$

Equation 29

where,

u is the control input

e is the error of the control variable

kp is the proportional gain

ki is the integral gain

kd is the derivative gain.

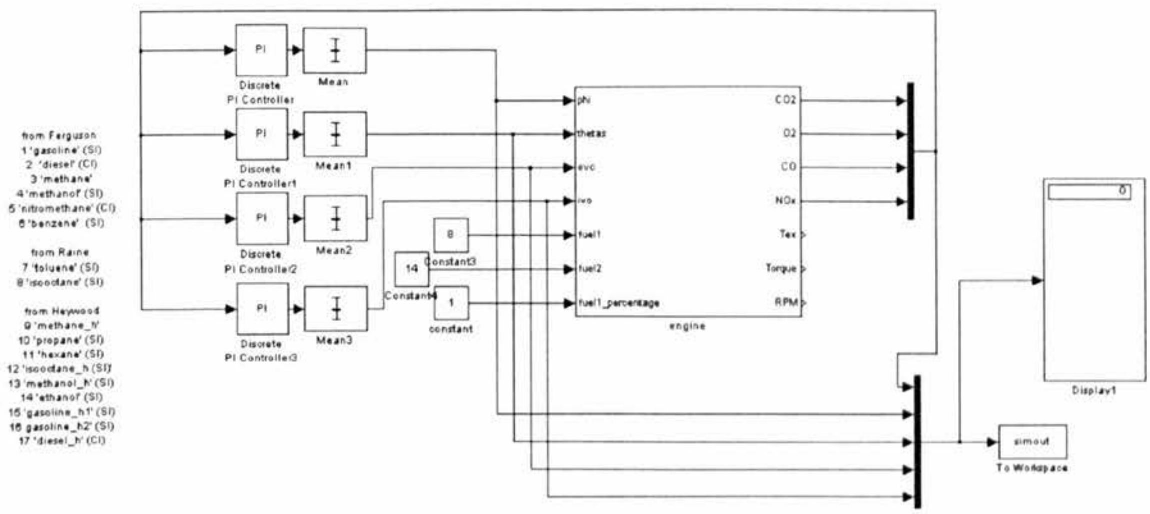

Figure 54 Simulation block of PI engine control

6.4.1 Engine simulation using PI controller

There are four control parameters and four control targets which have been discussed previously. In this simulation a simple PI controller is used to estimate the control variables. The reason for this is simply the implementation onto the engine simulation platform by considering only the error and the past data of emissions, where the D term, which predicted the future values is ignored. For MISO control, the Relative Gain Array (RGA) technique is used for different control biases. RGA finds the gain coupling between different control variables and penalised between control parameters and output error. The RGA can be obtained by the proportion of the plant output against control variables by observation. For example, the level of CO_2 is around 0.12 and the level of O_2 is around 0.01. The gain designed for O_2 is around 10 times bigger than for CO_2 in control of ignition timing. The objective is to control the level of the emissions to the minimum in various species within a range of control variables.

Figure 55 shows the result of the emission in a PI engine control and Figure 56 shows the input parameters calculated from PI controller. It is noted that the level of O_2 and NO can be stable after 1 second. Compared to the results of the CO_2 and CO level, they have the opposite relationship. CO level exceeds the emission limited of 1% at around 4 seconds, while the CO_2 level is successfully controlled to the minimum. It is concluded that the PI control has a slow response and the system is hardly stable over time. To improve the PID control for multi-variable system, several tuning method using eigenvalues can be used [79][94][100].

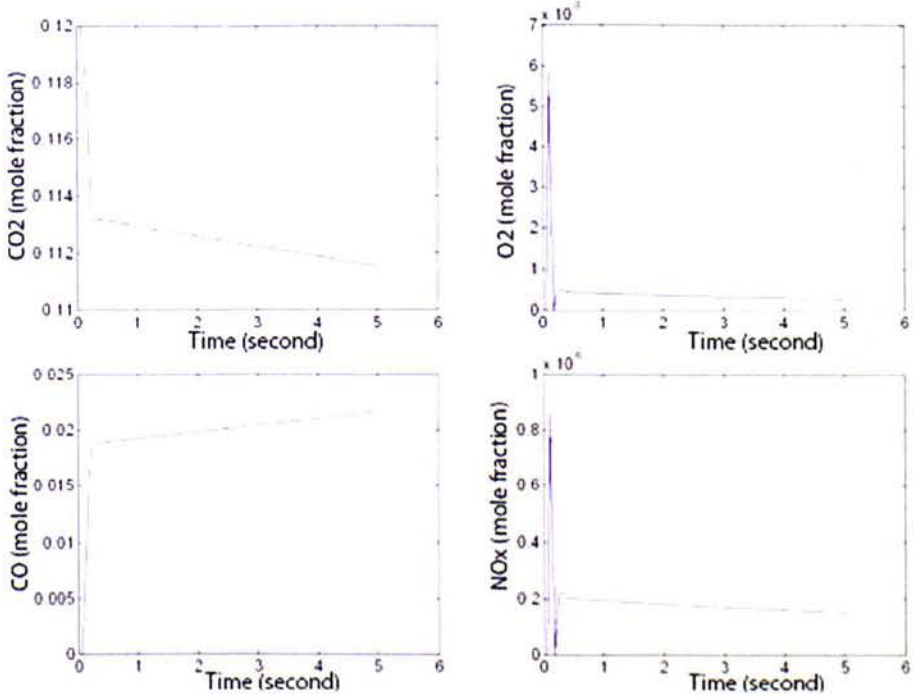

Figure 55 Level of CO2, O2, CO and NO found in fixed torque and speed condition for 10 seconds

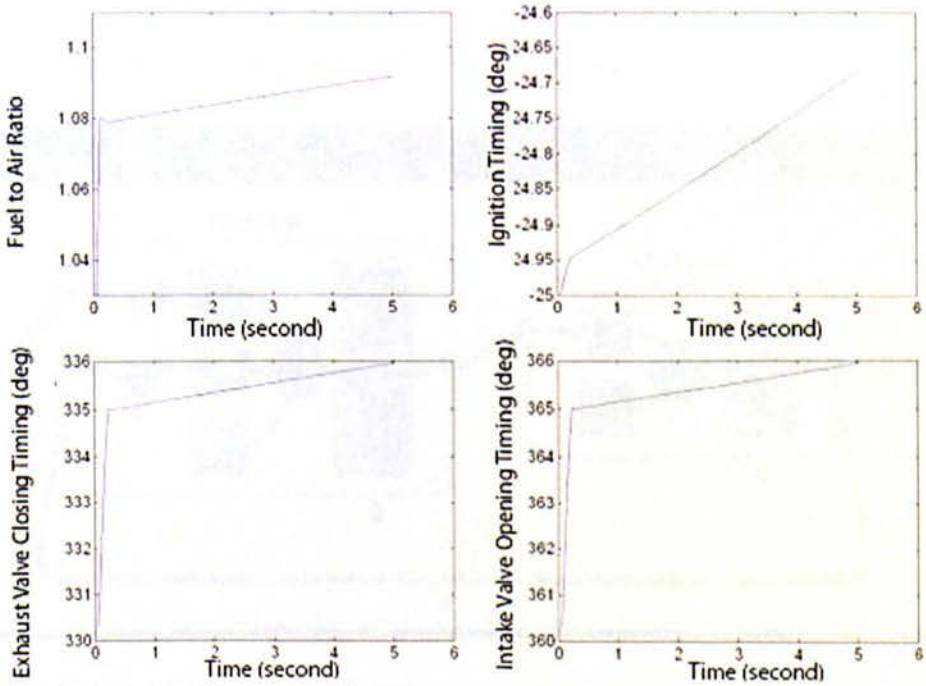

Figure 56 Control parameters of engine simulation in fixed torque and speed condition for 10 seconds

6.5 Non-linear Auto Regressive (NAR) Neural Network

Non-linear Auto Regressive (NAR) Neural Network is a neuro-controller which is a feed-forward neural network with an additional feedback input for the weighting of closed-loop linearisation. The feedback input uses the past values to remove nonlinearities of a system [14][82]. The block diagram of a NAR neural network for 4-input-4-output system presents in Figure 57. NAR neural network is able to predict the future behaviour, and the number of future sample predicted depends on the number of delays trained in the network, allows the weight to track the trajectory of the behaviour. The feed-forward neural network is trained regressively using the past values to approximate the linear output. In the definition of a NAR neural network model, the math representation shows in Equation 30 [4][88][97].

$$y(t) = f\left(y(t-1), y(t-2), \dots, y(t-n_y), u(t-1), u(t-2), \dots, u(t-n_u)\right)$$

Equation 30

where,

u is the control variable

y is the output

n_u is the number of delay used to train the control variable set

n_y is the number of delay used to train the output set

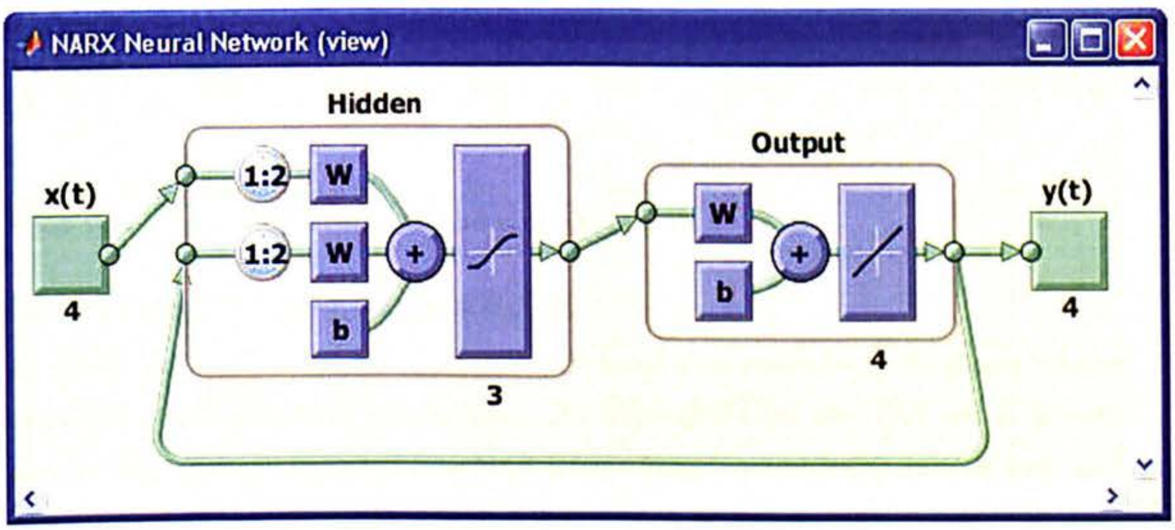

Figure 57 Closed-loop NAR neural network system

The number of past values is one of the factors determines the size of the network. Other than the main function of feed-forward neural network described in 5.2.1 which is non-linear system identification, NAR neural network can be used as system prediction in a time series. Once the system has been identified, the network output can be used as open-loop or closed-loop control. Open-loop NAR neural network control uses as the origin system identification, and closed-loop NAR neural network control have an additional input allowing the system update the forthcoming output. To train the closed-loop neural network, the specification of the training method uses is as same as feed-forward neural network, which is Levenberg Marquardt back-propagation algorithm. The number of past values is chosen as 2 and number of hidden layers is 3. The engine simulation system implement the NAR neural network presents in Figure 58. The control block is replaced the PI controller shown in Figure 56.

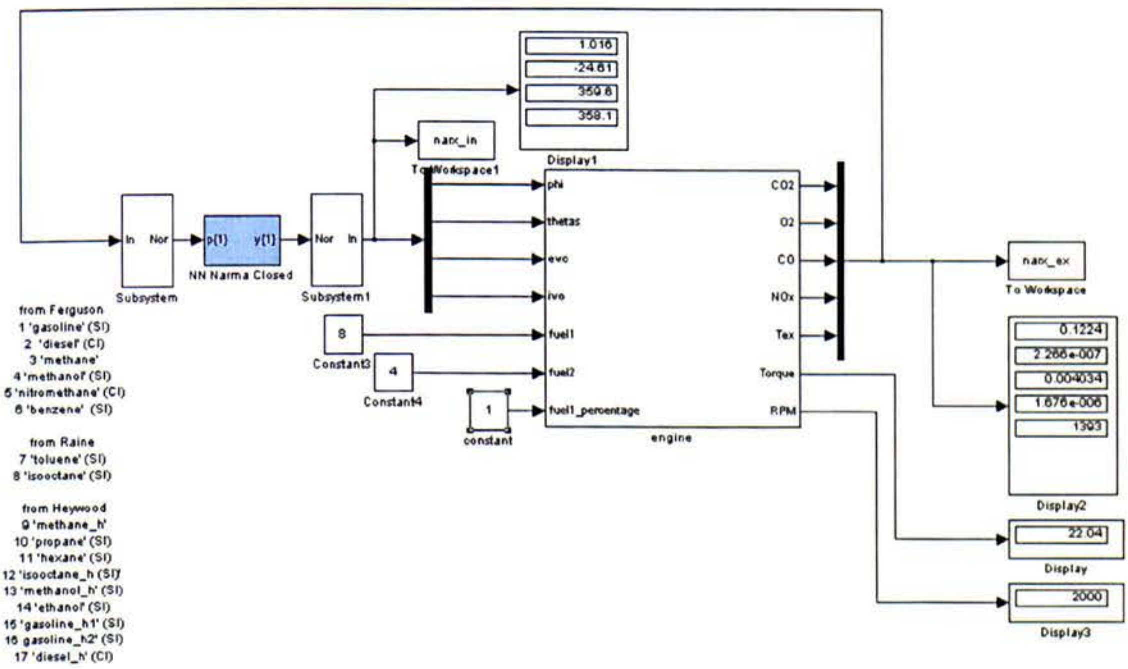

Figure 58 Simulation block of NAR neural network engine control

6.5.1 Open-loop NAR vs. closed-loop NAR

An open-loop NAR neural network is also developed to compare the performance between open-loop and closed-loop methodologies. The training of those two NAR neural networks uses the same dataset. In closed-loop NAR it has a better control in CO, but has been traded off with CO_2, O_2 and NOx. The results of the simulations are presented in Figure 59. The controllers settle at less than 0.6 seconds, which is equal to 10 revolutions at the speed of 2000RPM. They both provide quick and stable control.

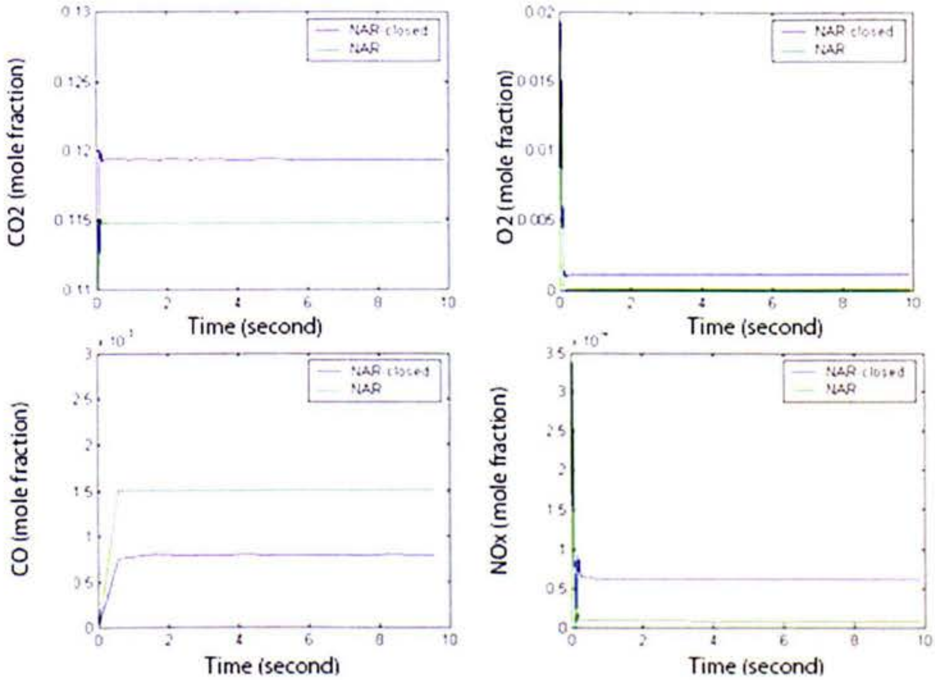

Figure 59 Result of NAR and closed-loop NAR control of CO_2, O_2, CO and NO levels found in fixed torque and speed condition for 10 seconds

6.6 State-feedback Model using LQR

A state-space is another approach, apart from neural network, to represent the behaviours of non-linear system using system identification. It consists of a set of nth order differential equations in the vector valued state which describe the dynamic of the system. The state-space model can also be designed as a closed-loop controller. The closed-loop control gain, K, can be developed using Linear Quadratic Regulator (LQR). The approach is first developed a state-space model and find K in the next stage. Figure 60 shows the block diagram of the systematic of state-space.

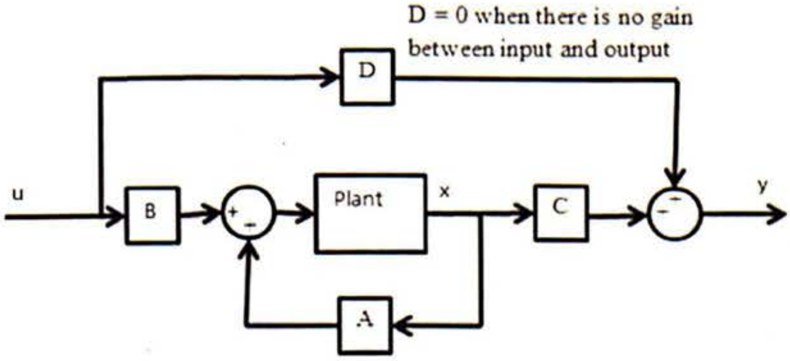

Figure 60 Block diagram of state-space system

For the real time system, the state-space representation, presented in Equation 31, is divided into two equations, state equation $x[t]$ and measurement equation $y(t)$[84]. The state equation records the behaviours of state, by the bias weights, at time t. The weighting bias between the pervious state and the current state is represented by the gain, A; and the weighting bias between input and state is represents by gain, B. The measurement equation records the behaviours between the state output and the system output with the gain. The weighting bias between them is represented by the gain, C. If there is some gain found between input and output, the gain, D, can represent the bias but if no gain happens between input and output, D is equalled to 0. For a multi-variables system, the gains can be represented in the form of matrix.

$$x[t+1] = Ax[t] + Bu[t],$$

$$y(t) = Cx[t] + Du[t]$$

Equation 31

where

x is the state vector,

u is the input vector,

y is the output vector,

A is a n-by-n state weighting matrix,

B is a n-by-m input weighting matrix,

C is a l-by-n output weighting matrix,

D is a m-by-m back propagate weighting matrix, zero when there is no gain between input and output,

n is the number of state order,

l is the number of outputs,

m is the number of inputs.

Since the linearisation is using sampling data in some time step, computer simulation is considered as a discrete time system. The state-space representation in discrete time is shown in Equation 32.

$$x[t+1] = Ax[t] + Bu[t]$$

$$y(t) = Cx[t] + Du[t]$$

Equation 32

where,

the state vector x is using the state value in the previous step, i.e. x[t+1].

The advantage of state-space is its ability to represent multi-variable systems, such as MIMO or MISO. The weighting matrix, *A*, *B*, *C* and *D* generate the weight between different correlations and prioritise the certain input parameters and states if needed. Figure 61 shows the overview of the weighting matrix in a MIMO system.

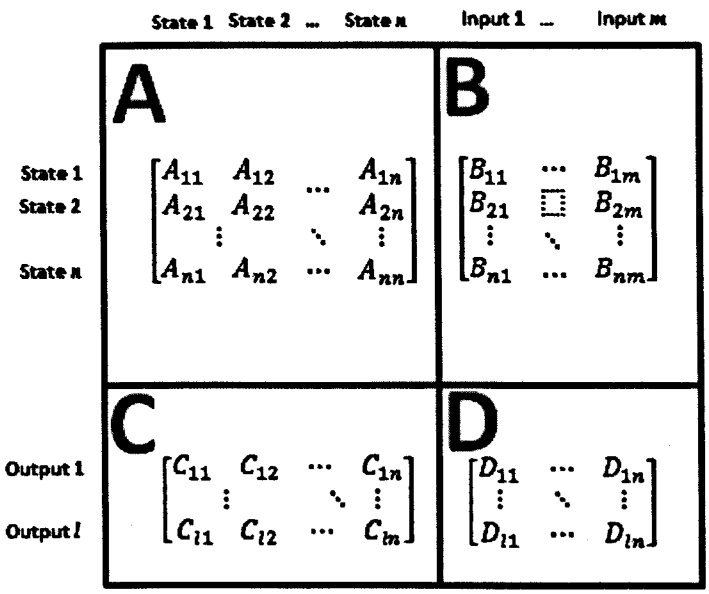

Figure 61 A, B, C and D matrix format in a MIMO system

Matrix A is often formed of a symmetric matrix, where the weighting only exists for each state. In some cases in state-space design, a different weighting can be between two different states, i.e. there is some gain between state 1 and state 2, A*12* and A*21* have the value for the correspondent weight instead of zeroes. Matrix B and C are the input and output weighting matrix where it prioritises the importance between two different inputs or outputs. Matrix D is usually formed of a zero matrix due to only rare cases when the outputs are formed with a gain of inputs. This gives the advantage in designing a multi-variable system control which the weighting between them can be adjusted.

Those four gains, A, B, C and D, can be estimated by the prediction error method (pem). Such method estimates the error of N^{th} order and finds the minimum cost by the following equations:-

$$\hat{\theta}_N = \arg \min_{\theta \in D_M} V_N(\theta, Z^N)$$

Equation 33

The cost function, $V_n(\Theta, Z^N)$, can be calculated using Equation 34 [41][89].

$$V_N(\theta, Z^N) = \frac{1}{N}\sum_{t=1}^{N} e_F{}^T(k,\theta)\Lambda^{-1}e_F(k,\theta)$$

Equation 34

where,

V_n is the cost function

Z_n is the measurement data

Λ is the weighting matrix

N is the number of samples

$e_F(k,\Theta)$ is the prediction error function and can be determined by [41]:-

$$e_F(k,\theta) = L(q,\theta)H^{-1}(q,\theta)\big(y(k) - G(q,\theta)u(k)\big)$$

Equation 35

where,

L is the monic prefilter that can be used to enhance certain frequency regions.

G is process model

H is white noise model

θ can be determined by the least squares method by minimizing the sum of the form of the output and the product of θ and the measurement data.

$$\sum_{t=1}^{N}[y(t) - z^T(t)\theta]^2$$

Equation 36

In the linearisation of the engine simulation, the state-space form consists of five emission parameters, namely CO_2, O_2, CO, NO and exhausts gas temperature. The state-space tries to identify the four engine control parameters, including fuel-to-air ratio, ignition timing and exhaust and intake valve events. To simplify the state-space and increase performance, the state-space is developed as a MISO system.

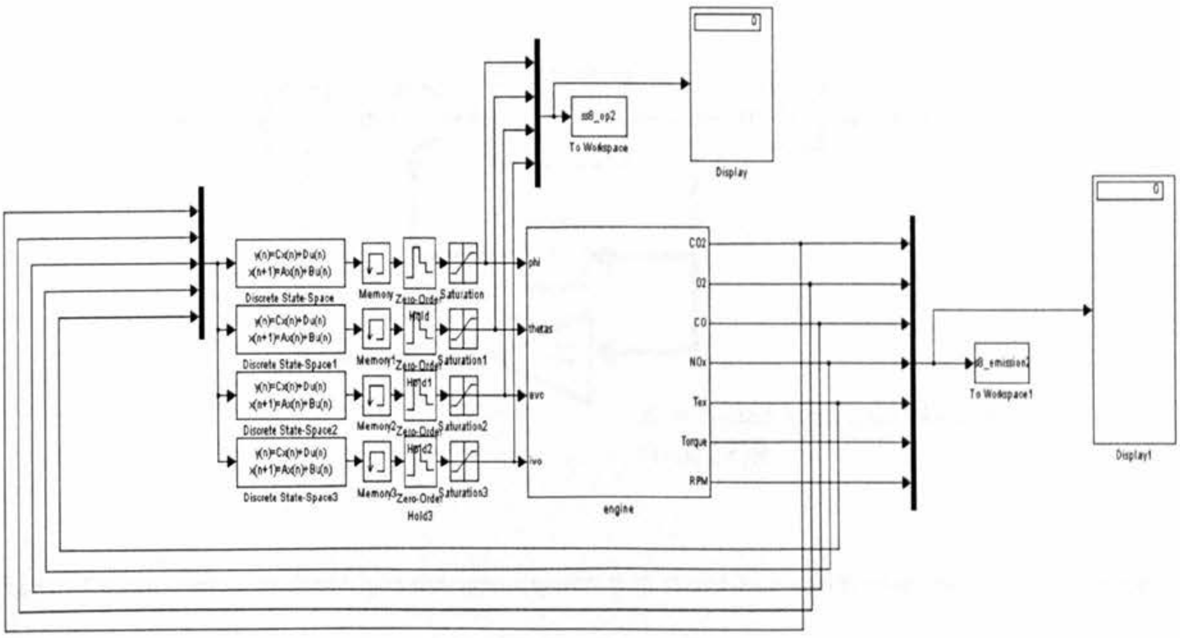

Figure 62 State-space engine model

The next step is to identify the state feedback control gain, K, which agrees the state feedback control law as shown in Equation 37.

$$u(t) = -Kx(t),$$

Equation 37

where,

u is the input

x is the state

K_i is the gain between input and output

and state-feedback controller presents in Figure 63 can be updated from state-space system Figure 60 by applying the input gain as

$$x(t+1)=A-BKx(t)$$

Equation 38

where,

K is the closed-loop gain

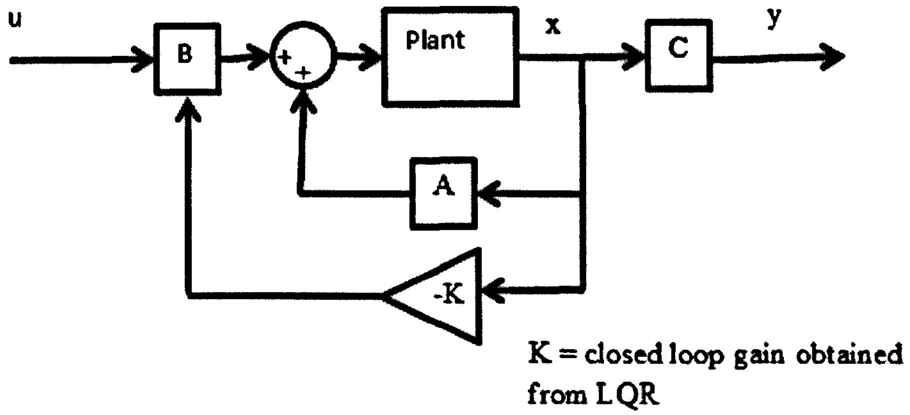

Figure 63 Block diagram of closed-loop state-space system with closed-loop gain K obtained from LQR method

Assume engine parameter is controllable against the emissions and performance, in the gain K can be obtained using linear quadratic regulator (LQR) method which optimises the system at the minimum cost. The state-space can be optimised by a LQR with the minimum cost. LQR is calculated to minimize the cost function J(u).

The cost function is:-

$$J(u) = \sum_{t=1}^{\infty}(x[t]^T Qx[t] + u[t]^T Ru[t] + 2x[t]^T Nu[t])$$

Equation 39

where,

Q is the state cost, = $Q^T \geq 0$

R is the input cost, $R = R^T \geq 0$ and

N is the time horizon

The LQR can be solved by Riccati equation with the condition $s = s^T \geq 0$:-

$$A^TSA - S - (A^TSB + N)(B^TSB + B)^{-1}(B^TSA + N^T) + Q = 0$$

Equation 40

The controller is to assume the simplest case to control the system by choosing $R = 1$, and $Q = C'.C$. The cost function corresponding to Q and R share the equal importance in the state variables although this can be tuned.

6.6.1 State-space engine simulation model without fuel estimation switch

The initial test develops four MISO state-spaces using one dataset contain all three fuel compositions, including Isooctane (C_8-H_{18}), Methanol (C_1-H_4-O_1) and Ethanol (C_2-H_6-O_1). This test did not include the fuel estimator. The state-spaces were developed using the 8th order. The engine simulation is run for 3 seconds with the fixed speed and torque. The aim is to find the set engine operating parameters in the lowest emissions in all constraints.

The results of the simulation in the level of emission and engine operating parameters show in Figure 64 & Figure 65 respectively. The controller is unstable and unable to find the set of engine operating parameters. One solution to improve the controller is to separate the controller according to the estimated fuel composition and controller switch to corresponding portion. Such fuel estimator developed in section 5.5. The state-space is developed in different fuel composition, Isooctane (Figure 67 and Figure 68), Methanol (Figure 69 and Figure 70) and Ethanol (Figure 71 and Figure 72). Results show that controllers are stabilised after the engine temperature saturates at 0.6 seconds.

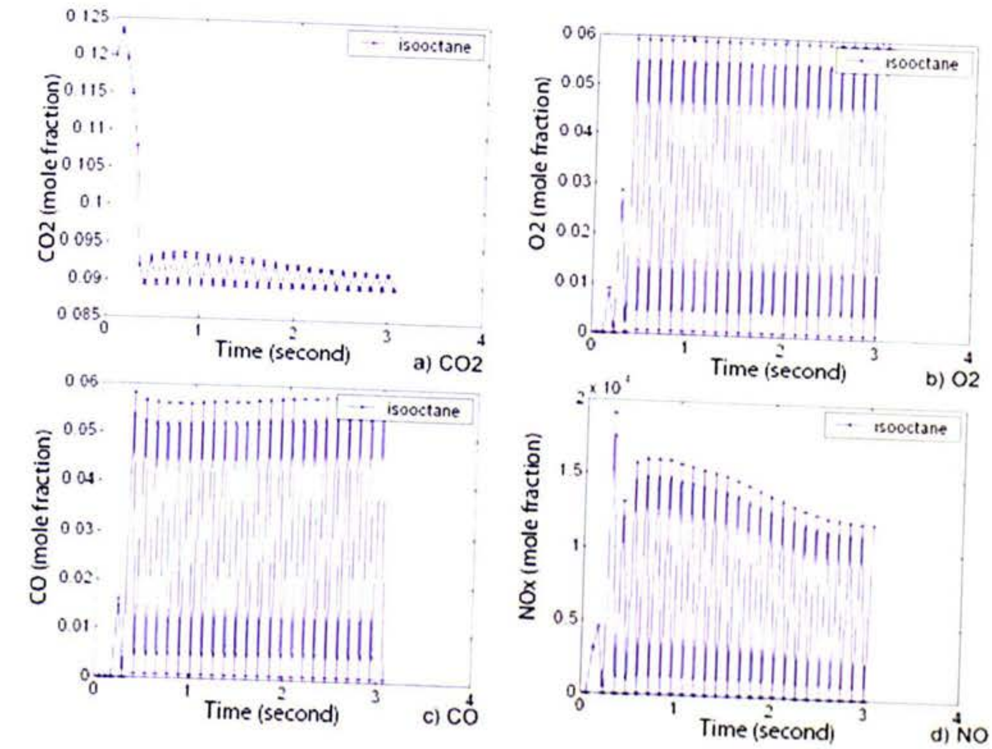

Figure 64 State-space result of emission level, a) CO_2, b) O_2, c) CO and d) NO

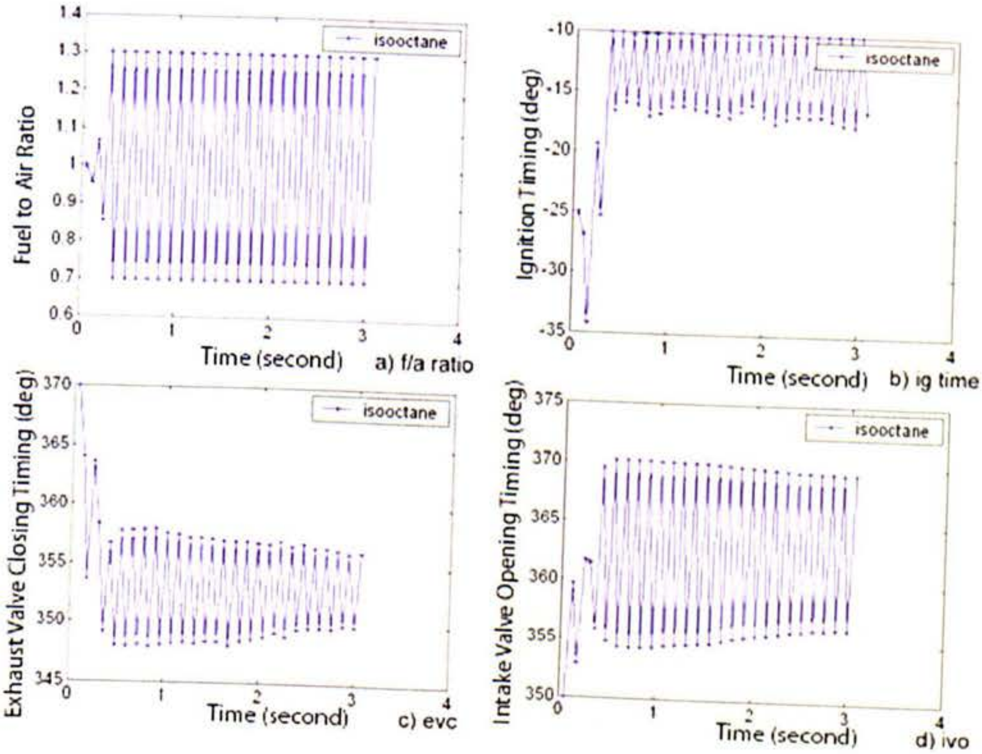

Figure 65 State-space result of emission level, a) fuel-to-air ratio, b) ignition timing, c) exhaust valve closed timing and d) Intake valve open timing

6.6.2 State-space engine simulation model with fuel estimation switch

Three separate state-space models have been developed based on three different types of fuel, Isooctane, Methanol and Ethanol. The fuel estimator which developed in Chapter 5 is added to give the proportion switch according to the fuel type estimated. Figure 66 shows the Simulink diagram. Four emission composition, CO_2, CO, O_2 and NOx in additional with exhaust temperature are used as the controller inputs. For each fuel type, four state-spaces are developed for each engine operating parameters, including 1) fuel-to-air ratio, 2) ignition timing, 3) exhaust valve closed timing, and 4) intake valve opening timing.

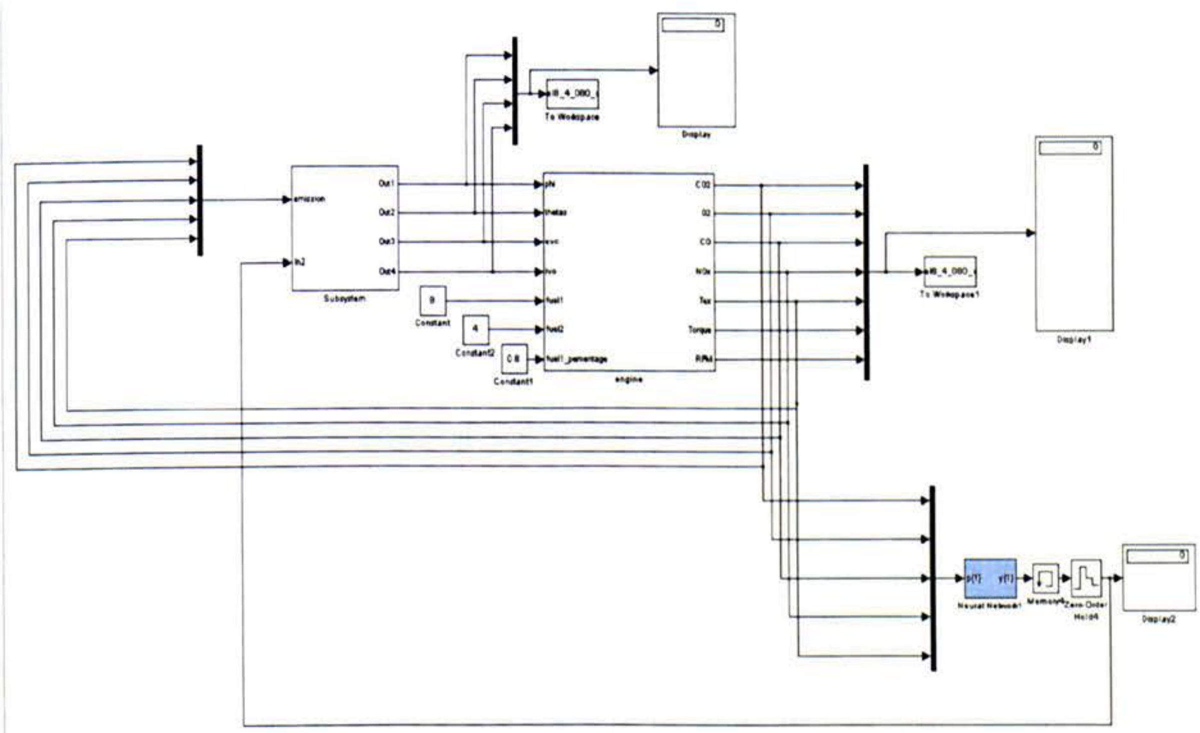

Figure 66 MATLAB Simulink model of a state-space control with aid of fuel estimator

Pure Isooctane

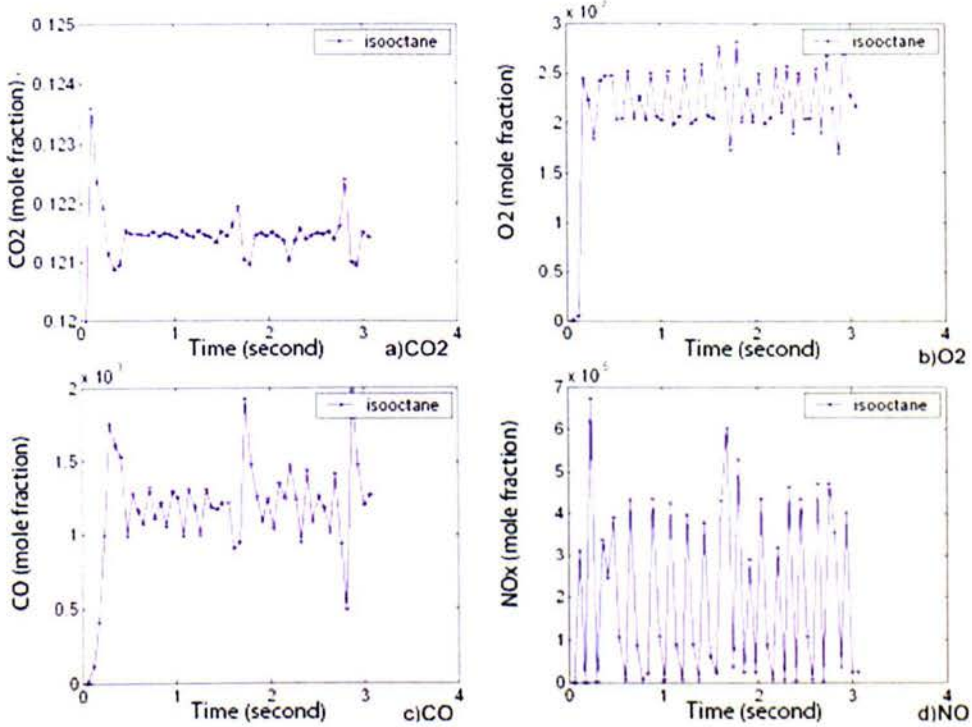

Figure 67 Pure Isooctane state-space result of emission level, a) CO_2, b) O_2, c) CO and d) NOx

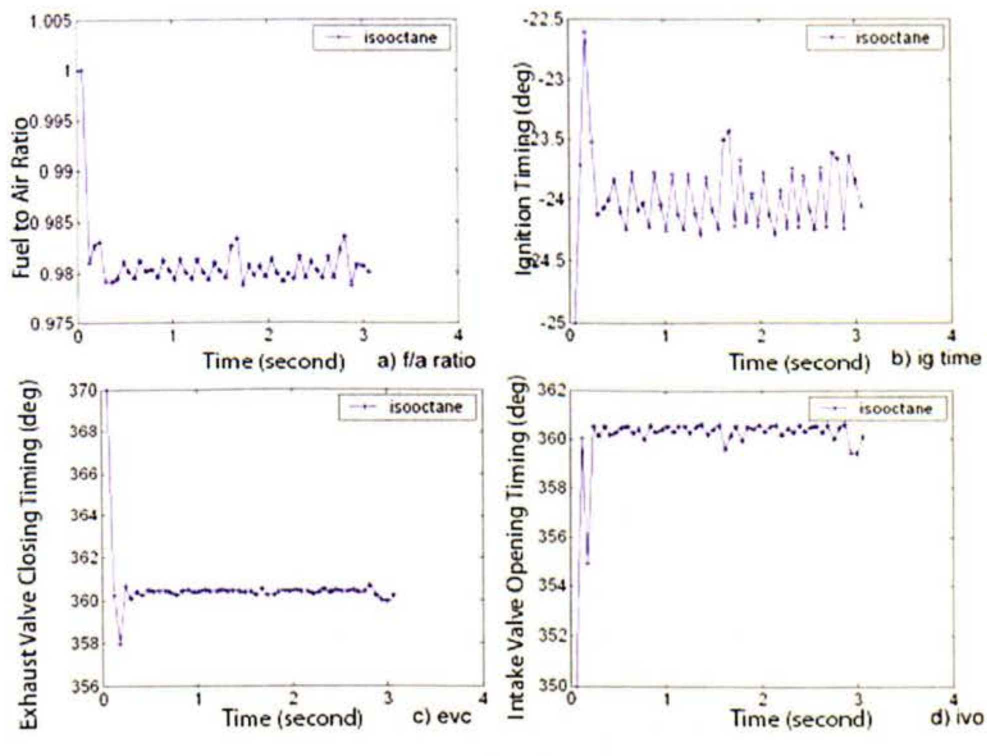

Figure 68 Pure isooctane state-space result of emission level, a) fuel-to-air ratio, b) ignition timing, c) exhaust valve closed timing and d) Intake valve open timing

Pure Methanol

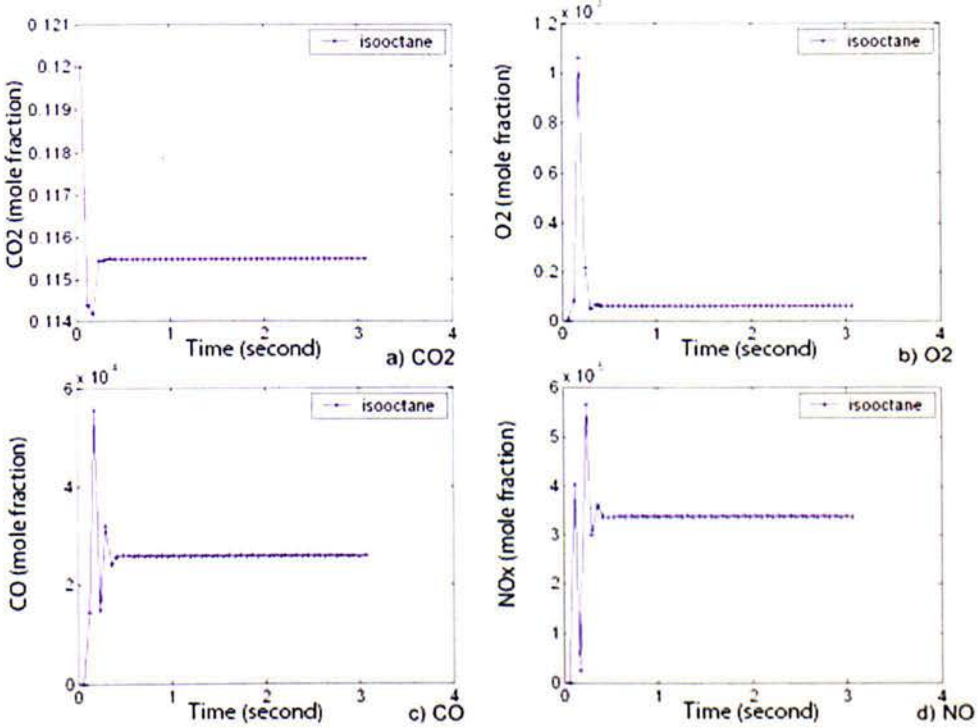

Figure 69 Pure methanol state-space result of emission level, a) CO_2, b) O_2, c) CO and d) NOx

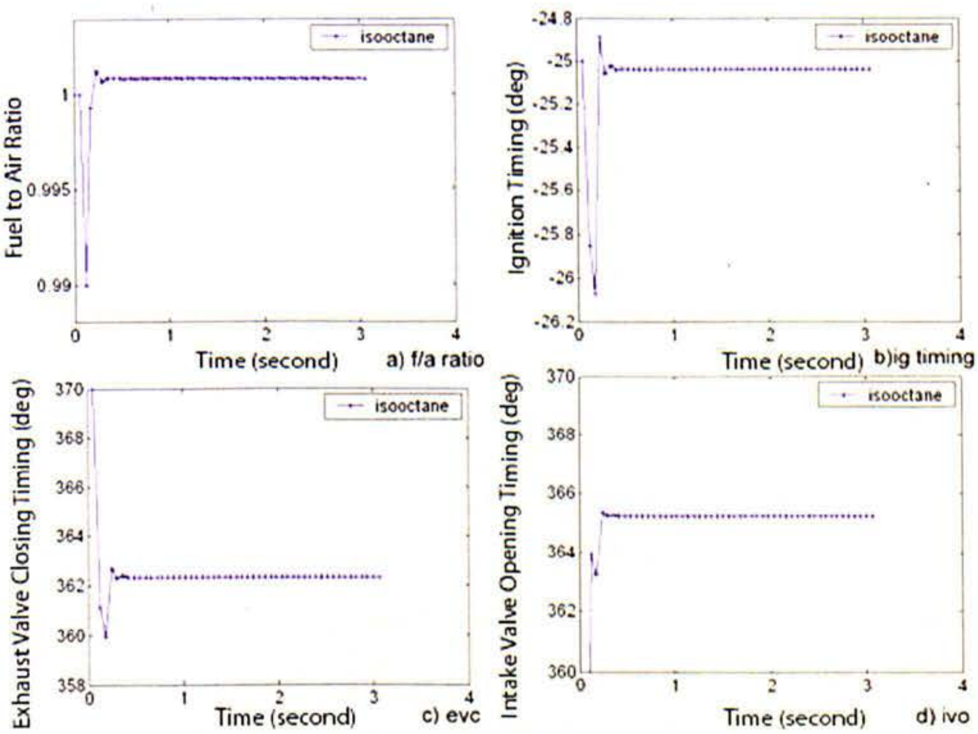

Figure 70 Pure methanol state-space result of emission level, a) fuel-to-air ratio, b) ignition timing, c) exhaust valve closed timing and d) Intake valve open timing

Pure Ethanol

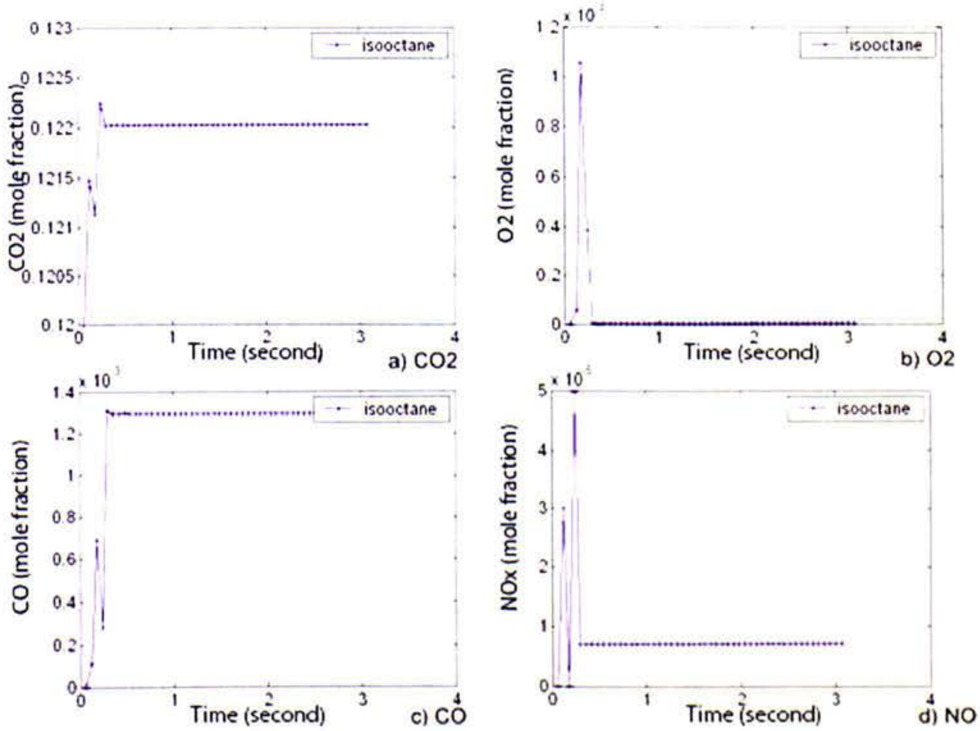

Figure 71 Pure ethanol state-space result of emission level, a) CO_2, b) O_2, c) CO and d) NO

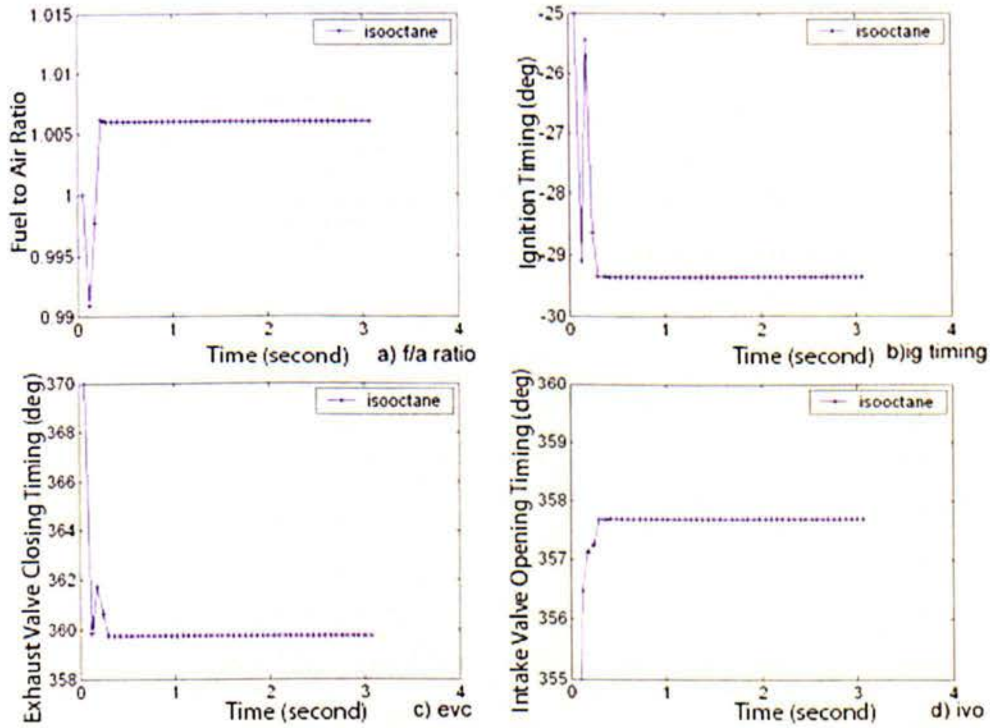

Figure 72 Pure ethanol state-space result of emission level, a) fuel-to-air ratio, b) ignition timing, c) exhaust valve closed timing and d) Intake valve open timing

6.6.3 Controller comparison

Considering the validation set of level of emission found in the engine, the state-space identified the optimal engine operating parameters. Figure 73 shows the results for Isooctane values used to compare the engine operating values between the original input and the state-space results. The red line denotes the random operating parameters without control. The blue lines are the optimal parameters identified by the state-space to provide the lowest emission level in all constraints. The black lines are the resulting of further control using state-space model with LQR. Results show that the optimal fuel-to-air ratio lies at around 1, which is in the stoichiometric ratio. The optimal ignition timing happened between -20 to -30 degrees.

However it is found that the state-space with LQR provided rather slow control for the valve timing. The exhaust valve closing timing and intake valve open timing have limited effect on emission composition by having significant effect on the resultant engine speed, although it is noted that late intake valve closing timing reduces the NOx emissions [81], intake valve closing timing was not include in this thesis. If the optimal valve timings found are beyond the realistic values, the controller can use a saturation block to limit the value of valve timing within a range.

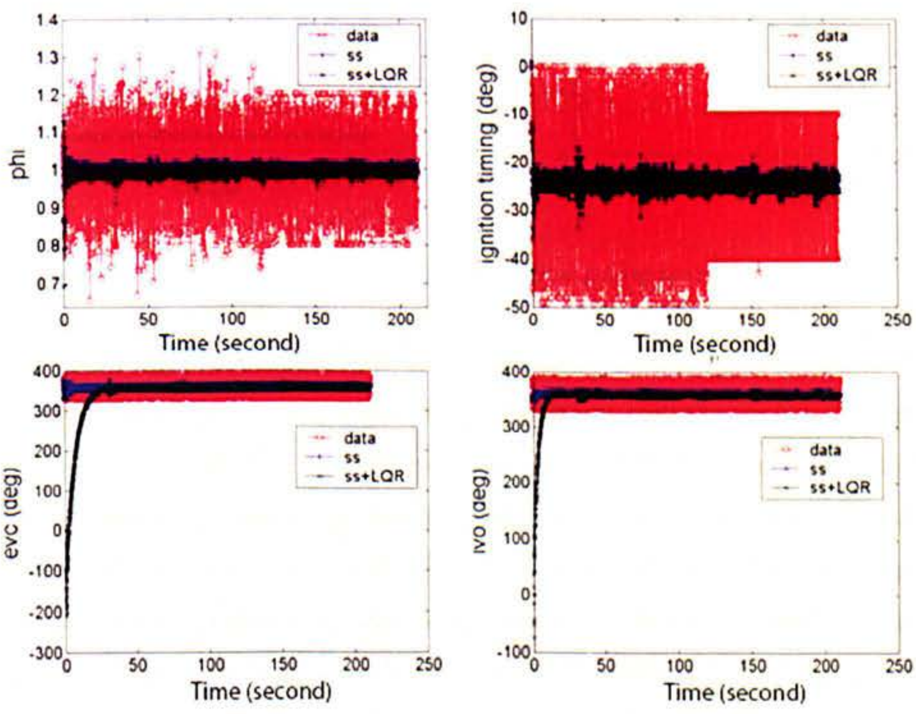

Figure 73 The engine operating parameter of simulation data in red, and the state-space optimized engine operating parameters in blue, state-space with LQR optimized engine operating parameters in black

6.7 Engine control in different speed with different fuel mixture

To test the controller working with different fuel mixtures, we use the same mixtures tested in 5.4.4, which are Isooctane-Methanol and Isooctane-Ethanol. The portion started with 100% Isooctane and gradually mixing with Methanol and Ethanol by 10% and 20%, respectively. The initial test used a steady-state where all operating parameters, speed and load are fixed. Results are shown in Figure 74 with the level of emissions found for four compositions. The controller is able to find similar emissions while the fuel composition is changing. The CO_2 level increased where the mixture is turned closer to Methanol, and decreased in O_2. The changes were not significant with the changes in CO_2 and O_2 were 0.1%.

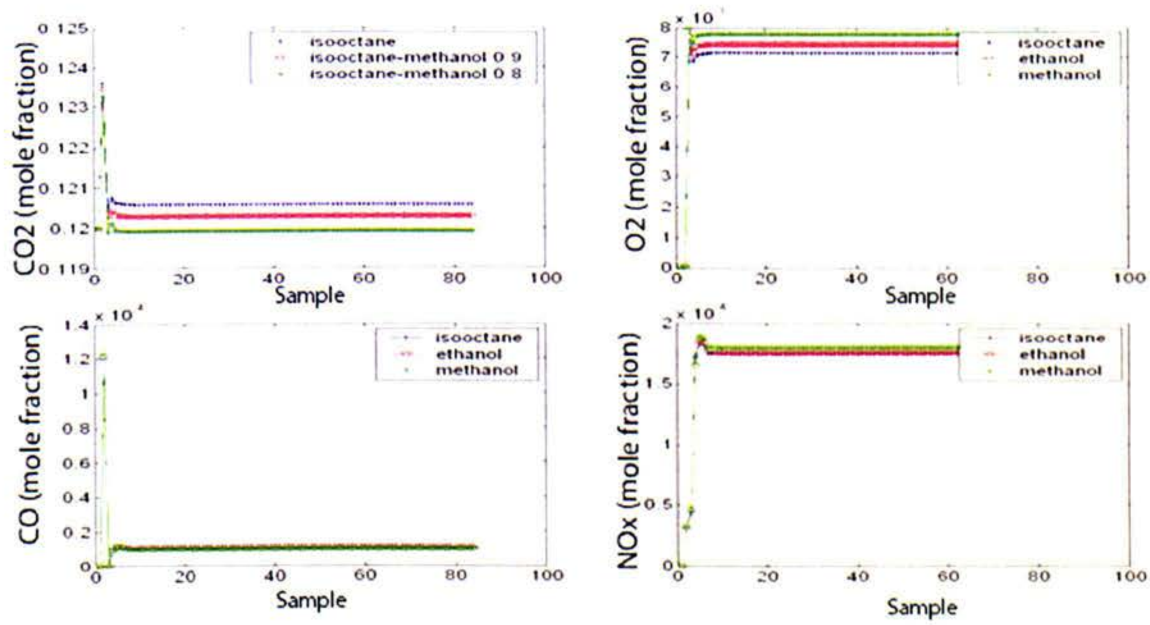

Figure 74 State-space and neural network comparison at different engine speed

6.7.1 Isooctane-Ethanol mixture with different speed

The next step is to take into account the realistic situation with the change in engine speed. The aim for the simulation is to use state-space model with fuel estimator to find the lowest emission while keeping similar performance. The first simulation used the Isooctane-Ethanol mixture by mixing Ethanol into Isooctane by 10%, 20%, 30% and 40%. The amount of throttle opened is set to constant at 25%, which allows the increase of speed. The performance measurement of the controller is in speed and the levels of the emissions, in compositions of CO_2, O_2, CO and NOx, found are at their minimum. Figure 75 shows the engine speed for 5 seconds and where it increases from idle speed at 1000 rpm to over 3000 rpm. The result showed that the controller was able to maintain similar speed. Thus it can be concluded that the performance didn't change significantly by using different mixtures when applying our proposed engine control.

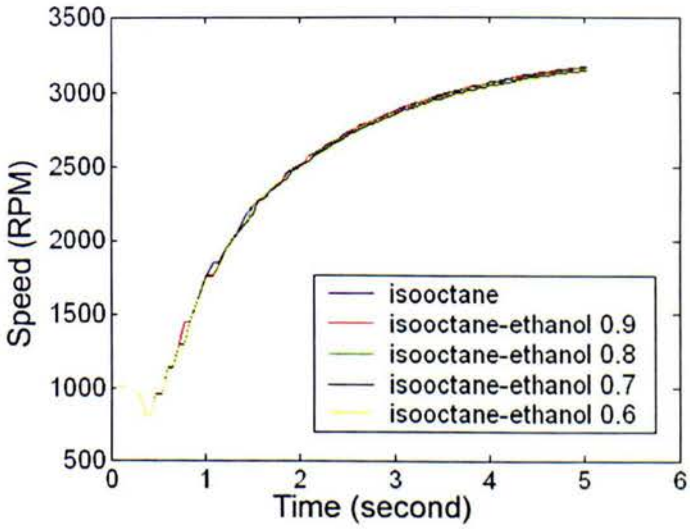

Figure 75 Speed of State-space control with fuel estimator in different portion of Isooctane-Ethanol mixture

The emissions produced from engine simulation are shown in Figure 76. The engine produced similar amount of CO_2, O_2 and NOx emissions. When larger portion of Ethanol was blended into Isooctane, CO emissions decreased. The engine operating parameters had about no difference in fuel-to-air ratio, ignition timing and valves timing. Therefore no control adjustment was needed and the level of CO dropped as presented in 2.5.5.

The results of engine control parameters are shown in Figure 77. The fuel-to-air ratio found throughout the simulation is slightly richer but the ratio was close to 1. The engine operating parameters did not change significantly, with fuel-to-air ratios were slight higher than 1 (slightly richer mixture) and ignition timing at around 25 degrees from 1^{st} second to 5^{th} second corresponding to 2000 to 3300 rpm, respectively (Figure 77). The exhaust valve timings show similar behaviour against ignition timing. For mixtures containing methanol, the controller found the later exhaust valve closed timing at 380 degree, whereas pure isooctane has its own optimal value at around 373 degree.

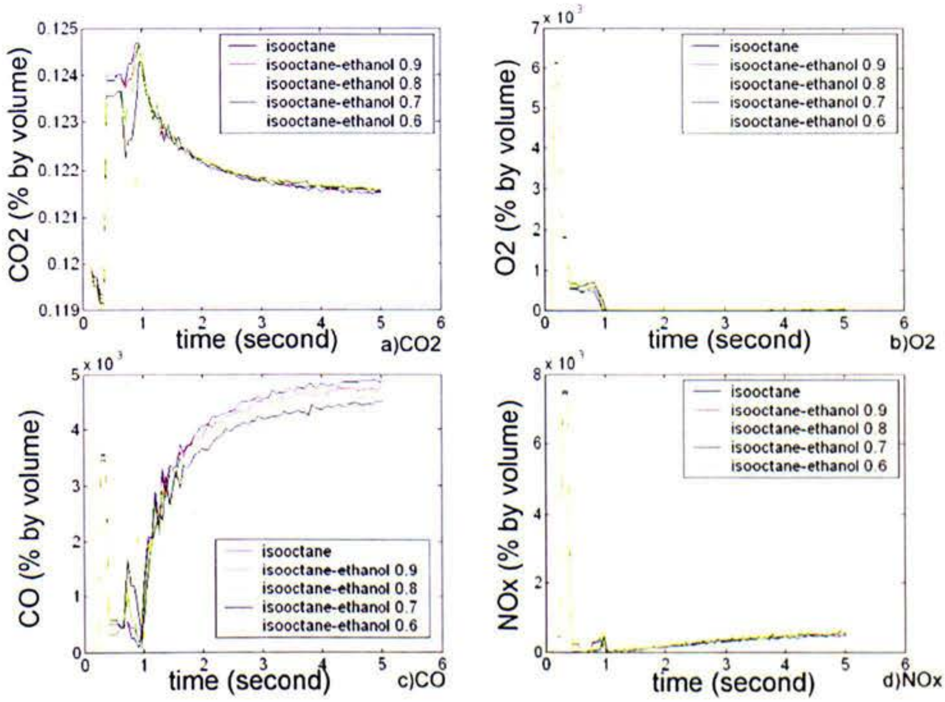

Figure 76 The level of emissions found in the engine simulation using state-space control with fuel estimator in different portion of Isooctane-Ethanol mixture. a) is CO_2, b) is O_2, c) is CO and d) is NOx

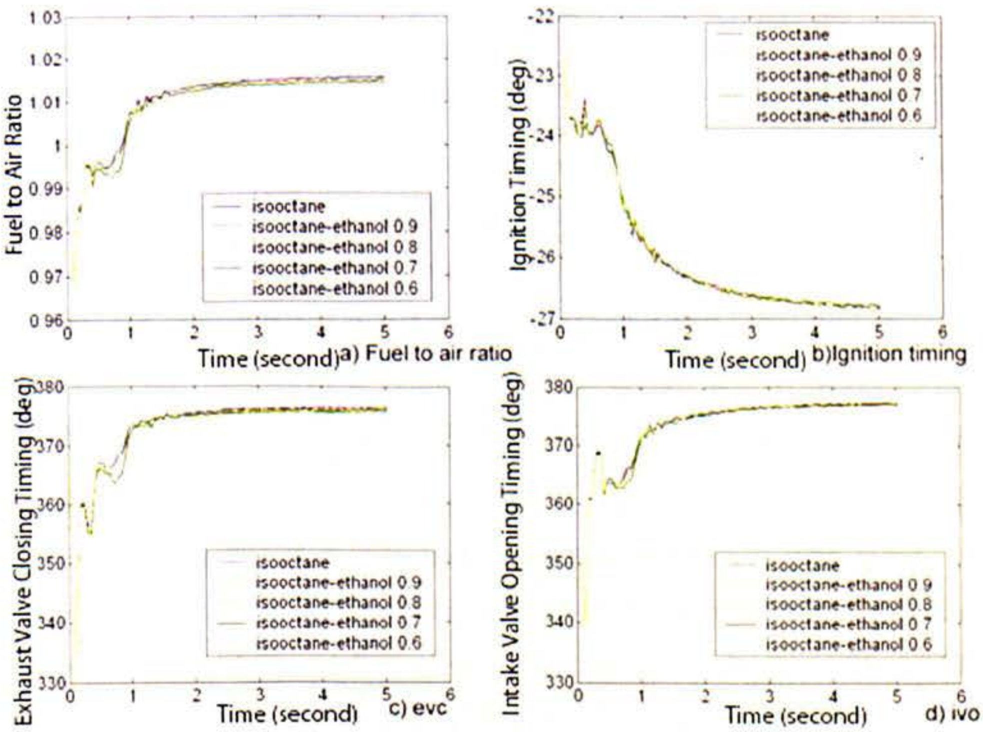

Figure 77 The engine operating parameters recorded in the engine simulation using state-space control with fuel estimator in different portion of Isooctane-Methanol mixture. a) is fuel-to-air ratio, b) is ignition timing is degree, c) is exhaust valve closed timing and d) is the intake valve opening timing

6.7.2 Isooctane-Methanol mixture with different speed

The same simulations were carried out, as shown in 6.7.1, but replacing the fuel with Isooctane-Methanol mixture. The portions of mixture are mixing Ethanol into Isooctane by 10%, 20%, 30% and 40%. The performance in terms of speed and levels of emission of CO_2, O_2, CO and NOx were recorded. The result showed in Figure 78 agreed that the performance in speed had no significant differences and can be concluded that the performance is similar with different mixtures after engine control is used.

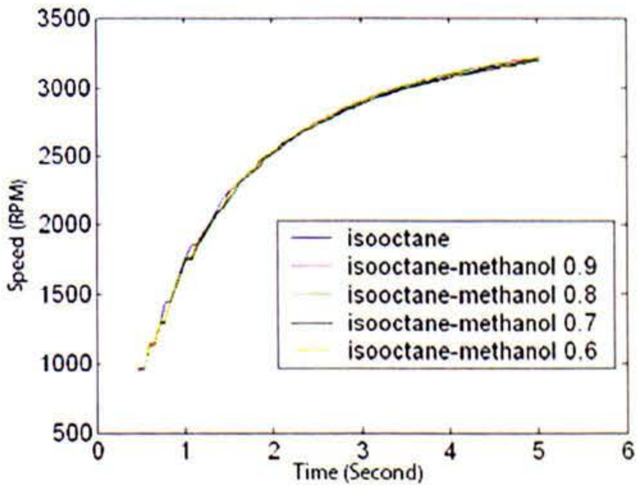

Figure 78 Speed of State-space control with fuel estimator in different portion of Isooctane-Methanol mixture

The emission levels found in the simulation are shown in Figure 79. Results showed that pure Isooctane has the minimum CO_2 whereas CO is the maximum. When the portion of methanol is increased, the CO_2 was kept relatively constant, but a gradually reduction of CO was noted. The level of O_2 and NOx (0.001% by volume) had not significant variations. The results also showed the variations in the levels of emission in larger at slow speeds, especially in CO_2 and CO. This is because the engine needs to warm up. Further tests are needed on slow speed.

The results of engine control parameters are shown in Figure 79. For pure Isooctane (shows in the blue line in Figure 79), the ignition timing was retarded to around 28 degree. The results also show that when the mixture was closer to Methanol, the fuel and air ratio turned closer to stoichiometric. The controller optimised the ignition timing according to different mixtures. It can be concluded that the results shown in Isooctane-Methanol mixture agreed the similar performance as shown in Isooctane-Ethanol. Both controllers provided optimised control and identified the minimum emissions without significant change in speed (in speed range between 1500-3300 rpm).

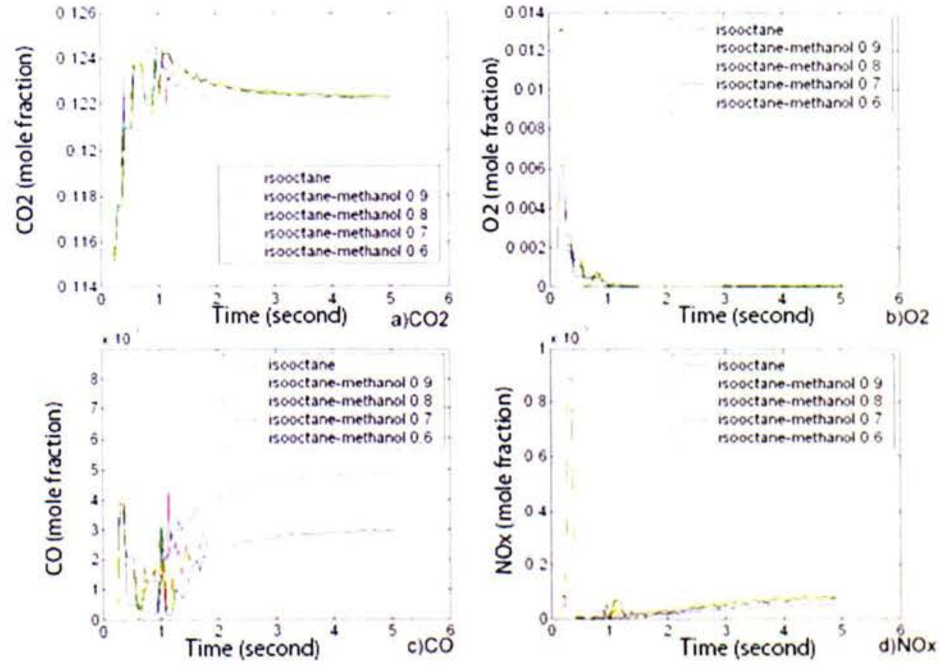

Figure 79 The level of emissions found in the engine simulation using state-space control with fuel estimator in different portion of Isooctane-Methanol mixture. a) is CO_2, b) is O_2, c) is CO and d) is NOx

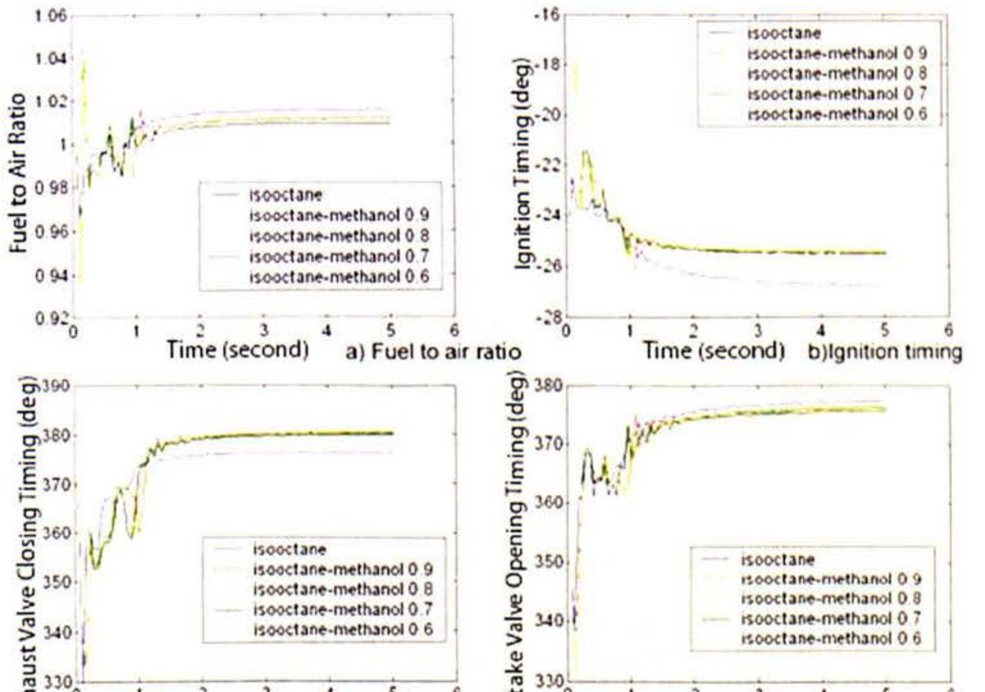

Figure 80 The engine operating parameter recorded in the engine simulation using state-space control with fuel estimator in different portion of Isooctane-Methanol mixture. a) is fuel-to-air ratio, b) is ignition timing is degree, c) is exhaust valve closed timing in degree and d) is intake valve open timing in degree

6.8 Engine control in basic engine cycle with different fuel mixture

The final tests in the engine control are implementing the controller onto the given engine cycle. They are the continuation of 6.7, where previous tests were run with the throttle constantly open, allowing the engine simulation while the speed is increasing exponentially. Here, an engine cycle is used with the change in speed, which is able to capture the behaviours of rapid and slow speed changes when the engine is accelerating or decelerating between 1000 rpm and 3000 rpm. The step of the change is two seconds, allowing the engine controller to settle the given speed. The engine cycle used is presented in Figure 81. It is noted that the tests are run on a fixed torque.

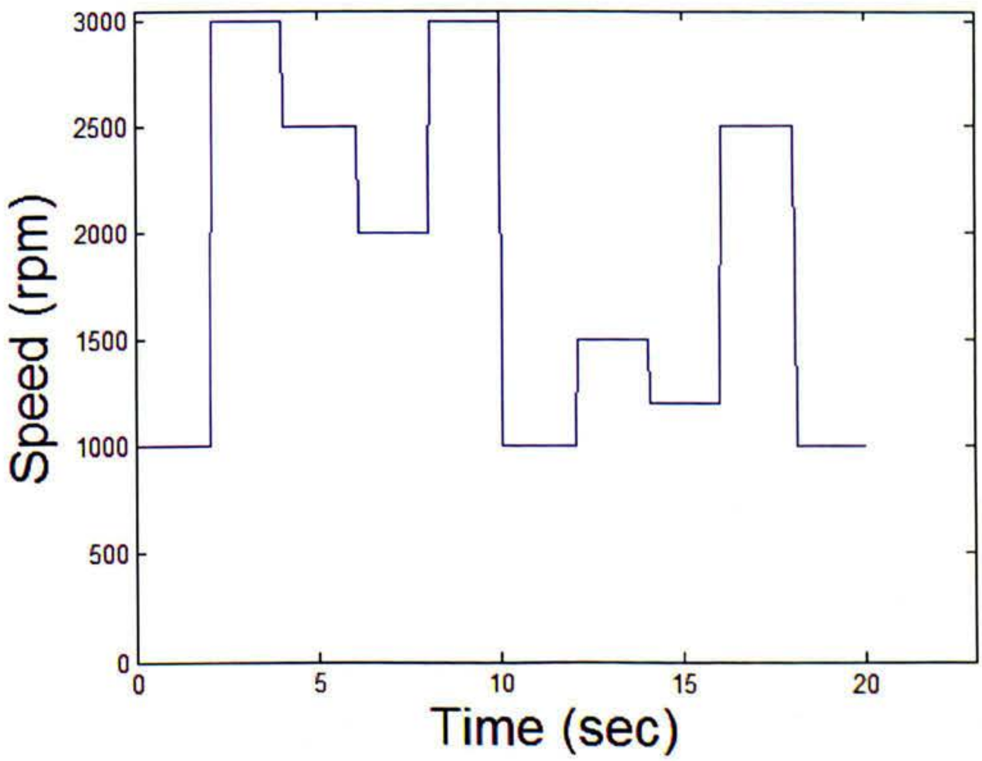

Figure 81 Engine cycle used in the final tests

6.8.1 Comparison of engine cycle tests with and without control

To test that the developed engine control provides the optimisation of emissions, two engine simulations were run with and without control, respectively in the engine cycle lasted 20 seconds. The engine parameters used without controller are fixed. The specifications of the engine run without control use two fuel-to-air ratios which are fixed at 0.95 and 1.05. The ignition timing is fixed at 25°. Exhaust valve closes at TDC (360°) and the intake valve opens at the same time. Two cases of Isooctane-Ethanol mixtures have been chosen for this comparison. The first case uses 90% Isooctane blended with 10% Ethanol while in the second case Ethanol portion was increased to 20% (i.e. 80% Isooctane).

The levels of emissions found in species of CO2, O2, CO and NOx with and without control are presented in Figure 82. The results show that when the engine has no control, the levels of emissions are not at their minimum at all constraints. When the fuel-to-air ratio is 1.05 at richer mixture (value over 1), the red lines denoted in the graph show the level of CO_2, O_2 and NOx are at the lowest compared to other two results, but the level of CO is over 1%, even exceeding the level allowed by legislation. Whereas when the fuel-to-air ratio is 0.95 at richer mixture, the black lines denoted in the graph show the level of CO_2 and CO are at the satisfactory level. The negative effect is the level of NOx which is about eight times larger than the resulting with control. Therefore it can be concluded that the controller found the better control in all level of emissions.

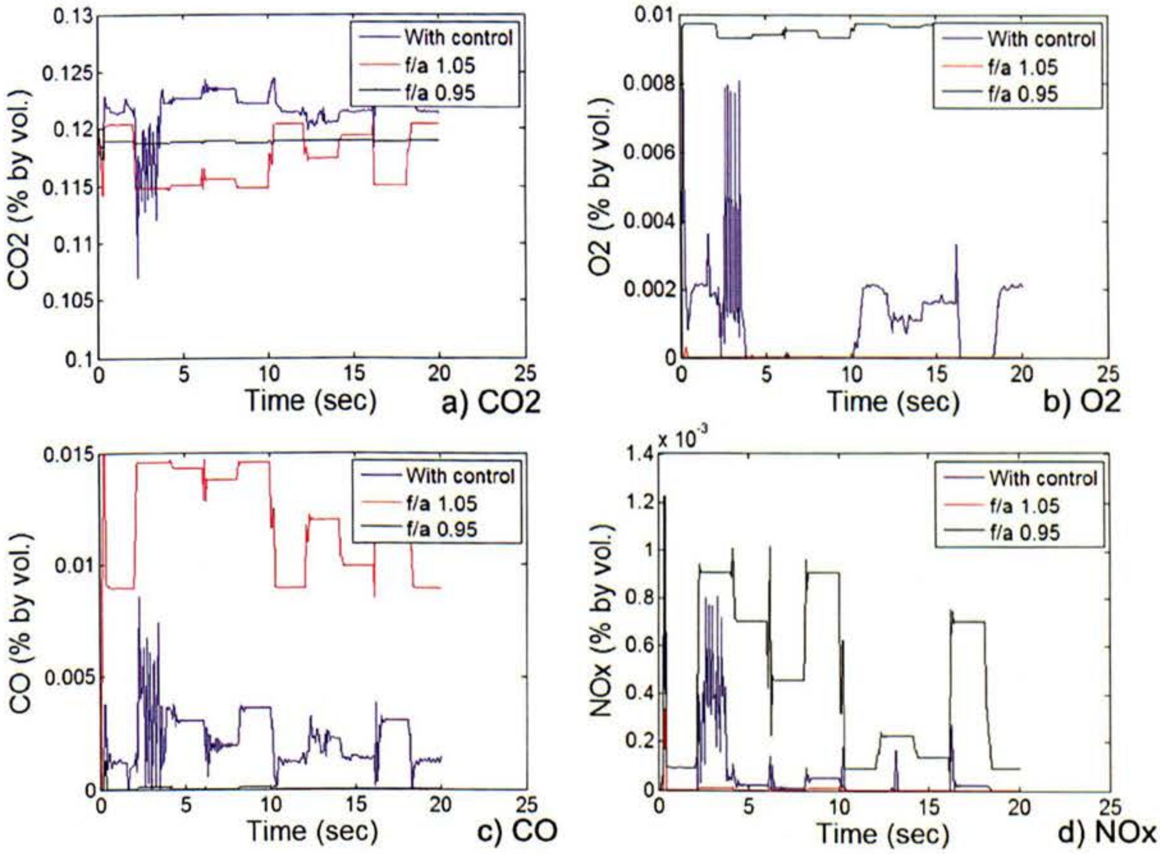

Figure 82 The level of emissions found in the engine simulation with and without control with given fuel-to-air ratio. a) is CO_2, b) is O_2, c) is CO and d) is NOx

- Case 1 Isooctane-Ethanol Mixture

Figure 83 presents the level of emissions generated from the simulation with the given engine cycle. The related engine operating parameters are presented in Figure 84. The results show that the controller provides quick responses in the emission control. In the 2nd second the emissions have rapid changes due to the speed increase from 1000 rpm to 3000 rpm. The controller is able to pick up the behaviours and the emissions are settled in the next few revolutions. For the performance of the steady control, we can draw the same conclusion as in 6.7.1.

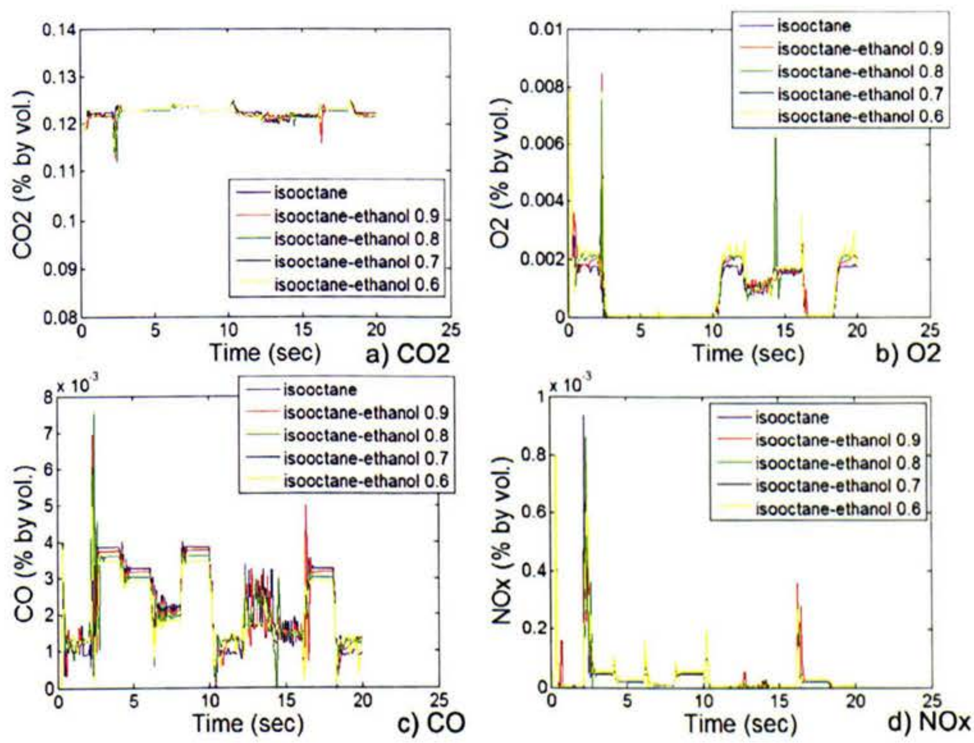

Figure 83 The level of emissions found in the engine control simulation of engine cycle in different portion of Isooctane-Methanol mixture. a) is CO_2, b) is O_2, c) is CO and d) is NOx

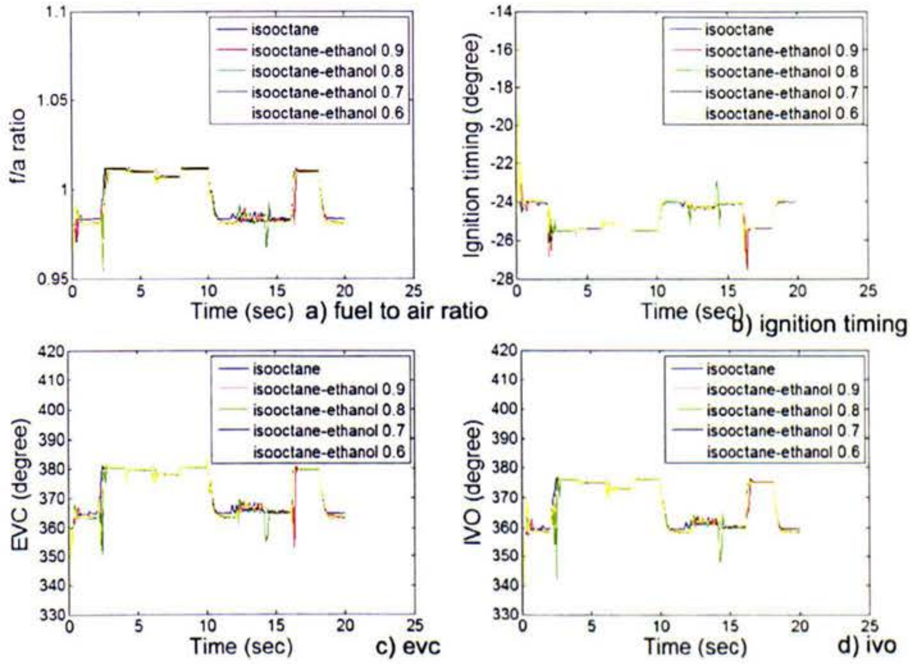

Figure 84 The engine operating parameters recorded in the engine control simulation of engine cycle in different portion of Isooctane-Methanol mixture. a) is fuel-to-air ratio, b) is ignition timing is degree, c) is exhaust valve closed timing and d) is the intake valve opening timing

- Case 2 Isooctane-Methanol Mixture

Case 2 tests on the engine run with Isooctane-Methanol mixture in the given engine cycle. Figure 85 presents the level of emissions generated from the simulation with the engine cycle. The related engine operating parameters are presented in Figure 86. The results show that when the speed is changing by the step, the controller settles quickly. It can be observed that when the speed varies, the emissions of CO_2 and NOx have rapid increases and CO decreases rapidly. The controller is able to settle the emissions quickly within a few engine revolutions.

One uncertainty found is in the result of 90% Isooctane and 10% of Methanol which is denoted by the red line. The controller has an unstable response between 2 to 4 seconds. The controller is unable to pick up the optimal engine operating parameters as shown in Figure 86 where the values of fuel-to-air ratio, ignition timing and valve events are fluctuating. The same trends happen at the results between 12 and 14 seconds. By analysing the speed at the moment where the uncertainties are found, we can note that they happen when the speed is increasing from 1000 rpm to higher speed. Therefore the controller performs worse at lower speed and the controller needs to improve by collecting more data while training the state-spaces. For the performance of the steady control, we can draw the same conclusion as in 6.7.2.

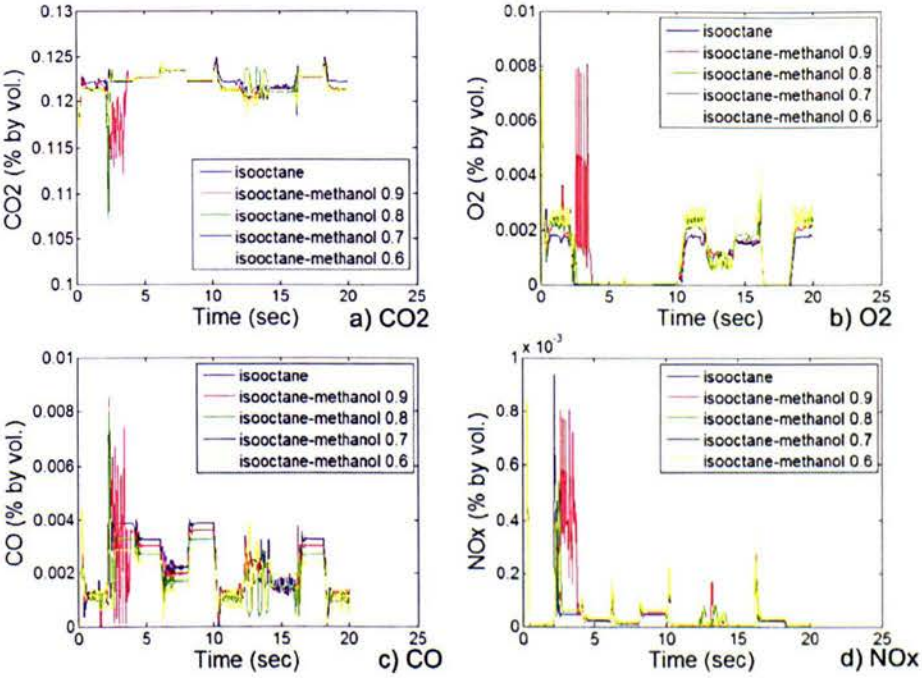

Figure 85 The level of emissions found in the engine control simulation of engine cycle in different portion of Isooctane-Methanol mixture. a) is CO_2, b) is O_2, c) is CO and d) is NOx

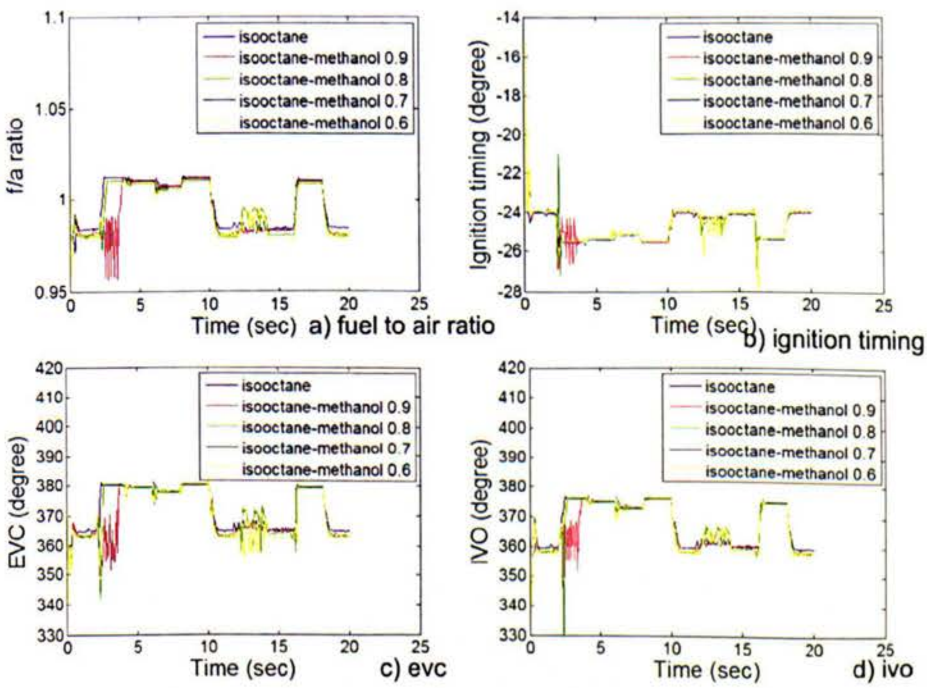

Figure 86 The engine operating parameters recorded in the engine control simulation of engine cycle in different portion of Isooctane-Methanol mixture. a) is fuel-to-air ratio, b) is ignition timing is degree, c) is exhaust valve closed timing and d) is the intake valve opening timing

6.9 Conclusions

The chapter discussed the development of the engine controller which is able to optimise engine control parameters resulting in the minimum levels of emissions while keeping the optimal performance in various speed. Three closed-loop controllers, PI control, NAR neural network and state-spaces with LQR have been investigated. Five input variables taken from the condition of exhaust gas have been identified, including the level of CO2, O2, CO and NOx in addition to the exhaust gas temperature. Four engine operating parameters are aiming to control the engine, including the fuel-to-air ratio, ignition timing, exhaust valve closed timing and intake valve opening timing. Three fuel mixtures have been used for the investigation, including 100% Isooctane, Isooctane-Methanol mixture and Isooctane-Ethanol mixture. The engine simulations were also run at different speeds to test the controller working in different conditions. The chapter can be concluded as follows:-

1) By comparing three closed-loop controllers, PI control performs poorly. The controller is not settling quickly enough for engine control applications.
2) The performance of NAR neural network is satisfactory for engine control applications. It is similar to the state-spaces control result.
3) Four MISO state-spaces have been developed for each control variable.
4) The controller improves by generating one set of state-spaces controller for each given fuel. The state-spaces provide the proportional control according to the probability of the fuels calculated from the fuel estimator.
5) The controller is tested in various conditions. The results show that the controller is able to control the engine where the emissions are minimal while keeping optimal performance.

6.10 Summary of Chapter 6

This chapter discusses the control algorithm to control four engine operating parameters to achieve lowest emission levels with different fuel mixture and at different engine speeds. The four control parameters used are fuel-to-air ratio, ignition timing, exhaust valve closed timing and intake valve open timing. The emission target is to maintain CO_2, O_2, CO and NOx to the minimum. The controller treats the system in discrete time, which is discussed in 6.3. Three different closed-loop multi input single output (MISO) control algorithms are ran in the engine simulation, which are PI control in 6.4, nonlinear auto-regressive (NAR) neural network in 6.5 and state-space model with linear quadratic regulator (LQR) in 6.6. Results show that state-space model with LQR combined with the fuel estimator are chosen for further study because they can achieve the minimum level of emissions in all constraints. Further studies on different mixture at different speeds while engine torque was fixed were performed. Results discussed in 6.7 and 6.8 showed the performance of the controller while fuelling with two mixtures, including Isooctane-Ethanol and Isooctane-Methanol. The simulations used different portions of Isooctane into Methanol or Ethanol by 90%, 80%, 70% and 60%. Results agreed that the emissions were kept the lowest possible while engine speed was increasing with constant opening of the throttle.

Chapter 7 Conclusions

7.1 Conclusion

This thesis is set out to research the spark ignition (SI) engine controller while fuel composition is continuously changing. The novel approaches developed the MIMO closed-loop control which is satisfied with the objectives listed in 1.4. The engine simulation model is used as the platform to test on the controller. The criteria of the engine simulation including 1) the variation of engine operating parameters fuel-to-air ratio, ignition timing, exhaust valve closed timing and intake valve open timing; 2) collection emissions composition including CO_2, O_2, CO and NOx, 3) choice of fuel compositions, including Isooctane, Methanol and Ethanol, and 4) capable of running engine in continuous time. The conclusion of this thesis can be divided into three parts:- the engine simulation model in 7.2, the fuel estimator in 7.3 and the non-linear MIMO closed-loop controller in 7.4.

7.2 Engine simulation model

Chapter 3 develops a single cylinder Spark-Ignition (SI) engine simulation model based on the first law of thermodynamics. In the development of engine model, additional sub-models are used for detailing the engine combustion process, including the heat release, heat transfer, gas exchange, blow-by and friction etc. The final version of engine simulation model is to complete the full engine simulation with intake manifold model is added which can calculates the change in speed. The theory is outlined by increase the amount of opening of throttle, more air enters into intake manifold. The manifold pressure changes and hence varies the pressure in cylinder. The relationship between intake manifold pressure and speed has been discussed in the chapter.

The specification of the engine maps the standard SI engine size. It contains one cylinder with four strokes engine combustion process. The reason of engine simulation using one cylinder is it can remove the unwanted effect between cylinders and can be focused on the improvement of the combustion.

The developed model has been compared with two reference models, Ricardo Wave [91] and Lotus Engine simulation [71]. The results have been discussed in Chapter 4. The parameters of the comparison are using the peak pressure and peak temperature timing during compression and combustion stroke. There are differences between the packages, since more detailed sub-models are included in the commercial packages based on laboratory works on engine materials. One example is cylinder wall material, which has effects on the cylinder heat transfer. The final version of the engine simulation generates the outputs of the condition of the emissions which are used in this thesis in the development of the controller.

7.3 Fuel estimator

The introduction of a fuel estimator aims to provide additional optimisation of engine control taken into account possible unknown fuel compositions after refuelling the engine. Two artificial intelligence methodologies, feed-forward neural network and Adaptive Neuro-Fuzzy Interface System (ANFIS) are investigated, and their comparison has been discussed. Three different fuels are used, which are 100% Isooctane, Isooctane-Methanol mixture, and Isooctane-Ethanol mixture. The measurement of the fuel estimation system is estimating the number of atoms of Carbon and Hydrogen.

7.3.1 Feed-forward artificial neural network

One methodology is the feed-forward artificial neural network which is an open-loop neural network. The first simulation is run by using the fixed value of ignition timing and variable fuel-to-air ratio. Results show that feed-forward neural network is capable to distinguish between three given fuels when the fuel-to-air ratio is less than 1. Accuracy drops with the mixture in learner ratio. The second simulation is run by using fixed value of fuel-to-air ratio and variable ignition timing. Results show that the accuracy of fuel estimation is not affected by different ignition timing. It can be concluded that fuel-to-air ratio is more sensitive than other engine operating parameters, including ignition timing, exhaust valve closed timing, and intake valve opening timing.

The final simulation is run by using two mixtures, namely Isooctane-Methanol and Isooctane-Ethanol. The simulation starts with pure Isooctane and gradually blended Methanol and Ethanol by the percentages of 5%, 10%, 15%, 20%, 25% and 30%. The results show that the neural network is able to identify the changes in different percentage of mixture and is able to provide proportional control to the engine by likelihood of fuels.

7.3.2 Adaptive Neuro-Fuzzy Interface System (ANFIS)

To compare with the performance of feed-forward neural network fuel estimation, a second methodology that uses Adaptive Neuro-Fuzzy Interface System (ANFIS) is investigated. One disadvantage found in this thesis is the complexity for systems that include many input variables. ANFIS requires a large set of fuzzy rules, resulting in long training time and excessive memory requirements to train the system. The controller provided slow response in consideration of large data sets. Thus the results prove that the performance of ANFIS is not better than feed-forward artificial neural network. Therefore, ANFIS is not suitable in multi-input control system and not been chosen in this thesis.

7.3.3 Fuel mixture estimation by probability distribution

Further in the thesis, the outputs of the fuel estimator which are the probability distributions of the three types of fuels provide control gains according to the likelihood of the fuel. In order to do that, the Softmax transfer function is used in the output layer of the neural network where the sum of the outputs is forced to be 1.

Three different mixtures were used, including 100% Isooctane, and blended Methanol and Ethanol into Isooctane by 10%, 20%, 30% and 40%. The simulation ran in continuous time and results show that the fuel estimator is able to identify the changes in blended portions of Methanol and Ethanol. It can be concluded that the fuel estimator is successfully developed. The fuel estimator uses artificial feed-forward methodology and the output is the probability distribution of a given fuel. Moreover, it is capable to providing further control to the engine parameters.

7.4 Engine operating parameters optimisation

Once the fuel type is estimated, the thesis developed engine controller strategies which were able to optimise the engine operating parameters resulting in the lowest emission in all constraints at different speeds. Three closed-loop controllers, PI controller, Non-linear Auto-Regressive (NAR) neural network, and state-space with LQR, are investigated. Five input variables of exhaust gas condition are used, including the level of CO_2, O_2, CO and NOx in addition to the exhaust gas temperature. The comparison of three controllers has been done and their performance can be concluded as follow:-

7.4.1 PI controller

PI controller is the most commonly used closed-loop controller. The controller provides the gains as update according to the error in the past values. The results of using PI in engine control found that PI controller returned slow responses in this application. To improve the performance of PI control in engines, it may need a faster approach in additional to speed up the controller. Methods include adaptive control which are combined with PI such as fuzzy-PID or neuro-PID which is not considered in this thesis.

7.4.2 Nonlinear Auto-Regressive neural network (NAR)

Nonlinear Auto-Regressive neural network (NAR) is a closed-loop neural network methodology where additional layer of extra neurons are added and the corresponding weights can be updated by past values. In this thesis, NAR in engine control was proposed since it provides good control in engine operating parameters. However, it was decided not to adopt it here since it is hard to implement onto the real application with the extra input of the NARX model require a real time input rather than the parallel input-output set which is tested in the thesis.

7.4.3 Closed-loop state-space control

Space-space is a system identification approach which records the behaviour of a system by nth number of order. In this thesis, a MIMO closed-loop state-space controller is developed. The state-space can be used as closed-loop control, i.e. state-feedback controller, by finding the closed-loop gain using LQR. The regulator updated the input matrix, B, by control law A-BK. Three state-space models are developed and each model contains the behaviour of one given fuel from Isooctane, Methanol and Ethanol. The controller gives proportional control according to the fuel likelihood generates from fuel estimator. The feedback gain, K, is calculated offline by using LQR methodology, where the variable, Q, is used simple example of Q = C'.C.

The results show that the closed-loop state-space controller together with the fuel estimator is able to find the stable control with lowest emissions in all constraints. Figure 73 shows the comparison of engine operating parameters between engine with control and without control. It can be concluded that the controller provides the optimal parameters, where the fuel-to-air ratio lied at around 1 and the ignition timing were between -20 to -30 degree. The state-space provides a rather slow control. By just considering the fuel composition changes while refuelling, the fast controller is not a concern in this thesis.

7.4.4 Engine control at different speed

The simulation run on the condition when the throttle is opening constantly, allows the engine to increase the speed. Two simulations were run by using two mixtures, Isooctane-Methanol and Isooctane-Ethanol. The results discussed in 6.7.1 and 6.7.2 prove that the lowest emissions were found and that the performance of engine in speed had no significant difference. We concluded that the proposed approach that generates separate state-space for each fuel component in combination with the fuel estimator that provides proportional control have good response and is able to achieve the target of the thesis.

7.5 Contributions

The novel engine controller combined with fuel estimation, allows vehicle users more choices while refuelling theirs vehicles. The thesis started with the development of the engine simulation platform. The performance of the developed model has been validated by comparing it to existing engine simulation packages that involved laboratory works in their development. The results of the comparison have been published in [21].

The next step in the study is the development of the fuel estimator. The artificial feed-forward neural network approach has been chosen. The simulations run with different portion of mixtures including Isooctane-Methanol and Isooctane-Ethanol. The results have been presented in [20][23].

The final stage of the thesis is to develop the engine control, which used state-space methodology to perform system identification. The LQR method has been used for the closed-loop control in the developed state-spaces. Five parameters have been identified as the control system inputs, which are the exhaust gas compositions, including CO_2, O_2, CO and NOx in addition to the exhaust gas temperature. The controller is developed as a MIMO system, five MISO models has been developed where each one has a single output, including fuel-to-air ratio, ignition timing, exhaust gas valve closed timing, and intake valve opening timing respectively. To improve the state-spaces performance, the system developed five MISO controllers for each given fuels, including Isooctane, Methanol and Ethanol. The controller used the developed fuel estimation as the proportional switch according to the likelihood of the fuel. The models used and the results of the controller have been presented in UKACC PhD showcase in 2011, 2012 and 2013 and the result of the complete controller with the engine cycle is published in [22].

7.6 Final version of virtual engine control system

The block diagram of the final model engine control of this thesis is shown in Figure 87. The final model includes a) the virtual machine, b) fuel estimator and c) closed-loop state-space controller.

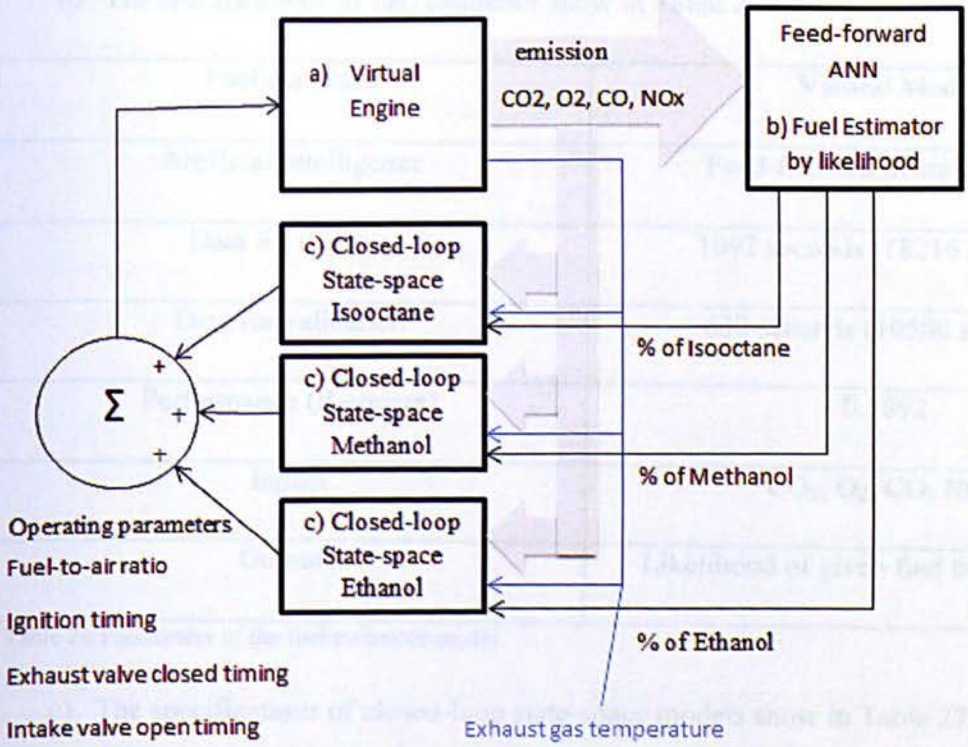

Figure 87 Block diagram of the final model engine control this thesis

a) The specifications of virtual engine show in Table 25.

Parameters	Values/ Model
Number of stroke	4
Number of cylinder	1
Combustion process	Spark Ignition
Fuel used (and mixtures between given fuel)	Isooctane (C_8H_{18}) Methanol ($C_1H_4O_1$) Ethanol ($C_2H_6O_1$)
Heat transfer model	Woschni
Heat release model	Wiebe
Engine size	Medium SI engine (refer to Table 6)

Table 25 Parameters of the final engine simulation model

b) The specifications of fuel estimator show in Table 26.

Fuel estimator	Values/ Model
Artificial intelligence	Feed-forward neural network
Data for training	1092 seconds (18216 samples)
Data for validation	630 seconds (10500 samples)
Performance (R-square)	0.7892
Inputs	CO_2, O_2, CO, NOx
Outputs	Likelihood of given fuel by percentage

Table 26 Parameters of the fuel estimator model

c) The specifications of closed-loop state-space models show in Table 27.

Closed-loop state-space	Values
Number of order	8^{th}
Closed-loop gain	Obtained from LQR
Data for training	1092 seconds (18216 samples)
Simulation	Real-time engine simulation with control
Inputs	CO_2, O_2, CO, NOx Exhaust gas temperature
Outputs	Fuel-to-air ratio Ignition timing Exhaust valve closed timing Intake valve opening timing

Table 27 Parameters of the final engine operating parameter control model

7.7 Recommendations and future works

Engine research is still at the early stages for full electronic engines. The limitations of developing electronic engines include 1) the engines are running mechanically, 2) emissions limitation is tightening and 3) possible fuel composition to run engines which can switch between compression ignition and spark ignition. This thesis provided new approaches on engine control that will work when feeding the engine with different fuel mixtures with unknown composition. Further research may be carried out in the following areas:-

- Implementation of the model to the engine controller

This thesis develops the control algorithm based on computer simulation. For practical use the implementation of the controller requires to research engines which can then download the model to ECU. More tests are needed so the control algorithm can be fitted on different combustion process, e.g. CI engines, HCCI engines, or PCCI engines.

- Valve timing of camless engine.

The thesis simulates the valve timing where practical variable valve timing systems require large mechanical components. The possibility of camless engine is discussed but further work is needed when the camless engine is practical ready.

- State-space model and fuel estimator with more fuel compositions

This thesis considers three fuel compositions that are suitable for its use in SI engines. Same approaches can be performed to CI engines, or HCCI and PCCI engines. More choices of fuel composition can be included in the development of state-space controller. In the current fuel composition, researchers focus on the use of biofuels, which have different compositions. The target is to provide consumers with more choices in composition. The work can be continued by using the same methodologies of training with new fuel estimator models and providing optimal control to engine parameters.

Reference

[1] Aaltonen, J., Huhtala, K., Vilenius, M., "Electrohydraulic Valvetrain for Extreme Value Diesel Engine," *SAE Technical Paper 2002-01-1282, (2002).*

[2] Agrell, F., Angstrom, H.E., Eriksson, B., Wikander, J., Linderyd J., "Control of HCCI During Engine Transients by Aid of Variable Valve Timings Through the use of Model-Based Non-Linear Compensation," *SAE Technical Paper 2005-01-0131, (2005).*

[3] Akbar, S.A., Dutta, P.K., Lee, C., "High-Temperature Ceramic Gas Sensor: A Review," *International Journal of Applied Ceramic Technology, issue 3, pp. 302–311, (2006).*

[4] Al-Zohary, T.A., Wahdan, A.M., Ghonaimy, M.A.R., Elshamy, A.A., "Adaptive Control of Nonlinear Multivariable Systems Using Neural Networks and Approximate Models," *Article, Math. Dept. Fac. Of Science Al-Azhar University.*

[5] Amba Prasad Rao, G., Kaleemuddin, S., "Development of variable timing fuel injection cam for effective abatement of diesel engine emission," *Applied Energy, Aug 2011, vol.88, issue 8, pp. 2653-2662, (2011).*

[6] Anca, R., Wagner, U., Velji, A., Spicher, U., "HCCI-A Possible Solution to Avoid Particulate/NOx Trade-Off for Future Compression Ignition Engines," *CONAT 2004, Brasov, International Automotive Congress, (2004).*

[7] Anderson, M., Tsao, T., Levin, M., "Adaptive lift control for a camless electrohydraulic valvetrain," *SAE Technical Paper 981029, (1998).*

[8] Aoyama, S., Nohara, T., Takamura, S., Tanaka, Y., "Variable compression ratio system for internal combustion engine and method for controlling the system," *Nissan Motor co. ltd. (2006).*

[9] Arsie, I., Marra, D., Pianese, C., Sorrentino, M., "Real-Time Estimation of Engine Nox Emissions Via Recurrent Neural Networks," *SAE International Journal of Passenger Cars, (2009).*

[10] Asad, U., Kumar, R., Han, X., Zheng, M., "Precise instrumentation of a diesel single-cylinder research engine," Measurement, vol.44, issue7, Aug 2011, pp. 1261-1278. (2011)

[11] Atkinson, C., Long, L.W., Hanzevack, L.,"Virtual Sensing: A Neural Network-based Intelligent Performance and Emissions Prediction System for On-Board Diagnostics and Engine Control," *International Congress and Exposition, Detrioit US, 23-26 Feb 1998, (1998).*

[12] Baburic, M., Bogdan, Z., & Duic, N., "A new approach to CFD research: Combining AVL's Fire code with user combustion model," *Information Technology Interfaces 2002, Proceedings of the 24th International Conference, vol. 1, (pp. 383-388), (2002).*

[13] Barclay, S., "Lotus omnivore engine - 10% better fuel economy than current leading gasoline engines," *Automotive Industries, vol. 189, no. 12, (2009).*

[14] Belikov, J. Petlenkov, E., "Model Reference Control of Nonlinear MIMO System by Dynamic Output Feedback Linearization of ANARX Models," *IEEE International Conference on Control and Automation, Christchurch New Zealand, Dec 9-11, 2009, pp. 536-541, (2009).*

[15] Bosch, R., "Bosch Automotive Handbook." *Wiley Blackwell, 7th Edition 26 Oct 2007, (2007)*

[16] Brijesh, P., Sreedhara, S., "Exhaust emission and its control methods in compression ignition engines: A review," *International Journal of Automotive Technology, April 2013, vol.14, issue 2, pp. 195-206, (2013).*

[17] Cassidy, J., "Emissions and Total Energy Consumption of a Multicylinder Piston Engine Running on Gasoline and a Hydrogen-Gasoline Mixture," *National Aeronautics and Space Administration Technical Note, May 1977, (1977).*

[18] Ceviz, M.A., Akin,M., "Design of a new SI engine intake manifold with variable length plenum," *Energy Conversion and Management, Nov 2010, vol. 51, issue 11, pp. 2239-2244, (2010).*

[19] Ceviz, M.A., "Intake plenum volume and its influence on the engine performance, cyclic variability and emissions," *Energy Conversion and Management, March 2007, vol. 48, issue 3, pp. 961-966, (2007).*

[20] Chan, K.Y., Ordys, A., Duran, O., Volkov, K., Deng, J., "SI Engine Simulation Using Residual Gas and Neural Network Modeling to Virtually Estimate the Fuel Composition", *World Congress on Engineering 2013, London, U.K., 3-5 July 2013, vol. 1, pp. 897-903, (2013).*

[21] Chan, K.Y., Ordys, A., Volkov, K., Duran, O., "Comparison of Engine Simulation Software for Development of Control System", *Modelling and Simulation in Engineering, Volume 2013 (2013), Article ID 401643, (2013)*

[22] Chan, K.Y., Ordys, Duran, O., A., Volkov, K., Deng, J., "Minimising engine emissions using State-feedback engine control with LQR and artificial intelligence fuel

estimator", *International Journal of Innovative Research in Technology & Science 2014, vol.2, issue 3, 30th May 2014, pp. 1-9, (2014).*

[23] Chan, K.Y., Ordys, A., Duran, O., Volkov, K., Deng, J., "Adaptive Neuro-Fuzzy Method to Estimate Virtual SI Engine Fuel Composition using Residual Gas Parameters", *UKACC 10th International Conference on Control, Loughborough University UK, 9-11th Jul 2014, (2014)*

[24] Chen, H., "Fuel Injection Control and Simulation of EFI Engine Based on ANFIS. Intelligent Computation Technology and Automation (ICICTA)", *2008 International Conference, Oct 2008, vol.1, pp. 191-194, (2008).*

[25] Ciniciz, M. Kose, H. Canli, E. Solmaz, O., "An experimental investigation on effects of methanolblended diesel fuels to engine performance and emissions of a diesel engine," *Scientific Research and Essays, 11 August, 2011, Vol. 6(15), pp. 3189-3199,* (2011).

[26] Conklin, J.C., Szybist, J.P., "A highly efficient six-stroke internal combustion engine cycle with water injection for in-cylinder exhaust heat recovery," *Energy 2010, vol. 35, issue 4, pp. 1658-1664, (2010).*

[27] Debnath, B.K., Sahoo, N., Saha, U.K., "Thermodynamic analysis of a variable compression ratio diesel engine running with palm oil methylester," *Energy Conversion and Management, Jan 2013, vol. 65, pp. 147–154, (2013).*

[28] Dembele, S., Wen, J.X., "Assessment of spectral narrow band and global gas radiation models for computational fluid dynamics simulations of pool fires," Numerical Heat Transfer - Part B: Fundamentals, *44(4), pp. 365-385. ISSN (print) 1040-7790, (2003).*

[29] Dembele, S., Wen, J., "Predicting Glazing Behaviour in a Fire Environment - Effect of Radiation Models," *FABIG Newsletter, R570(45), (2005).*

[30] Deng, J., Maass, B., Stobart, R., "Particulate Matter Prediction of Both Steady-State and Transient Operation in Diesel Engines", Proceedings of the Institution of Mechanical Engineers, Part D: Journal of Automobile Engineering, 226(2), pp. 260-274.

[31] Deng, J., Maass, B., Stobart, R., "Minimum Data Requirement for Neural Networks Based on Power Spectral Density Analysis," *Neural Networks and Learning Systems, IEEE Transactions, April 2012, vol. 23(4), pp. 587 - 595 , (2012).*

[32] Di Gennaro, S., Castillo Toledo, B., Benedetto, M.D., "Nonlinear Regulation of Electromagnetic Valves for Camless Engines," *45th IEEE Conference on Decision & Control, San Diego USA, Dec 13-15 2006, pp. 3578-3582, (2006).*

[33] Dinkelacker, F., Manickam, B. and Muppala, S.P.R., "Modelling and simulation of lean premixed turbulent methane/hydrogen/air flames with an effective Lewis number approach," *Combustion and Flame*, 158(9), *pp. 1742-1749. ISSN (print) 0010-2180, (2011).*

[34] Drangel, H., Olofsson, E., and Reinmann, R., "The Variable Compression (SVC) and the Combustion Control (SCC) - Two Ways to Improve Fuel Economy and Still Comply with World-Wide Emission Requirements," *SAE Technical Paper 2002-01-0996, (2002).*

[35] Duran, A., Lapuerta, M., Rodríguez-Fernandez, J., "Neural networks estimation of diesel particulate matter composition from transesterified waste oils blends," *Fuel, Nov 2005, vol. 84(16), pp. 2080–2085, (2005).*

[36] Ebrahimi, B., Tafreshi, R., Masudi, H., Franchek, M., Mohammadpour, J., Grigoriadis, K. A, "A parameter-varying filter PID strategy for air-fuel ratio control of spark ignition engines," *Control Engineering Practice, Aug 2012, vol. 20, issue 8, pp. 805-815, (2012).*

[37] Ebrahimi, R., Desmet, B., "An experimental investigation on engine speed and cyclic dispersion in an HCCI," *Fuel, Aug 2010, vol. 98, issue 8, pp. 2149-2156, (2010).*

[38] Epping, K., Aceves, S., Bechtold, R., Dec, J., "The Potential of HCCI Combustion for High Efficiency and Low Emissions," *SAE Technical Paper 2002-01-1923, (2002)*

[39] Ferguson, C.R. and Kirkpatrick A.T., "Internal Combustion Engines: Applied Thermoscience," *John Wiley and Sons, New York, (2001).*

[40] Figueroa, O.L., Lee, C., Akbar, S.A., Szabo, N.F., Trimboli, J.A., Dutta, P.K., Sawaki, N., Soliman, A.A., Verweij, H., "Temperature-controlled CO, CO2 and NOx sensing in a diesel engine exhaust exhaust stream," *Sensor and Actuator B: Chemical Jun 2005. vol. 107, issue 2, pp. 839-848, (2005)*

[41] Forsell, U., Ljung, L., "Closed-loop identification revisited," *Automatica, vol. 35, pp. 1215-1241, (1999).*

[42] Franceschi, E., Muske, K., Peyton Jones, J., Makki, I., "An Adaptive Delay-Compensated PID Air Fuel Ratio Controller," *SAE Technical Paper 2007-01-1342, (2007).*

[43] Ganesh, D., Nagarajan, G., "Homogeneous charge compression ignition (HCCI) combustion of diesel fuel with external mixture formation," *Energy, Jan 2009, vol. 35, issue 1, pp. 148-157, (2009).*

[44] Gao, F., Guo, Y., Liu, F., Li, H., Ji, H.; Tan, M., "Control of HCCI Engine Fueled with Gasoline with Electro-Hydraulic Variable Valve System," *2nd International Asia*

Conference on Informatics in Control, Automation and Robotics 2010, pp. 250-253, (2010).

[45] Ghaffari, A., Shamekhi, A.H., Saki, A., Kamrani, E., "Adaptive Fuzzy Control for Air-Fuel Ratio of Automobile Spark Ignition Engine," *World Academy of Science, Engineering and Technology 2008, vol.24, pp. 284 – 292, (2008).*

[46] Ghazikhani, M., Feyz, M.E., Joharchi, A., "Experimental investigation of the Exhaust Gas Recirculation effects on irreversibility and Brake Specific Fuel Consumption of indirect injection diesel," *Applied Thermal Engineering, Sep 2010, vol. 30, issue13, pp. 1711-1718, (2010).*

[47] Gibson, A., Kolmanovsky, I., "Modeling Positive Intake Valve Overlap Air Charge Response in Camless Engines," *American Control Conference 2003, Jun 4-6 2003, vol. 1, pp. 755-760, (2003).*

[48] Gu, Y., Fang, Z., "Experimental Study on Different Ignition System Matching Different Spark Plug Gap," *2009 International Conference on Computational Intelligence and Natural Computing, 6-7 Jun 2009, vol. 1, pp. 305-308, (2009).*

[49] Guzzella, L. and Onder, C.H., "Introduction to Modeling and Control of Internal Combustion Engine System," *Springer, (2004).*

[50] Hanks, T.C, Lumkes, J.H., "Adaptive Control System for Electrohydraulic Camless Engine Gas Valve Actuator," *American Control Conference, Portland, June 8-10 2005, vol. 6, 4369-4374, (2005).*

[51] Hanson, R., Kokjohn, S., Splitter, D., and Reitz, R., "An Experimental Investigation of Fuel Reactivity Controlled PCCI Combustion in a Heavy-Duty Engine," *SAE Int. J. Engines3(1) 2010, pp. 700-716, (2010).*

[52] He, Y. and Rutland, C.J. "Application of Artificial Neural Networks in Engine modelling," *International Journal of Engine Research, 2004, 5(4), 281-296, (2004).*

[53] Heisler, H., "Vehicle and Engine Technology," *2nd edition. (1999)*

[54] Heywood, J.B. "Internal Combustion Engine Fundamentals," *McGraw-Hill, New York, (1988).*

[55] Hillier, V.A.W., "Hillier's Fundaments of Automotive Electronics," *2nd edition, Nelson, Thornes, (1996).*

[56] Hillier, V.A.W., Coombes, P., "Hillier's Fundamentals of Motor Vehicle Technology," *5th edition 2004, Nelson Thornes Ltd, (2004).*

[57] Hoffmann, W., Peterson, K., Stefanopoulou, A.G., "Iterative learning control for soft landing of electromechanical valve actuator in camless engines," *IEEE Trans.Control Syst.Technol., 2003, vol. 11, no. 2, pp. 174-184, (2003).*

[58] Ibrahim, A., Bari, S., "An experimental investigation on the use of EGR in a supercharged natural gas SI engine," *Fuel, 2010, vol. 89, issue 7, pp. 1721-1730, (2010).*

[59] Ishida, M., Yamamoto, S., Ueki, H., Sakaguchi, D., "Remarkable improvement of NO_x -PM trade-off in a diesel engine by means of bio-ethanol and EGR," *Energy, Dec 2010, vol. 35, issue12, pp. 4572-4581, (2010).*

[60] Jaimoukha, I.M., El-Zobaidi H., Limebeer D.J.N., "Controller reduction for linear parameter-varying systems with a priori bounds," Automatica 2005, *vol. 41, pp. 273-279, (2005).*

[61] Jalili, N., Wagner, J., Dadfarnia, M., "A piezoelectric driven ratchet actuator mechanism with application to automotive engine valves," *Mechatronics, Oct 2003, vol. 13, issue 8-9, pp. 933-956, (2003).*

[62] Jang, J., Bar, C., "Effects of valve events on the engine efficiency in a homogeneous charge compression ignition engine fueled by dimethyl ether," *Fuel, Jul 2009, vol. 88, issue 7, pp. 1228-1234, (2009).*

[63] Jankovic, M., Wagner, S.W., "Cylinder air-charge estimation for advanced intake valve operation in variable cam timing engines," *JSAE Review Oct 2001, vol. 22, issue 4, pp. 445-452, (2001).*

[64] Jankovic, M., "Nonlinear Control in Automotive Engine Applications," *University of Notre Dame, (2002).*

[65] Joe Qin, S., "An overview of subspace identification," *Computer and Chemical Engineering, 12 Sep 2006, vol. 30, pp. 1502-1513, (2006).*

[66] Kapus, P., Fraidl, G., Sams, T., Kammerdiener, T., "Potential of VVA Systems for Improvements of CO2, Pollution Emission and Performance of Combustion Engines", SIA Variable Valve Actuation Conference 2006, IFP Rueil-Malmaison

[67] Kokjohn, S., Hanson, R., Splitter, D., and Reitz, R., "Experiments and Modeling of Dual-Fuel HCCI and PCCI Combustion Using In-Cylinder Fuel Blending," *SAE Int. J. Engines 2(2):24-39, (2010).*

[68] Lancefield, T., "The influence of variable valve actuation on the part-load fuel economy of a modern light-duty diesel engine," *SAE Technical Paper 2003-01-0028, (2003).*

[69] Larsen, G. J., "Reciprocating piston engine with a varying compression ratio," *US Patent US5025757 A, issued 1990-09-13*

[70] Leroy, T.; Chauvin, J.; Petit, N., "Motion planning for experimental air path control of a variable-valve-timing spark ignition engine," *Control Engineering Practice, Dec 2009, vol. 17, issue 12, pp. 1432-1439, (2009).*

[71] Lotus, "Lotus Engineering Software user menu", *Lotus Group plc (2011).*

[72] Maass, B., Deng, J., and Stobart, R. K., "Diesel Engine Emissions Prediction with Parallel Neural Networks," *American Control Conference 2009, Jun 10-12 2009, st. Louis US, pp. 1122-1127, (2009).*

[73] Mancaruso, E., Vaglieco,B.M., "Optical investigation of the combustion behaviour inside the engine operating in HCCI mode and using alternative diesel fuel," *Exp.Therm.Fluid Sci., April 2010, vol. 34, issue 3, pp. 346-351, (2010).*

[74] Manning, J. "Internal Combustion Engine Design," *Ricardo UK Limited (2012)*

[75] Megaritis, A., Yap, D., Wyszynski, M.L., "Effect of inlet valve timing and water blending on bioethanol HCCI combustion using forced induction and residual gas trapping," *Fuel 2008, vol. 87, pp. 732-739, (2008).*

[76] Milton, B.E., "Thermodynamics, Combustion and Engines," Chapman and Hall, 1st Edition, 1995. (1995)

[77] Miron, W., Ragazzi, R., Hollman, T., and Gallagher, G., "Ethanol-Blended Fuel as a CO Reduction Strategy at High Altitude," *SAE Technical Paper 860530, (1986).*

[78] Misztal, J., Xu, H.M., Wyszynski, M.L., Price, P., Stone, R., Qiao, J., "Effect of injection timing on gasoline homogeneous charge compression ignition particulate emissions," *International Journal of Engine Research. Jul 2009, vol.10 pp. 419 – 430, (2009).*

[79] Moradi, M.H., Katebi, M.R., Johnson, M.A., "Robust MIMO PID Tuning Method," *Conference on Control Applications, Proceedings of the 2002 IEEE International, 18-20 Sep 2002, vol. 1, pp. 247-252, (2002).*

[80] Moteki, K., Aoyama, S., Ushijima, K., Hiyoshi, R., "A Study of a Variable Compression Ratio System with a Multi-Link Mechanism," *SAE Technical Paper 2003-01-0921, (2003).*

[81] Murata, Y., Kusaka, J., Odaka, M., Daisho, Y., Kawano, D., Suzuki, H., Ishii, H., Goto, Y., "Emissions suppression mechanism of premixed diesel combustion with

variable valve timing," *International Journal of Engine Research, Jun 2007, vol. 8, issue 5, 415-428, (2007).*

[82] Narendra, K.S., Mukhopadhyay, S., "Adaptive Control Using Neural Networks and Approxiate Models," *IEEE Transactions on Neural Networks, May 1997, vol.8, no3, pp.475-485, (1997).*

[83] Ohyama, Y., "Engine Control Using a Combustion Model," *Seoul 2000 FISITA World Automotive Congress, June 12-15 2000, (2000).*

[84] Ordys, A.W., and Clarke, D.W., "A State-space Description for GPC Controllers," *International Journal of Systems Science 1993, vol. 24, no. 9, pp. 1727-*1744, (1993).

[85] Parlikar, T.A., Chang, W.S., Qiu, Y.H., Seeman, M.D., Perreault, D.J., Kassakian, J.G., Keim, T.A., "Design and experimental implementation of an electromagnetic engine valve drive," *IEEE/ASME Transactions on Mechatronics, 2005, vol. 10, no. 5, pp. 482-494, (2005).*

[86] Peng, Z., Jia, M., "Full engine cycle CFD investigation of effects of variable intake valve closing on diesel PCCI combustion and emissions," *Energy Fuels, 2009, vol.23, no. 12, pp. 5855-5864, (2009)*

[87] Piche, S.,"A Disturbance Rejection based Neural Network Algorithm for Control of Air Pollution Emissions. Neural Networks," 2005. IJCNN '05. Proceedings. 2005 IEEE International Joint Conference on, Aug *2005, vol.5,pp. 2937-2941, (2005).*

[88] Pukrittayakamee, A., De Jesus, O., Hagan, M.T., "Smoothing the Control Action for NARMA-L2 Controllers," *Circuits and Systems 2002, 4-7 Aug 2002, vol. 3, pp. III-37-III-40, (2002).*

[89] Pupeikis, R., "Closed-loop Robust Identification Using the Direct Approach," *INFORMATICA 2000, vol. 11, no. 2, pp 163-178, (2000).*

[90] Raine, R.R., "ISIS 319 user manual, computer modelling of nitric oxide formation in a spark ignition engine," *Oxford Engine Group, (2000).*

[91] Ricardo, "Ricardo software: WAVE user's manual," *Version 8.0, Ricardo Inc, (2009).*

[92] Sher, E., Bar-Kohany, T., "Optimization of variable valve timing event for maximizing performance of an unthrottled SI engine – a theoretic study," *Energy 2002. vol.27, issue 8, pp 757-775, (2002).*

[93] Sher, I., Levinzon-Sher, D., Sher, E., "Miniaturization limitations of HCCI internal combustion engines," Applied Thermal Engineering, Feb 2009, vol. 29, issue 2-3, pp. 400-411, (2009).

[94] Silva, E.I, Erraz, D.A., "An LQR Based MIMO PID Controller Synthesis Methos for Unconstrainted Lagrangian Mechanical Systems," *Proceedings of the 45th IEEE Conference on Decision & Control, San Diego US, 13-15 Dec 2006, pp. 6593-6598, (2006).*

[95] Soares, S.M.C., Sodré, J.R., "Effects of atmospheric temperature and pressure on the performance of a vehicle," *Proc.Inst.Mech.Eng.Pt.D: J.Automobile Eng., 2002, vol. 216, issue 6, pp. 473-477, (2002).*

[96] Sommer, A., Stiegler, L., Wormbs, T., Kabitzke, J., Buschmann, G., "Will we need variable valve trains for passenger-car diesel engines in the future?" SIA Conference on Variable Valve Actuation, 30 Nov 2006, IFP Rueil, (2006)

[97] Srakaew, K., Kananai, J., Chancharoen, R., "Trajectory Control of a Nonlinear Dynamical System using NARMA L2 Neurocontroller," *Journal of Computer and Information Technology, vol. 1, no. 1.*

[98] Srinivasa Pai, P., Shrinivasa Rao, B.R., "Artifical Neural Network based prediction of performance and emission characteristics of a variable compression ratio CI engine using WCO as a biodiesel at different injection timings," *Applied Energy Jul 2011, vol. 88, issue 7, pp. 2344-2354, (2011).*

[99] Sun, Z., Kuo, T.W., "Transient Control of Electro-Hydraulic Fully Flexible Engine Valve Actuation System," *IEEE Transactions on control systems technology May 2010, vol. 18, no.3, pp. 613-621, (2010).*

[100] Tamura, K., Ohmori, H., "Auto-Tuning Method of Expended PID Control for MIMO Systems," *SICE-ICASE 2006, International Joint Conference, 18-21 Oct 2006, pp. 3270-3275, (2006).*

[101] Turner, J.W.G., Blundell, D.W., Pearson, R., Patel, R., Larkman, D.B., Burke, P., "Project Omnivore: A Variable Compression Ratio ATAC 2-Stroke Engine for Ultra-Wide-Range HCCI Operation on a Variety of Fuels," *SAE Technical Papers, 2010-01-1249, (2010).*

[102] Urushihara, T., Hiraya, K., Kakuhou, A., and Itoh, T., "Expansion of HCCI Operating Region by the Combination of Direct Fuel Injection, Negative Valve Overlap and Internal Fuel Reformation," *SAE Technical Paper 2003-01-0749, (2003).*

[103] Verhelst, S., Demuynck, J., Sierens, R., Huyskens, P., "Impact of variable valve timing on power, emissions and backfire of a bi-fuel hydrogen/gasoline engine," *International Journal of Hydrogen Energy, vol. 35, no. 9, pp. 4399-4408, (2010).*

[104] Walter, B., Pacaud, P., Gatellier, B., "Variable valve actuation systems for homogeneous diesel combustion: How interesting are they?" *Oil and Gas Science and Technology, 2008, vol. 63, issue 4, pp. 517-534, (2008).*

[105] Wang, Y., He, L., Zhou, L., Li, W., "Effects of DME pilot quantity on the performance of a DME PCCI-DI engine," *Energy Conversion and Management, April 2010. vol. 51, issue 4, pp. 648-654, (2010).*

[106] Woo, L.Y., Glass, R.S., Novak, R.F., Visser, J.H., "Diesel engine dynamometer testing of impedancemetric NOx sensors," *Sensor and Actuator B: Chemical, Sep 2011. vol. 157, issue 1, pp. 115-121, (2011).*

[107] Woschni, G. "A universally applicable equation for the instantaneous heat transfer coefficient in the internal combustion engine," *SAE Paper, 1967, 670931, (1967).*

[108] Wu, B., Prucka, R. G., Filipi, Z. S., Kramer, D. M. and Ohl, G. L. "Cam-phasing Optimization using Artificial Neural Networks as Surrogate Models—Fuel Consumption and NOx Emissions," *SAE 2006-01-1512, (2006).*

[109] Yan, F., Wang, J., "Pressure-based transient intake manifold temperature reconstruction in Diesel engines," *Control Engineering Practice(20), 2012, pp. 531-538, (2012).*

[110] Yang, L., "Script files analysis and parameterization operation of GT-Power," *Mechanic Automation and Control Engineering (MACE), July 15-17 2011, pp.6812-6814, (2011).*

[111] Yao, M., Chen, Z., Zheng, Z., Zhang, B. et al., "Effect of EGR on HCCI Combustion fuelled with Dimethyl Ether (DME) and Methanol Dual-Fuels," *SAE Technical Paper 2005-01-3730, (2005).*

[112] Yap, D., Megaritis, A., Wyszynski, M.L., "Effect of inlet valve timing on booted gasoline HCCI with residual gas trapping," *SAE Technical Paper, 2005-01-2136, (2005).*

[113] Yap, W.K., Ho, T., Karri, V., "Exhaust emissions control and engine parameters optimization using artificial neural network virtual sensors for a hydrogen-powered vehicle," *Internal Journal of Hydrogen Energy 2012, vol. 37, issue 10, pp. 8704-8715, (2012).*

[114] Ye, Z., Washko, F., Lai, M.C., "Genetic Algorithm Optimization of Fuel Economy for PFI Engine with VVT-VCR," *Proceedings of the 2004 IEEE Internation Coference, 2-4 Sep 2004, vol.1, pp. 364-369 , (2004).*

[115] Zhang, S.M.; Tian, F., Ren, G.F., Yang, L., "SCR control strategy based on ANNs and Fuzzy PID in a heavy-duty diesel engine," *International Journal of Automotive Technology, August 2012, vol. 13, issue 5, pp. 693-699, (2012).*

[116] Zhao, J., Seethaler, R.J., "A Fully Flexible Valve Actuation System for Internal Combustion Engines," *IEEE ASME Transcations on Mechatronics, Apr 2011, vol. 16, no. 2, pp. 361-370, (2011).*

[117] Zhao, J., Seethaler, R.J., "Compensating combustion forces for automotive electromagnetic valves", *Mechatronics, Jun 2010,vol. 20, issue 4, pp.433-441, (2010).*

[118] Ziegler, J.G and Nichols, N. B., "Optimum settings for automatic controllers", *Transactions of the ASME 64, Nov 1942, pp. 759–768, (1942).*

[119] Zolotas, A.C., Chaudhuri, B., Jaimoukha, I., Korba, P., "A Study on LQG/LTR Control for Damping Inter-Area Oscillations in Power Systems," *IEEE Transcations on Control System Technology, Jan 2007, vol. 15, no. 1, pp. 151-160, (2007).*

Pending publication

[120] Chan, K.Y., Ordys, A., Volkov, K., Duran, O., Deng, J., "State-feedback Engine Emission Control under the Open Condition of the Dynamic Intake Manifold Model," *IEEE Transcations on Control System Technology.*

Appendix A

Current Engine Combustion Process

In principle, engine aims to design with the compression ratio as highest as possible. When compression ratio is high, the fuel and air particles are closely packed together and obtain a higher explosive velocity during combustion. However, the design and material used to manufacture engine cylinder and piston head has limitation of compression ratio. There are two different combustion process produced for vehicle engines available in the industry, Spark-Ignition (SI) process and Compression-Ignition (CI).

1.1.1 Spark-Ignition (SI) engine

In SI engine, the typical compression ratio is between 8 and 12, usually does not exceed 12 due to the material used in the production is not durable and engine knocking is possibly occurs if compression ratio is too high. The standard liquid fuel composition used contains 4 and 12 Carbon atom per molecule, named gasoline or petrol from the fuel supplier. However alternative auto gas, such as methane, methanol, nitromethane can be used as fuel. Fuel suppliers provided the standard gasoline can be a partly mixture with the listed autogas, with an octane number is a set standard to avoid engine knock. The air and fuel mixture compressed to the temperature at around 700K. The ignition starts when a spark plug fires a spark of high voltage electricity at 30,000V in a fraction of time, gives enough power and duration in combustion.

1.1.2 Diesel (CI) engine

In diesel engine, the typical compression ratio is in the range of 12 to 24. Because the compression ratio is higher, it has better efficiency compare to SI engine. Diesel engine also produces a high power output compared to SI engine. The application aims to heavy vehicles, such as trucks and coaches. The standard liquid fuel used contains 10 to 15 Carbon atoms and 18 to 28 Hydrogen atoms per molecule. This fuel has a lower boiling point at around 525K.

Comparison of SI engine and Diesel engine

Advantages of diesel engines against gasoline engine

- Better efficiency, higher compression ratio, higher power, larger expansion ratio.
- Better torque at low speed

- Better fuel economy while performing the same work against petrol engine.
- Lower temperature combustion, engine is more durable
- Less pollution in CO2

Disadvantages

- Harder to start in cold condition.
- Complex in design means more expensive to manufacture and repair

Combustion process	Fuel type	Compression Ratio typical values
Spark ignition	Gasoline	8:1 – 12:1
Compression ignition	Diesel	12:1 – 24:1

Table A1 Typical values of compression ratio

1.2 Future Engine Combustion Process

SI and CI engines are currently available engine combustion process in passenger vehicle engines. The advantages and disadvantages have been discussed in the Chapter 0. However the process of the combustion is almost fixed because the operation of an engine decided by mechanical part which cannot adaptively modified. The combustion can hardly be adjusted, and hence combustion perform can be adjusted using large mechanical parts or other factor, such as fuel-to-air ratio which is independent to camshaft. Therefore SI and CI combustion process cannot switch to one to another to provide a flexible control to internal combustion engines.

1.2.1 Homogeneous charge compression ignition engine (HCCI)

Homogeneous charge compression ignition is the combustion process which is widely developing. The mixture compressed to a self-ignition temperature to perform compression ignition [37][62][70][93][111]. The fuel use in the HCCI process can be gasoline, diesel fuel or other alternative fuel [38]. Homogeneous charge means air and fuel mix as a homogenous charge before entering the engine cylinder through the intake valve. The mixture performs compression ignition when the mixture is compressed and reached the ignition temperature. The important factors in HCCI process are the pressure and temperature control inside cylinder and the homogeneity of air and fuel, means the engine design aimed for a good air and fuel mixing system.

Homogeneous charge compression ignition engine can be controlled by ECU in order to optimize the pre-mixed air and gasoline/diesel enter into cylinder and compress to high pressure where high temperature [37][43][62][73][93]. It might also controlling temperature by closing the exhaust valve early. The hot residual gas left the high temperature in the combustion chamber and ECU calculates the best parameter for next combustion cycle such as amount of air and fuel needed. Because self-ignition react in those mixed air and fuel particles widely spread inside the cylinder, the ignition points can be discretely occurs at the particles. This overcomes the problem of SI engine has a port injection or direct injection where mixed air and fuel particles packed relatively near the injection point. So HCCI gives better power output compared to SI and diesel engine. HCCI has 15% more fuel efficiency compared to Otto-Cycle engines and also less pollutant. One main disadvantage is life of the engine can be shorter due to high temperature and compression ratio work frequently and engine part wear and tear faster. Work with computer controlled engine before it is mature enough for commercial use.

1.2.2 Premix charge compression ignition engine (PCCI)

The other method is similar to HCCI is Premix Charge Compression Ignition (PCCI). Homogenous charge is mixed before entering the cylinder. The portion of such mixture is not compressed to self-ignition. A remaining portion of premix charge mixture is directly injected into cylinder from a second pilot to perform ignition. It is the improvement of the diesel process with taken half of the idea of HCCI. The first portion of mixture entered into cylinder to let the mixed air and fuel particles widely spread, the second portion ignites the mixture therefore it can be achieve a longer combustion duration [105].

1.3 Mathematics representation of combustion process

By considering the movement of piston, the volume inside the cylinder is compressed and expanded. Boyle's law explained the relationship between pressure and volume. The combustion process can be best described with a P-V diagram or commonly called indicator diagram.

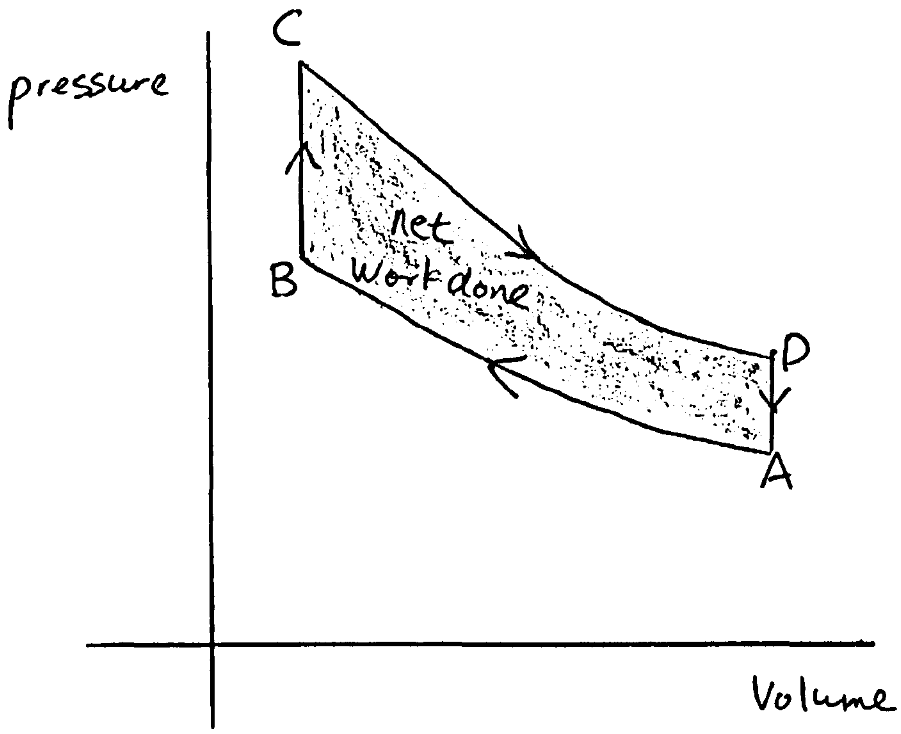

Figure A1 PV diagram of a 4-stroke engine cycle.

The indicator plots the ideal pressure difference against volume throughout the combustion process. In Figure A1, it shows the simplified form of indication diagram.

- From A to B – As the piston goes from BDC to TDC, the volume decreases. The gas injected into the cylinder has been compressed adiabatically. The compression causes pressure and temperature increases. The energy rises, work is done to the gas.

- From B to C – As the ignition starts, the mixture explodes and generate high temperature frame. Resultant further temperature increases which pressure proportionally have further increases.

- From C to D – The exploded mixture expands due to high temperature and pressure. This process generates the motion which pushes the piston down. Piston moves from TDC to BDC. While the volume increases, the temperature and pressure decreases. As the energy released through the expansion process, work is done by the gas.

- From D to A – The expansion process finished. Exhaust gas valve opens to warm exhaust gas discharged to atmosphere. Intake valve opens and fresh air enter the cylinder from atmosphere, which causes pressure drop through the pressure difference between cylinder and atmosphere.

1.3.1 Ideal gas law

The gas species which can be found in engine combustion process included working fluid, such as oxygen, nitrogen, carbon dioxide, fuel vapour, can be treated as ideal gas. This can be simply explained by the Ideal gas law shown in Equation A1.

$$pV = nRT$$

Equation A1

where

p is pressure

V is volume

n is the fraction of mass of gas and molecule weight

R is Gas constant

T is temperature

1.4 Number of stroke in engines

It can be divided into four process, intake, compression, ignition and expansion. In one stroke, piston moves from two positions between Top Dead Centre (TDC) and Bottom dead centre (BDC). For 2-stroke engine, one working cycle contains 2 strokes, i.e. 360° piston movement. For 4-stroke engine, one working cycle contains four strokes, i.e. 720° piston movement.

1.4.1 2-stroke engine

One working cycle consists of two strokes (four piston movements), corresponding to one crankshaft revolutions.

- 1st stroke – compression stroke

The piston moves from the BDC (0°) to TDC (180°). When the position of the piston is at the BDC, the piston let the both intake and exhaust ports open. Fresh air and fuel mixture enters to the cylinder. The upward movement of piston close both valves at some point. The mixture compressed to high pressure and temperature in the remaining space. Mixture ignites by a spark in SI process or fuel injected into cylinder in CI process.

- 2nd stroke – combustion stroke

The explored mixture expands and push piston downward. In the point of the valve position, exhaust valve opens and hot burned gas discharged from the cylinder. The cycle repeats with fresh mixture entering the cylinder.

1.4.2 4-strokes engine (SI process)

One working cycle consists of four strokes (four piston movements), corresponding to two crankshaft revolutions.

- 1st stroke – induction stroke

The piston moves from the TDC (0°) to BDC *(180°). During the induction stroke, the* intake valve opens and fresh mixture enters into combustion chamber. The downward movement of the piston during the induction stroke creates a partial vacuum in the cylinder, which means that prepared ignitable mixture is sucked and filled up the space.

- 2nd stroke – compression stroke

The piston moves from the BDC (180°) to TDC (360°). The intake and exhaust valves are closed. This makes the mixture without breathing to generate a higher pressure. The mixture is compressed by the upward movement of the piston to the 8th to 12th part of its original volume and thus heated to 400 to 500°C. The engine is designed to compress the mixture with the highest temperature without reaching self-ignition temperature. The combustion initiated by switching an ignition spark between the electrodes of the spark plug shortly before the top dead centre (TDC) is reached.

- 3rd stroke – combustion stroke

The piston moves from the TDC (360°) to BDC (540°). During the 3rd stroke, combustion of the compressed mixture takes place. The intake and exhaust valve are closed. During the process of combustion the combusted particle propagate to the space in the combustion chamber. This generates the rise in pressure and the expansion pushes the piston downwards and hence applies work to the crankshaft.

- 4th stroke – exhaust stroke

The piston moves from the BDC (540°) to TDC (720°). With the exhaust valve open, the exhaust gases are emitted by the upward movement of the piston (exhaust stroke). For emission, the piston must overcome a back pressure of approx. 0.2 bar. For this reason, the upward movement of the piston is supported by flywheel masses on the crankshaft. Before the next downward movement of the piston, the intake valve opens and the cylinder is charged with fresh mixture: the next working cycle starts.

1.4.3 4-strokes engine (CI process)

The different between the four-strokes SI engine and CI engine is the ignition temperature. In pratical, CI engine does not require a spark plug. The compression ignition start once fuel (diesel) injected into the combustion chamber. The combustion process is similar to SI engine, but the operating process is different:-

- 1st stroke – induction stroke

The piston moves from the TDC (0°) to BDC (180°). When the intake valve opens, fresh air enters the combustion chamber. The process is similar to spark ignition, while the piston moves download, it creates a partial vacuum in the cylinder which fresh air is sucked and filled up the space.

- 2nd stroke – compression stroke

The piston moves from the BDC (180°) to TDC (360°). Because of a higher compress ratio compared to spark ignition engine, the air being compressed to a higher temperature, at around. The temperature is high enough for an auto-ignition and ready for combustion start while fuel injected into cylinder.

- 3rd stroke – combustion stroke

The piston moves from the TDC (360°) to BDC (540°). The air compressed to the temperature which high enough for fuel ignite. Combustion starts by injecting fuel into cylinder through direct injection. It means fuel injector installed on the wall of cylinder and fuel enter cylinder directly. The burned gas expands and pushes the piston to downward direction.

- 4th stroke – exhaust stroke

The piston moves from the BDC (540°) to TDC (720°). This stroke has the same process as SI engine.

1.4.4 Overview of 2-stroke engine and 4-stroke

Comparing to the number of stroke in engine, 2-stroke and 4-stroke both have advantages and disadvantages and play a part in the industry. 2-stroke engine is easier to design and produce. The process is simple and have easy valve event. 2-stroke engine is also has a higher power density, producing power in every full cycle since combustion happens once the piston is compressing mixture. However, 2-stroke engine has poor emission and fuel consumption [Manning]. 4-stroke engine has better volumetric efficiency over engine speed range. The emission and fuel consumption is improved. It has a poorer power density since it produce power in every two full piston cycles. The usage of different engines, 2-stroke engines aims for light duty vehicle such as motorbikes and leisure vehicles. 4-stroke gasoline engine aims for light to medium duty vehicles, such as passenger cars. 4-stroke diesel engine aims for medium to heavy duty vehicles, such as trucks or buses.

1.4.5 6-stroke engines

There is more research on adding two more strokes in engine cycle [26]. This addition provides some advantages in emission. However it is not mature yet for commercial use, but in this research it is worth to discuss. The two extra strokes act as power stroke. It inserted between combustion stroke and exhaust stroke. The process works as distilled-water injected into combustion chamber. The residual gas left after the combustion chamber remains a certain high temperature. By injecting water, the water evaporates the water into stream and provides another expansion stroke. This reaction makes water expends by 1600 times and cylinder pressure increased. The power is designed to be enough to push the piston down. These two strokes make engine more efficient and reduce emissions. This is because the extra strokes work as a cooling effect which low temperature exhaust gas reduces the CO2 and CO level.

Appendix B

Electronic Throttle Control using Labview

Introduction

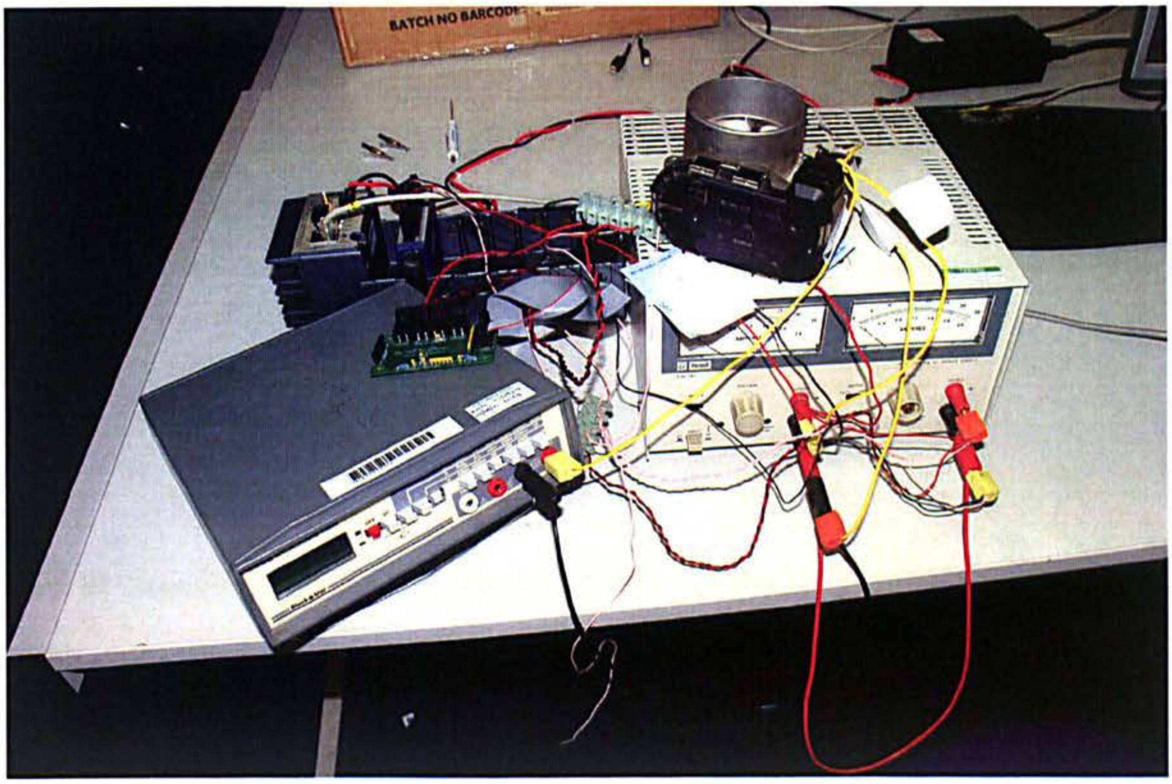

Figure B1 Throttle connected to CompactRio

Throttle is an air valve which controls the amount of air enter engine. It locates at the entrance of intake manifold. The main function of a throttle is by controlling the air flow rate, regulates the air-fuel ratio and pressure where it affect the power output of the engine and emission of exhaust gas. There is an air flow sensor installed after the throttle valve to measure the amount of air entered, and also a throttle position sensor send signals to E.C.U to determine the amount of fuel needed. Diesel engines do not need to control air volume.

Hardware

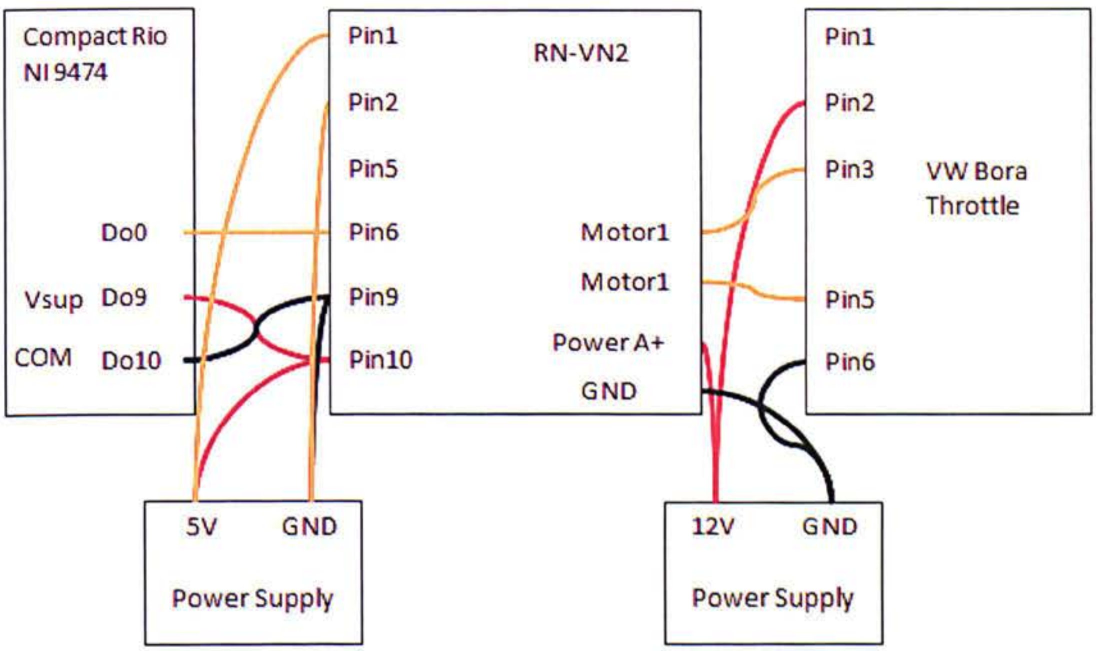

Figure B2 Connection diagram of the electronic throttle system

In this experiment, a real throttle is connected to computer and uses the computer to control the position of the throttle. The system contains three parts, a Voltswagen Bora throttle with 12V input, National Instrument CompactRio with NI9474 sourcing digital output module, and RN-VN2 dual motor controller with 5V input. The idea is by programming CompactRio using Labview, sends pulse width modulation (PWM) signal to motor controller where the controller controls DC motor in the throttle and adjusts the position needed. The direction of the throttle is determined by polarity of the controller board, therefore the PWM power sends to the motor controls the opening direction, and there is a strong return spring against the throttle and it is used to control the closing direction.

National Instrument Compact Rio

CompactRio is a programmable real-time embedded controller offer powerful stand-alone embedded execution for deterministic LabVIEW Real-Time applications. The controller contains reconfigurable IO modules and FPGA where it can be programmed by Labview. It communicates with computer through High-Speed Ethernet. The users can make their own controller by insert various modules which suit users' needs. In this experiment, NI9474 sourcing digital output module is used to produce pulse width modulation.

NI9474 – Pulse Width Modulation

Figure B3 NI9474 sourcing digital output module

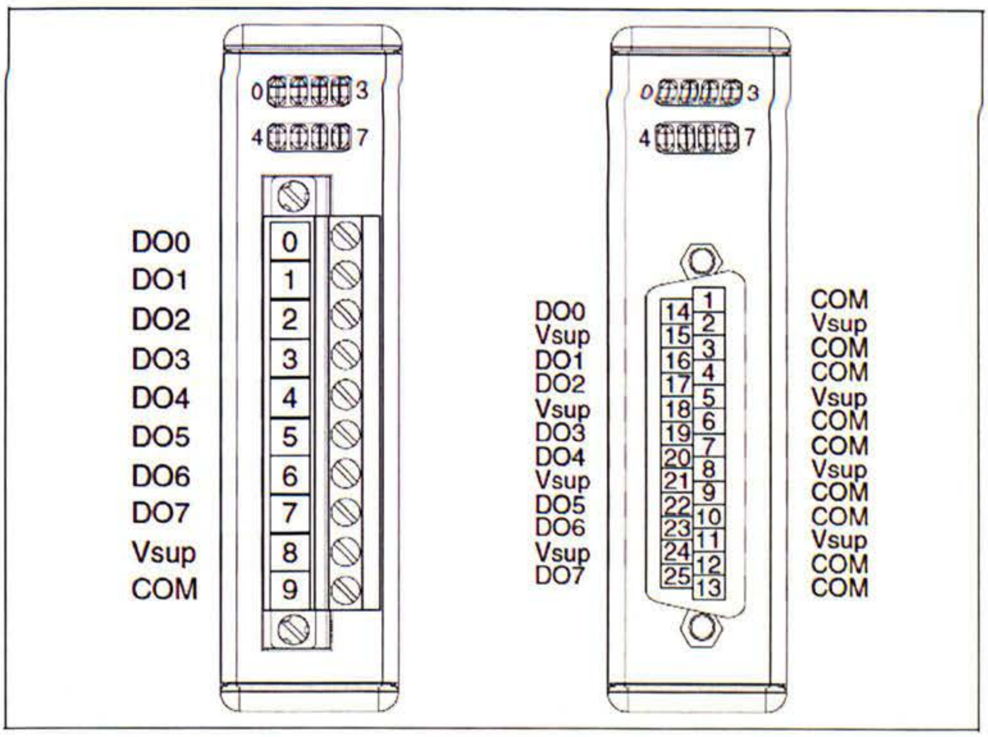

Figure B4 NI9474 Terminal pin assignment

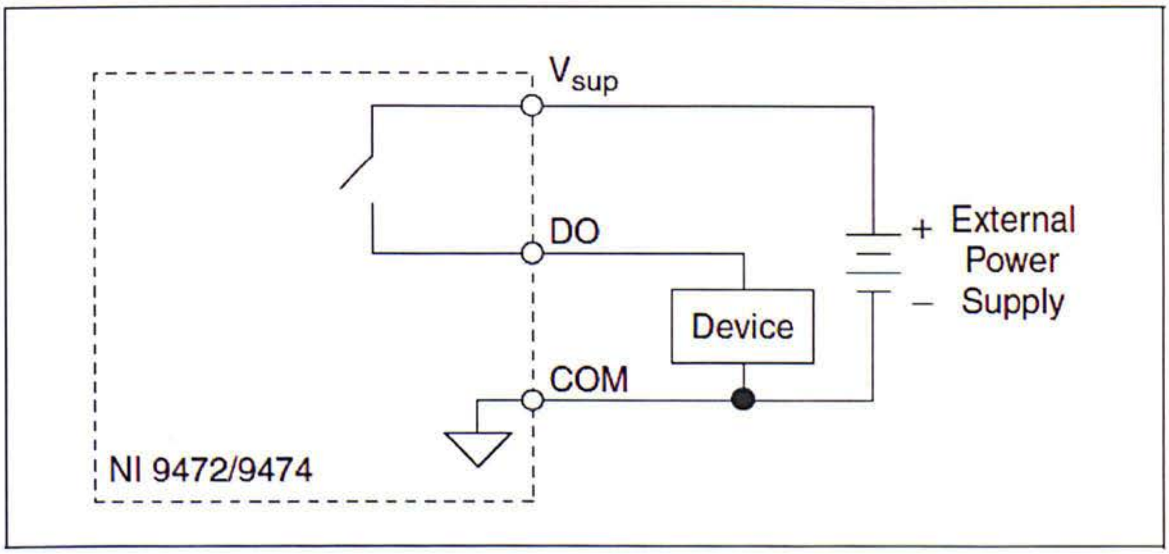

Figure B5 Connecting a device to NI9474

The main feature of NI9474 are 8 channels 1 μs high-speed digital output, 5 to 30 V, sourcing digital output. The module function as an on-off switch where the on time is depends on the pulse width where it can be controlled on Labview. The pulse is powered from an external power supply from pin 9 & 10. There is a set of LEDs indicate the state of the correspondent channel.

Connection of NI9474

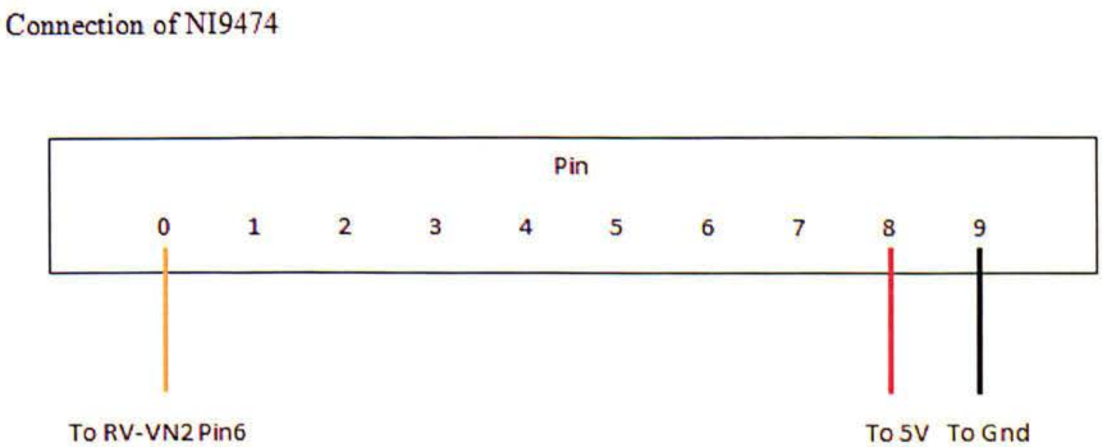

Figure B6 Connection diagram of NI9474

RV-VN2 Motor Controller

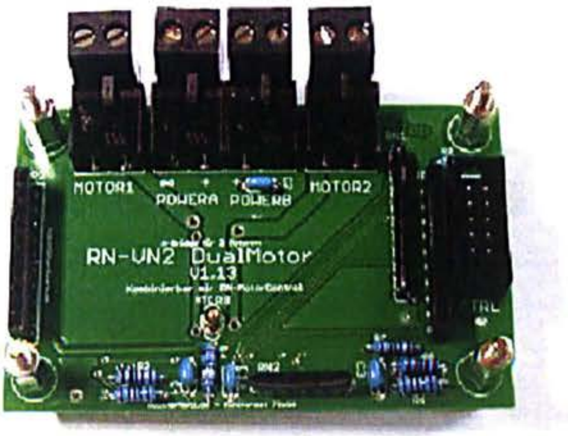

Figure B7 RV-VN2 board

This RN-VN2 is a dual motor controller used to control the DC motor inside the throttle. It contains two microcontrollers which is able to control two motors. The main component of the board is microcontroller VNH2SP30 which is a full bridge motor driver. In this experiment the controller input signals from CompactRio and send the correspondent signals to control the motor. There are three ports sufficient per engine. Two ports, pin 9 & pin 10 determine direction of rotation, which determined by polarity; and one port, pin 6, enabled by pulse width modulation which determine speed which is up to 20kHz.

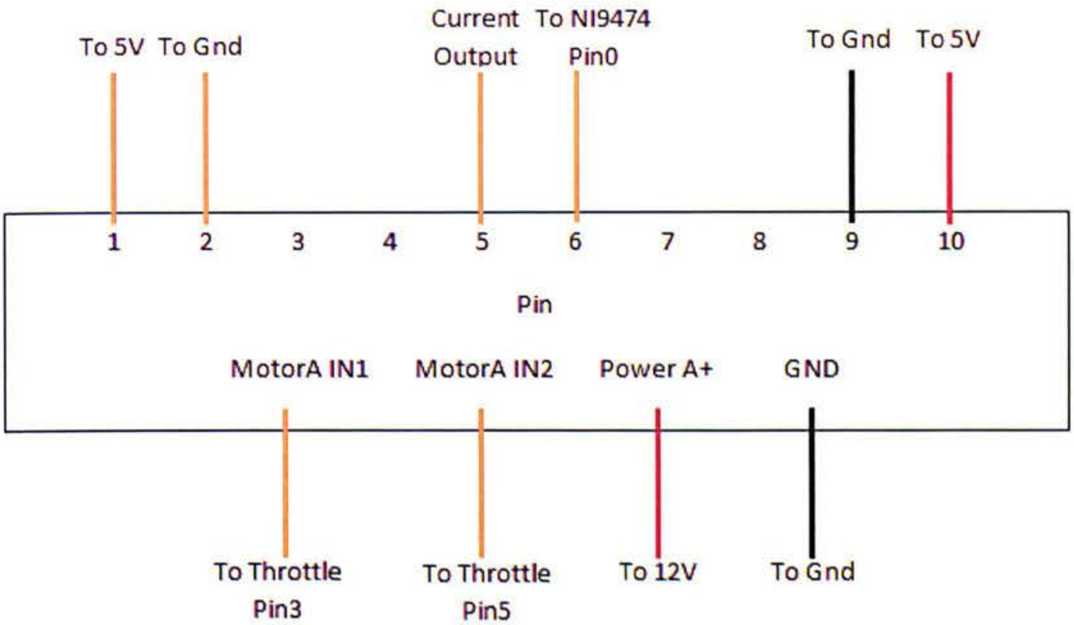

Figure B8 Connection diagram of RN-VN2

VNH2SP30

INA	INB	ENA	ENB	OUTA	OUTB	CS	Operating Mode
1	1	1	1	H	H	High Imp.	Brake to VCC
1	0	1	1	H	L	ISENSE=IOUT/K	Clockwise
0	1	1	1	L	H	ISENSE=IOUT/K	Counter clockwise
0	0	1	1	L	L	High Imp.	Brake to GND

Table B1 Truth table in normal operating conditions

VNH2SP30 is a full bridge motor driver which is able to drive the direction of the motor. Table 1 is a truth table of the chip. While EnA and EnB is on, the direction determined by InA and InB, act as a NAND gate. When InA is high and In B is low, the motor turns to clockwise direction, and vice versa.

Throttle body

Figure B9 VW Bora Throttles from 1999-2006

The Volkswagen Bora throttle uses DC Motor where the speed controlled by pulse width frequency and direction controlled by polarity. The input voltage of the throttle is 12V. There is a position sensor installed in the throttle and that is the only output. The signal is connected to ECU to determine the fuel usage.

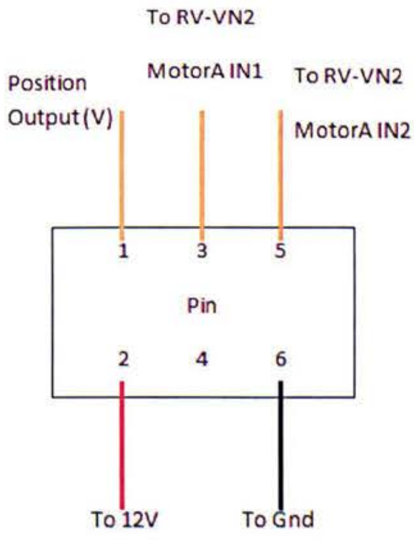

Figure B10 Connection diagram of VW Bora Throttle

Software

The system connects to CompactRio, therefore Labview is used for the ease of this experiment.

Labview

The program for this experiment is simple. Set NI9474 to PWM and set into a timed loop, the program is controlled by a Knob from 0 to 100 according to the percentage set to frequency for pulse width. The frequency range used in this experiment is set to 50Hz. The pulse width determines the frequency which input into motor controller pin6. To control direction, there is a strong return spring inside the throttle. Therefore only opening direction of control is needed and throttle close using return spring.

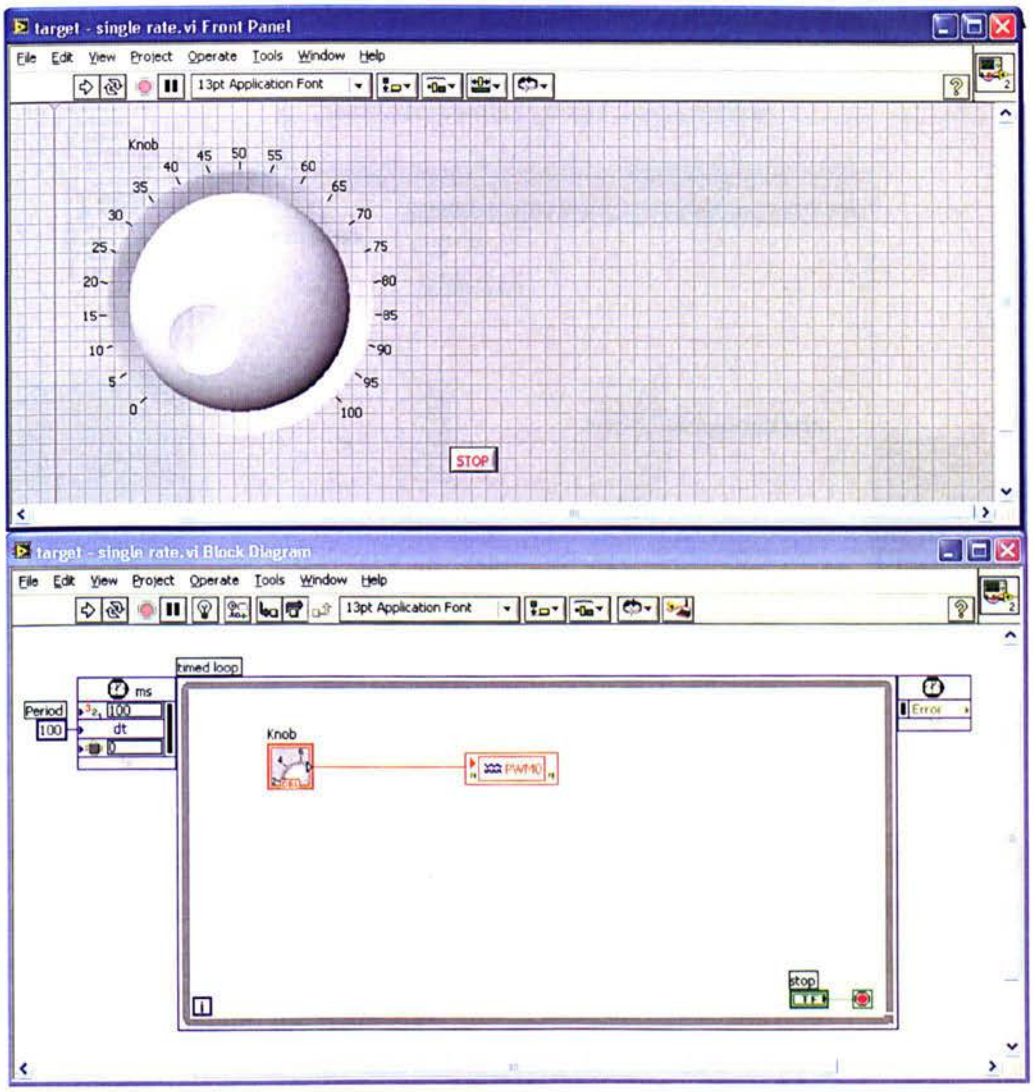

Figure B11 Labview program print screen in this experiment

To change frequency range, right click the module on project dialog. Choose Speciality Digital Configuration. Make sure Speciality Mode is "Pulse Width Modulation". By choosing channel 0, which is used in this experiment, choose frequency 50Hz.

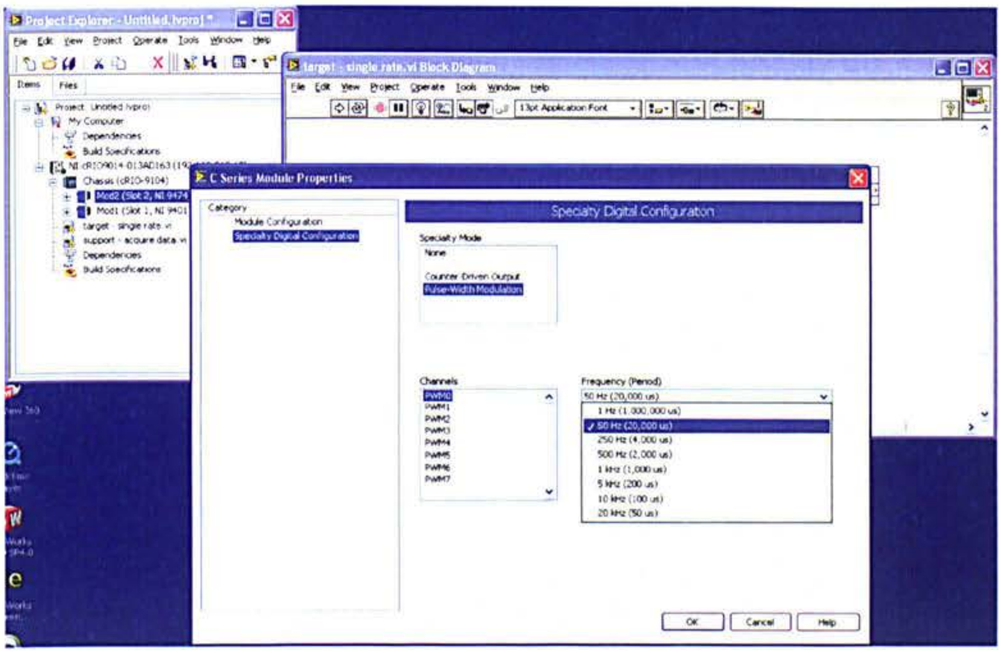

Figure B12 Change frequency range for PWM

Test Result

Determine the output by the output of position sensor (Pin1). To test the frequency of the pulse width needed for certain position, find the voltage from the position sensor at closed position and find the voltage at fully open position, and hence calculate the voltage needed at half open and record the frequency.

Frequency	Position	Position Sensor Voltage
12	Fully Closed	1.42
20	Half Open	4.85
28	Fully Open	8.27

Table B2 Throttle test results

To overcome the power of return spring, pulse width from 0-12 Hz is idle. The throttle starts to open when the pulse width is bigger than 25Hz. When the throttle is fully open, it needs around 28Hz. Pulse width bigger than 28Hz will keep throttle fully open.